

การประยุกต์ใช้ระบบเยื่อแผ่นเหลวที่พุงด้วยเส้นใยกลวงแยกไอออนตะกั่ว โปรท และสารหนู  
ออกจากน้ำสังเคราะห์และการทำนายผลการแยกด้วยแบบจำลองทางคณิตศาสตร์



นายศิระ สุहरินทร์

จุฬาลงกรณ์มหาวิทยาลัย  
CHULALONGKORN UNIVERSITY

วิทยานิพนธ์นี้เป็นส่วนหนึ่งของการศึกษาตามหลักสูตรปริญญาวิทยาศาสตรดุษฎีบัณฑิต

สาขาวิชาวิศวกรรมเคมี ภาควิชาวิศวกรรมเคมี  
บทคัดย่อและแฟ้มข้อมูลฉบับเต็มของวิทยานิพนธ์ตั้งแต่ปีการศึกษา 2554 ที่ให้บริการในคลังปัญญาจุฬาฯ (CUIR)  
คณะวิศวกรรมศาสตร์ จุฬาลงกรณ์มหาวิทยาลัย

เป็นแฟ้มข้อมูลของนิสิตเจ้าของวิทยานิพนธ์ ที่ส่งผ่านทางบัณฑิตวิทยาลัย  
ปีการศึกษา 2556

The abstract and full text of theses from the academic year 2011 in Chulalongkorn University Intellectual Repository (CUIR)  
ลิขสิทธิ์ของจุฬาลงกรณ์มหาวิทยาลัย

are the thesis authors' files submitted through the University Graduate School.

THE APPLICATION OF HOLLOW FIBER SUPPORTED LIQUID MEMBRANE TO  
SEPARATE LEAD, MERCURY AND ARSENIC IONS FROM SYNTHETIC WATER AND  
MATHEMATICAL MODEL FOR PREDICTION

Mr. Sira Suren

จุฬาลงกรณ์มหาวิทยาลัย  
CHULALONGKORN UNIVERSITY

A Dissertation Submitted in Partial Fulfillment of the Requirements  
for the Degree of Doctor of Engineering Program in Chemical Engineering

Department of Chemical Engineering

Faculty of Engineering

Chulalongkorn University

Academic Year 2013

Copyright of Chulalongkorn University

Thesis Title	THE APPLICATION OF HOLLOW FIBER SUPPORTED LIQUID MEMBRANE TO SEPARATE LEAD, MERCURY AND ARSENIC IONS FROM SYNTHETIC WATER AND MATHEMATICAL MODEL FOR PREDICTION
By	Mr. Sira Suren
Field of Study	Chemical Engineering
Thesis Advisor	Distinguished Professor Dr.Ura Pancharoen

---

Accepted by the Faculty of Engineering, Chulalongkorn University in Partial  
Fulfillment of the Requirements for the Doctoral Degree

.....Dean of the Faculty of Engineering  
(Professor Dr.Bundhit Eua-arporn)

#### THESIS COMMITTEE

.....Chairman  
(Professor Dr.Paisan Kittisupakorn)

.....Thesis Advisor  
(Distinguished Professor Dr.Ura Pancharoen)

.....Examiner  
(Assistant Professor Dr.Varong Pavarajarn)

.....Examiner  
(Assistant Professor Dr.Soorathep Kheawhom)

.....External Examiner  
(Associate Professor Dr.Anchaleeporn Waritswat Lothongkum)

ศิริระ สุหรินทร์ : การประยุกต์ใช้ระบบเยื่อแผ่นเหลวที่พุงด้วยเส้นใยกลวงแยกไอออนตะกั่ว  
ปรอท และสารหนูออกจากน้ำสังเคราะห์และการทำนายผลการแยกด้วยแบบจำลองทาง  
คณิตศาสตร์ . (THE APPLICATION OF HOLLOW FIBER SUPPORTED LIQUID  
MEMBRANE TO SEPARATE LEAD, 264 หน้า.

งานวิจัยนี้ศึกษาการแยกไอออนตะกั่ว ปรอท และสารหนู ออกจากสารละลายป้อนคือน้ำที่  
จากหลุมขุดเจาะแก๊สธรรมชาติและน้ำสังเคราะห์ผ่านระบบเยื่อแผ่นเหลวที่พุงด้วยเส้นใยกลวง ปัจจัยที่  
ศึกษา ได้แก่ ชนิดของสารสกัด (D2EHPA, TOA, Aliquat 336, Bromo-PADAP, Cyanex 471 และ  
Cyanex 923) ความเข้มข้นของสารสกัด ชนิดของสารละลายนำกลับ (น้ำกลั่น, HNO<sub>3</sub>, H<sub>2</sub>SO<sub>4</sub>, HCl,  
NaOH และไทโอยูเรีย) ความเข้มข้นของสารละลายนำกลับ ความเข้มข้นของ H<sub>2</sub>SO<sub>4</sub> ในสารละลายป้อน  
รูปแบบการไหลของสารละลายป้อนและสารละลายนำกลับ ชนิดของสารประกอบเชิงซ้อนของตะกั่วใน  
สารละลายป้อน ชนิดสารสกัดและสารละลายนำกลับในแต่ละมอดูลเส้นใยกลวงที่ต่อกันแบบอนุกรม  
ระยะเวลาปฏิบัติการ และอัตราการไหลของสารละลายป้อนและสารละลายนำกลับ สำหรับการแยก  
ไอออนปรอทและสารหนูออกจากน้ำที่จากหลุมขุดเจาะแก๊สธรรมชาติ พบว่าสามารถแยกปรอทได้ดีกว่า  
สารหนู การสกัดสารหนูเป็นแบบเสริมฤทธิ์โดยใช้สารสกัดผสมระหว่าง Aliquat 336 และ Cyanex 471  
สัมประสิทธิ์การสกัดแบบเสริมฤทธิ์มีค่า 2.8 สารละลายนำกลับที่ดีที่สุดคือไทโอยูเรีย 0.1 โมลต่อลิตร  
ความเข้มข้นของปรอทและสารหนูหลังการแยกมีค่าไม่เกินมาตรฐานน้ำทิ้ง โดยใช้สารสกัดผสม Aliquat  
336 และ Cyanex 471 0.22 และ 0.06 โมลต่อลิตร ความเข้มข้นของ H<sub>2</sub>SO<sub>4</sub> ในสารละลายป้อน 0.2  
โมลต่อลิตร และจำนวนรอบในการแยก 1 และ 3 รอบตามลำดับ สำหรับการแยกไอออนตะกั่วและ  
ปรอทออกจากน้ำสังเคราะห์ พบว่าการใช้มอดูลเส้นใยกลวง 2 มอดูลต่อกันแบบอนุกรม สามารถแยก  
ไอออนตะกั่วและปรอทแบบคัดเลือกจนเหลือความเข้มข้นไม่เกินมาตรฐานน้ำทิ้งในเวลา 80 นาที และ  
สามารถเพิ่มความเข้มข้นของตะกั่วและปรอทในสารละลายนำกลับได้ 2.7 และ 1.2 เท่าของความเข้มข้น  
ในสารละลายป้อนขาเข้า ภาวะที่เหมาะสมต่อการแยก คือ มอดูลที่ 1 ใช้ D2EHPA 0.03 โมลต่อลิตรเป็น  
สารสกัด และใช้ HCl 0.9 โมลต่อลิตรเป็นสารละลายนำกลับ มอดูลที่ 2 ใช้ Aliquat 336 0.06 โมลต่อ  
ลิตรเป็นสารสกัด และใช้ไทโอยูเรีย 0.9 โมลต่อลิตรเป็นสารละลายนำกลับ อัตราการไหลของสารละลาย  
ป้อนและสารละลายนำกลับเท่ากับ 100 มิลลิลิตรต่อนาที โดยให้สารละลายป้อนไหลผ่านมอดูลเส้นใย  
กลวงครั้งเดียว ส่วนสารละลายนำกลับให้ไหลวน นอกจากนี้ได้พัฒนาแบบจำลองทางคณิตศาสตร์สำหรับ  
ทำนายผลการแยกไอออนตะกั่วและปรอทโดยอาศัยสมการดุลมวลสาร ซึ่งพิจารณาเทอมของการพาและ  
การผสมของไอออนตะกั่วและปรอท รวมทั้งปฏิกิริยาที่ผิวสัมผัสของเยื่อแผ่นเหลว พบว่าผลการทำนาย  
ความเข้มข้นของไอออนตะกั่วและปรอททั้งในสารละลายป้อนและสารละลายนำกลับสอดคล้องกับค่าที่  
ได้จากการทดลอง แสดงให้เห็นว่าอัตราการถ่ายเทมวลของไอออนตะกั่วและปรอทจากสารละลายป้อน  
ไปยังสารละลายนำกลับขึ้นกับการพาและการผสมของไอออนตะกั่วและปรอท และปฏิกิริยาที่ผิวสัมผัส  
ของเยื่อแผ่นเหลว

ภาควิชา วิศวกรรมเคมี

ลายมือชื่อนิสิต .....

สาขาวิชา วิศวกรรมเคมี

ลายมือชื่อ อ.ที่ปรึกษาวิทยานิพนธ์หลัก .....

ปีการศึกษา 2556

# # 5170658021 : MAJOR CHEMICAL ENGINEERING

KEYWORDS: SEPARATION / LEAD / MERCURY / ARSENIC / HFSLM / MATHEMATICAL MODEL

SIRA SUREN: THE APPLICATION OF HOLLOW FIBER SUPPORTED LIQUID MEMBRANE TO SEPARATE LEAD, MERCURY AND ARSENIC IONS FROM SYNTHETIC WATER AND MATHEMATICAL MODEL FOR PREDICTION. ADVISOR: DISTINGUISHED PROFESSOR DR.URA PANCHAROEN, 264 pp.

This study investigated the separation of lead, mercury and arsenic ions from feed solution, i.e., produced water and synthetic water across hollow fiber supported liquid membrane (HFSLM). The influences of types of extractants (D2EHPA, TOA, Aliquat 336, Bromo-PADAP, Cyanex 471 and Cyanex 923), concentration of the extractants, types of stripping solutions (distilled water, HNO<sub>3</sub>, H<sub>2</sub>SO<sub>4</sub>, HCl, NaOH and thiourea), concentration of the stripping solutions, concentration of H<sub>2</sub>SO<sub>4</sub> in feed solution, flow patterns of feed and stripping solutions, types of lead complexes in the feed solution, types of extractants and stripping solutions in the HFSLM series, operating time, and flow rates of feed and stripping solutions were investigated. For the separation of mercury and arsenic ions from produced water, the superior performance in the extraction of mercury compared with arsenic was observed. Remarkably, the synergistic extraction of arsenic was discovered by using the mixture of Aliquat 336 and Cyanex 471 at the synergistic coefficient of 2.8. Thiourea of 0.1 M was found to be the suitable stripping solution. The concentrations of discharged mercury and arsenic ions complied with the regulatory discharge standards by using the mixture of 0.22 M Aliquat 336 and 0.06 M Cyanex 471 with 0.2 M H<sub>2</sub>SO<sub>4</sub> in feed solution at 1 and 3 cycle separations, respectively. In the case of the separation of Pb(II) and Hg(II) from synthetic water, it was found that by using a double-module HFSLM in series could extract lead and mercury ions below their regulatory discharge standards in 80 min. The concentrations of lead and mercury ions in the stripping solutions were higher than those in the inlet feed solution of about 2.7 and 1.2 times. The optimum conditions were achieved by using 0.03 M D2EHPA as the extractant and 0.9 M HCl as the stripping solution in the first module, and 0.06 M Aliquat 336 as the extractant and 0.1 M thiourea as the stripping solution in the second module. A single-pass flow pattern of feed solution and circulating flow pattern of the stripping solution of 100 mL/min were found to be the most suitable. In addition, a mathematical model to predict the separation of lead and mercury ions was developed by considering the material balance concept in terms of convection and accumulation of metal ions, and the reactions at the liquid-membrane interfaces. Consequently, the concentrations of lead and mercury ions in feed and stripping solutions predicted by the model agreed well with the experimental results. It indicated that the rates of lead and mercury ions transport from feed solution to the stripping solution corresponded to the convection and accumulation of lead and mercury ions and the reactions at the liquid-membrane interfaces.

Department: Chemical Engineering

Student's Signature .....

Field of Study: Chemical Engineering

Advisor's Signature .....

Academic Year: 2013

## ACKNOWLEDGEMENTS

I would like to extend my grateful thanks to my advisor, Distinguished Professor Dr. Ura Pancharoen, for his consistent kindness and support. He spent his time many years to advice me since I was his master student. I might never complete my doctoral dissertation without his encouragement. My deep appreciation also goes to the thesis committee, Professor Dr. Paisan Kittisupakorn, Assistant Professor Dr. Varong Pavarajarn, Assistant Professor Dr. Soorathep Kheawhom and Associate Professor Dr. Anchaleeporn Waritswat Lothongkum for many useful comments and suggestions, especially Associate Professor Dr. Anchaleeporn Waritswat Lothongkum who helped with proof reading and made corrections. Their comments and suggestions made this dissertation more valuable.

I also acknowledge the financial support from the Thailand Research Fund and Chulalongkorn University under the Royal Golden Jubilee Ph.D. Program as well as TRF Master Research Grant, the National Research University Project of CHE: Ratchadaphiseksomphot Endowment Fund (FW012A), the Asahi Glass Foundation, and Dutsadi Phiphat. Sincere thanks also go to the PTTEP Public Co., Ltd. for supplying produced water, and Cytec Canada Inc. for Cyanex 471. In addition, I would like to express my deep gratitude to Professor Dr. Milan Hronec for allowing me to do the research at his laboratory in Bratislava, Slovakia, giving me valuable suggestions and taking care of me during my stay in Slovakia. I am eternally grateful to my family for their blessings, encouragement, support and unconditional understanding at all times. I am also deeply grateful to my friends in the research group, the Separation Laboratory at the Department of Chemical Engineering, Chulalongkorn University, Bangkok, Thailand, and my friends at the Department of Organic Technology, Slovak University of Technology in Bratislava, Slovakia for their help. Many thanks are extended to Mr. Alan Wilcox, M.Ed. for reading of the research manuscripts and my dissertation.

## CONTENTS

	Page
THAI ABSTRACT .....	iv
ENGLISH ABSTRACT .....	v
ACKNOWLEDGEMENTS .....	vi
CONTENTS .....	vii
LIST OF TABLES .....	xiv
LIST OF FIGURES .....	xvi
CHAPTER I INTRODUCTION .....	1
1.1 Rationale of research problem .....	1
1.2 Lead, mercury and arsenic .....	4
1.2.1 Lead .....	4
1.2.1.1 Physical and chemical properties of lead .....	4
1.2.1.2 Applications of lead .....	5
1.2.1.3 Toxicity of lead .....	5
1.2.2 Mercury .....	6
1.2.2.1 Physical and chemical properties of mercury .....	6
1.2.2.2 Applications of mercury .....	7
1.2.2.3 Toxicity of mercury .....	7
1.2.3 Arsenic .....	8
1.2.3.1 Physical and chemical properties of arsenic .....	8
1.2.3.2 Applications of arsenic .....	9
1.2.3.3 Toxicity of arsenic .....	9
1.3 Extractants .....	10
1.4 Synergistic extraction .....	14
1.5 Stripping solutions .....	16
1.6 Patterns of HFSLM operations for metal ions separation .....	18
1.7 Mathematical modeling for separation of metal ions via HFSLM .....	22
1.8 Objectives of the dissertation .....	23

	Page
1.9 Scopes of the dissertation .....	24
1.10 Expected results .....	25
CHAPTER II SIMULTANEOUS REMOVAL OF ARSENIC AND MERCURY FROM NATURAL- GAS-CO-PRODUCED WATER FROM THE GULF OF THAILAND USING SYNERGISTIC EXTRACTANT VIA HFSLM .....	31
2.1 Abstract.....	32
2.2 Introduction .....	33
2.3 Theory .....	36
2.4 Experimental.....	42
2.4.1 Reagents and materials .....	42
2.4.2 Apparatus .....	43
2.4.3 Procedures .....	44
2.5 Results and discussion.....	46
2.5.1 The effects of extractants on the extraction of arsenic and mercury by solvent extraction.....	46
2.5.2 The effect of synergistic extractant concentration.....	48
2.5.3 The effect of H <sub>2</sub> SO <sub>4</sub> concentration in feed solution .....	49
2.5.4 The effects of stripping solutions.....	52
2.5.5 The effect of the number of separation cycles through the hollow fiber module .....	54
2.5.6 Distribution coefficients and extraction equilibrium constants.....	56
2.5.7 Permeability and mass transfer coefficients .....	58
2.6. Conclusion.....	61
2.7 Acknowledgements .....	61
2.8 References.....	62
CHAPTER III UPHILL TRANSPORT AND MATHEMATICAL MODEL OF Pb(II) FROM DILUTE SYNTHETIC LEAD-CONTAINING SOLUTIONS ACROSS HOLLOW FIBER SUPPORTED LIQUID MEMBRANE .....	68
3.1 Abstract.....	69



	Page
3.2 Nomenclature.....	70
3.3 Introduction .....	72
3.4 Theoretical background.....	76
3.4.1 Mathematical model for Pb(II) uphill transport through the hollow fiber system.....	76
3.4.2 The mass transfer coefficients .....	80
3.5 Experimental.....	83
3.5.1 Reagents .....	83
3.5.2 Apparatus .....	84
3.5.3 Procedures .....	85
3.6 Results and discussion.....	86
3.6.1 Effect of extractant concentration .....	86
3.6.2 Effects of stripping solutions .....	87
3.6.3 Effect of stripping solution concentration .....	88
3.6.4 Effects of flow patterns of feed and stripping solutions .....	89
3.6.5 Effects of lead species.....	92
3.6.6 Effects of flow rates of feed and stripping solutions .....	93
3.6.7 Reaction order and reaction rate constant .....	93
3.6.8 Prediction of Pb(II) concentration by mathematical model .....	95
3.7 Conclusion.....	97
3.8 Acknowledgements .....	98
3.9 References.....	98
CHAPTER IV SIMULTANEOUS EXTRACTION AND STRIPPING OF LEAD IONS VIA A HOLLOW FIBER SUPPORTED LIQUID MEMBRANE.....	106
4.1 Abstract.....	107
4.2 Introduction .....	107
4.3 Modeling of lead ion transport.....	111
4.3.1 Mechanism of lead ion transport across the liquid membrane phase ...	111

	Page
4.3.2 Developing the mathematical model .....	114
4.4 Experimental.....	119
4.4.1 Reagents and solutions .....	119
4.4.2 Apparatus .....	120
4.4.3 Procedures .....	121
4.5 Results and discussion.....	123
4.5.1 Influence of extractant concentration .....	123
4.5.2 Influences of stripping solutions.....	124
4.5.3 Influences of types of lead-containing solutions.....	125
4.5.4 Influences of flow rates of feed and stripping solutions.....	126
4.5.5 Reaction order and reaction rate constant .....	127
4.5.6 Validation of the model with experimental results .....	130
4.6 Conclusion.....	132
4.7 Acknowledgements .....	132
4.8 Appendix A. Solving mathematics for the model of lead ions transport via HFSLM.....	133
4.9 References.....	142
CHAPTER V A GENERATING FUNCTION APPLIED ON A REACTION MODEL FOR THE SELECTIVE SEPARATION OF Pb(II) AND Hg(II) VIA HFSLM .....	145
5.1 Abstract.....	146
5.2 Introduction .....	147
5.3 Modeling of lead and mercury ions transport.....	150
5.3.1 Transport mechanisms of lead and mercury ions across the liquid membrane phase .....	150
5.3.2 Developing the mathematical model .....	154
5.4 Experimental.....	158
5.4.1 Reagents and solutions .....	158
5.4.2 Apparatus .....	159

	Page
5.4.3 Procedures .....	161
5.5 Results and discussion.....	162
5.5.1 Influences of extractants.....	162
5.5.2 Influence of D2EHPA concentration on the selective extraction of lead ions .....	163
5.5.3 Influence of Aliquat 336 concentration on the selective extraction of mercury ions.....	164
5.5.4 Influences of setting modules .....	166
5.5.5 Influence of operating time.....	168
5.5.6 Parameters used in the model.....	170
5.5.7 Validation of the model with the experimental results.....	174
5.5.8 Comparison of the models.....	174
5.6 Conclusion.....	175
5.7 Acknowledgements .....	176
5.8 Appendix A. The developed-model mathematics and assumptions for metal-ion transport through HFSLM.....	176
5.9 References.....	184
CHAPTER VI MEASUREMENT ON THE SOLUBILITY OF ADIPIC ACID IN VARIOUS SOLVENTS AT HIGH TEMPERATURE AND ITS THERMODYNAMICS PARAMETERS .....	191
6.1 Abstract.....	192
6.2 Introduction .....	192
6.3 Experimental.....	194
6.3.1 Materials .....	194
6.3.2 Apparatus and procedures .....	195
6.3.3 Analyses.....	197
6.4 Results and discussion.....	198
6.4.1 Verification of the experimental method.....	198
6.4.2 Solubility of adipic acid in various solvents.....	200

	Page
6.4.3 Modeling of solubility data.....	201
6.4.4 Molar enthalpy and molar entropy of dissolutions .....	204
6.5 Conclusion.....	208
6.6 List of symbols .....	209
6.7 Acknowledgements .....	210
6.8 References.....	210
CHAPTER VII SOLUBILITY MEASUREMENT AND CORRELATION OF 4-ALKYL BENZOIC ACIDS IN AQUEOUS SOLUTIONS .....	214
7.1 Abstract.....	215
7.2 Introduction .....	216
7.3 Experimental.....	218
7.3.1 Chemicals .....	218
7.3.2 Apparatus and procedures .....	220
7.2.3 Analyses.....	221
7.4 Results and discussion.....	221
7.4.1 Solubilities of 4-alkyl benzoic acids.....	221
7.4.2 Modeling of solubility data.....	225
7.4.2.1 Empirical formula .....	225
7.4.2.2 $\lambda H$ equation .....	228
7.4.2.3 Modified Apelblat equation .....	231
7.4.2.4 Comparison of the models.....	235
7.4.3 Molar enthalpy and molar entropy of dissolutions .....	236
7.5 Conclusion.....	243
7.6 Nomenclature.....	243
7.7 Acknowledgements .....	245
7.8 References.....	245
CHAPTER VIII CONCLUSION .....	251

	Page
8.1 Conclusion.....	251
8.2 Recommendations for future studies.....	256
REFERENCES.....	257
VITA.....	264



จุฬาลงกรณ์มหาวิทยาลัย  
**CHULALONGKORN UNIVERSITY**

## LIST OF TABLES

TABLE	PAGE
Table 2. 1 Compositions of co-produced water (pH $\approx$ 6). .....	43
Table 2. 2 Properties of the hollow fiber module. ....	43
Table 2. 3 The reviewed methods for arsenic and mercury ions removal. ....	55
Table 2. 4 The distribution coefficients of arsenic and mercury at Cyanex 471 concentration from 0.02 to 0.07 M mixed with 0.22 M Aliquat 336 (0.5 M NaOH as the stripping solution). ....	57
Table 2. 5 The permeability coefficients of arsenic and mercury at TIBPS concentration from 0.02 to 0.07 M mixed with 0.22 M Aliquat 336 and 0.5 M NaOH as the stripping solution. ....	59
Table 3. 1 Examples of lead ions removal methods. ....	74
Table 3. 2 Literature reviews on metal ions removal by HFSLM. ....	75
Table 3. 3 Characteristics of the hollow fiber module. ....	83
Table 3. 4 Reaction order ( $n$ ) and reaction rate constant ( $k_f$ ). ....	94
Table 3. 5 Influences of equal flow rates of feed and stripping solutions on mass transfer coefficients. ....	97
Table 4. 1 Literature reviews on mathematical model for HFSLM. ....	110
Table 4. 2 Attributes of the hollow fiber module. ....	120
Table 4. 3 Reaction orders ( $m/n$ ) and reaction rate constants of Pb(II) extraction and stripping ( $k_{EX}$ and $k_{ST}$ ). ....	128
Table 5. 1 Attributes of the hollow fiber module. ....	159
Table 5. 2 Reaction orders ( $m/n$ ) versus reaction rate constants of Pb(II) and Hg(II) extraction and stripping ( $k_{EX}$ and $k_{ST}$ ). ....	170
Table 5. 3 Values of relevant parameters used in the model. ....	171
Table 6. 1 Source and mass fraction purity of chemicals. ....	195
Table 6. 2 Mole fraction of adipic acid solubility ( $x_i$ ) in solvents at different temperature (T). <sup>a</sup> .....	200
Table 6. 3 Parameters ( $A$ , $B$ and $C$ ) in the modified Apelblat equation model obtained by curve fitting the experimental solubility data and	

validity of the model for prediction of the adipic acid solubility in various solvents. <sup>a</sup> .....	202
Table 6. 4 Molar enthalpy of dissolution ( $\Delta_{sol}H$ ) of adipic acid in various solvents. <sup>a</sup> .....	206
Table 6. 5 Molar entropy of dissolution ( $\Delta_{sol}S$ ) of adipic acid in various solvents. <sup>a</sup> .....	207
Table 7. 1 Source and purity of the chemicals used.....	218
Table 7. 2 Mole fraction solubility ( $x_i$ ) of 4-alkyl benzoic acids.....	223
Table 7. 3 Parameters used in the $\lambda H$ equation model for 4-iso-propylbenzoic, 4-methylbenzoic and 4- <i>tert</i> -butylbenzoic acids in various solvents.....	229
Table 7. 4 Parameters ( $A$ , $B$ and $C$ ) in the modified Apelblat equation model obtained by fitting the experimental solubility data.....	232
Table 7. 5 Comparison of the validity of the $\lambda H$ equation and the modified Apelblat equation models for the prediction of the solubility of 4-iso-propylbenzoic, 4-methylbenzoic and 4- <i>tert</i> -butylbenzoic acids in various solvents. ....	236
Table 7. 6 Molar enthalpy and molar entropy of dissolutions ( $\Delta_{sol}H$ and $\Delta_{sol}S$ ) of 4-alkyl benzoic acids in various solvents.....	239

## LIST OF FIGURES

FIGURE	PAGE
Figure 1. 1 Schematic diagram of batch operation HFSLM.....	19
Figure 1. 2 Schematic diagrams of continuous operation HFSLM: (a) connecting the HFSLM modules in series, (b) connecting the HFSLM modules in parallel.....	20
Figure 1. 3 Schematic diagrams of semi-batch operation HFSLM: (a) connecting the HFSLM modules in series, (b) connecting the HFSLM modules in parallel.....	21
Figure 2. 1 Schematic mechanisms of the extraction and stripping of $H_2AsO_4^-$ , $H_3AsO_3$ , $H_3AsO_4$ and $HgCl_4^{2-}$ by a mixture of Aliquat 336 and TIBPS (Cyanex 471) with thiourea as the stripping solution. ....	38
Figure 2. 2 Schematic counter-current flow diagram for one-through-mode separation by hollow fiber supported liquid membrane: (1) inlet feed reservoir, (2) gear pumps, (3) inlet pressure gauges, (4) outlet pressure gauges, (5) flow meters, (6) outlet stripping reservoir, (7) hollow fiber module, (8) inlet stripping reservoir, (9) outlet feed reservoir [13].....	45
Figure 2. 3 The maximum percentages of metal ions extraction from co-produced water against types of the extractants by solvent extraction: (a) 0.22 M Aliquat 336, (b) 0.002 M Bromo-PADAP, (c) 0.06 M Cyanex 471, (d) 0.51 M Cyanex 923, (e) 0.22M Aliquat 336-0.06 M Cyanex 471.....	47
Figure 2. 4 The distribution coefficients of As(V) against types of the extractants. ....	48
Figure 2. 5 Percentages of metal ions extraction and recovery against the concentrations of the extractants via HFSLM by using 0.5 M NaOH as the stripping solution without the co-extractant: (a) Aliquat 336	



mixed with 0.06 M Cyanex 471, (b) Cyanex 471 mixed with 0.22 M Aliquat 336. ....	50
Figure 2. 6 Percentages of metal ions extraction and recovery against H <sub>2</sub> SO <sub>4</sub> concentration in feed solution as the co-extractant via HFSLM by using the mixture of 0.22 M Aliquat 336 and 0.06 M Cyanex 471 as the extractant and 0.5 M NaOH as the stripping solution. ....	51
Figure 2. 7 Percentage of metal ions recovery against types of stripping solutions via HFSLM by using the mixture of 0.22 M Aliquat 336 and 0.06 M Cyanex 471 as the extractant with 0.2 M H <sub>2</sub> SO <sub>4</sub> as the co-extractant. ....	52
Figure 2. 8 Percentage of metal ions recovery against the concentration of thiourea via 1-cycle HFSLM separation by using the mixture of 0.22 M Aliquat 336 and 0.06 M Cyanex 471 as the extractant and thiourea as the stripping solution with 0.2 M H <sub>2</sub> SO <sub>4</sub> as the co-extractant. ....	53
Figure 2. 9 Percentages of metal ions extraction and recovery against the number of separation cycles through HFSLM by using the mixture of 0.22 M Aliquat 336 and 0.06 M Cyanex 471 as the extractant and 0.1 M thiourea as the stripping solution with 0.2 M H <sub>2</sub> SO <sub>4</sub> as the co-extractant. ....	56
Figure 2. 10 The equilibrium constants: (a) plot of $[(CH_3R_3N^+)_2(H_2AsO_4^-)(TIBPS)_{4/5}]$ and $[H_2AsO_4^-][CH_3R_3N^+][TIBPS]^{4/5}$ at equilibrium for As(V), (b) plot of $[(CH_3R_3N^+)_2(HgCl_4^{2-})(TIBPS)]$ and $[HgCl_4^{2-}][CH_3R_3N^+]^2[TIBPS]$ at equilibrium for Hg(II). ....	60
Figure 3. 1 Schematic mechanisms of the extraction and stripping of Pb(II) by using D2EHPA as the extractant and HCl as the stripping solution. ....	77
Figure 3. 2 Schematic diagram of separation via HFSLM by counter-current continuous flow of feed and stripping solutions: (1) gear pumps, (2) flow meters, (3) inlet pressure gauges, (4) outlet pressure gauges, (5) hollow fiber module. ....	84

Figure 3. 3 Pb(II) concentration in feed and stripping solutions against concentration of D2EHPA at continuous feed and stripping solutions of 100 mL/min (1 mg/L Pb(NO <sub>3</sub> ) <sub>2</sub> and 0.5 M HNO <sub>3</sub> ). .....	86
Figure 3. 4 Pb(II) concentration in stripping solution against types of stripping solutions at continuous feed and stripping solutions of 100 mL/min (1 mg/L Pb(NO <sub>3</sub> ) <sub>2</sub> and 0.03 M D2EHPA). .....	88
Figure 3. 5 Pb(II) concentration in stripping solution against HCl concentration at continuous feed and stripping solutions of 100 mL/min (1 mg/L Pb(NO <sub>3</sub> ) <sub>2</sub> and 0.03 M D2EHPA). .....	89
Figure 3. 6 Pb(II) concentration of different flow patterns of feed and stripping solutions at equal flow rates of 100 mL/min against time (1 mg/L Pb(NO <sub>3</sub> ) <sub>2</sub> , 0.03 M D2EHPA, 0.9 M HCl). .....	91
Figure 3. 7 Pb(II) concentration in outlet Pb(NO <sub>3</sub> ) <sub>2</sub> and PbCl <sub>2</sub> feed solutions and stripping solution against time of continuous feed solution and circulating stripping solution at equal flow rates of 100 mL/min (0.03 M D2EHPA, 0.9 M HCl, blank symbol: outlet feed solution, bold symbol: outlet stripping solution).....	92
Figure 3. 8 Pb(II) concentration in outlet feed and stripping solutions against flow rates of feed and stripping solutions of continuous feed solution and circulating stripping solution (0.03 M D2EHPA, 0.9 M HCl, blank symbol: outlet feed solution, bold symbol: outlet stripping solution).....	94
Figure 3. 9 Outlet Pb(II) concentration in Pb(NO <sub>3</sub> ) <sub>2</sub> and PbCl <sub>2</sub> solutions of continuous feed solution and circulating stripping solution against equal flow rates of feed and stripping solutions (0.03 M D2EHPA, 0.9 M HCl). .....	96
Figure 4. 1 Schematic mechanism of Pb(II) transport across the liquid membrane phase using D2EHPA as the extractant.....	112
Figure 4. 2 Schematic transport mechanism of lead ions through the small segments: (a) feed phase (tube side), (b) stripping phase (shell side).....	116

Figure 4. 3 Schematic diagram of separated lead ions through HFSLM by continuous counter-current flow patterns of feed and stripping solutions: (1) gear pump, (2) flow meters, (3) inlet pressure gauges, (4) outlet pressure gauges, (5) hollow fiber module. ....	121
Figure 4. 4 Influences of D2EHPA concentration on Pb(II) extraction and stripping at flow rates of feed and stripping solutions of $1.7 \times 10^{-6}$ m <sup>3</sup> /s with 1 mg/L PbCl <sub>2</sub> as the feed solution and 0.5 M HNO <sub>3</sub> as the stripping solution. ....	123
Figure 4. 5 Influences of types of stripping solutions on Pb(II) stripping at flow rates of feed and stripping solutions of $1.7 \times 10^{-6}$ m <sup>3</sup> /s with 1 mg/L PbCl <sub>2</sub> as the feed solution and 0.03 M D2EHPA as the extractant.....	125
Figure 4. 6 Influences of types of lead-containing solutions on the extraction and stripping of Pb(II) using flow rates of feed and stripping solutions at $1.7 \times 10^{-6}$ m <sup>3</sup> /s with 0.03 M D2EHPA as the extractant and 0.9 M HCl as the stripping solution. ....	126
Figure 4. 7 Influences of flow rates of feed and stripping solutions on the extraction and stripping of Pb(II) using 0.03 M D2EHPA as the extractant with 0.9 M HCl as the stripping solution and 1 mg/L PbCl <sub>2</sub> as feed solution.....	127
Figure 4. 8 Plots of integral concentrations of Pb(II) versus time: (a) extraction reaction, (b) stripping reaction.....	129
Figure 4. 9 Comparison of Pb(II) concentration in the outlet feed and stripping solutions from the model and from the experiment at various flow rates of feed and stripping solutions using 0.03 M D2EHPA as the extractant with 0.9 M HCl as stripping solution and 1 mg/L PbCl <sub>2</sub> as feed solution.....	131
Figure 5. 1 Schematic of mass transport of Pb(II) across the liquid membrane phase using HR (D2EHPA) as the extractant and HCl as the stripping solution.....	152

Figure 5. 2 Schematic of mass transport of Hg(II) across the liquid membrane phase using $(\text{CH}_3\text{R}_3\text{N}^+)\text{Cl}^-$ (Aliquat 336) as the extractant and $\text{NH}_2\text{CSNH}_2$ (thiourea) as the stripping solution.....	152
Figure 5. 3 Schematic of the transport mechanism of metal ions through small segments: (a) feed phase (tube side), (b) stripping phase (shell side).....	156
Figure 5. 4 Schematic diagram of lead and mercury ion separation via HFSLM by counter-current flow patterns of feed and stripping solutions: (1) gear pumps, (2) flow meters, (3) inlet pressure gauges, (4) outlet pressure gauges, (5) hollow fiber modules. ....	160
Figure 5. 5 Percentages of metal ions versus types of extractants (0.03 M each) by single-module hollow fiber at flow rates of feed and stripping solutions of 100 mL/min with 0.9 M HCl. ....	163
Figure 5. 6 Percentages of metal ions versus concentration of D2EHPA by single-module hollow fiber at flow rates of feed and stripping solutions of 100 mL/min with 0.9 M HCl.....	164
Figure 5. 7 Percentages of metal ions versus concentration of Aliquat 336 by single-module hollow fiber at flow rates of feed and stripping solutions of 100 mL/min with 0.1 M thiourea. ....	165
Figure 5. 8 Percentages of extraction of metal ions versus setting modules with flow rates of feed and stripping solutions of 100 mL/min: (a) 0.9 M HCl and 0.1 M thiourea as the stripping solution for the first module and the second module, respectively, (b) 0.1 M thiourea and 0.9 M HCl as the stripping solution for the first module and the second module, respectively.....	167
Figure 5. 9 Concentration of metal ions versus operating time with flow rates of feed and stripping solutions of 100 mL/min, first module (a and c) using 0.03 M D2EHPA and 0.9 M HCl as the extractant and stripping solution, second module (b and d) using 0.06 M Aliquat 336 and 0.1 M thiourea as the extractant and stripping solution: (a) and (b) for Pb(II), (c) and (d) for Hg(II).....	169

Figure 5. 10 Concentrations of Pb(II) and Hg(II) versus flow rates of feed and stripping solutions: (a) first module using 0.03 M D2EHPA and 0.9 M HCl as the extractant and stripping solution, respectively, (b) second module using 0.06 M Aliquat 336 and 0.1 M thiourea as the extractant and stripping solution, respectively.....	172
Figure 5. 11 Comparison of concentrations of Pb(II) and Hg(II) in the feed solution, obtained from experimental results and mathematical model results: (a) first module using 0.03 M D2EHPA and 0.9 M HCl as the extractant and stripping solution, respectively, (b) second module using 0.06 M Aliquat 336 and 0.1 M thiourea as the extractant and stripping solution, respectively.....	173
Figure 6. 1 The experimental apparatus: (1) temperature control, (2) Teflon <sup>®</sup> container holder, (3) silicone oil bath, (4) stainless steel reactor, (5) Teflon <sup>®</sup> container, (6) Teflon <sup>®</sup> container hole, (7) magnetic bar, (8) stirrer controller.....	196
Figure 6. 2 Comparison of the literature and experimental mole fraction of adipic acid solubility ( $x_i$ ) against temperature: (a) in acetic acid and water, (b) in cyclohexanol and cyclohexnone.....	199
Figure 6. 3 Mole fraction of adipic acid solubility ( $x_i$ ) in various solvents against temperature obtained from experimental results and from the modified Apelblat equation model. ....	203
Figure 7. 1 Experimental apparatus: (1) temperature control, (2) container handle (3) silicone oil bath, (4) stainless steel vessel, (5) Teflon <sup>®</sup> container, (6) Teflon <sup>®</sup> container hole, (7) magnetic bar, (8) stirrer controller. ....	219
Figure 7. 2 Comparison of mole fraction solubility ( $x_i$ ) of 4-methylbenzoic acid in water. ....	222
Figure 7. 3 Mole fraction solubilities ( $x_i$ ) of acids in various solvents against temperature and their empirical formula correlation: (a) mole fraction solubility of 4-iso-propylbenzoic acid, (b) mole fraction	

solubility of 4-methylbenzoic acid, (c) mole fraction solubility of 4-  
tert-butylbenzoic acid..... 227

Figure 7. 4 Mole fraction solubilities ( $x_i$ ) of acids in various solvents against  
temperature obtained from experimental results and from the  
 $\lambda H$  equation model: (a) mole fraction solubility of 4-iso-  
propylbenzoic acid, (b) mole fraction solubility of 4-methylbenzoic  
acid, (c) mole fraction solubility of 4-*tert*-butylbenzoic acid. .... 231

Figure 7. 5 Mole fraction solubilities ( $x_i$ ) of acids in various solvents against  
temperature obtained from experimental results and from the  
modified Apelblat equation model: (a) mole fraction solubility of  
4-iso-propylbenzoic acid, (b) mole fraction solubility of 4-  
methylbenzoic acid, (c) mole fraction solubility of 4-*tert*-  
butylbenzoic acid..... 234

## CHAPTER I

### INTRODUCTION

#### 1.1 Rationale of research problem

Produced water from offshore oil and gas production, which is re-injected to rock formations from where oil and gas originated, is however contaminated with toxic metals such as lead, mercury and arsenic. Toxicities of lead, mercury and arsenic can cause acute and chronic poisoning in human beings depending on the exposure limit<sup>(1-4)</sup>. The amounts of these toxic metals exposed to the environment continuously intensify with the quantity of produced water. The concentrations of lead, mercury and arsenic in the produced water from various wells are different. In the Gulf of Thailand, the concentrations of lead and mercury in the produced water are 0.003 – 2 mg/L (or parts per million, ppm) and the concentration of arsenic is 1 – 4 mg/L. The regulated discharge limits of lead, mercury and arsenic from industrial wastewater by Thailand Ministry of Industry<sup>(5)</sup> and the Ministry of Natural Resources and Environment<sup>(6)</sup> must not be higher than 0.2, 0.005 and 0.25 mg/L, respectively. For this reason, Chevron Thailand developed a new technology to assure that the capability of their produced water treatment process meets the overboard discharge water quality specifications. The aforementioned patented technology associated with the treatment of the produced water contaminated with mercury and arsenic<sup>(7)</sup> is concluded as follows:

In the beginning, gas and condensate in the produced water are separated at a three-phase separator. The produced water from the separator is passed through de-sanding, de-oiling hydrocyclones and finally fed to the chemical treatment process which consists of a degasser, a retention tank and an induced gas flotation (IGF) unit. An oxidant (NaOCl), ferric ions (ferric chloride) and a flocculant (cationic polymer) are added in the degasser, the retention tank and the upstream of the IGF unit, respectively. A floatable sludge of ferric hydroxide, chemisorbed mercury, ferri-arsenate and hydrocarbons are formed. Arsenous acid in the produced water is oxidized to arsenic acid by adding the oxidant, while mercury is maintained in the elemental form. Due to too high amounts of mercury element and arsenic ions in produced water from the Gulf of Thailand fields for the oxidant –  $\text{Fe}^{3+}$  – flocculent process to meet high quality water complying with the regulatory discharged limits, the new patented technology has been developed. This technology consists of desanding hydro-cyclones to remove elemental Hg, HgS and sand particles. Then, the desanded water is treated with oxidant, ferric ions, a thiol, and the flocculant. The new thiol addition is effective in precipitating excess elemental Hg,  $\text{Hg}^{2+}$  and As that cannot be removed by the oxidant –  $\text{Fe}^{3+}$  – flocculent process. The Fe-As-Hg sludge is subsequently re-injected back into rock formations.

However, the injection of produced water or Fe-As-Hg sludge back into rock formations is still risk as the toxic metals may spill into the environment, and therefore an alternative method is required. Several studies have shown that hollow fiber supported liquid membrane (HFSLM) is an effective method for the separation of metal ions from aqueous solutions, particularly at a very low concentration in ppm or ppb level<sup>(8-14)</sup>. This method allows simultaneous extraction and stripping of



target ions in a single-step operation with high selectivity<sup>(15,16)</sup>. Other advantages of the HFSLM over traditional methods (e.g., chemical precipitation, coagulation, adsorption and ion exchange) include less extractant and solvent, low energy consumption, and low capital and operating costs<sup>(17)</sup>. The HFSLM has high surface area that contributes to high mass transfer rate for separation<sup>(18)</sup>, and can be applied in many fields such as industrial water treatment, pharmaceutical<sup>(19,20)</sup>, and food processings<sup>(21)</sup>. Hollow fiber modules can be connected in series or in parallel for a higher capacity<sup>(22)</sup>. Therefore, it is suitable to use as a secondary treatment after the any other traditional methods to eliminate a very low concentration of metal ions from aqueous solution. The outstanding advantages of the HFSLM draw a considerable interest of many researchers in applying the HFSLM to treat a large volume of wastewater contaminated with a very low concentration of toxic metal<sup>(23)</sup>. In applying the HFSLM to industrial application, reliable mathematical models are required since they help provide a necessary guideline to understand the transport mechanism of the target ions through liquid membrane as well as to predict the separation time and efficiency. In addition, the model is an important tool for cost estimation and scaling up consideration<sup>(24)</sup>.

The constraint of the injection of toxic metal-contaminated produced water and sludge back into rock formations, and the advantages of the HFSLM lead to the objectives of this work. The HFSLM was used to separate lead, mercury and arsenic ions from produced water and synthetic water. The effects of types of extractants (D2EHPA, TOA, Aliquat 336, Bromo-PADAP, Cyanex 471 and Cyanex 923), concentration of the extractants, types of stripping solutions (distilled water, HNO<sub>3</sub>, H<sub>2</sub>SO<sub>4</sub>, HCl, NaOH and thiourea), concentration of the stripping solutions,

concentration of  $\text{H}_2\text{SO}_4$  in feed solution, flow patterns of feed and stripping solutions, types of lead complexes in the feed solution, types of extractants and stripping solutions in the HFSLM series, operating time, and flow rates of feed and stripping solutions were investigated. The mathematical model to predict the extraction and stripping of lead and mercury ions by considering the convection and accumulation of metal ions in the feed and stripping solutions, and the reactions at liquid-membrane interfaces was developed. The mathematical model was solved by using two different methods, i.e., Laplace Transform and Generating Function. The reliability of the model was verified by the experimental results in terms of the average percent deviation.

## **1.2 Lead, mercury and arsenic**

### **1.2.1 Lead**

Lead (Pb), a heavy metallic element, with atomic number of 82 and atomic weight of 207.19 g/mole is found plentiful in the earth's crust. Major natural sources of lead are in igneous and metamorphic rocks<sup>(25)</sup>.

#### **1.2.1.1 Physical and chemical properties of lead**

At room temperature, lead is a bluish-white or silvery-grey<sup>(26)</sup>. Metallic lead is of high density and low strength. The melting point of lead is 327.5 °C and boiling point is 1,740 °C. It is soft and malleable. Lead dissolves very

slowly in hydrochloric acid but rapidly in nitric acid. The solubility of lead in pure water is low,  $3.11 \times 10^{-4}$  g/L. Lead does not dissolve in sulfuric acid<sup>(2)</sup>. Lead compounds are toxic and hazardous to health. The oxidation state of inorganic lead compounds is +2 rather than +4. Lead sulfate ( $\text{PbSO}_4$ ) has low solubility in water of  $8.6 \times 10^{-4}$  g/L. Lead(II) nitrate ( $\text{Pb}(\text{NO}_3)_2$ ) is soluble in water. Its solubility is 376.5 g/L. Lead dioxide ( $\text{PbO}_2$ ) is a brown powder and is insoluble in water. It reacts with hydrochloric acid forming  $\text{PbCl}_2$  which is soluble in cold water. The solubility of  $\text{PbCl}_2$  in water at room temperature is 919 g/L<sup>(25)</sup>.  $\text{PbCl}_2$  precipitates in chloride solution but in excess chloride, as in sea water, it will re-dissolve and associate to  $\text{PbCl}_4^{2-}$ <sup>(27)</sup>.

#### 1.2.1.2 Applications of lead

Lead is used in many applications. For example, it is extensively used as an industrial raw material in alloys, the production of storage batteries, electric appliances, computer components, electrical cable covering and circuit boards, soldering, water and noise proofing. Lead is also used to make ammunition, bearing metal, radiation and sound barriers or shields, and metal pipes to prevent corrosion in the chemical industry<sup>(2,27,28)</sup>.

#### 1.2.1.3 Toxicity of lead

Contamination of lead in soil, water and air is found more often in urban areas than in rural areas. All lead compounds are toxic<sup>(2)</sup>. Lead can accumulate in the body over a period of time. Therefore, long-term exposures to lower levels

can result in a buildup of lead in the body and more severe symptoms. The toxicity of lead can cause disorder symptoms in virtually every system in the body. Symptoms include headache, abdominal pain, malaise, acute kidney disease, cancer, stroke and death. Lead poisoning in children is more severe than in adults. Lead toxicity can affect the foetus of an unborn child prematurely leading to less IQ<sup>(29)</sup> and can also lead to reproductive effects in both male and female. In the male, it limits sperm count and morphology. In the female, it causes some adverse pregnancy outcomes<sup>(25)</sup>.

### 1.2.2 Mercury

Mercury (Hg) is a heavy liquid metallic element with atomic number of 80 and atomic weight of 200.59 g/mole. Mercury can be found in metallic form or in inorganic mercury compounds. The important mercury ore is cinnabar (HgS), which can be decomposed to the elements<sup>(27)</sup>.

#### 1.2.2.1 Physical and chemical properties of mercury

Mercury is silver-white. It has low viscosity at room temperature. The melting point of mercury is  $-39\text{ }^{\circ}\text{C}$  and boiling point is  $357\text{ }^{\circ}\text{C}$ <sup>(27)</sup>. Mercury does not react with oxygen at room temperature, but at its boiling point it forms mercury(II) oxide (HgO) with oxygen<sup>(27)</sup>. Mercury strongly forms complexes with the ligands comprising nitrogen, sulfur or phosphorous as donor atoms<sup>(30)</sup>. Mercury compounds have two valences 1 and 2: mercurous compounds (mercury(I) compounds) and mercuric

compounds (mercury(II) compounds)<sup>(31)</sup>. In sea water, the dominant form of mercury is  $\text{HgCl}_4^{2-}$ . The solubility of mercury element is  $2 \times 10^{-6}$  g/L. The solubilities of mercurous chloride ( $\text{Hg}_2\text{Cl}_2$ ) and mercuric chloride ( $\text{HgCl}_2$ ) are  $2 \times 10^{-3}$  and 69 g/L, respectively. The solubility of methylmercury chloride is higher than the solubility of mercurous chloride about three times<sup>(32)</sup>.

### 1.2.2.2 Applications of mercury

Mercury and many mercury compounds are toxic and tend to accumulate in higher animals. Mercury is used in thermometers, barometers, high vacuum pumps, gas and pressure regulators, electric relays, electrodes, standard cells and other scientific equipment. Industrially, mercury is used for example in fluorescent tubular lamps, high-pressure street lamps and mercury lamps<sup>(31,33)</sup>. Compounds of mercury are also used in various applications; some are used in medicine.

### 1.2.2.3 Toxicity of mercury

Mercury poisoning damage the tissue of any organ to which it makes bone marrow produce less red blood cells. Mercury mostly accumulates in the cerebellum and cerebral cortex quickly during exposure but it is released from the brain very slowly. The liver and kidneys may also be damaged by mercury accumulation. Organic mercury compounds are the most toxic. It can attach to red blood cells and then spread to all parts of the body and can pass through the

Blood-Brain-Barrier tissue that prevents toxins from the blood stream passing into the brain tissue. Methylmercury can be absorbed in the gastrointestinal tract up to 95–98%, but very little of it can be defecated in the form of waste. Inorganic mercury compounds are the least toxic. Less than 2% of inorganic mercury compounds are absorbed into the body by the digestive tract, and it is easily expelled from the body. Metal mercury can be easily absorbed into the body through the skin and breath. Mercury in vapor form is the most dangerous to human life as it cause acute poisoning<sup>(34)</sup>.

### 1.2.3 Arsenic

Arsenic (As) is a heavy metalloid element with atomic number of 33 and atomic weight of 74.91 g/mole. Trace arsenic and arsenic compounds are usually found in the earth's crust, rock, soil and water. They can be in crystalline, powder, vitreous or amorphous forms<sup>(35)</sup>.

#### 1.2.3.1 Physical and chemical properties of arsenic

Arsenic have four valences:  $-3$ ,  $0$ ,  $+3$  and  $+5$ <sup>(35)</sup>. Arsenic in groundwater can be found as arsenic(III) compounds ( $\text{H}_3\text{AsO}_3$  and  $\text{H}_2\text{AsO}_3^-$ ) and arsenic(V) compounds ( $\text{H}_2\text{AsO}_4^-$ ,  $\text{H}_3\text{AsO}_4$ ,  $\text{HAsO}_4^{2-}$  and  $\text{AsO}_4^{3-}$ ) depending on the pH of groundwater. At the pH of most groundwater of 6.7–8.8, arsenic(III) in form of  $\text{H}_3\text{AsO}_3$  is found more than  $\text{H}_2\text{AsO}_3^-$ , and arsenic(V) in form of  $\text{H}_2\text{AsO}_4^-$  is found more than  $\text{H}_3\text{AsO}_4$ ,  $\text{HAsO}_4^{2-}$  and  $\text{AsO}_4^{3-}$  <sup>(36)</sup>.

### 1.2.3.2 Applications of arsenic

In agriculture, arsenic and its compounds are used as raw material to produce insecticides, herbicides, cotton desiccant and wood preservatives. Industrially, arsenic compounds are used in manufacturing of batteries, doping agent in semiconductors, and low-melting glasses. It can be used with other metals such as lead, copper or alloys to provide corrosion resistance<sup>(35)</sup>. Arsenic element is included in some lead-based alloys to promote hardening.

### 1.2.3.3 Toxicity of arsenic

Arsenic is very toxic. Arsenic compounds are accumulative poisons. It can spread throughout the body and eventually cause death. Acute arsenic poisoning causes irritation to exposed tissue. Symptoms may include nausea, vomit and muscle contraction. Arsenic poisoning affects functioning of the heart and can lead to heart failure. Chronic arsenic poisoning causes skin, lung and liver cancer, ulcers or a hole in the nose, dark spots on the skin, skin thickening and numbness in hands and feet. Chronic poisoning also includes symptoms like burning sensation and weakness of the arms and legs. There has been an increase of chromosomal abnormalities in workers exposed to arsenic<sup>(4,37,38)</sup>.

### 1.3 Extractants

The metal extractants for HFSLM system are grouped into 5 classes according to their functional groups (carboxyl, sulfo, phosphate, phosphate ester, phosphine oxide, phosphine sulphide and amines)<sup>(39,40)</sup>, extraction mechanism and types of metal ions extracted (cation, neutral complex and anion), i.e., acidic extractants, chelating extractants, neutral extractants (or solvating type extractants), ligand substitution extractants, and basic extractants (or ion-pair extractants)<sup>(41,42)</sup>.

#### I. Acidic extractants

Acidic extractant contains a functional group of carboxyl (RCOOH), sulfo (RSO<sub>3</sub>H) or phosphate (HOPO(OR)<sub>2</sub>) where R is alkyl group<sup>(41,42)</sup>. The acidic extractant reacts with metal cation in the feed solution. In an organic solvent or liquid membrane, the carboxyl, sulfo or phosphate groups of the acidic extractant deprotonates to an anion species RCOO<sup>-</sup>, RSO<sub>3</sub><sup>-</sup> or OPO(OR)<sub>2</sub><sup>-</sup>, respectively. The anion species subsequently form organo-metal complexes with the cation species. Acidic extractant which is widely used is D2EHPA (di-2-ethylhexylphosphoric acid, HOPO(OC<sub>8</sub>H<sub>17</sub>)<sub>2</sub>)<sup>(41)</sup>. The extraction of Pb<sup>2+</sup> by D2EHPA is shown in Eq. (1.1)<sup>(43)</sup>.

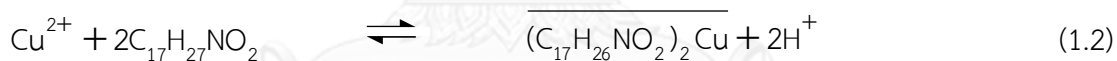


where the over bar represents the organo-metal complex in liquid membrane phase (organic phase).



## II. Chelating extractants

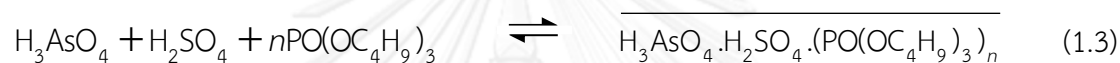
Chelating extractants are often derived from analytical reagents, such as  $\beta$ -diketones, 8-hydroxyquinoline, and hydroxyoximes<sup>(42)</sup>. They react with cation species same as the acidic extractants. The chelating extractants chemically bond to cation species at two sites in a manner similar to holding an object between the ends of the thumb and the index finger<sup>(41)</sup>. When the chelating extractant bonds to cation species, it releases hydrogen ion into the feed solution. Extractability of the chelating extractant increases with the pH of the feed solution. Decreasing of the pH promotes back-extraction or stripping. LIX 84-I or 2'-hydroxy-5'-nonylacetophenone ketoxime ( $C_{17}H_{27}NO_2$ ), which is representative of chelating extractants, is known as a good extractant for the extraction of  $Cu^{2+}$ . The extraction is shown in Eq. (1.2)<sup>(44)</sup>.



## III. Neutral extractants (Solvating type extractants)

Neutral extractant contains a functional group of phosphate ester ( $PO(OR)_3$ ), phosphine oxide ( $R_3PO$ ) or phosphine sulphide ( $R_3PS$ ). The neutral extractants are basic in nature and will coordinate to certain neutral metal complexes in the feed solution by replacing water molecules of hydration around neutral metal complexes, thereby causing the resulting organo-metal complex to become organic soluble and aqueous insoluble<sup>(41)</sup>. Examples of neutral extractants are tributyl phosphate (TBP,  $PO(OC_4H_9)_3$ ), trioctylphosphine oxide (Cyanex 921,  $(C_8H_{17})_3PO$ ) and tri-isobutylphosphine

sulfide (Cyanex 471,  $(C_4H_9)_3PS$ ). It is noted that the extractability of neutral metal complexes using the neutral extractant increases with the concentration of an acid or co-extractant in the feed solution<sup>(45,46)</sup>. The extraction of neutral metal complex  $H_3AsO_4$  by TBP and  $H_2SO_4$  as the co-extractant is shown in Eq. (1.3)<sup>(46)</sup>. Moreover, the neutral extractant can be used for the extraction of metal anions, for example  $AsO_4^{3-}$ , by adding  $H_2SO_4$  in the feed solution to transform metal anions to a neutral metal complex<sup>(45)</sup>. In case of the extraction of  $HgCl_4^{2-}$ , hydrochloric acid is used.



In general, extractions with solvating extractants are limited by:

- 1) the metal's ability to form neutral complexes with anions,
- 2) the co-extraction of acid at high acid concentrations, and
- 3) the solubility of the organo-metal complex in the organic carrier<sup>(41)</sup>.

#### IV. Ligand substitution extractants

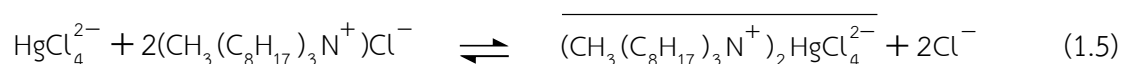
Ligand substitution extractants are similar to neutral extractants. They donate an electron pair to a metal anion ion, but ligand substitution extractants form inner shell complexes with metals and will displace other ligands. The neutral extractants coordinate to certain neutral metal complexes by replacing water molecules around neutral metal complexes. A ligand substitution extractant includes mono-oxime ( $R_2CNOH$ ) and dialkyl sulfides ( $R_2S$ ), for example, di-n-hexyl sulfide ( $(C_6H_{13})_2S$ ). Equation (1.4) shows the extraction of  $PdCl_4^{2-}$  using mono-oxime.



As shown in Eq. (1.4), two chloride ions of palladium are displaced by two molecules of mono-oxime resulting in a new complex species which is soluble in an organic extractant but insoluble in water<sup>(41)</sup>.

### V. Basic extractants (Ion-pair extractants)

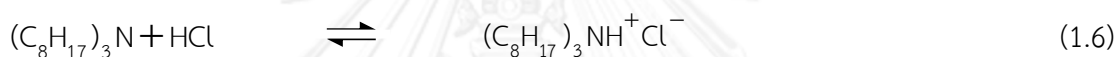
Basic extractants contain a functional group of primary amine (RNH<sub>2</sub>) or secondary amine (R<sub>2</sub>NH) or tertiary amine (R<sub>3</sub>N) or quaternary amine (R<sub>4</sub>N<sup>+</sup>). In general, the commercial basic extractants contain a functional group of tertiary amine or quaternary amine. The quaternary amines are usually in the form of alkyl ammonium salts (or amine salts). Metal anions in the feed solution can react with quaternary amine to form organo-metal complexes by replacing the common anions (e.g., Cl<sup>-</sup>, SO<sub>4</sub><sup>-</sup>, and F<sup>-</sup>) of the quaternary amines<sup>(41,47)</sup>. Examples of basic extractants which were studied in this work are quaternary amine ( trioctyl methyl ammonium chloride (Aliquat 336, (CH<sub>3</sub>(C<sub>8</sub>H<sub>17</sub>)<sub>3</sub>N<sup>+</sup>Cl<sup>-</sup>)) and tertiary amine (trioctylamine (TOA: (C<sub>8</sub>H<sub>17</sub>)<sub>3</sub>N)). Equation (1.5) shows the extraction of HgCl<sub>4</sub><sup>2-</sup> by Aliquat 336.



As shown in Eq. (1.5), the organo-metal complex from large positive charge (CH<sub>3</sub>(C<sub>8</sub>H<sub>17</sub>)<sub>3</sub>N<sup>+</sup> of Aliquat 336 reacted with anion HgCl<sub>4</sub><sup>2-</sup> is soluble in the liquid

membrane but insoluble in the feed solution while anion  $\text{Cl}^-$  of Aliquat 336 releases to the feed solution<sup>(30,41)</sup>.

In case of the extraction of metal anions by tertiary amine, the tertiary amine must be reacted with a mineral acid (e.g., HCl,  $\text{H}_2\text{SO}_4$ , or HF) to form an anion exchanger (amine salt) which is equivalent to quaternary amines<sup>(47)</sup>. The extraction by the tertiary amine, e.g., TOA occurs in two steps, i.e., amine salt formation, Eq. (1.6), and an anion-exchange reaction or extraction reaction, Eq. (1.7)<sup>(48,49)</sup>. The following equations show the extraction of  $\text{HgCl}_4^{2-}$  by TOA.



#### 1.4 Synergistic extraction

Synergistic extraction is the phenomenon in which the mixture of two types of extractants enhances the extraction of metal ions greater than the expected summation of the performance of the two extractants separately<sup>(42)</sup>. This phenomenon arises from the combination of two extractants resulting in a new complex (an adduct) which is more hydrophobic than each extractant. With more hydrophobic molecule, the adduct reacts more with metal ions<sup>(50)</sup>. Three different mechanisms are proposed to describe the synergistic extraction. The first mechanism involves an opening of one or more of the chelate rings and occupation by the adduct molecule(s) of the vacated metal coordination site(s). In the second

mechanism, the metal ions retain residual water(s) in the coordination sphere which can be replaced by the adduct molecules. The third mechanism is the expansion of the coordination sphere of the metal ion to allow bonding of the adduct molecules<sup>(51)</sup>.

The synergistic coefficient ( $R$ ) in terms of the distribution coefficients, as shown in Eq. (1.8), was defined to quantify the synergistic effect<sup>(52)</sup>. Generally,  $R$  is greater than 1. The greater synergistic coefficient shows higher extraction of metal ions by the synergistic extractant.

$$R = \frac{D_{1,2}}{(D_1 + D_2)} \quad (1.8)$$

where  $D_{1,2}$  is the distribution coefficient of the synergistic system to extract the specified ions,  $(D_1 + D_2)$  is the summation of the distribution coefficient in each single extraction system.

A number of synergisms are found in the literature but very few have been commercialized. This is due to the difficulty in maintaining the optimum ratio of the extractants in the liquid membrane phase to sustain synergism. The most common synergistic system consists of a mixture of neutral and acidic extractants<sup>(42)</sup>. Guezzen et al.<sup>(53)</sup> used the mixture of TBP (a neutral extractant) and D2EHPA (an acidic extractant) as the synergistic extractant to extract zinc ions. The synergistic coefficient is found to be 1.74. Wannachod et al.<sup>(54)</sup> observed the synergistic extraction of lanthanide ions by using the mixture of Cyanex 921 (a neutral extractant) and D2EHPA

as the synergistic extractant at the synergistic coefficient of 7.5. Wang et al.<sup>(55)</sup> used the mixture of Cyanex 921 and Cyanex 272 (Bis(2,4,4-trimethylpentyl)phosphinic acid, an acidic extractant) as the synergistic extractant to extract Zr(IV) and Hf(IV) from synthetic water. The synergistic coefficient for the extraction of Zr(IV) and Hf(IV) are 30.4 and 18.3, respectively. Other previous studies on neutral extractant mixed with basic extractant for synergistic extraction were investigated. Qiong et al.<sup>(56)</sup> used the mixture of TBP and N235 (trialkyl amine, a basic extractant) as the synergistic extractant to extract zinc ions from synthetic water. The synergistic coefficient of 12.3 was observed. In this work, the synergistic extraction of arsenic ions was studied by using the mixture of Cyanex 471 (a neutral extractant) and Aliquat 336 (a basic extractant) at the synergistic coefficient of 2.8.

### 1.5 Stripping solutions

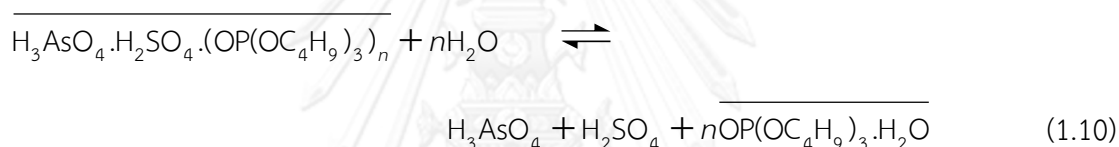
The selection of stripping solution for removal of metal ions from the organo-metal complexes depends on types of metal ions extracted (cation, neutral complex, and anion) and types of extractants (acidic extractants, chelating extractants, neutral extractants, ligand substitution extractants, and basic extractants) used in the extraction of metal ions.

In the extraction of metal cations, an acidic extractant or a chelating extractant is used. In order to strip metal cations from the organo-metal complexes, an acidic stripping solution is required. Hydrogen ions which dissociated from the acidic stripping solution replace metal cations in the organo-metal complexes. As a result, metal cations are released to the stripping solution. The stripping reaction of

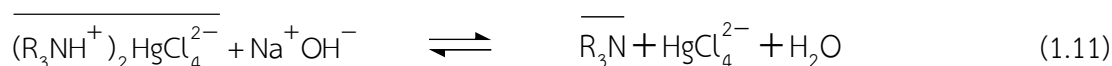
$\text{Pb}^{2+}$  from the organo-metal complex  $\overline{\text{Pb}(\text{OPO}(\text{OC}_8\text{H}_{17})_2)_2}$  by an acidic stripping solution is shown in Eq. (1.9)<sup>(43)</sup>.



For the extraction of neutral metal complexes, a neutral extractant is used. Neutral metal complexes can be stripped from the organo-metal complexes by a neutral stripping solution, for example, water as shown in Eq. (1.10)<sup>(42,57)</sup>.

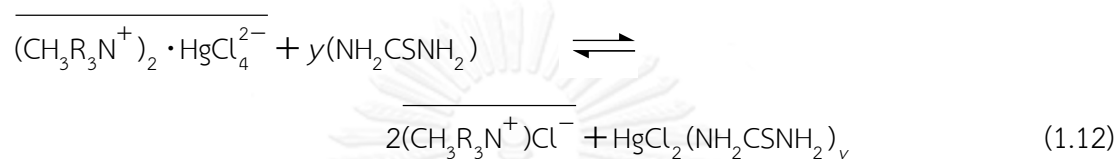


In the case of extraction of metal anions, a basic extractant or a neutral extractant is used. In order to strip metal anions from the organo-metal complexes, a basic stripping solution is required. Anions from the basic stripping solution replace metal anions in the organo-metal complexes. As a result, metal anions are released to the stripping solution. The stripping reaction of  $\text{HgCl}_4^{2-}$  from the organo-metal complex using NaOH as the stripping solution is shown in Eq. (1.11)<sup>(49)</sup>.



It is noted that quaternary ammonium extractants, for example, Aliquat 336 strongly form complexes with metal anions, and therefore the stripping of metal

anions from such complexes is rather difficult. In many cases, stripping can be accomplished by using a large anion or ligand containing phosphorous, nitrogen or sulfur as a donor atom<sup>(30,41)</sup>, e.g., thiourea ( $\text{NH}_2\text{CSNH}_2$ ). Equation (1.12) shows the stripping of  $\text{HgCl}_4^{2-}$  from mercury–quaternary-ammonium complex by thiourea.



## 1.6 Patterns of HFSLM operations for metal ions separation

The patterns of HFSLM operations for metal ions separation are mainly classified as follows: batch operation, continuous operation and semi-batch operation.

### I. Batch operation

The separation of metal ions by batch operation consists of a single HFSLM module, a feed reservoir, and a stripping reservoir, as shown in Figure 1.1. Feed and stripping solutions are circulated through the HFSLM module. Batch operation is suitable for the separation of metal ions from a small volume of feed solution, and slow extraction and stripping. By using batch operation, high percentage separation of the metal ions can be obtained.



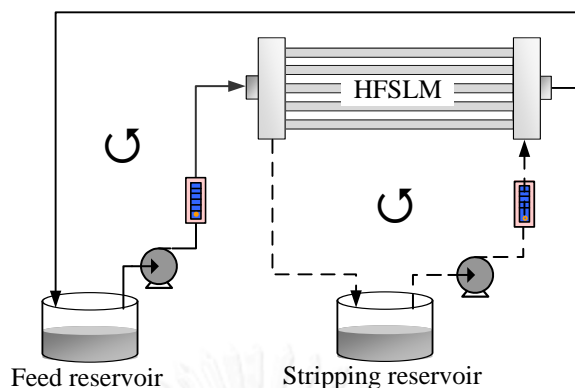


**Figure 1. 1** Schematic diagram of batch operation HFSLM

## II. Continuous operation

Continuous operation is suitable for the separation of metal ions from a large volume of feed solution and can be performed by connecting the HFSLM modules in series or in parallel as shown in Figures 1.2(a) and (b), respectively. The feed and stripping solutions are supplied in single-pass flow or one-through-mode.

Continuous operation by connecting the HFSLM modules in series provides higher residence time of feed and stripping solutions in the HFSLM modules. Therefore, the continuous operation with the HFSLM modules in series is recommended for slow extraction and stripping as they require long residence time to complete the reactions.

On the other hand, continuous operation by connecting the HFSLM modules in parallel provides shorter residence time than that in series. Therefore, continuous operation connecting the HFSLM modules in parallel is suitable for fast extraction and stripping.

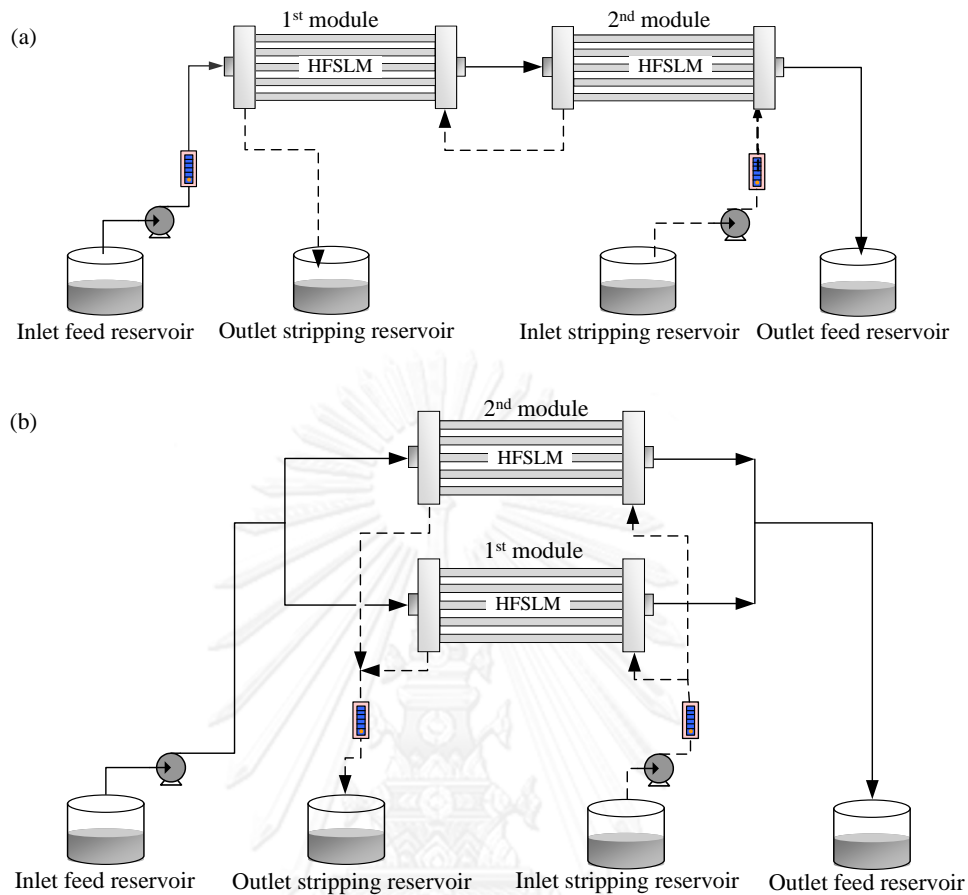


**Figure 1. 2** Schematic diagrams of continuous operation HFSLM: (a) connecting the HFSLM modules in series, (b) connecting the HFSLM modules in parallel

### III. Semi-batch operation

The separation of metal ions by semi-batch operation is carried out by using single-pass flow of feed solution but circulating flow of stripping solution. By using this pattern operation, the metal ions in the stripping solution can be concentrated until its concentration is constant and the reaction reaches the equilibrium. Figures 1.3(a) and (b) show semi-batch operation by connecting the HFSLM in series or in parallel. The operation using HFSLM modules in series is preferable for the selective

separation of metal ions which the extraction reaction is slow. In case of fast extraction reaction, the separation of metal ions does not need long residence time. Therefore, using HFSLM modules in parallel is suitable.

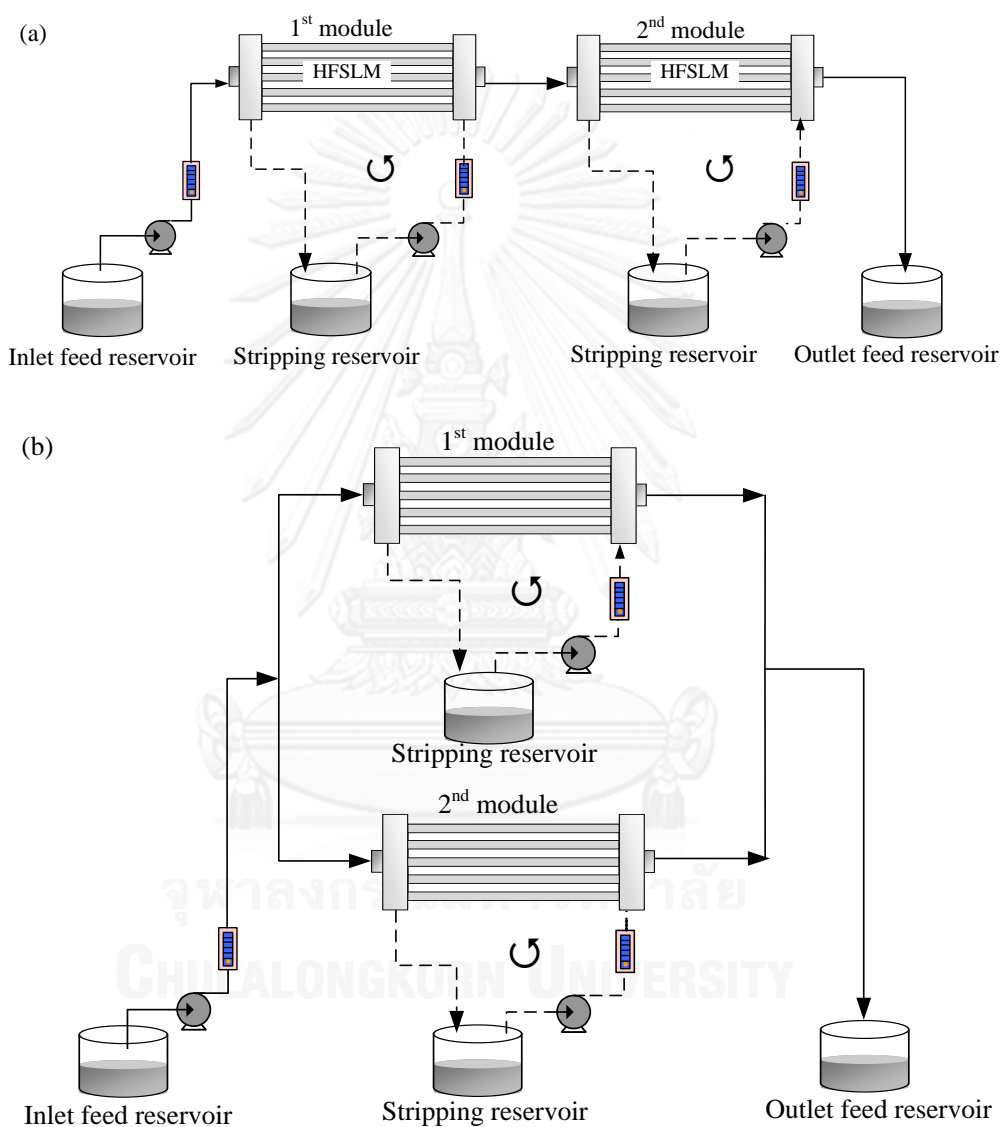


**Figure 1. 3** Schematic diagrams of semi-batch operation HFSLM: (a) connecting the HFSLM modules in series, (b) connecting the HFSLM modules in parallel

### 1.7 Mathematical modeling for separation of metal ions via HFSLM

Two types of the models have been developed to explain the extraction and stripping of metal ions via HFSLM. The first model is based on the convection of metal ions in the feed solution and the diffusion of metal ions in liquid membrane<sup>(12,24,58)</sup>. The second model considers the convection and accumulation of metal ions in the feed solution, and includes the reactions at feed-liquid-membrane interface<sup>(23,59)</sup>. Kandwal et al.<sup>(58)</sup> developed a mathematical model involving the convection of metal ions in the feed solution and the diffusion of metal ions in liquid membrane for the extraction of Cs(I) from synthetic water via HFSLM. The chemical reactions at liquid-membrane interfaces were neglected. Their model results were in good agreement with the experimental data. Vernekar et al.<sup>(24)</sup> studied the extraction of Co(II) via HFSLM. They developed a model considering the convection and the diffusion of metal ions, neglecting the extraction (complexation) and stripping (de-complexation) reactions at liquid-membrane interfaces. The model results showed that the controlling step of Co(II) extraction was the diffusion in liquid membrane phase. However, Yang and Kocherginsky<sup>(60)</sup> found that the model, which the extraction and stripping reactions at liquid-membrane interfaces were neglected, could not describe the extraction and stripping of Cu(II) via HFSLM. Thus, Pancharoen et al.<sup>(23)</sup> developed the reaction flux model considering the convection and accumulation of metal ions in the feed solution as well as the reactions at feed-liquid membrane interface but neglecting the diffusion of metal ions in liquid membrane to explain the extraction of Cu(II) via HFSLM. The model results were in good agreement with the experimental data at the average percentage of deviation

about 2%. It indicated that the extraction of Cu(II) via HFSLM depended on the convection and accumulation of metal ions in the feed solution, and the reactions at feed-liquid membrane interface. Another model in our group Chaturabul et al.<sup>(59)</sup> described not only the extraction but also the stripping of metal ions via HFSLM. We can conclude that not only types of extractants (single or synergistic) but also the facilitated transport mechanism (carrier-mediated transport) attributed to the extraction efficiency of metal ions.

In this work, a mathematical model considering the convection and accumulation of lead and mercury ions in the feed and stripping solutions and the reactions at liquid-membrane interfaces was developed to describe the extraction and stripping of the ions from synthetic water via HFSLM. The diffusion in liquid membrane was neglected.

### 1.8 Objectives of the dissertation

1. To study the influences of variables on the efficiency of extraction and stripping of lead, mercury and arsenic ions from synthetic water and produced water from the Gulf of Thailand via HFSLM.
2. To develop a reaction flux model for the extraction and stripping of lead and mercury ions.
3. To measure the solubilities of organic acids in various solvents by equilibrium method.

## 1.9 Scopes of the dissertation

This dissertation presents the separation of lead, mercury and arsenic ions via HFSLM as well as a reaction flux model to predict the extraction and stripping. The scopes of this dissertation are as follows:

1. The experiments were focused on the separation of lead, mercury and arsenic ions from synthetic water and produced water.
2. Supply feed and stripping solutions counter-currently with equal flow rates to tube and shell sides of the HFSLM, respectively.
3. The investigated parameters were
  - a) types of extractants: D2EHPA, TOA, Aliquat 336, Bromo-PADAP, Cyanex 471 and Cyanex 923
  - b) concentration of the selected extractants
  - c) types of lead complexes in feed solution, i.e.,  $\text{Pb}(\text{NO}_3)_2$  and  $\text{PbCl}_2$
  - d) concentration of  $\text{H}_2\text{SO}_4$  (a co-extractant) in produced water
  - e) types of stripping solutions: distilled water,  $\text{HNO}_3$ ,  $\text{H}_2\text{SO}_4$ ,  $\text{HCl}$ ,  $\text{NaOH}$  and thiourea
  - f) concentration of the selected stripping solutions
  - g) patterns of HFSLM operations
    - 1) continuous operation: single-pass flows of feed and stripping solutions
    - 2) batch operation: circulating flows of feed and stripping solutions
    - 3) semi-batch operation: single-pass flow of feed solution but circulating flow of stripping solution

- h) operating time
  - i) equal flow rates of feed and stripping solutions.
4. Develop the reaction flux model for the extraction and stripping of lead and mercury ions via HFSLM by considering the convection and accumulation of lead and mercury ions, and the reactions at liquid-membrane interfaces.
  5. Verify the reaction flux model by comparing the model results with the experimental data.

#### 1.10 Expected results

The expected results are as follows:

1. The outlet concentrations of lead, mercury and arsenic ions from HFSLM modules comply with the regulatory discharge limits by the Ministry of Industry and the Ministry of Natural Resources and Environment, Thailand.
2. High stripping of lead and mercury ions.
3. High accuracy reaction flux model.

#### 1.11 Descriptions of dissertation

This dissertation is divided into 8 chapters. Chapter I gives a brief introduction on separation of metal ions by HFSLM, important parameters involved such as types of extractants and stripping solutions, the concept of synergistic extraction, patterns of HFSLM operations, and mathematical model. Chapters II–VII present the published

articles showing the separation of lead, mercury and arsenic ions from synthetic water and produced water by HFSLM. Chapter VIII is the conclusion of this dissertation. Five parts of studies are involved and outlined as follows:

#### Part I

This part shows the simultaneous separation of mercury(II), arsenic(III) and arsenic(V) from produced water ( $\text{pH} \approx 6$ ) from the Gulf of Thailand which was supplied by the PTT Exploration and Production Public Company Limited (PTTEP). The concerned mercury(II) ions was about 0.279 ppm (regulatory discharge limit 0.005), and arsenic(III), arsenic(V) ions were 3.984 ppm (regulatory discharge limit 0.200). The influences of types of extractants (Aliquat 336, Bromo-PADAP, Cyanex 923 and Cyanex 471), concentration of the selected extractant, concentration of  $\text{H}_2\text{SO}_4$  (a co-extractant) in the feed solution, types of stripping solutions (NaOH, DI water,  $\text{HNO}_3$ ,  $\text{H}_2\text{SO}_4$  and thiourea), concentration of the selected stripping solution, and the number of separation cycles were studied. Details are available in Chapter II and the article in *Journal of Membrane Science*<sup>(61)</sup>.

#### Part II

This part focuses on the separation of lead(II) ions from synthetic water by HFSLM. The concentration of lead ions in synthetic water was 1 ppm which is the same concentration in the produced water from Bualuang field. As a matter of fact, produced water was contaminated by various contaminant metal ions. The produced water from Bualuang field has lead(II) and mercury(II) ions of about 1 ppm individually. Although it is likely that the extractability of the extractant depends



particularly on chemical structure of the extractant, types of metal ions and the interference of different ions on extraction efficiency, in this work, synthetic water firstly contained only lead(II) ions to observe the single effect of lead ions on D2EHPA, and to avoid the interference of other ions. D2EHPA was chosen as the extractant due to high lead extractability based on previous literature<sup>(28,43,62,63)</sup> and its low solubility in acid solution<sup>(64)</sup>. Concentration of extractant D2EHPA, types of stripping solutions (distilled water, HNO<sub>3</sub>, H<sub>2</sub>SO<sub>4</sub> and HCl) having high potential stripping of lead ions<sup>(28,43,62,63)</sup>, concentration of the selected tripping solution, patterns of HFSLM operations, types of lead complexes in the feed solution (Pb(NO<sub>3</sub>)<sub>2</sub> and PbCl<sub>2</sub>), and flow rates of feed and stripping solutions were investigated. High stripping of lead(II) ions is expected. In this study, the kinetics (reaction order and reaction rate constant) of Pb(NO<sub>3</sub>)<sub>2</sub> and PbCl<sub>2</sub> extraction were estimated. In addition, the experimental in this study were compared with the results estimated by a mathematical model from our research group (the reaction flux model), which considered the convection and accumulation of metal ions in the feed solution, and the reactions at feed-liquid membrane interface<sup>(23)</sup>. Details are described in Chapter III and the article in Chemical Engineering Journal<sup>(65)</sup>.

### Part III

This part applied the reaction flux model to predict the extraction and stripping of lead(II) ions from synthetic water by HFSLM. The model was solved by using Laplace Transform. The amount of lead ions in synthetic water was 1 ppm which is similar to its concentration in the produced water from Bualuang field. Same parameters as shown in Part II were studied using the optimum conditions from Part

II to validate the reaction flux model. The reaction order and reaction rate constant of the extraction and stripping reactions of lead ions were estimated. The model results were subsequently compared with the experimental results. Details are shown in Chapter IV and the article in Journal of Industrial and Engineering Chemistry<sup>(66)</sup>.

#### Part IV

This part highlights selective separation of lead(II) and mercury(II) ions from synthetic water by HFSLM. The concentrations of lead(II) and mercury(II) ions of 1 ppm individually in synthetic water same as the concentrations in the produced water were studied. The double-module HFSLM in series was applied to attain the selective separation of lead(II) and mercury(II) ions. At first, the influences of types of extractants (D2EHPA, Cyanex 471, Aliquat 336, and TOA) were investigated, and afterwards the concentration of the selected extractant was determined by using a single-module HFSLM. It was found that D2EHPA was preferable to lead ions and Aliquat 336 was preferable to mercury ions. D2EHPA with the optimum concentration was used in the first module of the HFSLM to extract lead(II) ions. Aliquat 336 with the optimum concentration was subsequently used in the second module of the HFSLM to extract mercury(II) ions. Thiourea the most preferable stripping solution for mercury(II) ions in Part I, and HCl the most preferable stripping solution for lead(II) ions in Part II were used. The concentrations of thiourea and HCl were fixed. The effects of operating time and flow rates of feed and stripping solutions on the extraction and stripping of lead(II) and mercury(II) ions were investigated finally.

Reaction rate constants and reaction order of the extraction and stripping of lead(II) and mercury(II) ions were estimated using integral and graphical methods. The reaction flux model considering the convection and accumulation of lead(II) and mercury(II) ions in the feed and stripping solutions, and the reactions at liquid-membrane interfaces to predict the extraction and stripping of lead(II) and mercury(II) ions was developed. The model was solved by using Generating Function and was verified by the experimental data in terms of the average percent deviation. Details are available in Chapter V and the article in Journal of Membrane Science<sup>(67)</sup>.

#### Part V

This part explains the measurement of the solubilities of organic acids (adipic acid, 4-methylbenzoic acid, 4-iso-propylbenzoic acid and 4-*tert*-butylbenzoic acid) in various solvents. Details are available in Chapters VI and VII.

Liquid membrane, an extractant dissolved in a diluent, plays a significant role in liquid membrane separation. It is embedded in the hollow-fiber micropores and in contact with feed and stripping solutions. It is known that the solubilities of the extractant in feed and stripping solutions have an important effect on the stability of the liquid membrane. Lifetime of the HFSLM is attributed to the stability of the liquid membrane. In this manner, the extractant should have low solubility in feed and stripping solutions but should have high solubility in the diluent<sup>(68)</sup>. The solubility data of the extractants in feed and stripping solutions must be known in order to select an appropriate extractant for the HFSLM system. However, the solubility data of some extractants in specific solutions do not exist. In this Part, the equilibrium method for the measurements of the solubilities of adipic acid, 4-methylbenzoic

acid, 4-iso-propylbenzoic acid and 4-*tert*-butylbenzoic acid in various solvents, i.e., water, acetic acid, acetic acid-water mixture, cyclohexanol and cyclohexanone was applied as learning cases for the measurement of the solubility of the extractant. The equilibrium method was validated by comparing the solubilities of these organic acids observed from this work with those solubilities reported in the literature<sup>(69-72)</sup>. The obtained solubility data were correlated with the modified Apelblat equation and the  $\lambda H$  equation<sup>(69-72)</sup>, and were used to calculate the molar enthalpy and the molar entropy of the dissolutions of the organic acids in the above solvents. The solubility of adipic acid is shown in Chapter VI and was published in Fluid Phase Equilibria<sup>(73)</sup>. The solubilities of 4-methylbenzoic acid, 4-iso-propylbenzoic acid and 4-*tert*-butylbenzoic acid are shown in Chapter VII and the article in Journal of Molecular Liquids<sup>(74)</sup>.

CHAPTER II

SIMULTANEOUS REMOVAL OF ARSENIC AND MERCURY FROM NATURAL-  
GAS-CO-PRODUCED WATER FROM THE GULF OF THAILAND USING  
SYNERGISTIC EXTRACTANT VIA HFSLM

Anchaleeporn Waritswat Lothongkum<sup>a</sup>, Sira Suren<sup>b</sup>, Srestha Chaturabul<sup>b</sup>,  
Noppawat Thamphiphit<sup>b</sup>, Ura Pancharoen<sup>b†</sup>

<sup>a</sup> *Department of Chemical Engineering, Faculty of Engineering, King Mongkut's  
Institute of Technology Ladkrabang, Chalongkrung Rd., Bangkok 10520, Thailand*

<sup>b</sup> *Department of Chemical Engineering, Faculty of Engineering, Chulalongkorn  
University, Bangkok 10330, Thailand*

จุฬาลงกรณ์มหาวิทยาลัย  
CHULALONGKORN UNIVERSITY

---

This article has been published in Journal: Journal of Membrane Science.

Page: 350–358. Volume: 369. Year: 2011.

---

## 2.1 Abstract

The simultaneous separation of arsenic and mercury ions from natural-gas-co-produced water was well achieved by a synergistic extractant through a hollow fiber supported liquid membrane (HFSLM). Aliquat 336, Bromo-PADAP, Cyanex 923 and Cyanex 471 dissolved in toluene were used as the organic extractants or carriers. The transport system was studied on several variables: types of the extractants, concentration of the synergistic extractant, concentration of  $H_2SO_4$  (a co-extractant) in feed solution, types of stripping solutions (NaOH, DI water,  $HNO_3$ ,  $H_2SO_4$  and thiourea), and the number of separation cycles. The results indicated the superior performance of mercury removal to arsenic by every single extractant in this study. The synergistic effect on arsenic removal was observed by adding Cyanex 471 in Aliquat 336 resulting in the synergistic coefficient of 2.8. The regulate mercury discharge to the environment not higher than 5 ppb was attained within 1-cycle separation by using the mixture of 0.22 M Aliquat 336 and 0.06 M Cyanex 471 as the synergistic extractant and 0.1 M thiourea as the stripping solution with 0.2 M  $H_2SO_4$  in feed solution. By 3-cycle separation, 94% arsenic extraction, which was below the legislation limit of 250 ppb, was obtained.

**Keywords:** Arsenic; Mercury; Synergistic; HFSLM; Co-produced Water.

## 2.2 Introduction

In offshore oil and gas production, co-produced water contaminated with organic and inorganic compounds, salts, hydrocarbons, radioactive elements, trace heavy and toxic metals, and chemical additives used during well drillings came along with oil and gas [1]. The amounts of the constituents that expose to the environment increase with the amount of co-produced water due to high petroleum demand and older oil and gas wells. In practice, co-produced water is partially reused and treated before discharging to the environment or re-injecting into the originated reservoir depending on its quality and the environmental constraints. Basically, in the Gulf of Thailand, trace heavy and toxic metals in co-produced water are arsenic and mercury. The arsenic appears in As(V) form [2] whereas the mercury appears predominantly in the element form with the rest in inorganic (such as  $\text{HgCl}_2$ ), organic (such as  $\text{CH}_3\text{HgCH}_3$  and  $\text{C}_2\text{H}_5\text{HgC}_2\text{H}_5$ ) and organo-ionic compounds (such as  $\text{ClHgCH}_3$ ) [3,4]. Arsenic and mercury toxicity can occur both severe acute and chronic poisoning to human health [5–7].

According to the permissible discharge limits by both the Ministry of Industry and the Ministry of Natural Resources and Environment, Thailand, it is a must for the operators to remove arsenic and mercury from the offshore waste discharges to no greater than 250 ppb and 5 ppb, respectively [8]. Chevron, Thailand has been applied a continuous chemical treatment process to fit these regulations. However, sometimes the on-line As and Hg monitors have been problematic to achieve the desired discharge concentrations [3]. In addition, it is reported that the conventional methods of metal treatment, for example, precipitation, coagulation, electrolysis,

reverse osmosis, carbon adsorption, solvent extraction, ion exchange, chemical oxidation and reduction are, however, ineffective at a very low concentration of the contaminated metal ions [9].

In accordance with several studies of using liquid membrane (LM) to remove trace metal ions from aqueous solutions, in particular, the simultaneous separation of mercury and lignosulfonate from dilute synthetic solution by a flat sheet supported liquid membrane [6] and our previous works via hollow fiber supported liquid membrane (HFSLM) for industrial wastewaters [10,11] and co-produced waters [12,13], inevitably, HFSLM is a promising method to treat a very low metal ions concentration effectively. The selection of types of the extractants and stripping solutions for arsenic and/or mercury separation was reviewed from the following literature because they played important role in the separation. Iberhan and Wisniewski [14] extracted As(III) and As(V) by Cyanex 925, Cyanex 301 and their mixtures of different volumetric ratios by liquid-liquid extraction with sulfuric acid as a co-extractant. The result showed that As extraction increased with sulfuric acid concentration in the synthetic aqueous feed. Cyanex 301 provided higher extraction of As(III) than As(V). The mixture of Cyanex 925 with Cyanex 301 helped remove As(V) significantly, while pure Cyanex 925 could extract As(V) a little better than As(III). Fabrega and Mansur [15] also used liquid-liquid extraction to remove Hg(II) from HCl solution by Aliquat 336 dissolved in commercial Kerosene Exxol D-80 as the extractant. Mercury was almost totally extracted within 5 min at  $\text{pH} \geq 1$  and satisfactorily stripped of about 99% by using thiourea as the stripping solution. Chakrabarty et al. [6] found that in the supported liquid membrane (SLM) system, trioctylamine (TOA) could extract Hg(II) from pure solution better than lignosulfonate-



mixed solution. Sangtumrong et al. [16] simultaneously separated Hg(II) and As(III) ions from chloride media via HFSLM by TOA dissolved in toluene as the extractant and NaOH as the stripping solution; about 95% Hg(II) was recovered but none of As(III). Prapasawat et al. [17] applied HFSLM to separate As(III) and As(V) ions from sulfate media and used Cyanex 923 dissolved in toluene as the extractant and water as the stripping solution. It was found that As(V) could be extracted more than As(III); and the percentage of extraction increased with the concentration of H<sub>2</sub>SO<sub>4</sub>, a co-extractant, in feed solution. Uedee et al. [18] attained 100% extraction and 97% recovery of Hg(II) ions from chloride media via HFSLM using TOA dissolved in kerosene as the extractant and NaOH as the stripping solution.

Recently, Pancharoen et al. separated arsenic and mercury ions from co-produced water from different gas fields in the Gulf of Thailand by HFSLM. For co-produced with pretreatment of mercury to nil, about 91% arsenic was extracted by Aliquat 336 dissolved in kerosene, and 72% was stripped by NaOH [12]. In the case of co-produced water from a different gas field without mercury pretreatment, mercury were highly selective extracted by TOA dissolved in toluene with NaOH as the stripping solution. The amount of mercury ions that complied with the regulatory limit was obtained in 6-cycle separation by using 2% (v/v) TOA and 0.5 M NaOH at a pH of feed solution of 2.5, and equal flow rates of feed and stripping solutions of 50 ml/min [13]. Therefore, this current work focuses on the synergistic extraction to enhance the simultaneous arsenic and mercury separation from co-produced water via HFSLM for their regulatory discharge limits because various combinations of two or more extractants can produce a synergistic effect which the extractability of a mixture of the extractants is greater than the sum of their individual extractabilities

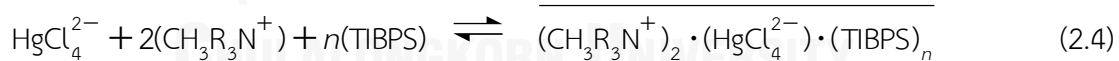
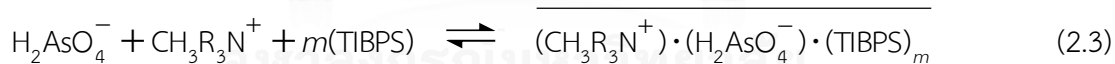
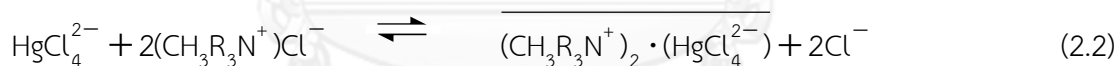
[19–25]. The mechanism of the synergistic extraction, types of the extractants, concentration of the synergistic extractant, concentration of  $\text{H}_2\text{SO}_4$  (co-extractant) in feed solution, types of stripping solutions (NaOH, DI water,  $\text{HNO}_3$ ,  $\text{H}_2\text{SO}_4$  and thiourea), and the number of separation cycles were studied.

### 2.3 Theory

The HFSLM system consists of an aqueous feed containing metal ions and a stripping solution. Feed and stripping phases are separated by the supported liquid membrane embedded with one type of an organic extractant or a mixture of two types of extractants to enhance the separation. As shown in Figure 2.1, the target metal ions react with the extractant at the feed-membrane interface to form complex species. Subsequently, the complex species diffuse across the liquid membrane (organic phase) to react with the stripping solution at the opposite interface of the membrane then are stripped into the stripping phase. Thus, the target metal ions can be extracted and stripped simultaneously in a single step. The transportation rate of metal ions is driven by the concentration gradient between feed and stripping phases.

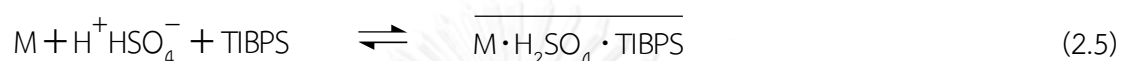
It is noted that co-produced water from the Gulf of Thailand consists of arsenic in undissociated forms ( $\text{H}_3\text{AsO}_3$ ,  $\text{H}_3\text{AsO}_4$ ) and dissociated form ( $\text{H}_2\text{AsO}_4^-$ ), mostly  $\text{H}_2\text{AsO}_4^-$ , residual mercury after pretreatment as  $\text{HgCl}_2$  and so on. The dissociated form of  $\text{H}_2\text{AsO}_4^-$  is usually converted to  $\text{H}_3\text{AsO}_4$ . In general,  $\text{HgCl}_2$  is converted to  $\text{HgCl}_4^{2-}$  in the presence of chloride ions [12,26,27]. Due to the hazardous waste management regulations, various attempts have been made to

treat  $\text{H}_2\text{AsO}_4^-$  and  $\text{HgCl}_4^{2-}$  from co-produced water simultaneously. The synergistic extraction by using a mixture of the selected extractants with favor on specific forms is of great interest. It is known that the extractant plays an important role on a separation of metal ions. A hard base extractant, for example, Aliquat 336 (tri-octyl methyl ammonium chloride:  $\text{CH}_3\text{R}_3\text{N}^+\text{Cl}^-$ ) can extract both dissociated and undissociated forms in a basic or weak acidic condition but dissociated forms are high favor. While a neutral extractant like Cyanex 471 (tri-isobutylphosphine sulfide: TIBPS), which is classified by a hard soft acid base theory [28,29] as a soft base, normally reacts with undissociated forms but in an acidic condition it can react with dissociated forms [12,17,28–32]. The extraction reaction of  $(\text{CH}_3\text{R}_3\text{N}^+)\text{Cl}^-$  with  $\text{H}_2\text{AsO}_4^-$  and  $\text{HgCl}_4^{2-}$  in co-produced water are shown in Eqs. (2.1) and (2.2), and by  $(\text{CH}_3\text{R}_3\text{N}^+)\text{Cl}^-$  mixed with TIBPS are in Eqs. (2.3) and (2.4):



where the over bars represent the complex species,  $m$  and  $n$  are the stoichiometric coefficients to be calculated from the distribution coefficients of the relevant ions at various concentrations of the extractant used.

To enhance the extraction of undissociated forms by either basic or neutral extractant, commonly, it is recommended to add acid solution as a co-extractant [6,16–18,31]. Thus, the reaction of undissociated arsenic of  $\text{H}_3\text{AsO}_3$  and  $\text{H}_3\text{AsO}_4$  from co-produced water with TIBPS is as follows:



where M stands for  $\text{H}_3\text{AsO}_3$  or  $\text{H}_3\text{AsO}_4$  and the over bar is the complex species.

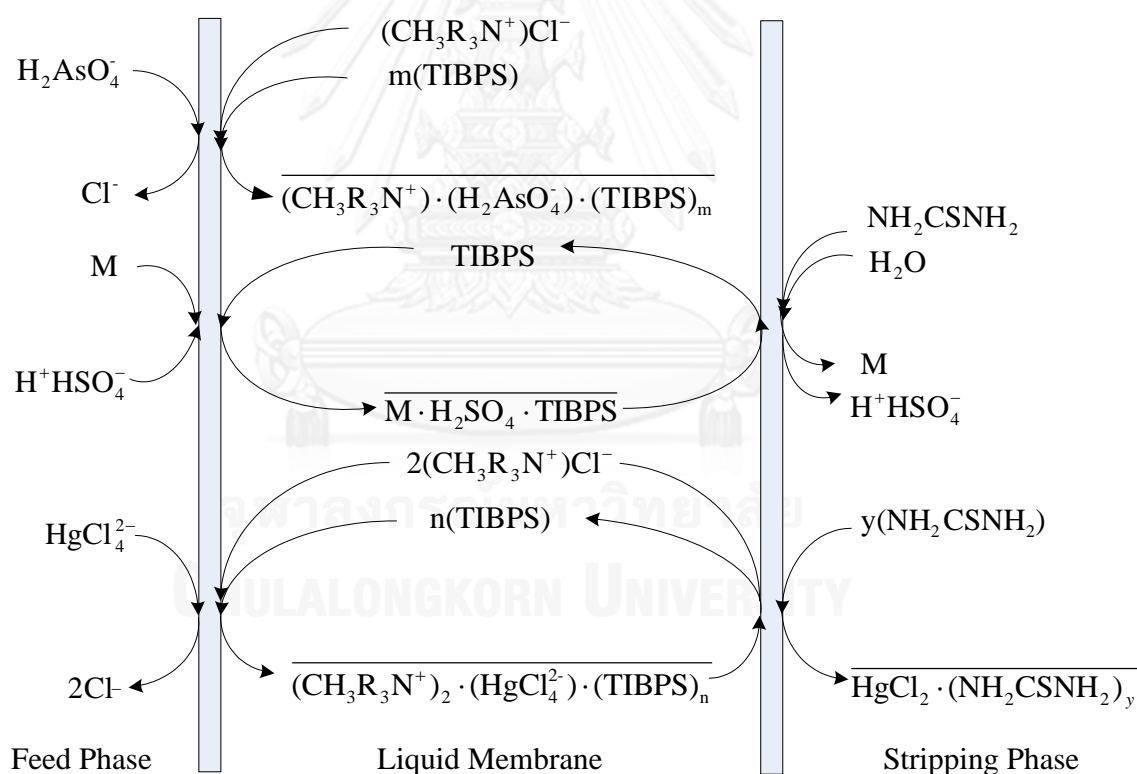
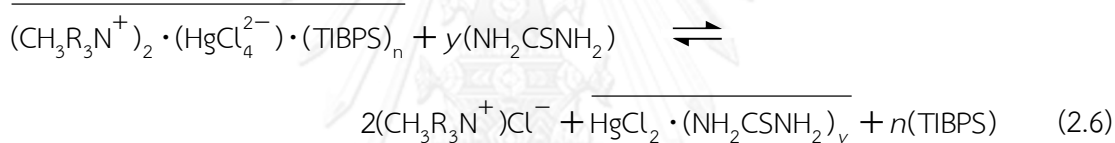


**Figure 2. 1** Schematic mechanisms of the extraction and stripping of  $\text{H}_2\text{AsO}_4^-$ ,  $\text{H}_3\text{AsO}_3$ ,  $\text{H}_3\text{AsO}_4$  and  $\text{HgCl}_4^{2-}$  by a mixture of Aliquat 336 and TIBPS (Cyanex 471) with thiourea as the stripping solution.

Figure 2.1 shows the descriptive schematic mechanisms of  $\text{H}_2\text{AsO}_4^-$  and  $\text{HgCl}_4^{2-}$  with the synergistic extractant and stripping solution. The complex species reacted with the stripping solution. Large anion in the structure of thiourea ( $\text{NH}_2\text{CSNH}_2$ ) was strong enough to strip mercury complex ion from Aliquat 336, which was composed of a large organic cation associated with a chloride ion [15]. The undissociated complex form of  $\text{H}_3\text{AsO}_3$  or  $\text{H}_3\text{AsO}_4$  was stripped by an aqueous solution of thiourea. Water in thiourea solution was presumed to take part as the stripping solution same as Prapasawat et al. used pure water in As(III) and As(V) separation [17]. The stripping reactions can be proposed in Eqs. (2.6) and (2.7):



Luo et al. determined the synergistic coefficient ( $R$ ) in terms of the distribution coefficients [25].

$$R = \frac{D_{\max}}{(D_1 + D_2)} \quad (2.8)$$

where  $D_{\max}$  is the maximum distribution coefficient or distribution ratio of the synergistic system to extract the specified ions. For example, the synergistic systems are the mixture of the extractants A and B or A and C to extract arsenic ions.

$(D_1 + D_2)$  is the summation of the distribution coefficient in each single extraction system, viz. A, B or A, C. The greater synergistic coefficient of A and B system than that of A and C system is, the higher extraction of arsenic by the mixture of A and B was obtained.

The extraction equilibrium constants ( $K_{ex}$ ) of arsenic and mercury ions are as follows:

$$K_{ex,As} = \frac{[(CH_3R_3N^+) \cdot (H_2AsO_4^-) \cdot (TIBPS)_m]}{[H_2AsO_4^-][CH_3R_3N^+][TIBPS]^m} \quad (2.9)$$

$$K_{ex,Hg} = \frac{[(CH_3R_3N^+)_2 \cdot (HgCl_4^{2-}) \cdot (TIBPS)_n]}{[HgCl_4^{2-}][CH_3R_3N^+]^2[TIBPS]^n} \quad (2.10)$$

The distribution coefficients ( $D$ ) for arsenic and mercury extractions by the mixture of Aliquat 336 and Cyanex 471 can be calculated by

$$D_{As} = \frac{[(CH_3R_3N^+) \cdot (H_2AsO_4^-) \cdot (TIBPS)_m]}{[H_2AsO_4^-]} = K_{ex,As} [CH_3R_3N^+] [TIBPS]^m \quad (2.11)$$

$$D_{Hg} = \frac{[(CH_3R_3N^+)_2 \cdot (HgCl_4^{2-}) \cdot (TIBPS)_n]}{[HgCl_4^{2-}]} = K_{ex,Hg} [CH_3R_3N^+]^2 [TIBPS]^n \quad (2.12)$$

The permeability coefficient ( $P$ ) by Denesi [33] is expressed as

$$-V_f \ln\left(\frac{C_f}{C_{f,o}}\right) = AP \frac{\beta}{\beta + 1} t \quad (2.13)$$

where

$$\beta = \frac{Q_f}{PL \epsilon L \pi r_i} \quad (2.14)$$

where  $P$  is the permeability coefficient (cm/s);  $V_f$  is the volume of the feed (cm<sup>3</sup>);  $C_{f,o}$  is the mercury ion concentration at time 0 (mol/L);  $C_f$  is the mercury ion concentration at time  $t$  (mol/L);  $A$  is the effective area of the hollow fiber module (cm<sup>2</sup>);  $t$  is the time (min);  $Q_f$  is the volumetric flow rate of feed solution (cm<sup>3</sup>/s);  $L$  is the length of the hollow fiber (cm);  $\epsilon$  is the porosity of the hollow fiber (%);  $N$  is the numbers of hollow fibers in the module;  $r_i$  is the internal radius of the hollow fiber (cm).

The relevant mass transfer coefficients ( $k_i$  and  $k_s$ ) and permeability coefficient are as follows:

$$\frac{1}{P} = \frac{1}{k_i} + \frac{r_i}{r_{lm}} \cdot \frac{1}{P_m} + \frac{r_i}{r_o} \frac{1}{k_s} \quad (2.15)$$

$r_{lm}$  and  $r_o$  are the log-mean and external radius of the hollow fiber.  $P_m$  is the membrane permeability coefficient which is related to the distribution coefficient as shown [34]:

$$P_m = Dk_m \quad (2.16)$$

Therefore, the membrane permeability coefficients for arsenic ( $P_{m,As}$ ) and mercury ( $P_{m,Hg}$ ) are as follows:

$$P_{m,As} = K_{ex,As} k_m [CH_3R_3N^+][TIBPS]^m \quad (2.17)$$

$$P_{m,Hg} = K_{ex,Hg} k_m [CH_3R_3N^+]^2 [TIBPS]^n \quad (2.18)$$

where  $k_m$  is the membrane mass transfer coefficient.

## 2.4 Experimental

### 2.4.1 Reagents and materials

The feed solution was co-produced water from the gas separation plant in the Gulf of Thailand and supplied by the PTT Exploration and Production Public Company Limited (PTTEP). The compositions of the co-produced water, shown in Table 2.1, were analyzed by the inductively coupled plasma spectroscopy (ICP). Different types of extractants dissolved in toluene were Aliquat 336 (tri-octyl methyl ammonium chloride, 94% purity from Cognis Ltd.), Bromo-PADAP (2-(5-bromo-2-pyridylazo)-5-(diethylamino)phenol, 98% purity from Sigma-Aldrich PTE Ltd.), Cyanex 471 (tri-isobutylphosphine sulfide, 98% purity from Cytec Canada Inc.) and Cyanex 923 (trioctylphosphine oxide, 94% purity from Cytec Canada Inc.). Sulfuric acid,



analytical grade, was used as the co-extractant. Four stripping solutions from Merck Ltd. were sodium hydroxide (98% purity), nitric acid (65% purity), sulfuric acid (97% purity) and thiourea (98% purity). All stripping solutions were aqueous solutions except thiourea was dissolved in dilute HCl acid solution.

**Table 2. 1** Compositions of co-produced water (pH  $\approx$  6).

Compositions	Concentration (ppm)
As	3.984
Hg	0.279
Fe	0.169
Mg	2.014
Ca	15.167
Na	1821.5

#### 2.4.2 Apparatus

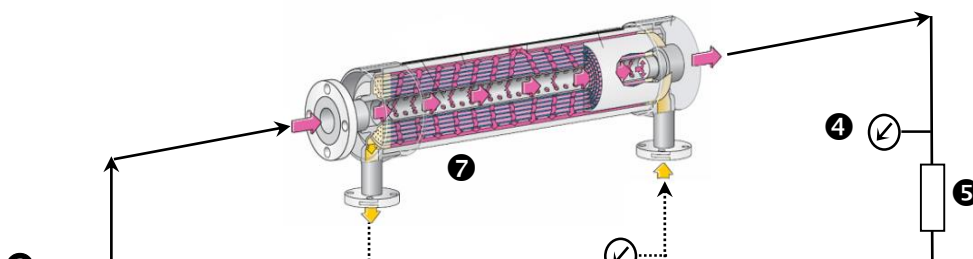
The hollow fiber supported liquid membrane (HFSLM) system from Liqui-Cel<sup>®</sup> Laboratory Liquid/Liquid Extraction System, which was composed of two gear pumps, two variable flow rate controllers, two rotameters and four pressure gauges, was used. This hollow fiber module was Celgard<sup>®</sup> microporous polypropylene fibers woven into fabric and wrapped around a central-tube feeder to supply the shell side fluid. The property of hollow fiber module is shown in Table 2.2. The concentrations of arsenic and mercury were determined by the ICP.

**Table 2. 2** Properties of the hollow fiber module.

Properties	Descriptions
Material	Polypropylene
Number of fibers	10,000
Module length	20.3 cm
Module diameter	6.3 cm
Porosity	30%
Pore size	0.03 $\mu\text{m}$
Contact area	1.4 $\text{m}^2$
Area per unit volume	29.3 $\text{cm}^2/\text{cm}^3$
Fiber ID	240 $\mu\text{m}$
Fiber OD	300 $\mu\text{m}$

### 2.4.3 Procedures

The potential extractants from literature reviews to remove arsenic and mercury were tested by solvent extraction using various concentrations to select a suitable type of the extractant and its concentration of the highest arsenic and mercury extractability for further study in the HFSLM system. The single-module HFSLM operation is shown in Figure 2.2.



3

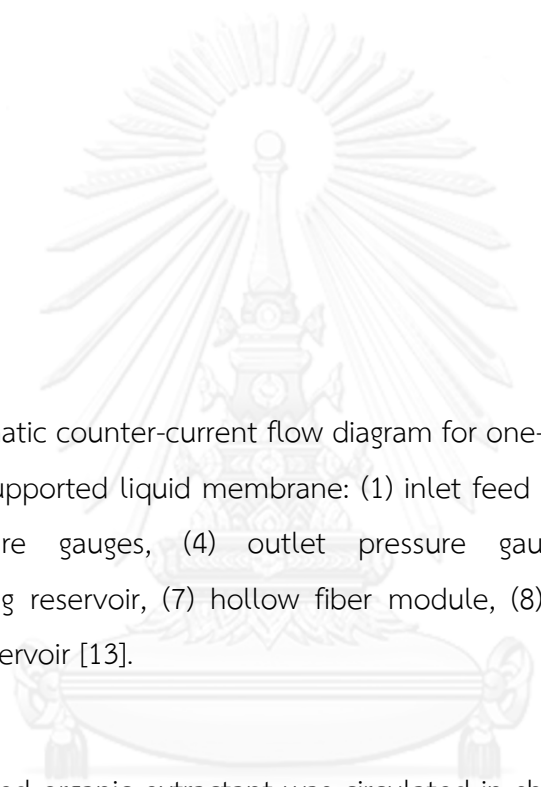


**Figure 2. 2** Schematic counter-current flow diagram for one-through-mode separation by hollow fiber supported liquid membrane: (1) inlet feed reservoir, (2) gear pumps, (3) inlet pressure gauges, (4) outlet pressure gauges, (5) flow meters, (6) outlet stripping reservoir, (7) hollow fiber module, (8) inlet stripping reservoir, (9) outlet feed reservoir [13].

The selected organic extractant was circulated in shell and tube sides of the hollow fiber module for 20 min to ensure the extractant was entirely embedded in micropores of the fibers. The co-produced water feed solution and stripping solution were pumped counter-currently into the tube side and shell side of the HFSLM, respectively. The effects of types of the extractants, concentration of the synergistic extractant, concentration of  $\text{H}_2\text{SO}_4$  (a co-extractant) in feed solution from 0 to 0.9 M, types of stripping solutions (NaOH, DI water,  $\text{HNO}_3$ ,  $\text{H}_2\text{SO}_4$  and thiourea), and the number of separation cycles on arsenic and mercury removal were studied. According to our previous work, the optimum flow rates of feed and stripping

solutions of 100 ml/min for the highest mass transfer by HFSLM were fixed [18]. The operating time for each separation cycle was 40 min. A 10-ml sample was taken from the feed and recovery reservoirs to determine arsenic and mercury ion concentrations by the ICP.

## 2.5 Results and discussion

### 2.5.1 The effects of extractants on the extraction of arsenic and mercury by solvent extraction

The maximum percentages of arsenic and mercury extraction from co-produced water (pH about 6) of each potential extractant at its concentration are shown in Figure 2.3. It was found that all of the extractants had much higher extractability of mercury than arsenic. The single basic extractants, 0.22 M Aliquat 336 and 0.002 M bromo-PADAP, could extract arsenic more than the single neutral extractants of 0.06 M Cyanex 471 and 0.51 M Cyanex 923 due to the extractive capability of both dissociated and undissociated arsenic forms [32]. When Cyanex 471 was added with Aliquat 336, the percentage of arsenic extraction abruptly increased. This is because of synergistic effect of Cyanex 471 with the synergistic coefficient ( $R$ ) to arsenic ions of 2.8 by Eq. (2.8) [25] and Figure 2.4. Higher synergistic coefficient of Aliquat 336 and Cyanex 471 system than 1 means that the system has the synergism on arsenic extraction. The combination of these extractants is considered to generate the complex species,  $(\text{CH}_3\text{R}_3\text{N}^+) \cdot (\text{H}_2\text{AsO}_4^-) \cdot (\text{TIBPS})_m$  in the membrane phase (see Figure 2.1), that are more hydrophobic than the species obtained by the single

extractant of Aliquat 336 or Cyanex 471. This agreed with those found and explained by Atanassova and Gaikwad [35,36]. As a result, by using a binary mixture of Aliquat 336 (a hard base extractant) and Cyanex 471 (a neutral extractant classified as a soft base) in this study, the amount of As which could not be extracted much by only one extractant increased due to the synergistic effect.

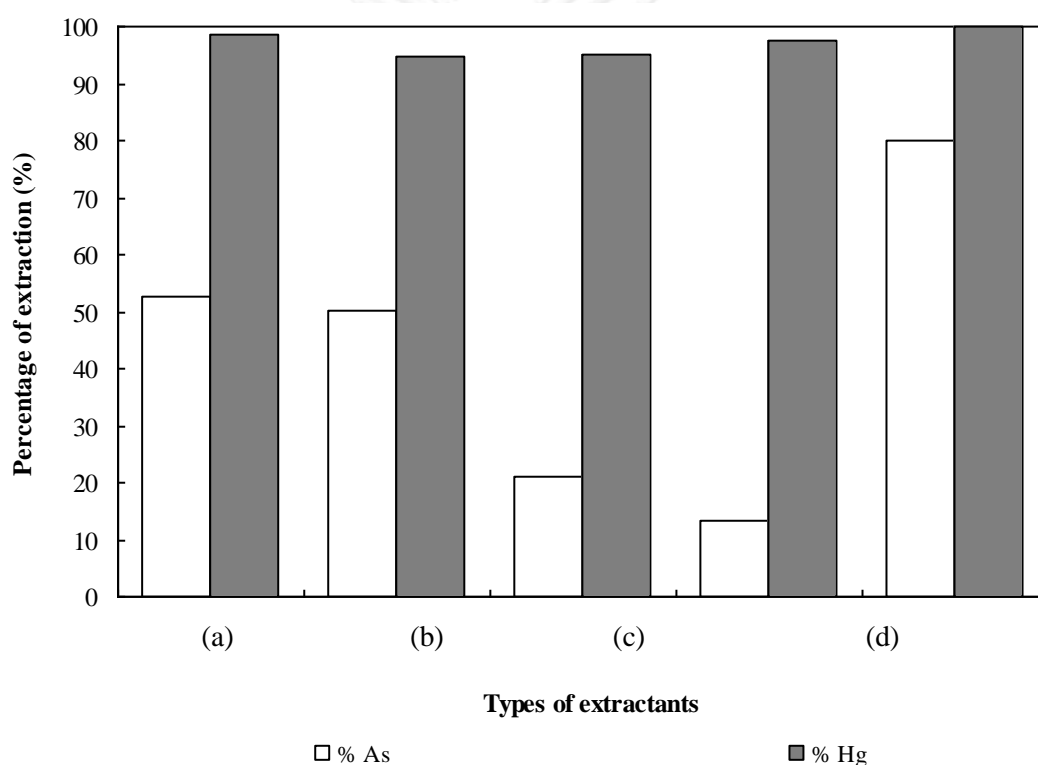


**Figure 2. 3** The maximum percentages of metal ions extraction from co-produced water against types of the extractants by solvent extraction: (a) 0.22 M Aliquat 336, (b) 0.002 M Bromo-PADAP, (c) 0.06 M Cyanex 471, (d) 0.51 M Cyanex 923, (e) 0.22M Aliquat 336-0.06 M Cyanex 471.

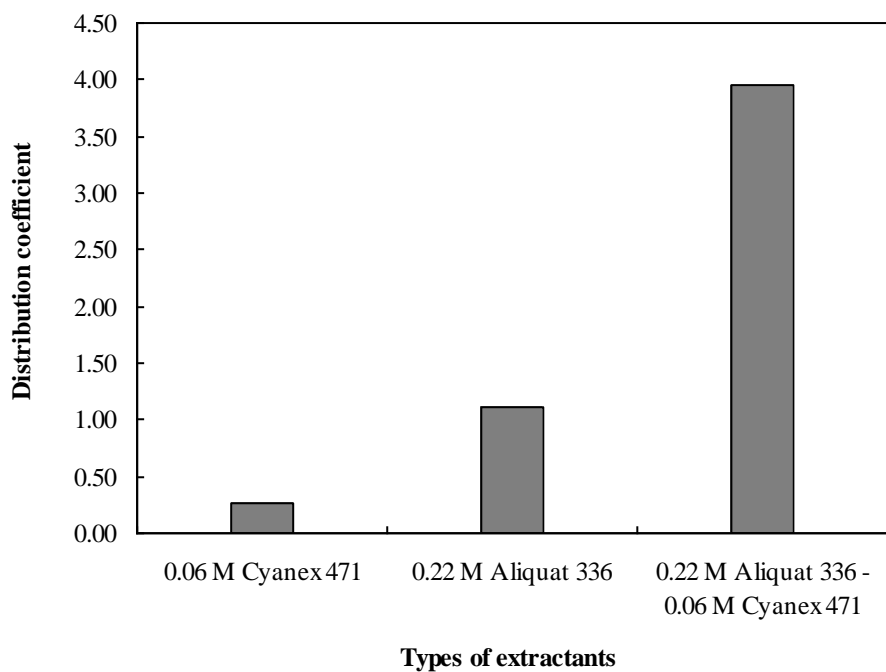


**Figure 2. 4** The distribution coefficients of As(V) against types of the extractants.

The sequences of percentages extraction of metal ions were shown as follows:

As: Aliquat 336-Cyanex 471 > Aliquat 336 > Bromo-PADAP >Cyanex 471>Cyanex 923,

Hg: Aliquat 336-Cyanex 471 > Aliquat 336 > Cyanex 923 >Bromo-PADAP≈Cyanex 471.

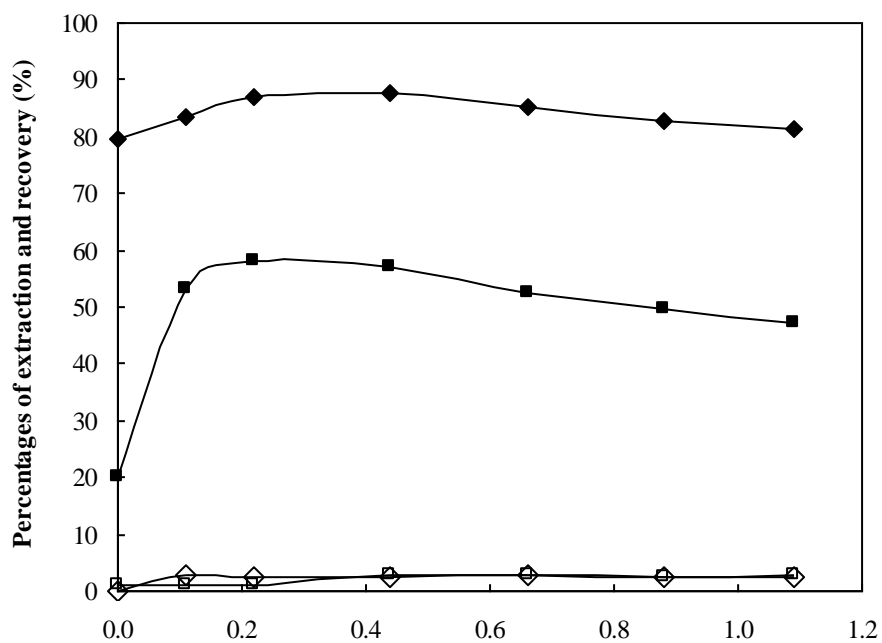
### 2.5.2 The effect of synergistic extractant concentration

Figure 2.5 shows the correlation between the percentages of extraction and recovery against the concentration of the mixture of the synergistic extractant of Aliquat 336 and Cyanex 471. From Figure 2.5(a), the percentages of arsenic and mercury extractions increased when the concentration of Aliquat 336 in the synergistic extractant increased. The same phenomena were observed in case of

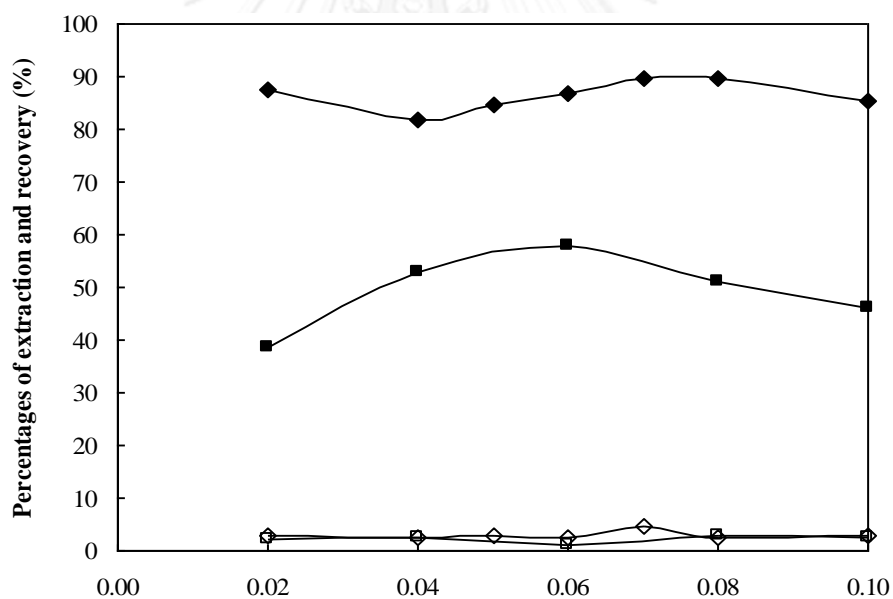
Cyanex 471 in Figure 2.5(b). The percentage of mercury extraction was slightly increased while that of arsenic was distinctly increased because most of mercury ions was almost completely extracted by a single extractant of Aliquat 336 and Cyanex 471; while arsenic ions could be extracted actively by the synergistic effect of the selected extractants [25,37]. This could be explained by Le Chatelier's principles that the extraction increased when the concentration of the extractant increased. The maximum arsenic extraction was attained at the concentrations of Aliquat 336 and Cyanex 471 in the mixture of synergistic extractant of 0.22 M and 0.06 M, respectively. The percentage of arsenic extraction was then decreased due to the excessive viscosity from high concentration. According to the molecular kinetic interpretation by Stokes and Einstein, the increase in high viscosity leads to lower diffusion coefficient resulting in lower extraction. Chakrabarty et al. [38] also observed that the viscosity of membrane phase increased with the extractant (TOA) concentration, resulting in the decrease of flux.

### 2.5.3 The effect of $H_2SO_4$ concentration in feed solution

The results in Figure 2.6 imply that by adding  $H_2SO_4$  (0–0.9 M) in feed solution of co-produced water helps increase the extraction and recovery of arsenic and mercury by the mixture of basic and neutral extractant. It is reported that the highest extraction of mercury was obtained by using TOA, a basic extractant, with a weak acidic feed containing 0.2 M HCl [16]. Perez et al. [31] found that a neutral extractant (Cyanex 921) reacted well with arsenic in feed added 1.6 M  $H_2SO_4$ . The extraction percentage was lower at very low concentration of  $H_2SO_4$ .



(a) Aliquat 336 concentration (M)



(b) Cyanex 471 concentration (M)

■ % As extraction                      ◆ % Hg extraction  
 □ % As recovery                        ◇ % Hg recovery

**Figure 2. 5** Percentages of metal ions extraction and recovery against the concentrations of the extractants via HFSLM by using 0.5 M NaOH as the stripping solution without the co-extractant: (a) Aliquat 336 mixed with 0.06 M Cyanex 471, (b) Cyanex 471 mixed with 0.22 M Aliquat 336.



In accordance with the results shown in Figure 2.6, a basic extractant as Aliquat 336 performed effectively in a basic solution in general, or in weak acidic solution (low acid concentration in feed solution). Therefore, we recommend to add a little  $\text{H}_2\text{SO}_4$  (0.2 M) in feed solution to enhance the extractability for arsenic and mercury of the extractant as found in this work and for a longer lifetime of the membrane.

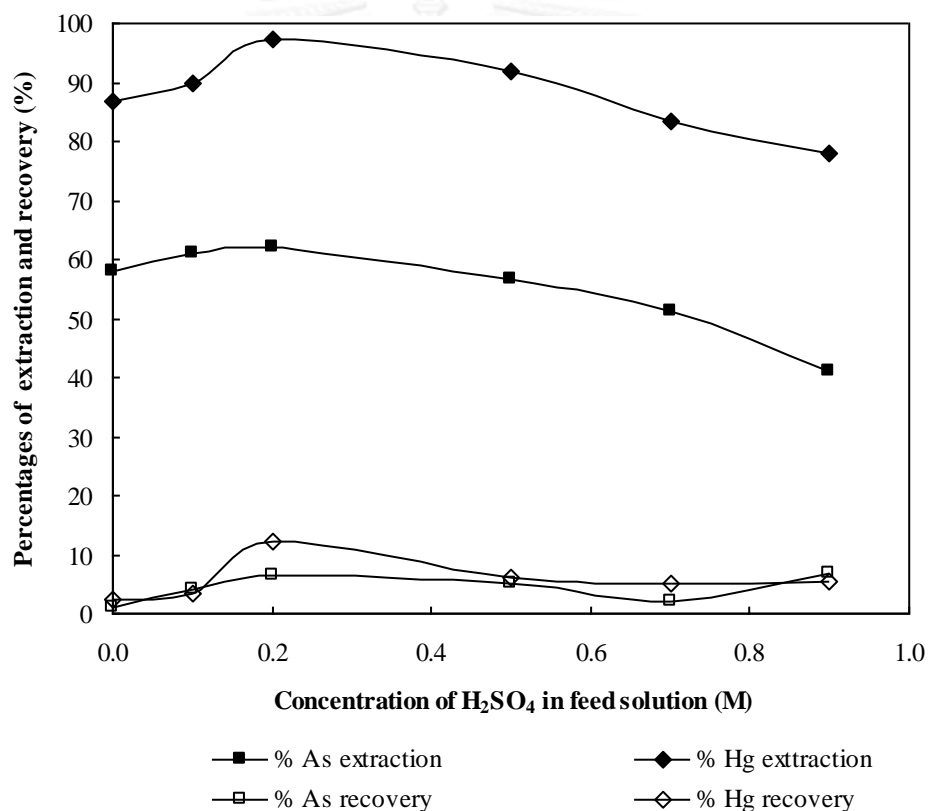


**Figure 2. 6** Percentages of metal ions extraction and recovery against  $\text{H}_2\text{SO}_4$  concentration in feed solution as the co-extractant via HFSLM by using the mixture of 0.22 M Aliquat 336 and 0.06 M Cyanex 471 as the extractant and 0.5 M NaOH as the stripping solution.

### 2.5.4 The effects of stripping solutions

Among the stripping solutions used in this work, i.e., NaOH, DI water, HNO<sub>3</sub>, H<sub>2</sub>SO<sub>4</sub>, and thiourea (NH<sub>2</sub>CSNH<sub>2</sub>) was found to be the best stripping solution for arsenic and mercury as seen in Figure 2.7. With large anion in the structure, thiourea was strong enough to strip mercury complex ion. NaOH showed less performance in metal ion stripping than thiourea, moreover, it yielded precipitates of HgO or Hg that could cause membrane fouling leading to low transport of mercury ions while no precipitates were found by using thiourea [6,15].

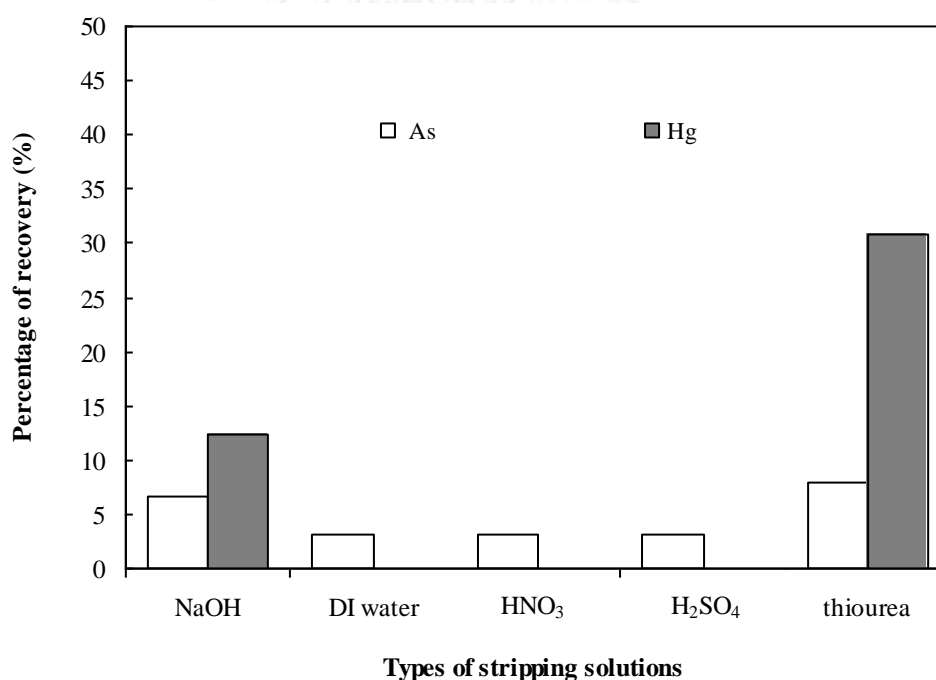


**Figure 2. 7** Percentage of metal ions recovery against types of stripping solutions via HFSLM by using the mixture of 0.22 M Aliquat 336 and 0.06 M Cyanex 471 as the extractant with 0.2 M H<sub>2</sub>SO<sub>4</sub> as the co-extractant.

The effect of thiourea concentration of 0.01–0.4 M on the recovery of mercury and arsenic ions were shown in Figure 2.8. The percentage of mercury recovery progressively increased with thiourea concentration up to 0.1 M, subsequently decreased. Based on Le Chatelier's principle the stripping reaction moved forward when the concentration of the stripping solution increased. The percentage of mercury recovery is much higher than arsenic due to higher extractability of mercury than arsenic in the extraction stage. From Figure 2.8, for 1-cycle separation, the highest percentage of mercury recovery about 46% was achieved at 0.1 M thiourea.

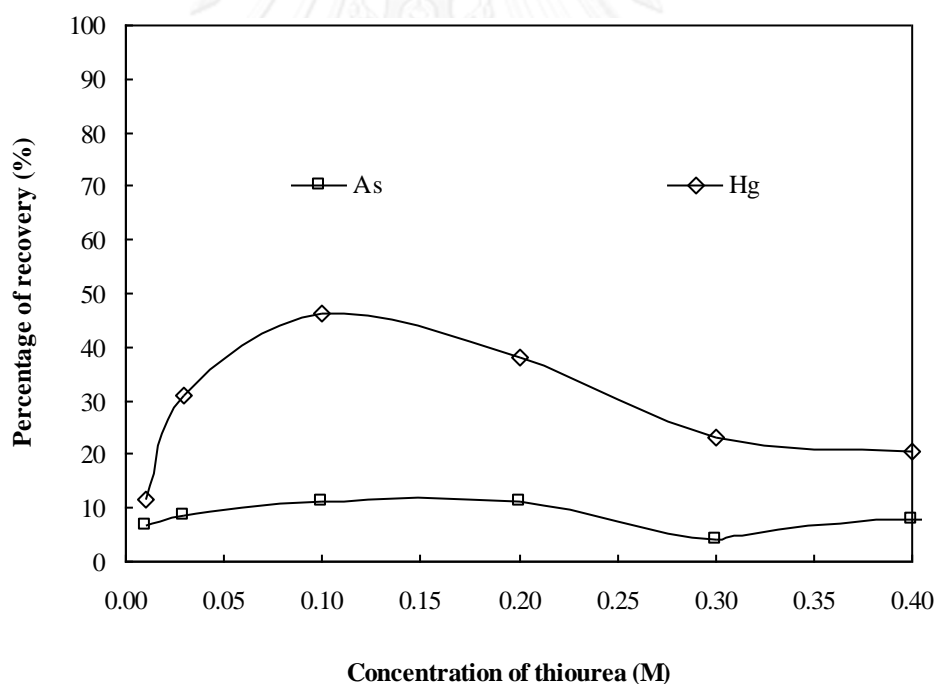


**Figure 2. 8** Percentage of metal ions recovery against the concentration of thiourea via 1-cycle HFSLM separation by using the mixture of 0.22 M Aliquat 336 and 0.06 M Cyanex 471 as the extractant and thiourea as the stripping solution with 0.2 M  $\text{H}_2\text{SO}_4$  as the co-extractant.

### 2.5.5 The effect of the number of separation cycles through the hollow fiber module

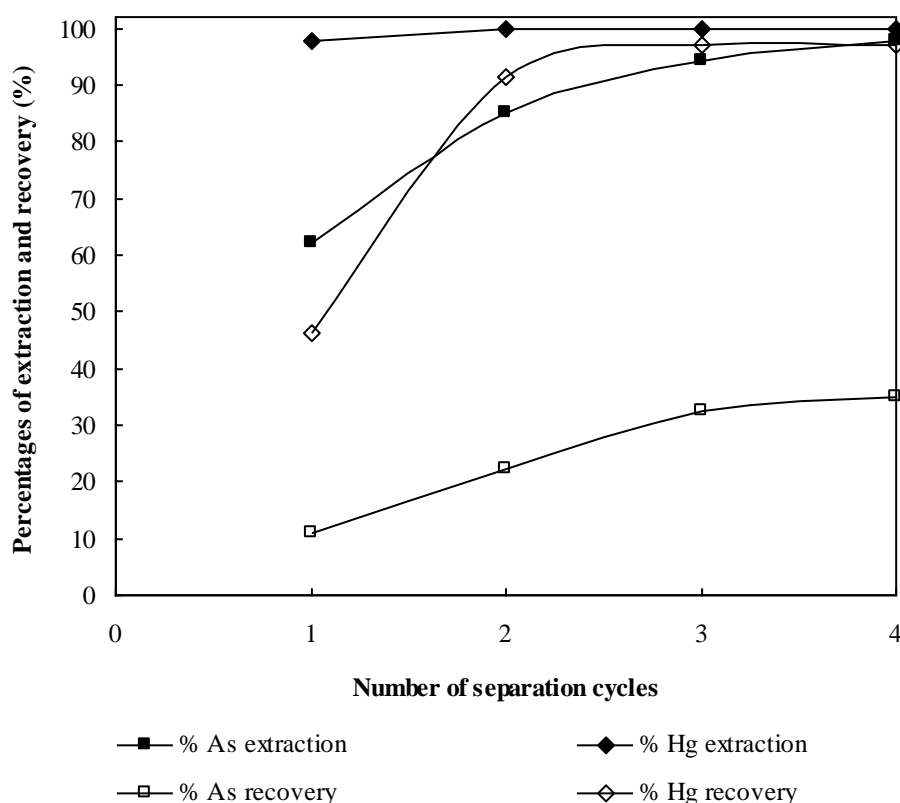
It was found that by 1-cycle separation using the synergistic extractant via HFSLM, the percentages of extraction of arsenic and mercury were 62% and 97%, whereas the percentages of recovery were 11% and 46%, respectively. The mercury level in co-produced water reached the regulation of wastewater discharge issued by the Ministry of Industry, Thailand, i.e., less than 5 ppb. From Figure 2.9, to enhance the extractability and recovery, a multiple-cycle was investigated. The results were obtained with highly achievement. By 3-cycle separation, 94% arsenic was removed; the arsenic level in co-produced water decreased below the legislation discharge of 250 ppb.

Table 2.3 summarises previous studies on arsenic and mercury treatment using different methods. It is obvious that HFSLM is an efficient method to separate a very low concentration of arsenic and mercury from the feeds containing the contaminations, e.g., co-produced water in this work. It is worth to be noted that for the feed having more than one contaminated metals or the same metal with different oxidation states, by using a single extractant may not be enough to accomplish the treatment. The well-matched extractants must be considered for their synergism.

**Table 2. 3** The reviewed methods for arsenic and mercury ions removal.

Authors	Feed solutions	Ions removal (concentration of feed solutions: ppm)	Extractants	Methods	Separation(%)
Arpa et al. [39]	Synthetic water	Pb(II), Hg(II), Cd(II) (100 each)	-	IE	1.81 for Hg and Pd, and 1.4 for Cd
Wisniewski [30]	Synthetic water	As(III) (5,000), As(V) (5,000)	Cyanex 923	LL	40 for As(III) 63 for As(V)
Francis et al. [40]	Wastewater from Board of Radiation and Isotope Technology (BRIT), India	Hg(II) (20)	Cyanex 471X	LL	≈100
Meera et al. [41]	Synthetic water	Hg(II) (20)	Cyanex 923	LL	≈100
Huebra et al. [42]	Contaminated sludge	Hg(II) (4.75)	LIX 34	LL	95
Fabrega and Mansur [15]	Synthetic water	Hg(II) (401.2)	Aliquat 336	LL	≈100
Jabbari et al. [43]	Synthetic water	Hg(II) (10)	DC18C6	BLM	95
Perez [31]	Synthetic water	As(V) (75)	Cyanex 921	SLM	94
Fontas et al. [44]	Synthetic water, Sea water	Hg(II) (10)	N-benzoyl-N',N'- diheptadecylthiourea	HFSLM	100
Sangtumrong et al. [16]	Synthetic water	Hg(II) (20), As(III) (20)	TOA	HFSLM	100
Prapasawat et al. [17]	Synthetic water	As(III) (20), As(V) (20)	Cyanex 923	HFSLM	46
Pancharoen et al. [12]	Co-produced water	As(III) (1.2842)	Aliquat 336	HFSLM	91
Pancharoen et al. [13]	Co-produced water	Hg(II) (1.248)	TOA	HFSLM	≈100
This work	Co-produced water	As(V) (0.279), Hg(II) (3.982)	Mixture of Aliquat 336 and Cyanex 471	HFSLM	98 for As 100 for Hg

*Note:* IE, ion exchange; LL, liquid-liquid extraction; BLM, bulk liquid membrane; SLM, supported liquid membrane; and HFSLM, hollow fiber supported liquid membrane.



**Figure 2. 9** Percentages of metal ions extraction and recovery against the number of separation cycles through HFSLM by using the mixture of 0.22 M Aliquat 336 and 0.06 M Cyanex 471 as the extractant and 0.1 M thiourea as the stripping solution with 0.2 M  $H_2SO_4$  as the co-extractant.

### 2.5.6 Distribution coefficients and extraction equilibrium constants

The distribution coefficients ( $D$ ) of arsenic and mercury from the separation by HFSLM, shown in Table 2.4, were estimated from the linear curve in Figure 2.5(b) and used Eqs. (2.11) and (2.12). The increasing of the distribution coefficient indicates the enhancement of extractability. From Table 2.4, the distribution coefficients increased with the concentration of Cyanex 471. The maximum distribution coefficients of

arsenic and mercury were attained at 0.06 M Cyanex 471 and 0.07 M Cyanex 471, respectively.

Table 2. 4 The distribution coefficients of arsenic and mercury at Cyanex 471 concentration from 0.02 to 0.07 M mixed with 0.22 M Aliquat 336 (0.5 M NaOH as the stripping solution).

Cyanex 471 (M)	Distribution coefficients	
	Arsenic	Mercury
0.02	0.63	–
0.04	1.13	4.52
0.05	1.32	5.57
0.06	1.47	6.59
0.07	–	8.72

The distribution coefficients in Eqs. (2.11) and (2.12) were rewritten as follows:

$$\log D_{As} = \log (K_{ex,As} \cdot [CH_3R_3N^+]) + m \log [TIBPS] \quad (2.19)$$

$$\log D_{Hg} = \log (K_{ex,Hg} \cdot [CH_3R_3N^+]^2) + n \log [TIBPS] \quad (2.20)$$

The stoichiometric coefficients ( $m$  and  $n$ ) were calculated from the plots of  $\log D_{As}$  and  $\log D_{Hg}$  against  $\log [TIBPS]$ . The linear relationships with slopes  $m = 0.7917$  or  $4/5$  for arsenic extraction and  $n = 1$  for mercury were obtained. The slopes,  $m$  and  $n$ , were substituted in the synergistic extraction equations (Eqs. (2.3) and (2.4)). The equilibrium constants of arsenic ( $K_{ex,As}$ ) and mercury ( $K_{ex,Hg}$ ) were determined by Eqs.

(2.9) and (2.10) and the slopes obtained in Figure 2.10(a) and (b). The equilibrium constant of mercury ( $1622 \text{ (L/mol)}^3$ ) was much higher than that of arsenic ( $62.7 \text{ (L/mol)}^{9/5}$ ) suggesting that the extraction of mercury was higher than arsenic which was in accordance with the results obtained from the pilot scale.

### 2.5.7 Permeability and mass transfer coefficients

The permeability coefficients of arsenic and mercury, which related to the concentration of Cyanex 471 from 0.02 to 0.07 M, were obtained from Eqs. (2.13) and (2.14) and the slopes ( $AP\beta/(\beta+1)$ ) of the plot between  $-V_f \ln(C_f/C_{f,o})$  versus  $t$ . From Table 2.5, it could be observed that the permeability coefficients increased with the concentration of TIBPS. The permeability coefficients of mercury were higher than those of arsenic, implying higher mass transfer or higher extraction of mercury ions.

Eqs. (2.21) and (2.22) were attained by substituting the membrane permeability coefficients ( $P_{m,As}$ ) and ( $P_{m,Hg}$ ) in Eqs. (2.17) and (2.18) to Eq. (2.15); assuming the stripping reactions of arsenic and mercury were instantaneous and no contribution of the stripping phase:

$$\frac{1}{P_{m,As}} = \frac{1}{k_i} + \frac{r_i}{r_{lm}} \cdot \frac{1}{K_{ex,As} k_m [\text{CH}_3\text{R}_3\text{N}^+][\text{TIBPS}]^{4/5}} \quad (2.21)$$

$$\frac{1}{P_{m,Hg}} = \frac{1}{k_i} + \frac{r_i}{r_{lm}} \cdot \frac{1}{K_{ex,Hg} k_m [\text{CH}_3\text{R}_3\text{N}^+]^2 [\text{TIBPS}]} \quad (2.22)$$



The organic-phase and aqueous-phase mass transfer coefficients ( $k_m$  and  $k_i$ ) of arsenic were determined from the plot of  $1/P_{m,As}$  against  $1/([CH_3R_3N^+][TIBPS]^{4/5})$ . The slope and the ordinate were  $(r_i/r_{lm})(1/K_{ex,As} k_m)$  and  $1/k_i$ . Accordingly,  $k_m$  and  $k_i$  of arsenic were  $1.02 \times 10^{-4}$  and  $0.0392$  cm/s. Similarly, the values of mercury were  $1.27 \times 10^{-5}$  and  $2.210$  cm/s from the plot of  $1/P_{m,Hg}$  against  $1/([CH_3R_3N^+]^2[TIBPS])$ . The organic-phase mass transfer coefficients were lower than the aqueous-phase mass transfer coefficients showing that the mass transfer within the membrane was the rate controlling step.

**Table 2. 5** The permeability coefficients of arsenic and mercury at TIBPS concentration from 0.02 to 0.07 M mixed with 0.22 M Aliquat 336 and 0.5 M NaOH as the stripping solution.

TIBPS (M)	P ( $\times 10^3$ cm/s)	
	Arsenic	Mercury
0.02	5.47	–
0.04	8.90	33.98
0.05	9.81	40.94
0.06	11.54	48.37
0.07	–	53.14

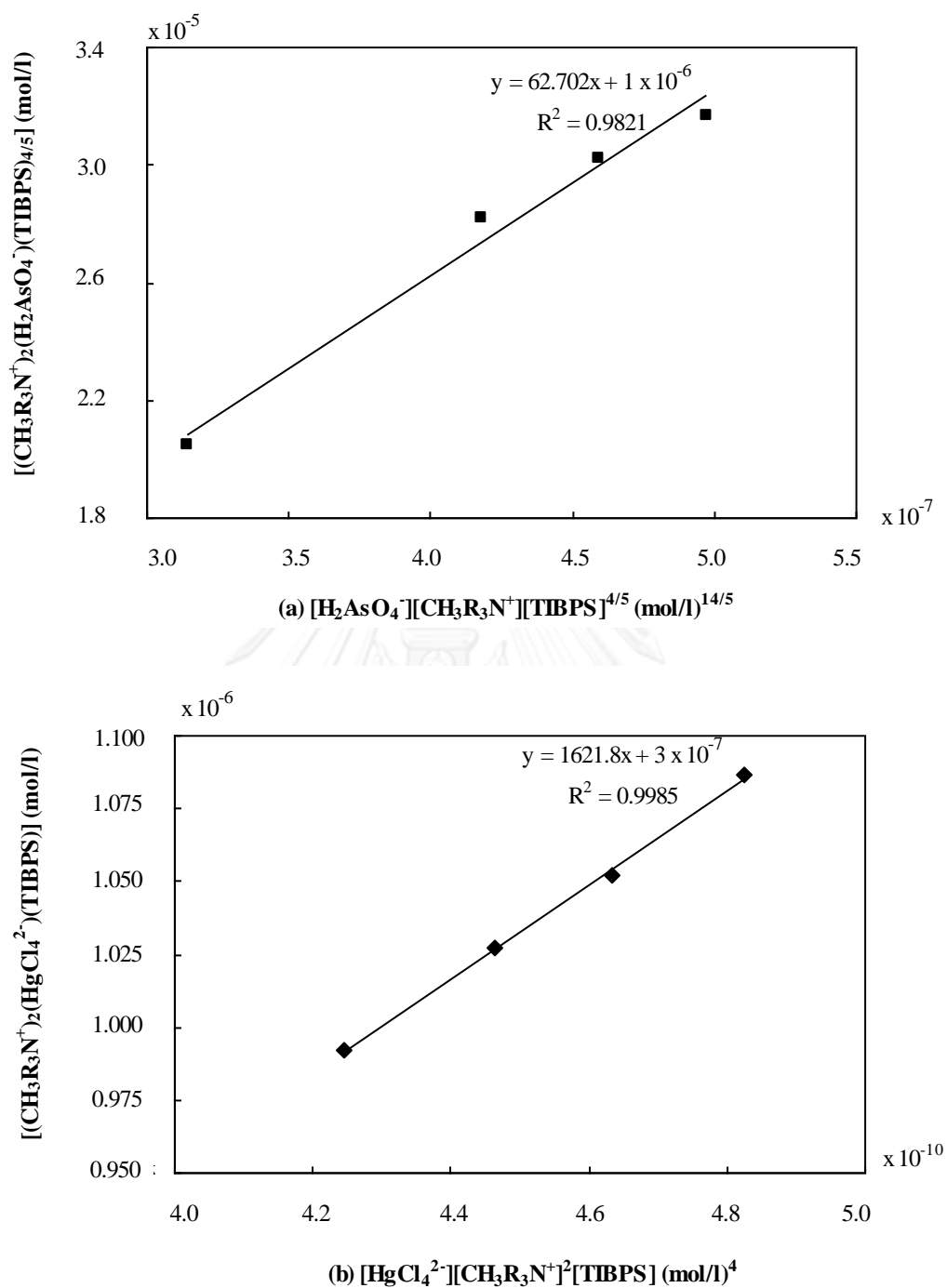


Figure 2. 10 The equilibrium constants: (a) plot of  $[(\text{CH}_3\text{R}_3\text{N}^+)_2(\text{H}_2\text{AsO}_4^-)(\text{TIBPS})_{4/5}]$  and  $[\text{H}_2\text{AsO}_4^-][\text{CH}_3\text{R}_3\text{N}^+][\text{TIBPS}]^{4/5}$  at equilibrium for As(V), (b) plot of  $[(\text{CH}_3\text{R}_3\text{N}^+)_2(\text{HgCl}_4^{2-})(\text{TIBPS})]$  and  $[\text{HgCl}_4^{2-}][\text{CH}_3\text{R}_3\text{N}^+]^2[\text{TIBPS}]$  at equilibrium for Hg(II).

## 2.6. Conclusion

The outstanding feature of HFSLM technique is its ability to treat metal ions of a very low concentration that are hardly treated or not possible by general separation techniques. Moreover, the target metal ions can be extracted and stripped simultaneously in a single step. In this work, the mercury contaminated in co-produced water was almost totally extracted by every single organic extractant used. A greater mercury extraction was observed than arsenic extraction. Of all the single extractants, Aliquat 336 showed superior mercury extraction. However, the synergistic effect on arsenic extraction was obviously found by using the mixture of 0.06 M Cyanex 471 and 0.22 M Aliquat 336. The calculated synergistic coefficient to arsenic ions was 2.8. Thiourea was found to be the best stripping solution. The discharge concentrations of mercury and arsenic in co-produced water to the environment complied with the legislation limits determined by 1-cycle separation and 3-cycle separation, respectively. The highest percentages of arsenic and mercury extractions were achieved by using 0.2 M  $\text{H}_2\text{SO}_4$  in feed solution, the synergistic extractant of 0.22 M Aliquat 336 mixed with 0.06 M Cyanex 471, and 0.1 M thiourea as the stripping solution at 4-cycle separation

## 2.7 Acknowledgements

The authors highly appreciate a financial support by Thailand Research Fund (TRF) and The National Research University Project of CHE: Ratchadaphiseksomphot

Endowment Fund (FW012A). Sincere thanks also go to Cytec Canada Inc. for supplying Cyanex 471 and the PTTEP Public Co., Ltd. for co-produced water.

## 2.8 References

- [1] J.M. Neff, N.N. Rabalais, D.F. Boesch, Offshore oil and gas development activities potentially causing long-term environmental effects, in: D.F. Boesch, N.N. Rabalais (Eds.), *Long-Term Environmental Effects of Offshore Oil and Gas Development*, Elsevier Applied Science Publishers, London, 1987, pp. 149–170.
- [2] N.E. Korte, Q. Feernando, A review of arsenic(III) in groundwater, *Crit. Rev. Environ. Control* 21 (1) (1991) 2–5.
- [3] D.L. Gallup, J.B. Strong, *Removal of Mercury and Arsenic from Produced Water*, Chevron Corporation, 2007, pp. 1–9.
- [4] G. Corvini, J. Stiltner, Keith Clark, *Mercury Removal from Natural Gas and Liquid Streams*, UOP LLC, 2007, p. 3.
- [5] United States Environmental Protection Agency EPA-600/8-83-021F, *Health Assessment Document for Inorganic Arsenic*, vol. 2, 1984, pp. 10–28.
- [6] K. Chakrabarty, P. Saha, A.K. Ghoshal, Simultaneous separation of mercury and lignosulfonate from aqueous solution using supported liquid membrane, *J. Membr. Sci.* 346 (2010) 37–44.
- [7] R. van der Vaart, J. Akkerhuis, P. Feron, B. Jansen, Removal of mercury from gas streams by oxidative membrane gas absorption, *J. Membr. Sci.* 187 (2001) 151–157.
- [8] Thailand Regulatory Discharge Standards 2, Ministry of Industry, Thailand, 1996.

- [9] B. Stephen Inbaraj, J.S. Wang, J.F. Lu, F.Y. Siao, B.H. Chen, Adsorption of toxic mercury(II) by an extracellular biopolymer poly( $\gamma$ -glutamic acid), *Bioresour. Technol.* 100 (2009) 200–207.
- [10] A.W. Lothongkum, Y. Khemglad, N. Usomboon, U. Pancharoen, Selective recovery of nickel ions from wastewater of stainless steel industry via HFSLM, *J. Alloy. Compd.* 476 (2009) 940–949.
- [11] P. Usapein, A.W. Lothongkum, P. Ramakul, U. Pancharoen, Efficient transport and selective extraction of Cr(VI) from waste pickling solution of the stainless steel-cold rolled plate process using Aliquat 336 via HFSLM, *Korean J. Chem. Eng.* 26 (3) (2009) 791–798.
- [12] U. Pancharoen, W. Poonkum, A.W. Lothongkum, Treatment of arsenic ions from produced water through hollow fiber supported liquid membrane, *J. Alloy Compd.* 482 (2009) 328–334.
- [13] U. Pancharoen, S. Somboonpanya, S. Chaturabul, A.W. Lothongkum, Selective removal of mercury as  $\text{HgCl}_4^{2-}$  from natural gas well produced water by TOA via HFSLM, *J. Alloy Compd.* 489 (2010) 72–79.
- [14] L. Iberhan, M. Wisniewski, Extraction of arsenic(III) and arsenic(V) with Cyanex 925, Cyanex 301 and their mixtures, *Hydrometallurgy.* 63 (2002) 23–30.
- [15] F.d.M. F. brega, M.B. Mansur, Liquid-liquid extraction of mercury (II) from hydrochloric acid solutions by Aliquat 336, *Hydrometallurgy* 87 (2007) 83–90.
- [16] S. Sangtumrong, P. Ramakul, C. Satayaprasert, U. Pancharoen, A.W. Lothongkum, Purely separation of mixture of mercury and arsenic via hollow fiber supported liquid membrane, *J. Ind. Eng. Chem.* 13 (2007) 751–756.

- [17] T. Prapasawat, P. Ramakul, C. Satayaprasert, U. Pancharoen, A.W. Lothongkum, Separation of As(III) and As(V) by hollow fiber supported liquid membrane based on the mass transfer theory, *Korean J. Chem. Eng.* 25 (2008) 158–163.
- [18] E. Uedee, P. Ramakul, U. Pancharoen, A.W. Lothongkum, Performance of hollow fiber supported liquid membrane on the extraction of mercury(II) ions, *Korean J. Chem. Eng.* 25 (2008) 1486–1494.
- [19] J.N. Mathur, Synergism of trivalent actinides and lanthanides solvent extraction and ions exchange, *Solvent Extr. Ion Exch.* 1 (2) (1983) 349–412.
- [20] T. Hosseini, F. Rashchi, E. Vahidi, N. Mostoufi, Investigating the synergistic effect of D2EHPA and Cyanex 302 on zinc and manganese separation, *Sep. Sci. Technol.* 45 (2010) 1158–1164.
- [21] J. Brunette, M. Taheri, G. Goetz-Grandmont, M. Leroy, Extraction of In(III) from chloride medium with 1-phenyl-3-methyl-4-acylpyrazol-5-ones: synergistic effect with high molecular weight ammonium salts, *Polyhedron* 1 (5) (1982) 457–460.
- [22] M. Atanassova, V. Jordanov, I. Dukov, Effect of the quaternary ammonium salt Aliquat 336 on the solvent extraction of lanthanoid(III) ions with thenoyltrifluoroacetone, *Hydrometallurgy* 63 (2002) 41–47.
- [23] I. Dukov, M. Atanassova, Synergistic solvent extraction and separation of lanthanides using mixtures of 1-phenyl-3-methyl-4-benzoyl-pyrazol-5-one and Aliquat 336: influence of the ammonium salt anion, *Sep. Sci. Technol.* 39 (1) (2004) 227–239.

- [24] S. Umetani, M. Matsui, H. Kanano, T. Nagai, Solvent extraction of zinc and cadmium with 4-benzoyl-3-methyl-1-phenyl-5-pyrazolone and quaternary ammonium salt, *Anal. Sci.* 1 (1985) 55–58.
- [25] F. Luo, D. Li, P. Wei, Synergistic extraction of zinc(II) and cadmium(II) with mixtures of primary amine N1923 and neutral organophosphorous derivatives, *Hydrometallurgy* 73 (2004) 31–40.
- [26] S.R. Kanel, J.M. Greneche, H. Choi, Arsenic(V) removal from ground water using nano scale zero-valent iron as a colloidal reactive barrier material, *Environ. Sci. Technol.* 40 (2006) 2045–2050.
- [27] Y. Kawamura, M. Mitsuhashi, H. Tanibe, H. Yoshida, Adsorption of metal ions on polyaminated highly porous chitosan chelating resin, *Ind. Eng. Chem. Res.* 32 (1993) 386–391.
- [28] [http://en.wikipedia.org/wiki/HSAB\\_theory#Theory](http://en.wikipedia.org/wiki/HSAB_theory#Theory), 30/9/2010.
- [29] Z. Hubicki, H. Hubicka, Studies of extractive removal of silver(I) from nitrate solutions by Cyanex 471X, *Hydrometallurgy* 37 (1995) 207–219.
- [30] M. Wisniewski, Extraction of arsenic from sulphuric acid solutions by Cyanex 923, *Hydrometallurgy* 46 (1997) 235–241.
- [31] M.E.M. Perez, J.A. Reyes-Aguilera, T.I. Saucedo, M.P. Gonzalez, R. Navarro, M. Avila-Rodriguez, Study of As(V) transfer through a supported liquid membrane impregnated with trioctylphosphine oxide (Cyanex 921), *J. Membr. Sci.* 302 (2007) 119–126.
- [32] S.T. Yang, S.A. White, S.T. Hsu, Extraction of carboxylic acids with tertiary and quaternary amines: effect of pH, *Ind. Eng. Chem. Res.* 30 (6) (1991) 1335–1342.

- [33] P.R. Danesi, A simplified model for the coupled transport of metal ions through hollow-fiber supported liquid membranes, *J. Membr. Sci.* 20 (1984) 231–248.
- [34] N.S. Rathore, J.V. Sonawane, A. Kumar, A.K. Venugopalan, R.K. Singh, D.D. Bajpai, J.P. Shukla, Hollow fiber supported liquid membrane: a novel technique for separation and recovery of plutonium from aqueous acidic wastes, *J. Membr. Sci.* 189 (2001) 119–128.
- [35] M. Atanassova, Synergistic solvent extraction and separation of lanthanide(III) ions with 4-benzoyl-3-phenyl-5-isoxazolone and the quaternary ammonium salt, *Solvent Extr. Ion Exch.* 27 (2009) 159–171.
- [36] A.G. Gaikwad, Synergic transport of yttrium metal ions through supported liquid membrane, *Chem. Biochem. Eng. Q.* 17 (4) (2003) 327–334.
- [37] P. Ramakul, U. Pancharoen, Synergistic extraction and separation of mixture of lanthanum and neodymium by hollow fiber supported liquid membrane, *Korean J. Chem. Eng.* 20 (2003) 724–730.
- [38] K. Chakrabarty, K.V. Krishna, P. Saha, A.K. Ghoshal, Extraction and recovery of lignosulfonate from its aqueous solution using bulk liquid membrane, *J. Membr. Sci.* 330 (2009) 135–144.
- [39] C. Arpa, E. Basyilmaz, S. Bektas, O. Genċ , Y. Yurum, Cation exchange properties of low rank Turkish coals: removal of Hg, Cd and Pb from waste water, *Fuel Process. Technol.* 68 (2000) 111–120.
- [40] T. Francis, T. Prasada Rao, M.L.P. Reddy, Cyanex 471X as extractant for the recovery of Hg(II) from industrial wastes, *Hydrometallurgy* 57 (2000) 263–268.



- [41] R. Meera, T. Francis, M.L.P. Reddy, Studies on the liquid–liquid extraction of mercury(II) from acidic chloride solutions using Cyanex 923, *Hydrometallurgy* 61 (2001) 97–103.
- [42] M. Huebra, M.P. Elizalde, A. Almela, Hg(II) extraction by LIX 34: mercury removal from sludge, *Hydrometallurgy* 68 (2003) 33–42.
- [43] A. Jabbari, M. Esmaeili, M. Shamsipur, Selective transport of mercury as  $\text{HgCl}_4^{2-}$  through a bulk liquid membrane using  $\text{K}^+$ -dicyclohexyl-18-crown-6 as carrier, *Sep. Purif. Technol.* 24 (2001) 139–144.
- [44] C. Fontas, M. Hidalgo, V. Salvado, E. Antico, Selective recovery and preconcentration of mercury with a benzoylthiourea-solid supported liquid membrane system, *Anal. Chem. Acta* 547 (2005) 255–261.

CHAPTER III

UPHILL TRANSPORT AND MATHEMATICAL MODEL OF Pb(II) FROM  
DILUTE SYNTHETIC LEAD-CONTAINING SOLUTIONS ACROSS  
HOLLOW FIBER SUPPORTED LIQUID MEMBRANE

Sira Suren<sup>a</sup>, Thidarat Wongsawa<sup>a</sup>, Ura Pancharoen<sup>at</sup>  
Tatchanok Prapasawat<sup>b</sup>, Anchaleeporn Waritswat Lothongkum<sup>bt</sup>

<sup>a</sup> *Department of Chemical Engineering, Faculty of Engineering, Chulalongkorn University, Bangkok 10330, Thailand*

<sup>b</sup> *Department of Chemical Engineering, Faculty of Engineering, King Mongkut's Institute of Technology Ladkrabang, Chalongkrung Rd., Bangkok 10520, Thailand*

จุฬาลงกรณ์มหาวิทยาลัย  
CHULALONGKORN UNIVERSITY

---

This article has been published in Journal: Chemical Engineering Journal.

Page: 503-511. Volume: 191. Year: 2012.

---

### 3.1 Abstract

This work presents an experimental investigation and mathematical model of Pb(II) separation and stripping from relatively low-level lead-containing synthetic solutions through a hollow fiber supported liquid membrane (HFSLM) by using di-2-ethylhexyl phosphoric acid (D2EHPA) in toluene as an extractant or carrier. The separation was studied on several variables: concentration of D2EHPA, types of stripping solutions (distilled water, HNO<sub>3</sub>, H<sub>2</sub>SO<sub>4</sub> and HCl), concentration of the selected stripping solution, flow patterns of feed and stripping solutions, types of lead-containing solutions (Pb(NO<sub>3</sub>)<sub>2</sub> and PbCl<sub>2</sub>), and flow rates of feed and stripping solutions. The results remarkably showed that HFSLM could successfully reduce a very low concentration of Pb(II) in feed solution to less than the regulatory discharge limit of 0.2 mg/L issued by the Ministry of Industry and the Ministry of Natural Resource Environment, Thailand. The highest extraction and stripping results were achieved by using 0.03 M D2EHPA, 0.9 M HCl at equal flow rates of feed and stripping solutions of 100 mL/min using a single-pass of feed solution and circulating of stripping solution. High percentages of extraction and stripping were observed from both (Pb(NO<sub>3</sub>)<sub>2</sub> and PbCl<sub>2</sub> solutions. The kinetics of (Pb(NO<sub>3</sub>)<sub>2</sub> and PbCl<sub>2</sub> separation were corresponded to second-order reaction with the rate constants of 1.49 and 1.51 L/mg min, respectively. The prediction of Pb(II) concentrations in the outlet (Pb(NO<sub>3</sub>)<sub>2</sub> and PbCl<sub>2</sub> feed solutions obtaining from mathematical model were in good agreement with the experimental results at the average percent deviations of 4% for (Pb(NO<sub>3</sub>)<sub>2</sub> solution and 8% for PbCl<sub>2</sub> solution.

**Keywords:** Uphill transport; Mathematical model; Lead ions; Liquid membrane; Hollow fiber.

### 3.2 Nomenclature

$A_c$	cross-sectional area of the hollow fiber
$C_A$	concentration of lead ions
$C_{Expt.}$	experimental concentration
$C_{Theo}$	theoretical concentration from the model
$d_i$	effective module inside diameter
$d_o$	effective module outside diameter
$D_{Pb}$	diffusion coefficient of lead ions in the solution
$Expt.$	experimental value
$F_i$	inlet feed solution
$F_o$	outlet feed solution
$k_f$	reaction rate constant
$k_m$	mass transfer coefficient in membrane phase of the HFSLM
$k_s$	mass transfer coefficient in shell side of the HFSLM
$k_t$	mass transfer coefficient in tube side of the HFSLM
$L$	effective length of the hollow fiber
$M$	molecular weight of solvent
$N$	number of hollow fibers in the membrane module
$n$	reaction order
$q$	volumetric flow rate of feed and stripping solutions

$r_A$	reaction rate
Re	Reynolds number
$r_i$	internal radius of the hollow fiber
$r_o$	outside radius of the hollow fiber
Sc	Schmidt number
Sh	Sherwood number
$S_o$	outlet stripping solution
$T$	temperature
$t$	time
<i>Theo.</i>	theoretical value
$V_A$	molar volume of solute A at its boiling temperature
$x$	direction of hollow fiber axis

#### Greek letters

$\varepsilon$	porosity of the hollow fiber module
$\eta$	dynamic viscosity of solvent
$v$	linear velocity of feed solution in the tube side
$\phi$	solvent association factor
$\rho$	density of feed and stripping solutions
$\tau$	tortuosity of the hollow fiber module

### 3.3 Introduction

Lead is extensively used in many manufacturing processes, therefore without an appropriate treatment of lead-containing wastewaters it may contaminate the ecosystem through surface water, underground water and soil. As it is non-biodegradable, long-term exposures to lead or its compounds even at very low levels can affect a gene function and induce a variety of adverse physiological responses in human, nephrotoxic, neurotoxic, including carcinogenesis, reproductive and developmental defects [1,2]. As a result, to lower its impact, many countries as well as the Ministry of Industry and the Ministry of Natural Resources and Environment, Thailand have been issuing the regulatory discharge limit of lead from industrial wastewaters not higher than 0.2 mg/L [3]. Examples of the methods for lead treatment are shown in Table 3.1.

Generally, chemical precipitation, carbon adsorption, solvent extraction and ion exchange are conventional methods for metal ions separation. However, they are always ineffective at a very low concentration in ppm or ppb level, e.g., lower than 100 mg/L [12]. Furthermore, one of the main handicaps of adsorption is its powder adsorbents, which is inconvenient for recycling, and the adsorption is not a continuous process [13]. Although, adsorption is an easy operation, simple maintenance and low-energy consumption, it requires many steps, particularly common adsorbents (e.g., activated carbons, silica gel) are nonselective and suffer from long equilibrium time and mechanical and thermal stability leading to difficult application for recovery or reuse of target species. In addition, pore sizes of zeolites (size-selective adsorbent) are close to the sizes of hydrated metal ions, thus they are

not suitable for heavy metal separation [13]. In recent years, several works have been done to resolve these limitations, e.g., most of Yeung's group by using new adsorbents and surface-modified MCM-41 (LUS-type) membranes for toxic metal removal and precious metal recovery [13–16]. Chen et al. [14] reported that chitosan biosorbent showed high selectivity for gold adsorption from multi-component solutions. The residual gold concentration of 1.5 ppm was attained. Chen et al. [15] separated chromium(VI) oxyanions selectively from various aqueous systems by magnetic MCM-41 nanosorbents. However, the remaining concentration of chromium(VI) oxyanions in the sample of 4.8 ppm was still over water-quality standard. Thus, supported liquid membrane, particularly hollow fiber supported liquid membrane (HFSLM), is also an alternative method to cope with the drawbacks of the conventional methods, and the constraint due to very low-level metal concentration. The HFSLM is a secondary treatment using after the conventional methods to reduce the trace metal concentrations to meet the mandatory water-quality standards. In case of precious metal ions, it is in practice to recover as the HFSLM system combines simultaneous separation and recovery steps in one single-step operation that makes the process very compact [17,18]. As an intraphase-mass-transfer process at low capital and operating costs without the energy-intensive step of creating or introducing a new phase [19,20], the HFSLM can be applied for industrial applications such as food and biological processing [21–23] and industrial water treatment [24–27]. Recent development and commercialization of hydrophobic hollow fiber membrane contactors to use a porous support and to reach high membrane surface area per unit volume with satisfactory membrane stability was reported by Kocherginsky et al. [21]. High surface area of these systems

gives the sufficient separation rates for industrial purposes. This technology is easily scalable and payback time is decreased with the plant size increase. For a large scale capacity or industrial purposes, the hollow fiber modules are connected consecutively in series or parallel and able to reduce a very low concentration of metal ions to a regulatory environmental acceptance permits [28,29]. The literature reviews on metal ions separation by using HFSLM are described in Table 3.2.

**Table 3.** 1Examples of lead ions removal methods.

Methods	Metal ions (conc. in mg/L)	Feed solutions	Reducing agents	% Separation	Refs.
ACM	Pb(II) (10) Cd(II) (10)	Synthetic water	D2EHPA	≈100	[4]
Precipitation	Pb, Cu, Cr, and Zn (100 each)	Synthetic water	Lime	≈100	[5]
PIM	Pb(II) (120)	Synthetic water	D2EHPA	99	[6]
Biomaterial	Pb(II) (100)	Wastewater from lead acid battery recharge unit	AC of Biomaterial	98	[7]
ELM	Pb(II) (4.2)	Wastewater from storage battery industry	D2EHPA	98	[8]
Adsorption	Pb(II) (250) Cd(II) (50)	Synthetic water	Clay	96 (Pb) 78 (Cd)	[9]
BLM	Pb(II) (20.72)	Synthetic water	BzA12C4+Oleic	95	[10]
IE	Pb(II) (14.45) Hg(II) (0.85) Cd(II) (2.95)	Wastewater from mining industry plant	Low rank coal	75 (Pb) 73 (Hg) 67 (Cd)	[11]

*Note:* AC, activated carbon; ACM, activated composite membrane; PIM, polymer inclusion membrane; ELM, emulsion liquid membrane; BLM, bulk liquid membrane; IE, ion exchange.



**Table 3.** Literature reviews on metal ions removal by HFSLM.

Authors	Initial ion concentration (mg/L)	Extractants/ Stripping solutions	% Separation
Guell et al. [24]	Cr(VI):	Aliquat 336/ HNO <sub>3</sub>	
	in electroplating rinse water (0.12)		90
	in spiked river water (0.15)		81
	in spiked tap water (0.0132)		78
Ansari et al. [25]	Am(III) in wastewater from Bhabha Atomic Research Centre (n/a)	Mixture of TODGA and DHOA/ distilled water	≈ 100
	As (3.984) and Hg(II) (0.279)	Mixture of Aliquat 336 and Cyanex 471/ thiourea	≈ 100 (Hg) 94 (As)
Lothongkum et al. [26]	in produced water		
Rathore et al. [27]	Pu(IV) in acidic waste from nuclear chemical facility (8)	TBP/ NH <sub>2</sub> OH·HCl in HNO <sub>3</sub>	90
Fontas et al. [30]	Hg(II) in synthetic water,	N-benzoyl-N',N'-	≈ 100
	sea water (10)	diheptadecylthiourea/ thiourea	
Pancharoen et al. [31]	Hg(II) in produced water (1.248)	TOA/ NaOH	≈ 100
Yang et al. [32]	Cu(II) in spent ammoniacal etching solution (150,000)	LIX 54/ H <sub>2</sub> SO <sub>4</sub>	≈ 100
Lothongkum et al. [33]	U(VI) in trisodium phosphate from monazite processing (45)	Mixture of TBP and Aliquat 336/ HNO <sub>3</sub>	99
Pancharoen et al. [34]	As(III) in produced water (1.2842)	Aliquat 336/ NaOH	91
Lothongkum et al. [35]	Ni(II) in wastewater from the stainless steel industry (8.12)	LIX 860-I/ H <sub>2</sub> SO <sub>4</sub>	87
Usapein et al. [36]	Cr(VI) spent pickling solution (342.2)	Aliquat 336/ NaCl	70
Kumar et al. [37]	Au(I) synthetic water (5000)	Mixture of TOPO and LIX 79/ NaOH	80

Despite the numerous advantages, a major limitation in applying HFSLM is fouling of suspended or dissolved substances and/or non-dissolved substances on the surface of the hollow fibers or deposition inside pore mouths of the hollow

fibers. It is noted that membrane stability depends largely on nature and concentration of solutes and solvents, molecular structure of the extractant, membrane type, pore structure and pore size distribution, surface characteristics, and material of membranes [38,39]. Authors such as Neplenbroek et al. [40] studied the instability effects on supported liquid membranes. Thus, to control fouling and enhance membrane stability for industrial use, a careful choice of membrane conditions and materials is significant. Different approaches have been used separately or in combination: feed pretreatment, membrane surface modification, back flushing, pulsing, membrane cleaning, etc. [38,41].

The present work studies the effects of parameters which influence the effectiveness separation of low-level lead ions of 1 mg/L from synthetic solutions by HFSLM. Di-2-ethylhexyl phosphoric acid (D2EHPA) was selected as the extractant due to high lead extractability based on previous literature [4,6,8,42]. Finally, the experimental data of Pb(II) concentrations in outlet feed solution after treatment were compared with the results from the mathematical model based on hollow fiber system.

### 3.4 Theoretical background

#### 3.4.1 Mathematical model for Pb(II) uphill transport through the hollow fiber system

Wastewaters contaminated by lead ions are mostly generated from battery manufacturing industries, activities of offshore oil and gas production, production of lead compounds and pigments [7,8,43]. To develop a mathematical model

describing mass transport across the hollow fiber module, synthetic wastewater solutions of  $\text{Pb}(\text{NO}_3)_2$  and  $\text{PbCl}_2$  were represented feed solutions. Feed and stripping solutions in the HFSLM operation are separated by the supported liquid membrane embedded with an organic extractant. For schematic mass transport in Figure 3.1,  $\text{Pb}(\text{II})$  in feed solution as target ions reacts with the organic extractant ( $\text{D2EHPA}$ ,  $\overline{\text{HR}}$ ) at the feed-membrane interface to form complex species ( $\overline{\text{PbR}_2}$ ). Subsequently, the complex species diffuse across the liquid membrane to the membrane-stripping interface and react with the stripping solution. As a result,  $\text{Pb}(\text{II})$  releases into the stripping phase, while the free anions of  $\overline{\text{HR}}$  combine with the hydrogen ions in the stripping solution and diffuse back to the feed-membrane interface to react again with free ion of  $\text{Pb}(\text{II})$ . Over a period of time, as long as the concentration of hydrogen ion in the stripping solution is higher than that in feed solution, the continuous transport of  $\text{Pb}(\text{II})$  from feed solution across the membrane to stripping solution can occur despite higher  $\text{Pb}(\text{II})$  concentration in the stripping solution. This is referred to as the uphill transport [28,44].

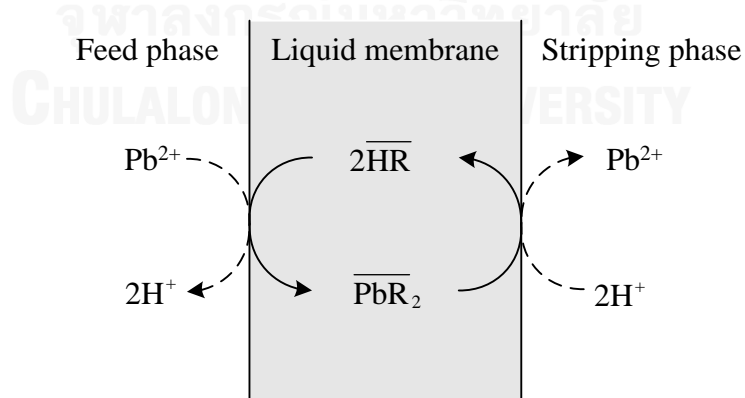
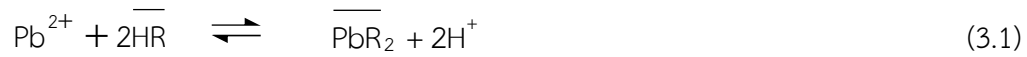


**Figure 3. 1** Schematic mechanisms of the extraction and stripping of  $\text{Pb}(\text{II})$  by using D2EHPA as the extractant and HCl as the stripping solution.

The extraction of Pb(II) from feed solution by D2EHPA is shown in Eq. (3.1).



The overbar denotes the species in the organic liquid membrane phase.

The complex species,  $\overline{\text{PbR}_2}$ , react continuously with hydrogen ion at the membrane-stripping interface to strip Pb(II) to the stripping phase as follows:



Eq. (3.1) can be simplified as follows:



where, A is lead ion, B is extractant (HR), C is complex species, D is hydrogen ion.  $a$ ,  $b$ ,  $c$  and  $d$  represent stoichiometric coefficients. Thus, the reaction rate ( $r_A$ ) is

$$r_A = -k_f C_A^n(x, t) \quad (3.4)$$

where  $C_A$  is concentration of lead ions (mg/L);  $k_f$  is the reaction rate constant;  $n$  is reaction order;  $x$  is direction of hollow fiber axis (dm); and  $t$  is time (min).

According to the hollow fiber model derived by Pancharoen et al. [45], the mass balance in hollow fiber can be described as follows:

$$-\frac{q}{A_c} \frac{\partial C_A(x,t)}{\partial x} + r_A(x,t) = \frac{\partial C_A(x,t)}{\partial t} \quad (3.5)$$

where  $q$  is volumetric flow rate (mL/min) and  $A_c$  is cross-sectional area of the hollow fiber (dm<sup>2</sup>).

In the case of  $n \neq 0, 1$ , Eq (3.5) can be:

at initial condition ( $t = 0$ )

$$C_A(x,0) = \left[ C_A^{1-n}(0,0) + \frac{(n-1)k_f A_c}{q} x \right]^{\frac{1}{1-n}} \quad (3.6)$$

at any time  $t$  ( $t \neq 0$ )

$$\bar{C}_A(L,t) = e^{-\beta} \bar{C}_A(L,t - \tau_0) \cdot u(t - \tau_0) \quad (3.7)$$

where

$$\bar{C}_A(x,t) = C_A(x,t) - C_A(x,0)$$

$$\beta = \left( \frac{A_c k_f n}{q \gamma} \right) \ln \left( \frac{L \gamma + \lambda}{\lambda} \right)$$

$$u(t - \tau_0)$$

$$\gamma = \frac{(n-1)A_c k_f}{q}$$

$$\lambda = C_A^{1-n}(0,0)$$

$L$  is an effective length of the hollow fiber (cm) and  $u(t - \tau_0)$  is a unit function.

The percentage of deviation can be calculated by Eq. (3.8)

$$\% \text{Deviation} = \frac{\sum_{i=1}^j \left( \frac{C_{\text{Expt.}} - C_{\text{Theo.}}}{C_{\text{Expt.}}} \right)_i}{j} \times 100 \quad (3.8)$$

$C_{\text{Expt.}}$  and  $C_{\text{Theo}}$  in mg/L are concentrations obtaining from the experiment and the model.

### 3.4.2 The mass transfer coefficients

Mass transfer coefficients in the tube side ( $k_t$ ), membrane phase ( $k_m$ ) and shell side ( $k_s$ ) of the HFSLM can be determined based on empirical correlations [46,47].

The mass transfer coefficient in the tube side with laminar flow of feed solution can be calculated as:

$$k_t = \frac{1.62D_{pb}}{2r_i} \times \left( \frac{4r_i^2 \nu}{D_{pb}L} \right)^{1/3} \quad (3.9)$$

where  $D_{pb}$  is the diffusion coefficient of lead ions in the solution and can be approximated by the equation of Wilke and Chang [48] as shown in Eq. (3.10);  $r_i$  is internal radius of the hollow fiber (cm);  $\nu$  is the linear velocity of feed solution in the tube side (cm/s).

$$D_{pb} = \frac{7.4 \times 10^{-8} (\phi M)^{1/2} T}{\eta V_A^{0.6}} \quad (3.10)$$

where  $\phi$  is the solvent association factor which is equal to 2.6;  $M$  is the molecular weight of the solvent (g/mol);  $T$  is the temperature (K);  $\eta$  is the dynamic viscosity of the solvent (cP);  $V_A$  is the molar volume of solute A at its boiling temperature (cm<sup>3</sup>/mol).

The mass transfer coefficient in the membrane phase can be approximated as follows:

$$k_m = \frac{\varepsilon D_{pb}}{r_i \tau \ln(r_o / r_i)} \quad (3.11)$$

where  $\varepsilon$  is porosity of the hollow fiber;  $\tau$  is tortuosity of the hollow fiber;  $r_o$  is outside radius of the hollow fiber.

The mass transfer coefficient in the shell side can be determined by the shell side mass transfer correlations in a cross-flow module which was developed by Schonert et al. [49] as shown below:

$$\text{Sh} = \frac{k_s(d_o^2 - d_i^2 - 4Nr_o^2)}{2D_{pb}Nr_o} \quad (3.12)$$

where Sh is Sherwood number;  $d_o$  and  $d_i$  are effective module outside and inside diameters;  $N$  is number of fibers in the membrane module.

The Sherwood number can be determined by the following correlation [47]:

$$\text{Sh} = 1.76\text{Re}^{0.82}\text{Sc}^{0.33} \quad (3.13)$$

where

$$\text{Re} = \frac{q\rho(d_o + d_i)\ln(d_o/d_i)}{\pi\eta LNr_o} \quad (3.14)$$

$$\text{Sc} = \frac{\eta}{\rho D_{pb}} \quad (3.15)$$

Re and Sc are Reynolds and Schmidt numbers, and  $\rho$  is density of feed and stripping solutions.



### 3.5 Experimental

#### 3.5.1 Reagents

AR grades of D2EHPA as the extractant, toluene (99.5%), and the stripping solutions ( $\text{HNO}_3$ ,  $\text{H}_2\text{SO}_4$  and  $\text{HCl}$ ) were obtained from Merck Ltd.  $\text{Pb}(\text{NO}_3)_2$  and  $\text{PbCl}_2$  for feed solutions were obtained from Merck Ltd. and Sigma–Aldrich Co. LLC.

**Table 3. 3** Characteristics of the hollow fiber module

Characteristics	Descriptions
Material	Polypropylene
Module diameter	6.3 cm
Module length	20.3 cm
Number of hollow fibers	10,000
Inside diameter of the hollow fiber	240 $\mu\text{m}$
Outside diameter of the hollow fiber	300 $\mu\text{m}$
Effective length of the hollow fiber	15 cm
Contact area	1.4 $\text{m}^2$
Area per unit volume	29.3 $\text{cm}^2/\text{cm}^3$
Pore size	0.03 $\mu\text{m}$
Porosity	25%
Tortuosity	2.6

### 3.5.2 Apparatus

The single-module HFSLM operation in this study, shown in Figure 3.2, consisted of a hollow fiber module, two gear pumps, two rotameters with variable flow rate controllers, and four pressure gauges as seen in Figure 3.2. The hollow fiber module was Celgard® microporous polypropylene fibers woven into fabric and wrapped around a central-tube feeder to supply the shell side fluid. The characteristics of the hollow fiber module are listed in Table 3.3. The magnetic stirrer (model CMT-V1) from Protronics Intertrade Co., Ltd. was used for stir feeding and stripping solutions. The Pb(II) concentrations were analyzed by atomic absorption spectrometer (AAS, model AA280FS) from Unicam Ltd.

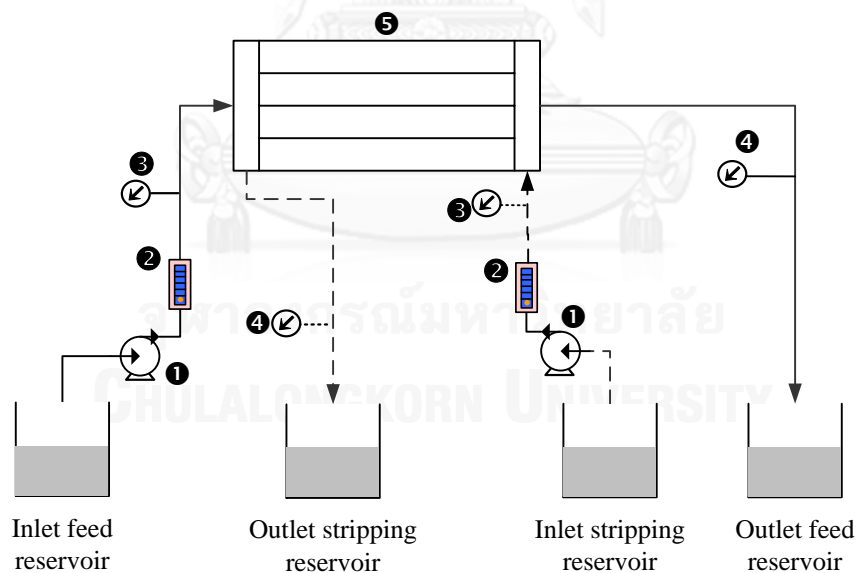


**Figure 3. 2** Schematic diagram of separation via HFSLM by counter-current continuous flow of feed and stripping solutions: (1) gear pumps, (2) flow meters, (3) inlet pressure gauges, (4) outlet pressure gauges, (5) hollow fiber module.

### 3.5.3 Procedures

Synthetic wastewater (feed solution) was prepared by dissolving  $\text{Pb}(\text{NO}_3)_2$  or  $\text{PbCl}_2$  in distilled water. D2EHPA was selected as the extractant. D2EHPA dissolving in 500 mL of toluene (liquid membrane phase) was circulated along shell and tube sides of the hollow fiber module for 25 min to assure perfect trapping in the micropores of the hollow fibers. Distilled water was subsequently fed through the hollow fibers to remove the excess liquid membrane. The separation was studied on the following variables: concentration of D2EHPA, types of stripping solutions (distilled water,  $\text{HNO}_3$ ,  $\text{H}_2\text{SO}_4$  and  $\text{HCl}$ ), concentration of the selected stripping solution, flow patterns of feed and stripping solutions, types of lead-containing solutions ( $\text{Pb}(\text{NO}_3)_2$  and  $\text{PbCl}_2$ ), and flow rates of feed and stripping solutions. To study the effects of concentration of D2EHPA, types of stripping solutions and concentration of the selected stripping solution, the single-pass modes using 1 L of feed and stripping solutions were applied. Feed and stripping solutions (10 mL each) were sampled at 10 min to analyze  $\text{Pb}(\text{II})$  concentrations by the AAS. In the case of flow patterns and flow rates of feed and stripping solutions, and types of lead-containing solutions, the single-pass and the circulating modes were used. Feed and stripping solutions were sampled at every 10 min up to 70–80 min. Three experiments were made for each variable and the results were averaged. The reaction order and rate constant were estimated from  $\text{Pb}(\text{II})$  extraction by the circulating modes using equal volumes of  $\text{Pb}(\text{NO}_3)_2$  and  $\text{PbCl}_2$  feed solutions, and the selected concentration of D2EHPA. The average results from the experiments were compared with those from the mathematical model.

### 3.6 Results and discussion

#### 3.6.1 Effect of extractant concentration

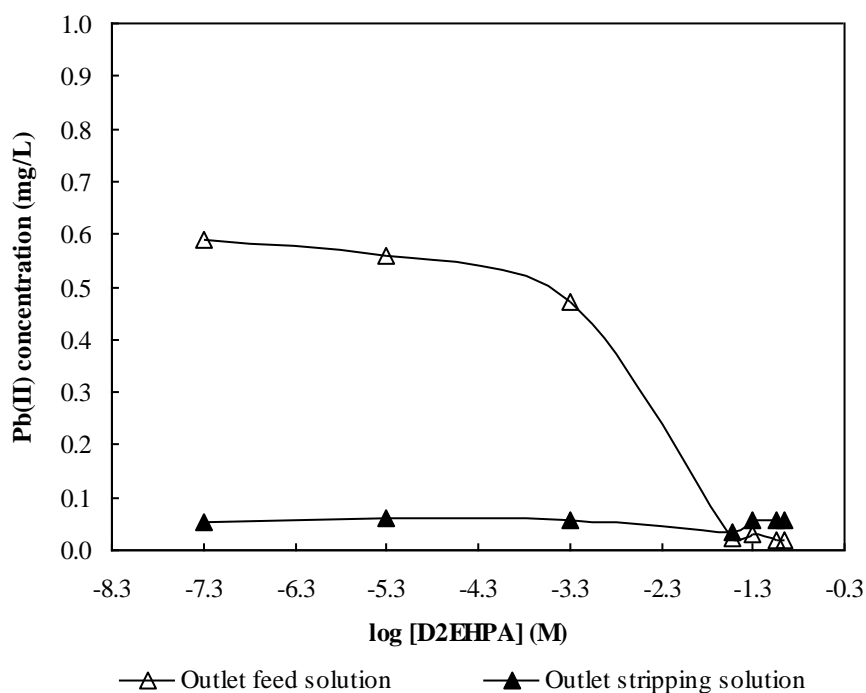


**Figure 3. 3** Pb(II) concentration in feed and stripping solutions against concentration of D2EHPA at continuous feed and stripping solutions of 100 mL/min (1 mg/L  $\text{Pb}(\text{NO}_3)_2$  and 0.5 M  $\text{HNO}_3$ ).

As shown in Figure 3.3, the concentration of Pb(II) in outlet feed solution decreased with the concentration of D2EHPA. This corresponded to Le Chatelier's principles that the increase in extractant concentration resulted in higher fluxes, subsequently the flux decreased apparently because the increase in film viscosity became dominant and obstructed mass transfer. The initial Pb(II) concentration of 1 mg/L in feed solution decreased to 0.03 mg/L at a concentration of D2EHPA up to

0.03 M ( $\log [D2EHPA] = -1.52$ ). Thus, 0.03 M of D2EHPA was used in the following studies on other variables.

### 3.6.2 Effects of stripping solutions

Distilled water,  $HNO_3$ ,  $H_2SO_4$  and HCl of 0.5 M were investigated to determine a suitable stripping solution. The role of the stripping solution is providing hydrogen ions for continuous uphill transport. The results are shown in Figure 3.4. HCl was found to be the best stripping solution for Pb(II) while distilled water showed an opposite result. This attributed to lower pH of the stripping phase or more hydrogen ions by acid stripping solutions ( $HNO_3$ ,  $H_2SO_4$  and HCl) resulting in higher mass transport. Hydrogen ions in acid stripping solutions reacted with the complex species  $\overline{PbR_2}$  in liquid membrane at the membrane-stripping interface to  $Pb(NO_3)_2$  and  $PbSO_4$  in case of using  $HNO_3$ ,  $H_2SO_4$ . Correspondingly, the  $Pb(NO_3)_2$  and  $PbSO_4$  in the stripping solution dissociated to  $Pb^{2+}$  and subsequently reacted with the extractant ( $\overline{HR}$ ), a reversible reaction in Eq. (3.2), leading to a decrease in  $Pb^{2+}$  in the stripping solution. In case of HCl, hydrogen ions reacted with  $\overline{PbR_2}$  to  $PbCl_2$ . With excess HCl concentration,  $PbCl_2$  continued converting to undissociated  $PbCl_4^{2-}$  [50], which could not react with the extractant ( $\overline{HR}$ ). As a result, compared to  $HNO_3$  and  $H_2SO_4$ , higher amount of Pb(II) in the stripping phase was observed. Therefore, HCl was selected as the stripping solution for further studies on other relevant variables.

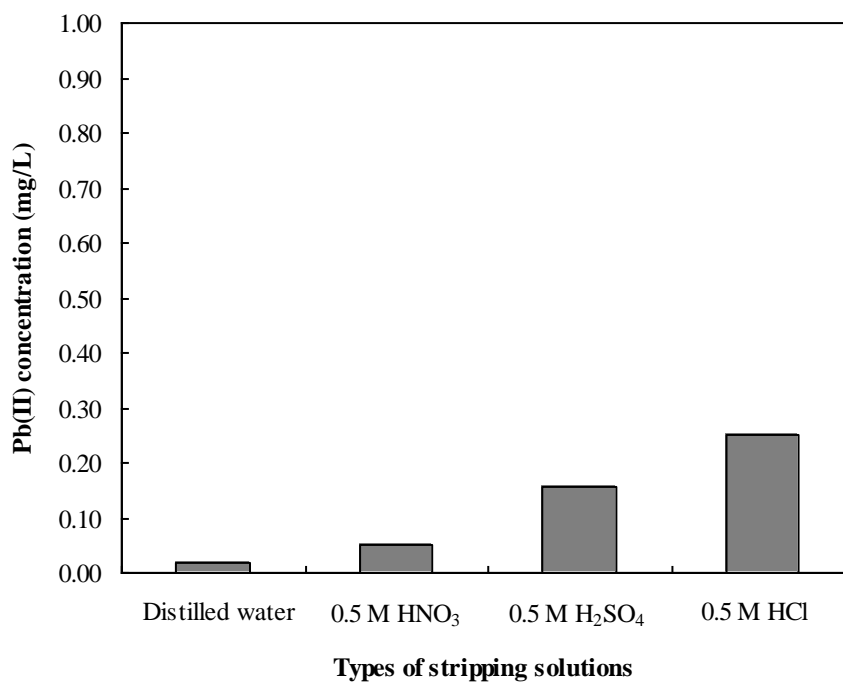


**Figure 3. 4** Pb(II) concentration in stripping solution against types of stripping solutions at continuous feed and stripping solutions of 100 mL/min (1 mg/L Pb(NO<sub>3</sub>)<sub>2</sub> and 0.03 M D2EHPA).

### 3.6.3 Effect of stripping solution concentration

The effect of the concentration of stripping solution was studied by varying HCl concentration from  $5 \times 10^{-6}$  to 0.9 M using single-pass flow patterns of feed and stripping solutions. From Figure 3.5, the amount of Pb(II) stripped by HCl increased with HCl concentration. This corresponded to the chemical kinetics that the tripping rate of Pb(II) increased with HCl concentration. However, for a longer lifetime of polypropylene hollow fibers, 0.9 M of HCl was recommended.

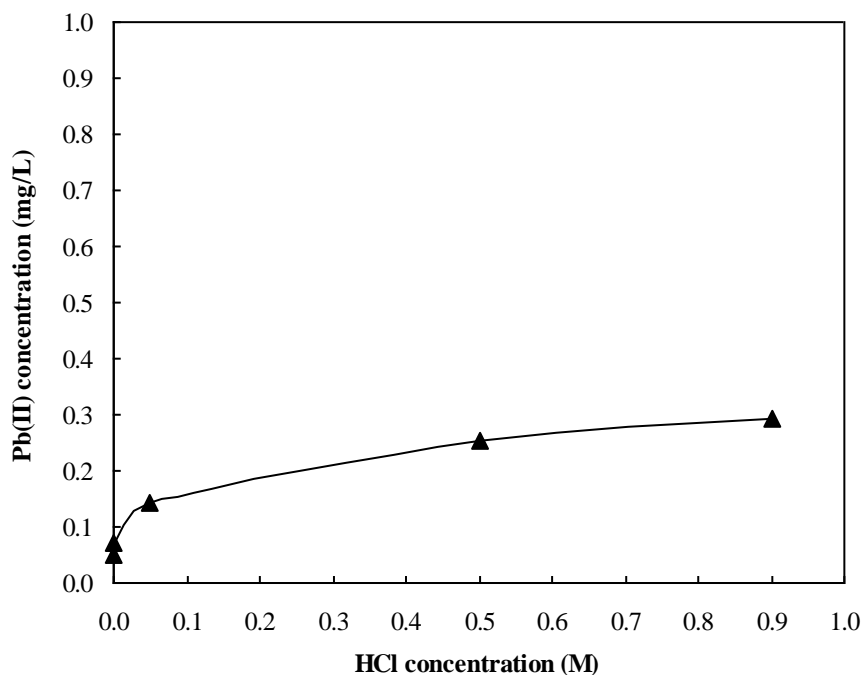
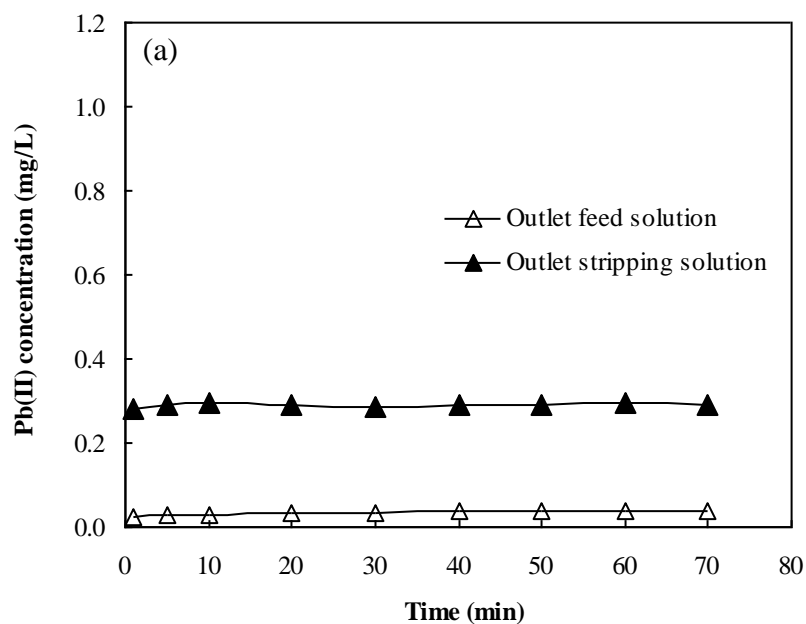


**Figure 3. 5** Pb(II) concentration in stripping solution against HCl concentration at continuous feed and stripping solutions of 100 mL/min (1 mg/L Pb(NO<sub>3</sub>)<sub>2</sub> and 0.03 M D2EHPA).

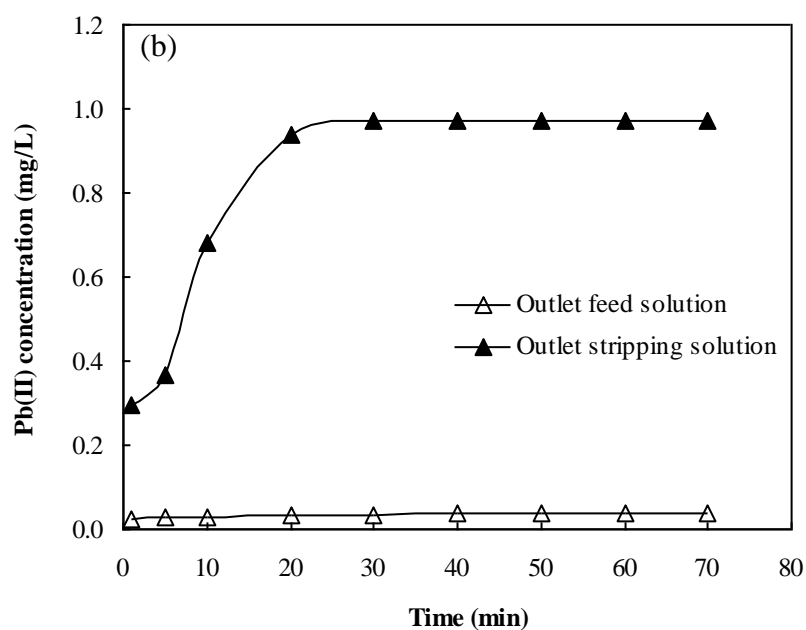
#### 3.6.4 Effects of flow patterns of feed and stripping solutions

The effects of three types of flow patterns of feed and stripping solutions (single-pass of feed and stripping solutions, circulating of feed and stripping solutions, and single-pass of feed solution and circulating of stripping solution) were investigated. For single pass and circulating operations, 7 L and 1 L of the solutions were used, respectively. Equal flow rates of feed and stripping solutions of 100 mL/min were applied to avoid a leakage of liquid membrane due to unbalanced pressure. In fact, single-pass flow pattern generally consumed a large amount of the solution and provided short residence time. Although the extraction reaction was

fast, the stripping reaction took a longer time due to high mass transfer resistance. Thus, for high performance extraction and stripping but less-solution consumption, the circulating mode was used.

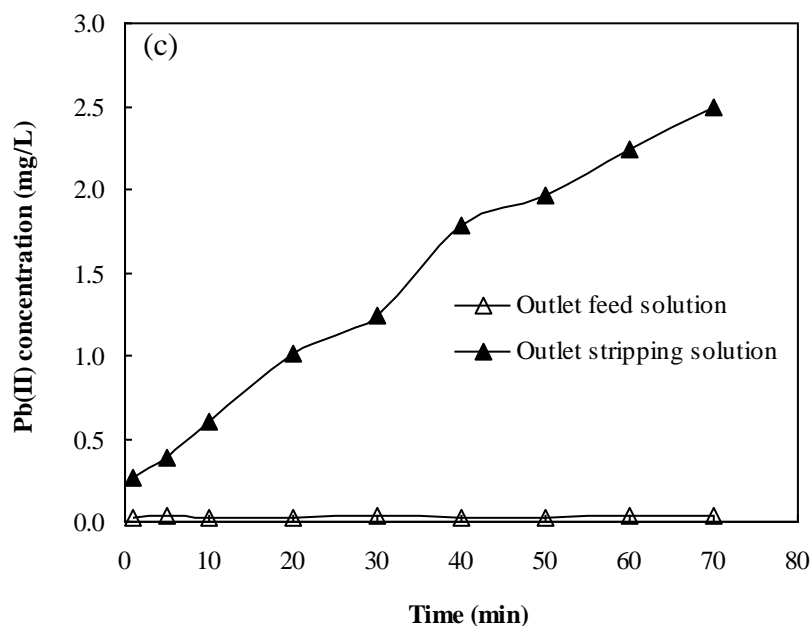


Single-pass of feed and stripping solutions



Circulating of feed and stripping solutions





Single-pass of feed solution and circulating of stripping

**Figure 3. 6** Pb(II) concentration of different flow patterns of feed and stripping solutions at equal flow rates of 100 mL/min against time (1 mg/L Pb(NO<sub>3</sub>)<sub>2</sub>, 0.03 M D2EHPA, 0.9 M HCl).

The results were shown in Figure 3.6(a)–(c). By a single-pass flow pattern of stripping solution, in Figure 3.6(a), Pb(II) could be stripped only 0.29 mg/L, but in Figure 3.6(b)–(c) by using circulating stripping solution at the same operating time, the amounts of stripped Pb(II) were comparatively higher (particularly at the operating time >10 min). This is because of the accumulation of Pb(II) in the circulating stripping solution. These results agreed with Rathore et al. [27] using circulating feed and stripping solutions for the separation of Pu(IV) from acidic wastes via HFSLM. As shown in Figure 3.6(b), by using circulating feed and stripping solutions, Pb(II) of 1 mg/L in feed solution was almost totally stripped in 20 min. For single-pass feed solution and circulating stripping solution, as shown in Figure 3.6(c), Pb(II) was totally stripped in 20 min. The amount of Pb(II) in the stripping solution kept increasing

continuously with time and was apparently higher than in feed solution due to excess HCl and the continuing Pb(II) accumulation. Therefore, it is recommended to use the single-pass flow pattern of feed solution and circulating flow pattern of stripping solution to attain high separation and stripping.

### 3.6.5 Effects of lead species

Pb(NO<sub>3</sub>)<sub>2</sub> and PbCl<sub>2</sub> solutions were selected to study because these compounds mostly contaminated in wastewaters. As seen in Figure 3.7, Pb(II) in both solutions could react well with D2EHPA and decreased to about 0.03 mg/L in 80 min. The maximum concentration of Pb(II) in the stripping solution of about 3.07 mg/L was achieved accordingly.

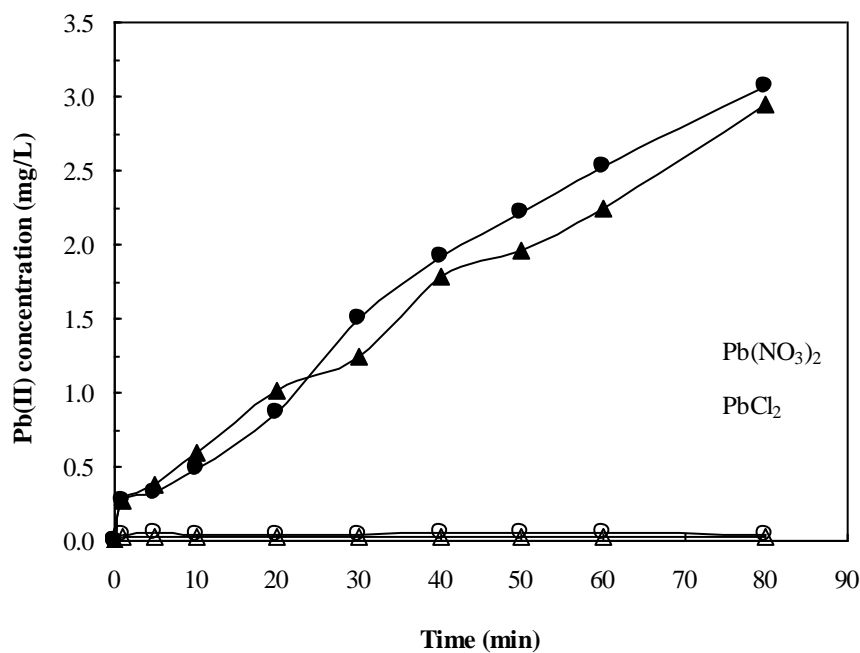


**Figure 3. 7** Pb(II) concentration in outlet Pb(NO<sub>3</sub>)<sub>2</sub> and PbCl<sub>2</sub> feed solutions and stripping solution against time of continuous feed solution and circulating stripping

solution at equal flow rates of 100 mL/min (0.03 M D2EHPA, 0.9 M HCl, blank symbol: outlet feed solution, bold symbol: outlet stripping solution).

### 3.6.6 Effects of flow rates of feed and stripping solutions

Equal flow rates of the single-pass feed solution and circulating stripping solution were varied from 60 to 400 mL/min. The effects of the flow rates were shown in Figure 3.8. The concentrations of Pb(II) in  $\text{Pb}(\text{NO}_3)_2$  and  $\text{PbCl}_2$  solutions were nearly constant. Percentages of Pb(II) extraction from both solutions were 96–97%. The concentrations of Pb(II) in stripping solutions were almost constant up to 100 mL/min and slowly decreased with higher flow rates of feed and stripping solutions due to less residence time same as stated by Uedee et al. [51]. According to this work for high extraction, high Pb(II) concentration in stripping solution and less separation time, the flow rates of feed and stripping solutions of 100 mL/min were approached.

### 3.6.7 Reaction order and reaction rate constant

The reaction order and rate constant in Eq. (3.4) were determined by integration and graphical method. The results from the plots between integral concentration of Pb(II) in feed solution ( $1/C_A - 1/C_{A0}$ ) versus time, shown in Table 3.4, represented the second-order reaction of highest  $R^2$ . The reaction rate constants of 1.49 L/mg min for  $\text{Pb}(\text{NO}_3)_2$  solution and 1.51 L/mg min for  $\text{PbCl}_2$  solution were obtained.

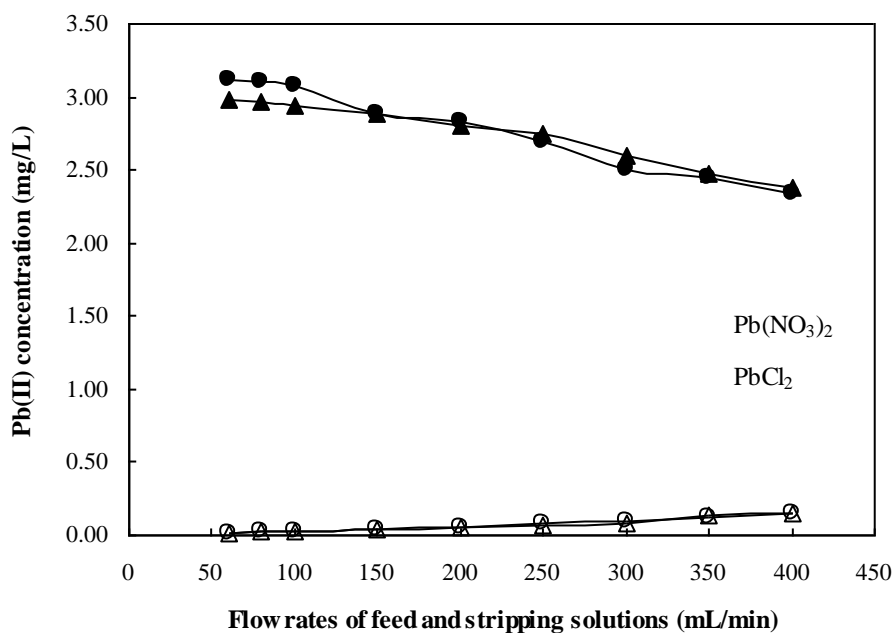


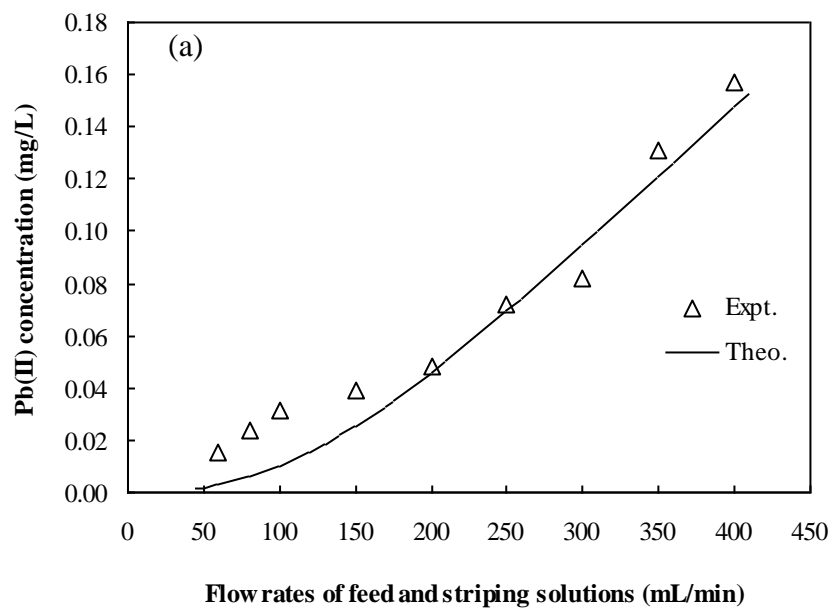
**Figure 3. 8** Pb(II) concentration in outlet feed and stripping solutions against flow rates of feed and stripping solutions of continuous feed solution and circulating stripping solution (0.03 M D2EHPA, 0.9 M HCl, blank symbol: outlet feed solution, bold symbol: outlet stripping solution).

**Table 3. 4** Reaction order ( $n$ ) and reaction rate constant ( $k_f$ ).

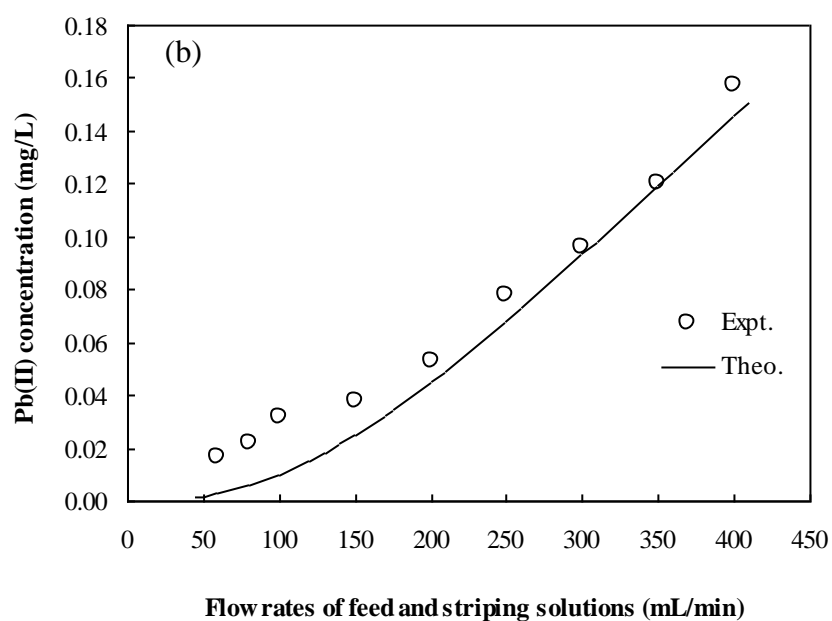
n	Plot of	$k_f$		$R^2$	
		Pb(NO <sub>3</sub> ) <sub>2</sub>	PbCl <sub>2</sub>	Pb(NO <sub>3</sub> ) <sub>2</sub>	PbCl <sub>2</sub>
1	$\ln(C_{A0}/C_A)$ and time	0.56 min <sup>-1</sup>	0.57 min <sup>-1</sup>	0.5641	0.5667
2	$1/C_A - 1/C_{A0}$ and time	1.49 L/mg min	1.51 L/mg min	0.9838	0.9788
3	$1/(2C_A^2) - 1/(2C_{A0}^2)$ and time	4.85 L <sup>2</sup> /mg <sup>2</sup> min	4.00 L <sup>2</sup> /mg <sup>2</sup> min	0.8590	0.8263

### 3.6.8 Prediction of Pb(II) concentration by mathematical model

Figure 3.9 shows the experimental Pb(II) concentration in  $\text{Pb}(\text{NO}_3)_2$  and  $\text{PbCl}_2$  solutions and theoretical values calculated by Eqs. (3.6) and (3.7). The results estimated by mathematical model based on hollow fiber system fitted well with the experimental results at average percentage of deviation about 4% for  $\text{Pb}(\text{NO}_3)_2$  solution and 8% for  $\text{PbCl}_2$  solution. Nevertheless, the model was unsatisfactory at flow rates of feed and stripping solutions lower than 200 mL/min. Because the lower flow rates generated the lower shear force and increased the mass transfer resistance [52]. In other words, mass transfer in terms of the diffusion in tube and shell sides decreased with flow rates of the solutions. As a result, the experimental results of Pb(II) concentration observed from outlet feed solutions at flow rates lower than 200 mL/min were higher than the values from the model, which did not consider the mass transfer resistance due to diffusion, as shown in Figure 3.9. From Table 3.5, at the flow rates of feed and stripping solutions of 60–400 mL/min, mass transfer coefficients in tube and shell sides increased gradually while the residence time extremely decreased. Hence, the separation of Pb(II) from  $\text{Pb}(\text{NO}_3)_2$  and  $\text{PbCl}_2$  solutions decreased gradually with flow rates higher than 200 mL/min. This corresponded to Yang et al. that described detailed theoretical mechanisms of the facilitated transport of Cu(II) from ammonium wastewater through HFSLM of which its mass transfer in tube sides decreased with flow rate of feed solution [32].



Pb(NO<sub>3</sub>)<sub>2</sub> solution



PbCl<sub>2</sub> solution

**Figure 3. 9** Outlet Pb(II) concentration in Pb(NO<sub>3</sub>)<sub>2</sub> and PbCl<sub>2</sub> solutions of continuous feed solution and circulating stripping solution against equal flow rates of feed and stripping solutions (0.03 M D2EHPA, 0.9 M HCl).

**Table 3. 5** Influences of equal flow rates of feed and stripping solutions on mass transfer coefficients.

Flow rate, $q$ (mL/min)	Residence time (s)	Mass transfer coefficients ( $10^4$ cm/s)		
		Tube side, $k_t$	Liquid membrane, $k_m$	Shell side, $k_s$
60	238	8.3	18	0.32
80	178	9.7	18	0.47
100	143	11.1	18	0.50
150	95	12.0	18	0.79
200	71	13.2	18	1.01
250	57	14.2	18	1.21
300	48	15.1	18	1.40
350	41	15.9	18	1.59
400	36	16.6	18	1.78

### 3.7 Conclusion

HFSLM using D2EHPA dissolving in toluene as the extractant can successfully reduce a relatively low concentration of Pb(II) from  $\text{Pb}(\text{NO}_3)_2$  and  $\text{PbCl}_2$  solutions (1 ppm) to meet the regulatory discharge limit of 0.2 mg/L. The highest Pb(II) extraction from both solutions (approximately 96–97%) were obtained by using 0.03 M D2EHPA as the extractant, 0.9 M HCl as the stripping solution, and single-pass flow pattern of feed solution and circulating flow pattern of stripping solution of 100 mL/min. To obtain a high concentration of Pb(II) in the stripping solution and less-solution consumption, the single-pass feed solution and circulating stripping solution are

recommended. The extraction of  $\text{Pb}(\text{NO}_3)_2$  and  $\text{PbCl}_2$  were second-order reaction with respect to the rate constants of 1.49 and 1.51 L/mg min. The final Pb(II) concentrations in outlet feed solutions predicted by mathematical model were in good agreement with the experimental results at the average percent deviation of 4% for  $\text{Pb}(\text{NO}_3)_2$  solution and 8% for  $\text{PbCl}_2$  solution.

### 3.8 Acknowledgements

The authors highly appreciate the financial supports by Thailand Research Fund and Chulalongkorn University under the Royal Golden Jubilee Ph.D. Program (grant no. PHD/0324/2551), and the Asahi Glass Foundation. Sincere thanks also go to our research group and the Separation Laboratory, Department of Chemical Engineering, Chulalongkorn University, Bangkok, Thailand.

### 3.9 References

- [1] W.J. Liu, F.X. Zeng, H. Jiang, X.S. Zhang, Adsorption of lead (Pb) from aqueous solution with *Typha angustifolia* biomass modified by  $\text{SOCl}_2$  activated EDTA, Chem. Eng. J. 170 (2011) 21–28.
- [2] M.Z. Barciszewska, M. Szymanski, E. Wyszko, J. Pas, L. Rychlewski, J. Barciszewski, Lead toxicity through the leadzyme, Mutat. Res. Rev. Mutat. Res. 589 (2005) 103–110.
- [3] Thailand regulatory discharge standards, Ministry of Industry, Thailand, 1996.



- [4] T. Gumi, M. Oleinikova, C. Palet, M. Valiente, M. Munoz, Facilitated transport of lead(II) and cadmium(II) through novel activated composite membranes containing di-(2-ethyl-hexyl)phosphoric acid as carrier, *Anal. Chim. Acta* 408 (2000) 65–74.
- [5] Q. Chen, Z. Luo, C. Hills, G. Xue, M. Tyrer, Precipitation of heavy metals from wastewater using simulated flue gas: sequent additions of fly ash, lime and carbon dioxide, *Water Res.* 43 (2009) 2605–2614.
- [6] C.-V.I. Gherasim, G. Bourceanu, R.-I. Olariu, C. Arsene, Removal of lead(II) from aqueous solutions by a polyvinyl-chloride inclusion membrane without added plasticizer, *J. Membr. Sci.* 377 (2011) 167–174.
- [7] M. Singanan, A. Abebaw, S. Vinodhini, Removal of lead ions from industrial waste water by using biomaterials – a novel method, *Bull. Chem. Soc. Ethiop.* 19 (2005) 289–294.
- [8] L. Gurel, L. Altas, H. Buyukgungor, Removal of lead from wastewater using emulsion liquid membrane technique, *Environ. Eng. Sci.* 22 (2005) 411–420.
- [9] D. Ozdes, C. Duran, H.B. Senturk, Adsorptive removal of Cd(II) and Pb(II) ions from aqueous solutions by using Turkish illitic clay, *J. Environ. Manage.* 92 (2011) 3082–3090.
- [10] A.W. Lothongkum, U. Pancharoen, T. Prapasawat, Treatment of heavy metals from industrial wastewaters using hollow fiber supported liquid membrane, in: K. Demadis (Ed.), *Water Treatment Processes*, Nova Science Publishers, Inc., 2011.

- [11] C. Arpa, E. Basyilmaz, S. Bektas, O. Genc, Y. Yurum, Cation exchange properties of low rank Turkish coals: removal of Hg, Cd and Pb from waste water, *Fuel Process. Technol.* 68 (2000) 111–120.
- [12] B. Stephen Inbaraj, J.S. Wang, J.F. Lu, F.Y. Siao, B.H. Chen, Adsorption of toxic mercury(II) by an extracellular biopolymer poly( $\gamma$ -glutamic acid), *Bioresour. Technol.* 100 (2009) 200–207.
- [13] K.F. Lam, H. Kassab, M. Pera-Titus, K.L. Yeung, B. Albela, L. Bonneviot, MCM-41 LUS: alumina tubular membranes for metal separation in aqueous solution, *J. Phys. Chem. C* 115 (2011) 176–187.
- [14] X. Chen, K.F. Lam, S.F. Mak, K.L. Yeung, Precious metal recovery by selective adsorption using biosorbents, *J. Hazard. Mater.* 186 (2011) 902–910.
- [15] X. Chen, K.F. Lam, K.L. Yeung, Selective removal of chromium from different aqueous systems using magnetic MCM-41 nanosorbents, *Chem. Eng. J.* 172 (2011) 728–734.
- [16] K.F. Lam, K.L. Yeung, G. McKay, Selective mesoporous adsorbents for  $\text{Cr}_2\text{O}_7^{2-}$  and  $\text{Cu}^{2+}$  separation, *Microporous Mesoporous Mater.* 100 (2007) 191–201.
- [17] P. Kandwal, S. Dixit, S. Mukhopadhyay, P.K. Mohapatra, Mass transport modeling of Cs(I) through hollow fiber supported liquid membrane containing calix-[4]-bis(2,3-naphtho)-crown-6 as the mobile carrier, *Chem. Eng. J.* 174 (2011) 110–116.
- [18] W. Zhang, C. Cui, Z. Ren, Y. Dai, H. Meng, Simultaneous removal and recovery of copper(II) from acidic wastewater by hollow fiber renewal liquid membrane with LIX984N as carrier, *Chem. Eng. J.* 157 (2010) 230–237.

- [19] I.M. Coelho, M.M. Cardoso, R.M.C. Viegas, J.P.S.G. Crespo, Transport mechanisms and modelling in liquid membrane contactors, *Sep. Purif. Technol.* 19 (2000) 183–197.
- [20] M.F. San Roman, E. Bringas, R. Ibanez, I. Ortiz, Liquid membrane technology: fundamentals and review of its applications, *J. Chem. Technol. Biotechnol.* 85 (2010) 2–10.
- [21] N.M. Kocherginsky, Q. Yang, L. Seelam, Recent advances in supported liquid membrane technology, *Sep. Purif. Technol.* 53 (2007) 171–177.
- [22] B.F. Jirjis, S. Luque, in: Z.F. Cui, H.S. Muralidhara (Eds.), *Practical Aspects of Membrane System Design in Food and Bioprocessing Applications*, Butterworth–Heinemann, Elsevier, USA, 2010, pp. 179–212.
- [23] F. Lipnizki, Cross-flow membrane applications in the food industry, in: K.-V. Peinemann, S.P. Nunes, L. Giorno (Eds.), *Membranes for Food Applications*, Wiley–VCH, Weinheim, Germany, 2010, pp. 1–24.
- [24] R. Guell, E. Antico, V. Salvado, C. Fontas, Efficient hollow fiber supported liquid membrane system for the removal and preconcentration of Cr(VI) at trace levels, *Sep. Purif. Technol.* 62 (2008) 389–393.
- [25] S.A. Ansari, P.K. Mohapatra, D.R. Raut, V.C. Adya, S.K. Thulasidas, V.K. Manchanda, Separation of Am(III) and trivalent lanthanides from simulated high-level waste using a hollow fiber-supported liquid membrane, *Sep. Purif. Technol.* 63 (2008) 239–242.
- [26] A.W. Lothongkum, S. Suren, S. Chaturabul, N. Thamphiphit, U. Pancharoen, Simultaneous removal of arsenic and mercury from natural-gas-co-produced

- water from the Gulf of Thailand using synergistic extractant via HFSLM, *J. Membr. Sci.* 369 (2011) 350–358.
- [27] N.S. Rathore, J.V. Sonawane, A. Kumar, A.K. Venugopalan, R.K. Singh, D.D. Bajpai, J.P. Shukla, Hollow fiber supported liquid membrane: a novel technique for separation and recovery of plutonium from aqueous acidic wastes, *J. Membr. Sci.* 189 (2001) 119–128.
- [28] U. Pancharoen, A.W. Lothongkum, S. Chaturabul, Mass transfer in hollow fiber supported liquid membrane for As and Hg removal from produced water in upstream petroleum operation in the Gulf of Thailand, in: M. El-Amin (Ed.), *Mass Transfer in Multiphase Systems and Its Applications*, InTech, India, 2011, pp. 499–524.
- [29] A.W. Lothongkum, U. Pancharoen, T. Prapasawat, Treatment of heavy metals from industrial wastewaters using hollow fiber supported liquid membrane, in: K. Demadis (Ed.), *Water Treatment Processes*, Nova Science Publishers, Inc., USA, 2012 (Section III Removal Techniques: Chapter 12).
- [30] C. Fontas, M. Hidalgo, V. Salvado, E. Antico, Selective recovery and preconcentration of mercury with a benzoylthiourea-solid supported liquid membrane system, *Anal. Chim. Acta* 547 (2005) 255–261.
- [31] U. Pancharoen, S. Somboonpanya, S. Chaturabul, A.W. Lothongkum, Selective removal of mercury as  $\text{HgCl}_4^{2-}$  from natural gas well produced water by TOA via HFSLM, *J. Alloys Compd.* 489 (2010) 72–79.
- [32] Q. Yang, N.M. Kocherginsky, Copper recovery and spent ammoniacal etchant regeneration based on hollow fiber supported liquid membrane technology: from bench-scale to pilot-scale tests, *J. Membr. Sci.* 286 (2006) 301–309.

- [33] A.W. Lothongkum, P. Ramakul, W. Sasomsub, S. Laoharochanapan, U. Pancharoen, Enhancement of uranium ion flux by consecutive extraction via hollow fiber supported liquid membrane, *J. Taiwan Inst. Chem. Eng.* 40 (2009) 518–523.
- [34] U. Pancharoen, W. Poonkum, A.W. Lothongkum, Treatment of arsenic ions from produced water through hollow fiber supported liquid membrane, *J. Alloys Compd.* 482 (2009) 328–334.
- [35] A.W. Lothongkum, Y. Khemglad, N. Usomboon, U. Pancharoen, Selective recovery of nickel ions from wastewater of stainless steel industry via HFSLM, *J. Alloys Compd.* 476 (2009) 940–949.
- [36] P. Usapein, A.W. Lothongkum, P. Ramakul, U. Pancharoen, Efficient transport and selective extraction of Cr(VI) from waste pickling solution of the stainless steel-cold rolled plate process using Aliquat 336 via HFSLM, *Korean J. Chem. Eng.* 26 (2009) 791–798.
- [37] A. Kumar, R. Haddad, G. Benzal, R. Ninou, A.M. Sastre, Use of modified membrane carrier system for recovery of gold cyanide from alkaline cyanide media using hollow fiber supported liquid membranes: feasibility studies and mass transfer modeling, *J. Membr. Sci.* 174 (2000) 17–30.
- [38] Z.F. Cui, Y. Jiang, R.W. Field, Fundamentals of pressure-driven membrane separation processes, in: Z.F. Cui, H.S. Muralidhara (Eds.), *Membrane Technology: A Practical Guide to Membrane Technology and Applications in Food and Bioprocessing*, Butterworth–Heinemann, Elsevier, UK, 2010, p. 12, 16.

- [39] M.F. San Roman, E. Bringas, R. Ibanez, I. Ortiz, Liquid membrane technology: fundamentals and review of its applications, *J. Chem. Technol. Biotechnol.* 85 (2010) 2–10.
- [40] A.M. Neplenbroek, D. Bargaen, C.A. Smolders, Supported liquid membranes: instability effects, *J. Membr. Sci.* 62 (1992) 121–132.
- [41] X.J. Yang, A.G. Fane, J. Bi, H.J. Griesser, Stabilization of supported liquid membranes by plasma polymerization surface coating, *J. Membr. Sci.* 168 (2000) 29–37.
- [42] A. Escobar, K.A. Schimmel, J. de Gyves, E.R. de San Miguel, Hollow-fiber dispersion-free extraction and stripping of Pb(II) in the presence of Cd(II) using D2EHPA under recirculating operation mode, *J. Chem. Technol. Biotechnol.* 79 (2004) 961–973.
- [43] C.E. Housecroft, A.G. Sharpe, *Inorganic Chemistry*, 2nd ed., Prentice Hall, New Jersey, 2004.
- [44] D. Nanda, M.S. Oak, B. Maiti, H.P.S. Chauhan, P.K. Dutta, Selective and uphill transport of uranyl ion in the presence of some base metals and thorium across bulk liquid membrane by di (2-ethylhexyl) phosphoric acid, *Sep. Sci. Technol.* 37 (2002) 3357–3367.
- [45] U. Pancharoen, T. Wongsawa, A.W. Lothongkum, A reaction flux model for extraction of Cu(II) with LIX84I in HFSLM, *Sep. Sci. Technol.* 46 (2011) 2183–2190.
- [46] W.J.D. Bruyn, E.S. Saltzman, Diffusivity of methyl bromide in water, *Mar. Chem.* 57 (1997) 55–59.

- [47] Q. Yang, N.M. Kocherginsky, Copper removal from ammoniacal wastewater through a hollow fiber supported liquid membrane system: modeling and experimental verification, *J. Membr. Sci.* 297 (2007) 121–129.
- [48] C.R. Wilke, P. Chang, Correlation of diffusion coefficients in dilute solutions, *AIChE J.* 1 (1955) 264–270.
- [49] P. Schoner, P. Plucinski, W. Nitsch, U. Daiminger, Mass transfer in the shell side of cross flow hollow fiber modules, *Chem. Eng. Sci.* 53 (1998) 2319–2326.
- [50] C.W. Wood, A.K. Holliday, *Inorganic Chemistry*, 3rd ed., Butterworth, England, 1967.
- [51] E. Uedee, P. Ramakul, U. Pancharoen, A.W. Lothongkum, Performance of hollow fiber supported liquid membrane on the extraction of mercury(II) ions, *Korean J. Chem. Eng.* 25 (2008) 1486–1494.
- [52] Z. Ren, W. Zhang, Y. Liu, Y. Dai, C. Cui, New liquid membrane technology for simultaneous extraction and stripping of copper(II) from wastewater, *Chem. Eng. Sci.* 62 (2007) 6090–6101.

CHAPTER IV  
SIMULTANEOUS EXTRACTION AND STRIPPING OF LEAD IONS VIA A  
HOLLOW FIBER SUPPORTED LIQUID MEMBRANE

Sira Suren, Ura Pancharoen \*, Soorathep Kheawhom \*\*

*Department of Chemical Engineering, Faculty of Engineering, Chulalongkorn  
University, Bangkok 10330, Thailand*



จุฬาลงกรณ์มหาวิทยาลัย  
CHULALONGKORN UNIVERSITY

---

This article has been published in Journal: Journal of Industrial and Engineering  
Chemistry. Page: 2584–2593. Volume: 20. Year: 2014.

---



#### 4.1 Abstract

An investigation on the separation of Pb(II) from synthetic wastewater via a hollow fiber supported liquid membrane (HFSLM) and its model is presented. Maximum percentages of Pb(II) extraction and stripping achieved were 97% and 30% using 0.03 M D2EHPA as the extractant, 0.9 M HCl as the stripping solution. The extraction and stripping of Pb(II) were second-order reaction with reaction rate constants of 0.03 and 0.19 L/mg s, respectively. A mathematical model is developed and shows that the model results fit in well with the experimental results. Average percent deviation was 3% for predictions in both feed and stripping sides.

**Keywords:** Extraction; Stripping; Lead ion; Model; HFSLM.

#### 4.2 Introduction

Many industries, in the process of manufacturing storage batteries, leaded glass, fuels, pigments, matches, photographic materials, explosives, etc. as well as offshore oil and gas industries, generate wastewater contaminated with lead [1–3]. Lead leaks continuously into the environment because of inappropriate treatment of wastewater. Lead or its compounds contaminate the ecosystem via surface water, soil and underground water. Its pollution can cause acute and chronic disease in humans [4,5]. Discharge limits for lead from industrial wastewaters are regulated by the Thailand Ministry of Industry as well as the Ministry of Natural Resources and Environment. Discharge limits for lead should not be higher than 0.2 mg/L [6].

Traditional methods currently used to remove lead ions from wastewater are precipitation, coagulation, ion exchange, solvent extraction and adsorption [7–11]. However, these methods are always ineffective when the concentration of contaminated metal ions is at a very low mM or nM level [12].

Accordingly, a hollow fiber supported liquid membrane (HFSLM) was used to separate trace metal ions from various solutions. HFSLM is an effective method for separating diluted concentrations of metal ions. This system has specific characteristics that allow simultaneous extraction and stripping processes of target ions in a single-step operation, with high selectivity [13]. HFSLM has many advantages over conventional methods. For example, it has lower energy consumption, lower capital and operating costs and less solvent is used [14]. The high surface area of the HFSLM system attains high separation rates [15]. Hollow fiber modules can be connected in series or in parallel for a larger capacity [16]. HFSLM, therefore, is most suitable to use as a secondary method in order to manage a very low concentration of metal ions.

Recently, several studies have investigated the use of HFSLM for separating various trace metal ions from aqueous solutions or wastewater. Güell et al. for instance [17], used HFSLM to separate Cr(VI) at low concentration of nM level from various aqueous matrices. The extractant used was trioctyl methyl ammonium chloride (Aliquat 336). Results showed that HFSLM was most efficient in separating Cr(VI) from various aqueous samples. The liquid membrane was found to be stable through 8 days operation non-stop. Buachuang et al. [18] investigated the separation of Ta(V) and Nb(V) from hydrofluoric media via HFSLM. The liquid membrane used

was Aliquat 336 diluted in kerosene. Optimum tantalum extraction of 80% was achieved at 3% (v/v) Aliquat 336 using 0.2 M NaClO<sub>4</sub> as stripping solution.

Mafu et al. [19] studied the separation of As(III) from wastewater via HFSLM. The liquid membrane used was the mixture of *n*-undecane and di-*n*-hexyl ether (3:1%, v/v). Stripping solution used was H<sub>2</sub>SO<sub>4</sub>. Percentage of As(III) separation achieved was 50%. Ansari et al. [20] reported that Am(II) was totally separated from synthetic wastewater by using HFSLM with 0.1 M TODGA (*N,N,N',N'*-tetraoctyl diglycolamide) and 0.5 M DHOA (*N,N*-di-*n*-hexyl octanamide) mixtures as the extractant and distilled water as the stripping solution. Furthermore, Mtibe et al. [21] separated dibutyl phthalate (DBP), benzyl butyl phthalate (BBP) and diethylhexyl phthalate (DEHP) from wastewater via HFSLM.

HFSLM is widely used for the separation of several components. Most models, however, have been established to describe the transport of target ions only on the feed side. To this end, mathematical models were developed which focus on describing the transport mechanism of target components across the liquid membrane from feed phase to stripping phase. The models aid in the scaling-up of the HFSLM system [22]. The transport of target ions across liquid membrane correspond to the following parameters i.e. diffusion transport, convection transport, mass accumulation and reaction. Some parameters, though, were neglected in order to develop and simplify the mathematical model. Examples of mathematical models developed, describing the transport of target ions, are shown in Table 4.1.

On the stripping side, mathematical models are mostly lacking since they are difficult to resolve. Chaturabul et al. [23] refined a mathematical model for feed and

stripping sides based on chemical reactions at the liquid membrane interfaces. This model, however, did not fit well with the experimental results.

**Table 4. 1** Literature reviews on mathematical model for HFSLM.

Authors	Transport ions	Extractants/ Strippings	Considered parameters				Model described in/ %deviation
			DT	CT	MA	R	
Vernekar et al. [22]	Co(II)	D2EHPA/ H <sub>2</sub> SO <sub>4</sub>	✓	✓	-	-	feed side/ n/a
Chaturabul et al. [23]	Pd(II)	TRHCl-OA/NaNO <sub>2</sub>	-	✓	✓	✓	feed and stripping sides/ ≈11% and ≈2%
Kandwal et al. [24]	Cs(I)	CNC/ distilled water	✓	✓	-	-	feed side/ n/a
Ramakul et al. [25]	Ce(IV) and La(II)	D2EHPA/ H <sub>2</sub> SO <sub>4</sub>	✓	-	-	-	feed side/ n/a
Zhang et al. [26]	Cu(II)	D2EHPA/ HCl	✓	✓	-	-	feed side/ n/a
Choi et al. [27]	Co(II) and Ni(II)	HEH/ H <sub>2</sub> SO <sub>4</sub>	✓	✓	✓	-	feed side/ n/a
Yang and Kocherginsky [28]	Cu(II)	LIX54/ H <sub>2</sub> SO <sub>4</sub>	✓	✓	-	✓	feed side/ n/a
Pancharoen et al. [29]	Cu(II)	LIX84/ H <sub>2</sub> SO <sub>4</sub>	-	✓	✓	✓	feed side/ 2%
This work	Pb(II)	D2EHPA/ HCl	-	✓	✓	✓	feed and stripping sides/ 3% for both sides

Note: DT; diffusion transport, CT; convection transport, MA; mass accumulation, R; reaction.

This work studied the separation of Pb(II) at a very low concentration from synthetic wastewater. Di-(2-ethylhexyl)phosphoric acid (D2EHPA) – which is shown to be effective for the extraction of lead ions [1,30–32] and has low solubility in acid solution [33] – was used as the extractant. Concentration of the extractant, types and concentration of the stripping solutions, types of lead-containing solutions as well as

flow rates of both feed and stripping solutions were studied. A mathematical model concerning convection transport, mass accumulation and reactions at liquid-membrane interfaces was improved to predict Pb(II) concentration in both feed and stripping phases. The model equation was verified by the results obtained from the experiment.

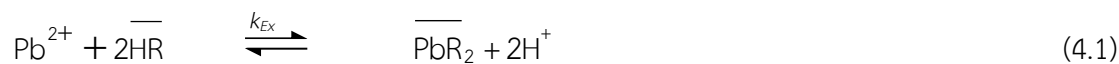
### 4.3 Modeling of lead ion transport

#### 4.3.1 Mechanism of lead ion transport across the liquid membrane phase

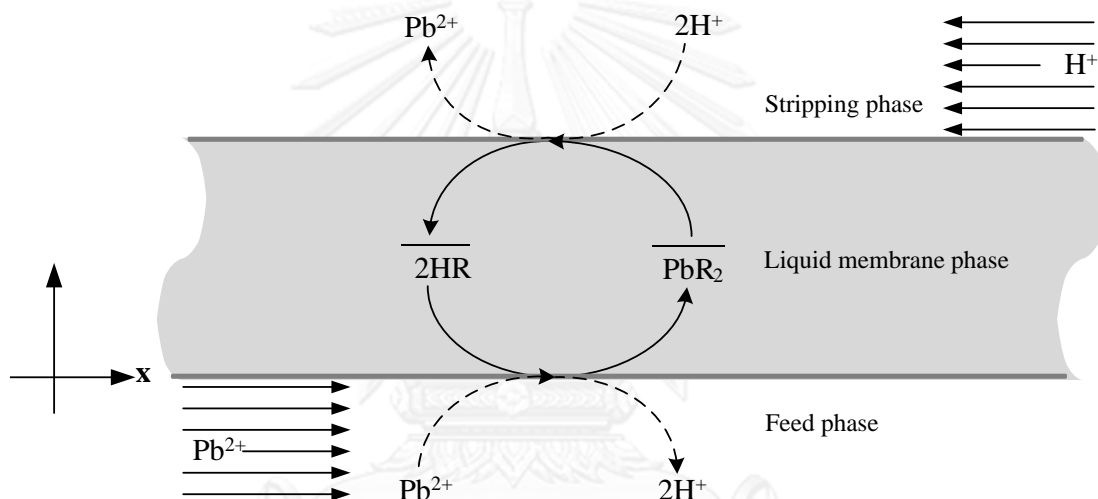
$\text{PbCl}_2$  and  $\text{Pb}(\text{NO}_3)_2$  dissolved in distilled water were used as aqueous feed solutions. In the aqueous solution, they dissociated to cations. In the operation of HFSLM, feed and stripping solutions are fed into the tube and shell sides of the hollow fibers, respectively. Both solutions are separated by the supported liquid membrane filled with an organic extractant.

Figure 4.1 shows the schematic mass transport of Pb(II) via the liquid membrane phase. The target Pb(II) in the feed solution reacts with the extractant ( $\text{D2EHPA}$ ,  $\text{HR}$ ) at the feed-liquid-membrane interface forming the lead-extractant complex ( $\text{PbR}_2$ ). Subsequently, the complex diffused across the liquid membrane phase to the liquid-membrane-stripping interface because of its concentration gradient. Then, it reacted with  $\text{H}^+$  from the stripping phase. Finally, Pb(II) was released into the stripping phase while the extractant diffused back toward the feed-liquid-membrane interface and reacted once again with the Pb(II) from the feed phase.

The extraction of Pb(II) from the feed phase by D2EHPA, as illustrated in Figure 4.1, is expressed in Eq. (4.1) [31]:



The overbar represents the species in the liquid membrane phase.



**Figure 4. 1** Schematic mechanism of Pb(II) transport across the liquid membrane phase using D2EHPA as the extractant.

The stripping reaction of complex  $\overline{\text{PbR}_2}$  and  $\text{H}^+$  at the liquid-membrane-stripping interface is represented as follows [32]:



Since, in the hollow fiber operation, Pb(II) is stripped out continuously by  $H^+$  at the liquid-membrane-stripping interface, the overall reaction in Eq. (4.1) is taken into account as the forward reaction.

The reaction rate of lead ion extraction  $r_{A,Ex}(x,t)$  can be expressed as follows:

$$r_{A,Ex}(x,t) = -k_{Ex} C_{A,F}^m(x,t) \quad (4.3)$$

where  $x$  is the longitudinal axis of the hollow fiber in the tube side,  $k_{Ex}$  is the reaction rate constant of extraction,  $t$  is the separation time,  $C_{A,F}(x,t)$  is the concentration of lead ions in the feed solution and  $m$  is the order of extraction reaction.

In order to strip the lead ions, hydrogen ions ( $H^+$ ), in the stripping solution, is kept in plentiful supply higher than that in the feed solution resulting in a higher forward reaction than a backward reaction. Therefore, the overall reaction of Pb(II) stripping in Eq. (4.2) can be considered as the forward reaction. Thus, the reaction rate of lead ion stripping,  $r_{A,St}(\bar{x},t)$ , is represented as:

$$r_{A,St}(\bar{x},t) = k_{St} C_{A,St}^n(\bar{x},t) \quad (4.4)$$

where  $\bar{x}$  is the longitudinal axis of the hollow fiber in the shell side and equal to  $L - x$ ,  $k_{St}$  is the reaction rate constant of stripping,  $C_{A,St}(\bar{x},t)$  is the concentration of lead ions in the stripping solution and  $n$  is the order of stripping reaction.

Using Taylor series to linearize the reaction rates of extraction and stripping in Eqs. (4.3) and (4.4), the following equations are obtained:

$$r_{A,Ex}(x_i, t) = -[\beta C_{A,F}(x_i, t) + \alpha] \quad (4.5)$$

where  $\beta = mk_{Ex} C_{A,F}^{m-1}(0,0)$

$$\alpha = (1-m)k_{Ex} C_{A,F}^m(0,0)$$

$$r_{A,St}(\bar{x}_i, t) = \varphi C_{A,St}(\bar{x}_i, t) + \gamma \quad (4.6)$$

given  $\varphi = nk_{St} C_{A,St}^{n-1}(\bar{x}_0,0)$

$$\gamma = (1-n)k_{St} C_{A,St}^n(\bar{x}_0,0)$$

### 4.3.2 Developing the mathematical model

A mathematical model based on the conservation of mass was improved in order to predict the concentration of lead ions in both feed and stripping solutions. Parameters considered in the model were axial convection, mass accumulation and reactions at the liquid-membrane interfaces.

In the feed phase, the mathematical model was developed under the following assumptions:

1. The feed-phase physical properties e.g. volume, temperature and pressure are constant.



2. The hollow-fiber inside diameter is very small. Therefore, the radial concentration profile of lead ions is constant.
3. The extraction reaction occurring at the feed-liquid-membrane interface is slow. This means that the diffusion fluxes of lead ions in the feed phase occurring in the axial direction can be neglected.
4. Only the lead-extractant complex arising from the extraction reaction, not lead ions, can transport into the liquid membrane phase.

For the stripping phase, the mathematical model was developed as follows:

1. The stripping-phase physical properties e.g. volume, temperature and pressure are constant.
2. The stripping reaction occurring at liquid-membrane-stripping interface is also slow. Then, the diffusion fluxes of lead ions in the stripping phase occurring in the axial direction can also be neglected.
3. Only lead ions resulting from the stripping reaction at the liquid-membrane-stripping interface, not lead-extractant complex, can transport into the stripping phase.

In order to determine the model equation, the tube and shell sides of the hollow fiber are dissected into segments. Each segment is very small as shown in Figure 4.2.

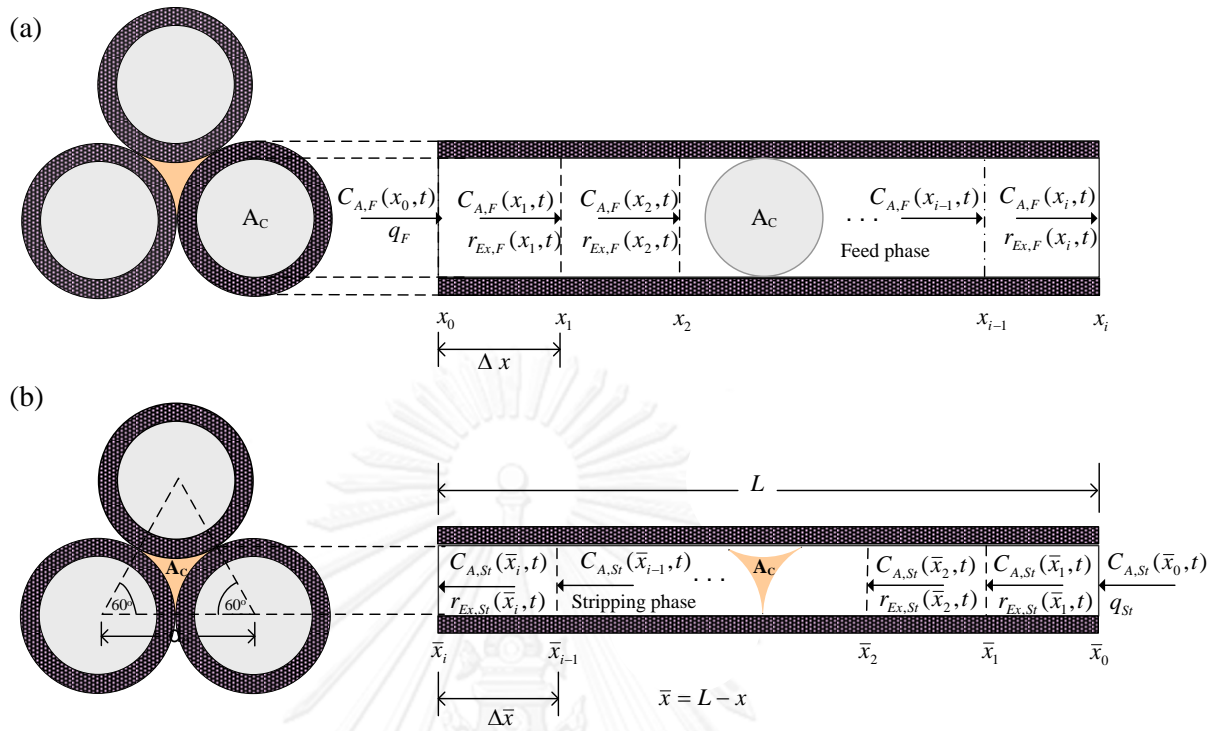


**Figure 4. 2** Schematic transport mechanism of lead ions through the small segments: (a) feed phase (tube side), (b) stripping phase (shell side).

Upon examining a small segment in the tube side of the hollow fiber, the conservation of mass for lead ions can be represented as below:

$$q_F C_{A,F}(x_{i-1}, t) - q_F C_{A,F}(x_i, t) + r_{A,Ex}(x_i, t) V_p = V_t \frac{dC_{A,F}(x_i, t)}{dt} \quad (4.7)$$

where

$$V_t = \pi r_i^2 \Delta x$$

$$V_p = \pi (r_o^2 - r_i^2) \Delta x \varepsilon$$

$$\Delta x = \frac{L}{i}$$

given  $q_F$  is the volumetric flow rate of the feed solution,  $i$  is the number of small segments,  $V_P$  is the pore volume of a small segment of the hollow fiber,  $V_t$  is the volume of a small segment of the tube side of the hollow fiber,  $r_i$  and  $r_o$  are the inner and outer radius of the hollow fibers,  $\varepsilon$  is the porosity of the hollow fiber and  $L$  is the effective length of the hollow fiber.

Eq. (4.7) is solved through Laplace transform as described in detail in Appendix A. Thus, the concentration of lead ions in the outlet feed solution,  $C_{A,F}(x_i, t)$ , can be calculated:

$$C_{A,F}(x_i, t) = \left(\frac{1}{a}\right)^i \left[ 1 - \sum_{j=1}^i \frac{1}{(j-1)!} \left(\frac{taq_F}{V_t}\right)^{j-1} e^{-\frac{taq_F}{V_t}} \right] C_{A,F}(x_0, t) - \sum_{j=1}^i \left(\frac{b}{a^j}\right) \left[ 1 - \sum_{j=1}^i \frac{1}{(j-1)!} \left(\frac{taq_F}{V_t}\right)^{j-1} e^{-\frac{taq_F}{V_t}} \right] \quad (4.8)$$

where

$$a = 1 + \frac{V_P}{q_F} \beta$$

$$b = \frac{V_P}{q_F} \alpha$$

For the stripping phase, mass conservation of lead ions was examined for each small segment in the shell side of the hollow fiber as shown below:

$$q_{St} C_{A,St}(\bar{x}_{i-1}, t) - q_{St} C_{A,St}(\bar{x}_i, t) + r_{A,St}(\bar{x}_i, t) V_P = V_s \frac{dC_{A,St}(\bar{x}_i, t)}{dt} \quad (4.9)$$

given

$$V_s = \left( \frac{\sqrt{3}}{4} d_o^2 - \frac{\pi r_o^2}{2} \right) \Delta \bar{x}$$

$$\Delta \bar{x} = \frac{L}{i}$$

where  $q_{St}$  represents the volumetric flow rate of the stripping solution and  $V_s$  is the volume of a small segment on the shell side of the hollow fiber,  $d_o$  is the outer diameter of the hollow fiber.

Solving Eq. (4.9) using Laplace transform, as described in detail in Appendix A, results in an equation for the calculation of lead ion concentration in the outlet stripping solution,  $C_{A,St}(\bar{x}_i, t)$ , as shown below:

$$C_{A,St}(\bar{x}_i, t) = \left(\frac{1}{g}\right)^i \left[ 1 - \sum_{j=1}^i \frac{1}{(j-1)!} \left(\frac{tgq_{St}}{V_s}\right)^{j-1} e^{-\frac{tgq_{St}}{V_s}} \right] C_{A,St}(\bar{x}_0, t) + \sum_{j=1}^i \left(\frac{h}{g^j}\right) \left[ 1 - \sum_{j=1}^i \frac{1}{(j-1)!} \left(\frac{tgq_{St}}{V_s}\right)^{j-1} e^{-\frac{tgq_{St}}{V_s}} \right] \quad (4.10)$$

where

$$g = 1 - \frac{V_P}{q_{St}} \phi$$

$$h = \frac{V_P}{q_{St}} \gamma$$

## 4.4 Experimental

### 4.4.1 Reagents and solutions

For the feed solutions,  $\text{PbCl}_2$  and  $\text{Pb}(\text{NO}_3)_2$  were used to prepare the synthetic wastewater. Di-(2-ethylhexyl)phosphoric acid (D2EHPA), diluted in toluene, was used as the extractant. The stripping solutions were  $\text{HCl}$ ,  $\text{H}_2\text{SO}_4$  and  $\text{HNO}_3$ . All chemicals used were AR grade obtained from Merck (Germany).

#### 4.4.2 Apparatus

The hollow fiber module used in studying the separation of Pb(II) consisted of microporous polypropylene fibers woven into fabric and wrapped around a central feeder tube to supply the shell-side fluid. The HFSLM system is comprised of a hollow fiber module, gear pumps, rotameters with variable flow rate controllers and pressure gauges, as shown in Figure 4.3. The attributes of the hollow fiber module are shown in Table 4.2. The concentration of Pb(II) was determined using an inductively coupled plasma optical emission spectrometer (ICP-OES) (model JY-2000; HORIBA Jobin Yvon, Edison, NJ, USA).

**Table 4. 2** Attributes of the hollow fiber module.

Attributes	Details
Material	Polypropylene
Module diameter	0.063 m
Number of hollow fibers	10,000
Inside diameter of a hollow fiber	$2.4 \times 10^{-4}$ m
Outside diameter of a hollow fiber	$3.0 \times 10^{-4}$ m
Effective length of a hollow fiber	0.203 m
Contact area	$1.4 \text{ m}^2$
Area per unit volume	$2.93 \times 10^3 \text{ m}^2/\text{m}^3$
Pore size	$3 \times 10^{-8}$ m
Porosity	25%
Tortuosity	2.6

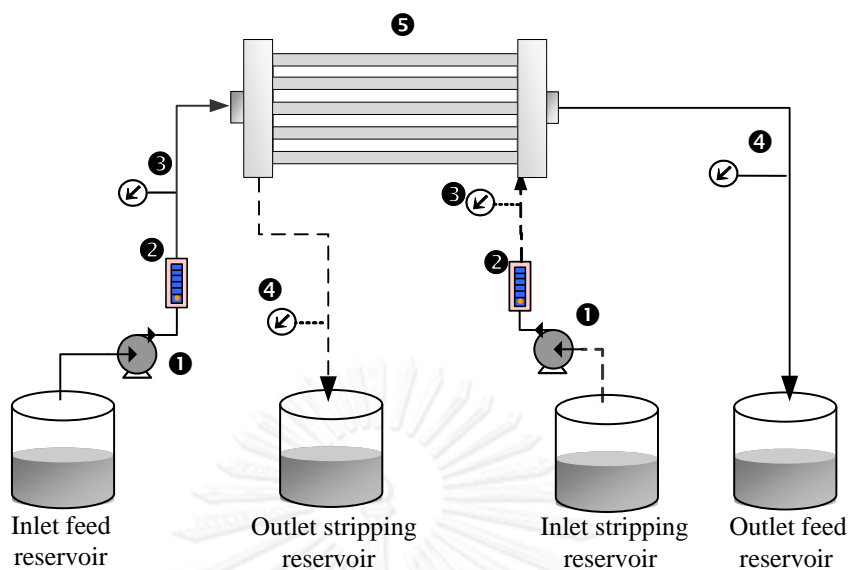


**Figure 4. 3** Schematic diagram of separated lead ions through HFSLM by continuous counter-current flow patterns of feed and stripping solutions: (1) gear pump, (2) flow meters, (3) inlet pressure gauges, (4) outlet pressure gauges, (5) hollow fiber module.

#### 4.4.3 Procedures

Feed solutions were prepared by dissolving  $\text{PbCl}_2$  and  $\text{Pb}(\text{NO}_3)_2$  in distilled water at a concentration of 1 mg/L. D2EHPA dissolved in toluene was used as the liquid membrane. Then, it was simultaneously circulated along the tube and shell sides of the hollow fibers until it was entirely embedded in the hollow-fiber micropores. Subsequently, distilled water was fed through both sides of the hollow fibers to flush out excess liquid membrane. After that, both feed and stripping solutions were fed into the tube and shell sides of the hollow fibers with single-pass modes. Finally, 10 cm<sup>3</sup> of feed and stripping solutions were collected at 600 s in order to determine the concentration of lead ions by ICP-OES.

Further, the influence of the concentration of D2EHPA, the type and concentration of stripping solutions, the lead-containing solutions as well as flow rates of both feed and stripping solutions were studied. The optimum condition obtained from the experiment was used to verify the validity of the model as shown by the average percent deviation in Eq. (4.19). The reaction order and reaction rate constant of Pb(II) extraction and stripping were carried out in batch liquid-liquid extraction. The standard uncertainty of the experiment was  $\pm 3\%$ . The hollow fiber module can be regenerated for a new separation cycle by feeding the surfactant through the hollow fibers to eliminate the liquid membrane in the tubes, shells and pores of the hollow fibers. Subsequently, distilled water flowed into the hollow fibers which then were dried with isopropyl alcohol.

$$\% \text{Deviation} = \frac{\sum_{k=1}^N \left( (C_{\text{Expt.}} - C_{\text{Model}}) / C_{\text{Expt.}} \right)_k}{N} \times 100 \quad (4.19)$$

where  $N$  is the number of experimental data,  $C_{\text{Expt.}}$  is the concentration of lead ions observed from the experiment and  $C_{\text{Model}}$  is the concentration of lead ions calculated from the model.



## 4.5 Results and discussion

### 4.5.1 Influence of extractant concentration

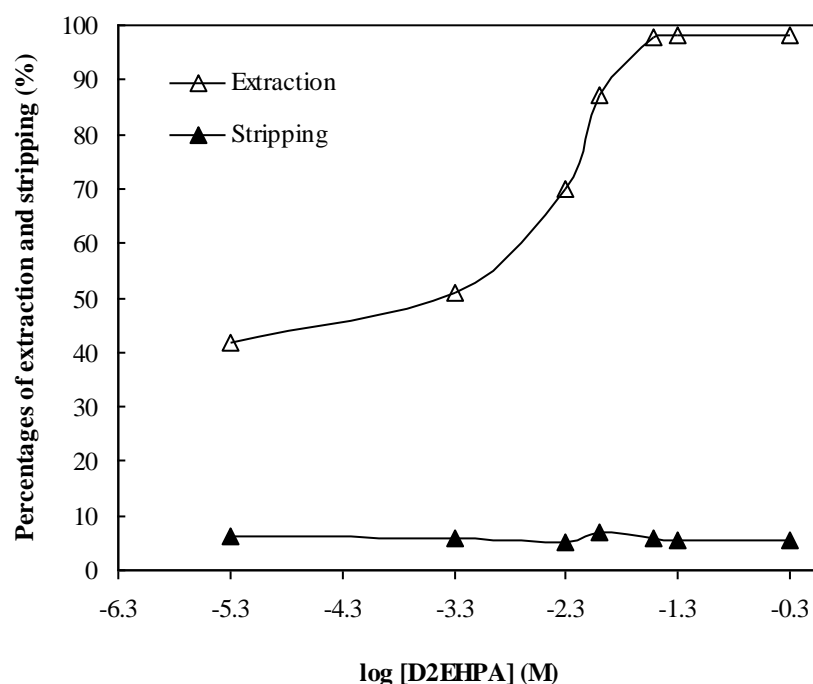


**Figure 4. 4** Influences of D2EHPA concentration on Pb(II) extraction and stripping at flow rates of feed and stripping solutions of  $1.7 \times 10^{-6} \text{ m}^3/\text{s}$  with  $1 \text{ mg/L PbCl}_2$  as the feed solution and  $0.5 \text{ M HNO}_3$  as the stripping solution.

The influence of extractant concentration on the extraction of lead ions was investigated by varying D2EHPA concentration from  $5.0 \times 10^{-6}$  to  $0.5 \text{ M}$  (log [D2EHPA] from  $-5.3$  to  $-0.3$ ). As shown in Figure 4.4, the percentage of Pb(II) extraction increased when the concentration of D2EHPA was increased. This agreed with Le Chatelier's principle that if any reactant in a system is added, the system reacts in a way to reduce it. The percentage of Pb(II) extraction achieved reached 97% at

D2EHPA concentration up to 0.03 M ( $\log [D2EHPA] = -1.52$ ). Therefore, 0.03 M D2EHPA was chosen in order to investigate other variables.

#### 4.5.2 Influences of stripping solutions

Hydrogen ions, in the stripping solution, play an important role in the continuous transport of Pb(II) from feed phase to stripping phase. Therefore, HCl, H<sub>2</sub>SO<sub>4</sub> and HNO<sub>3</sub>, which provide hydrogen ions, were investigated to find out the most suitable stripping solution. As shown in Figure 4.5, HCl was found to be the best stripping solution for Pb(II) stripping. This can be explained by the fact that the hydrogen ions in the acid stripping solutions reacted with the lead-extractant complex ( $\overline{PbR_2}$ ) at the liquid-membrane-stripping interface forming PbCl<sub>2</sub>, Pb(NO<sub>3</sub>)<sub>2</sub> and PbSO<sub>4</sub> when HCl, HNO<sub>3</sub> and H<sub>2</sub>SO<sub>4</sub> were used [34]. PbCl<sub>2</sub> in excess HCl concentration continued converting to anions [35] which could not react with the extractant ( $\overline{HR}$ ). In the case of Pb(NO<sub>3</sub>)<sub>2</sub> and PbSO<sub>4</sub> in HNO<sub>3</sub> and H<sub>2</sub>SO<sub>4</sub>, respectively, they dissociated to cations. Subsequently, they reacted with the extractant at the liquid-membrane-stripping interface resulting in a reversible reaction, as shown in Eq. (4.2). This caused Pb(II) in the stripping solution to decrease.

Finally, it was noted that when the concentration of stripping solutions was increased, the percentage of Pb(II) stripping increased. This corresponds to chemical kinetics that the rate of Pb(II) stripping increased when the concentration of stripping solutions was increased. However, a high concentration of acid can destroy the polypropylene hollow fibers. Therefore, in order to ensure a longer lifetime of the polypropylene hollow fibers, only 0.9 M ( $\log [H^+] = -0.05$ ) of each stripping solution

was investigated. Optimum percentage of stripping solution was obtained at 0.9 M HCl. Thus, 0.9 M HCl was recommended.

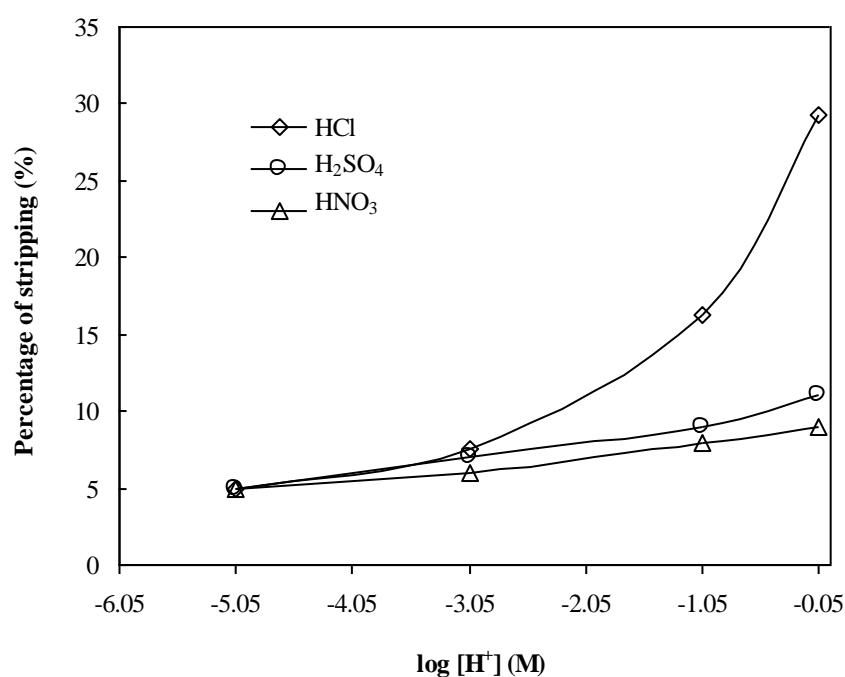


**Figure 4. 5** Influences of types of stripping solutions on Pb(II) stripping at flow rates of feed and stripping solutions of  $1.7 \times 10^{-6} \text{ m}^3/\text{s}$  with 1 mg/L PbCl<sub>2</sub> as the feed solution and 0.03 M D2EHPA as the extractant.

#### 4.5.3 Influences of types of lead-containing solutions

PbCl<sub>2</sub> and Pb(NO<sub>3</sub>)<sub>2</sub> solutions were selected in order to study the influence of lead-containing solutions. PbCl<sub>2</sub> generally contaminates water produced by the activities of offshore oil and gas production. Pb(NO<sub>3</sub>)<sub>2</sub> is widely used as raw material in chemical production. As shown in Figure 4.6, Pb(II) in both solutions reacted well with D2EHPA. It can be stated that D2EHPA and HCl can extract and strip Pb(II) whether Pb(II) in feed solution was PbCl<sub>2</sub> and Pb(NO<sub>3</sub>)<sub>2</sub>. The percentages of Pb(II)

extraction and stripping for both  $\text{Pb}(\text{NO}_3)_2$  and  $\text{PbCl}_2$  solutions were 97% and 30%, respectively.

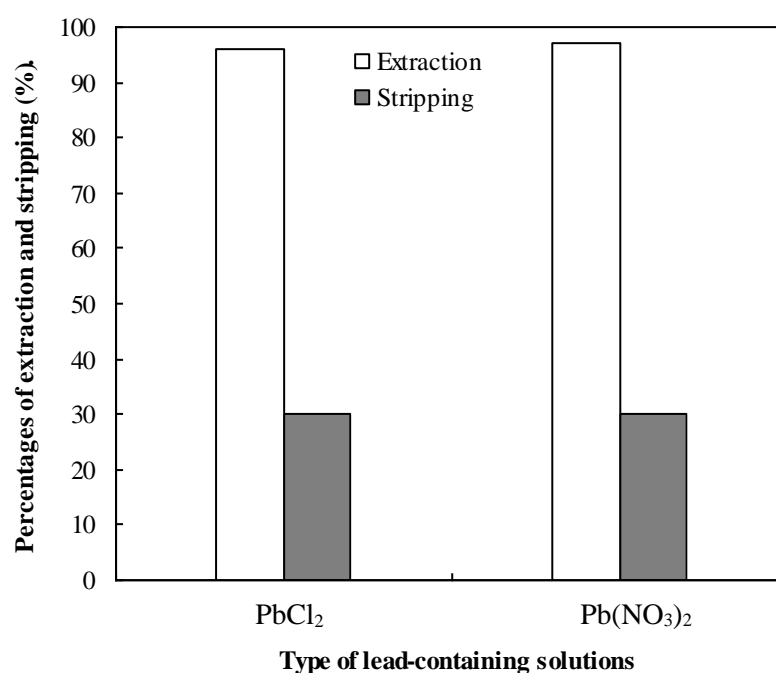


**Figure 4. 6** Influences of types of lead-containing solutions on the extraction and stripping of Pb(II) using flow rates of feed and stripping solutions at  $1.7 \times 10^{-6} \text{ m}^3/\text{s}$  with 0.03 M D2EHPA as the extractant and 0.9 M HCl as the stripping solution.

#### 4.5.4 Influences of flow rates of feed and stripping solutions

The influence of flow rates of feed and stripping solutions were investigated using  $\text{PbCl}_2$  solution as feed solution. Flow rates were varied from  $1.7 \times 10^{-6}$  to  $6.7 \times 10^{-6} \text{ m}^3/\text{s}$ . As shown in Figure 4.7, the percentages of Pb(II) extraction and stripping slowly decreased when the flow rates of feed and stripping solutions were increased. This was because of less residence time, as mentioned by Uedee et al. [36]. Optimum

percentages of Pb(II) extraction and stripping were obtained at flow rates of feed and stripping solutions of  $1.7 \times 10^{-6} \text{ m}^3/\text{s}$  where the Reynolds Number [28] was equal to 0.2.

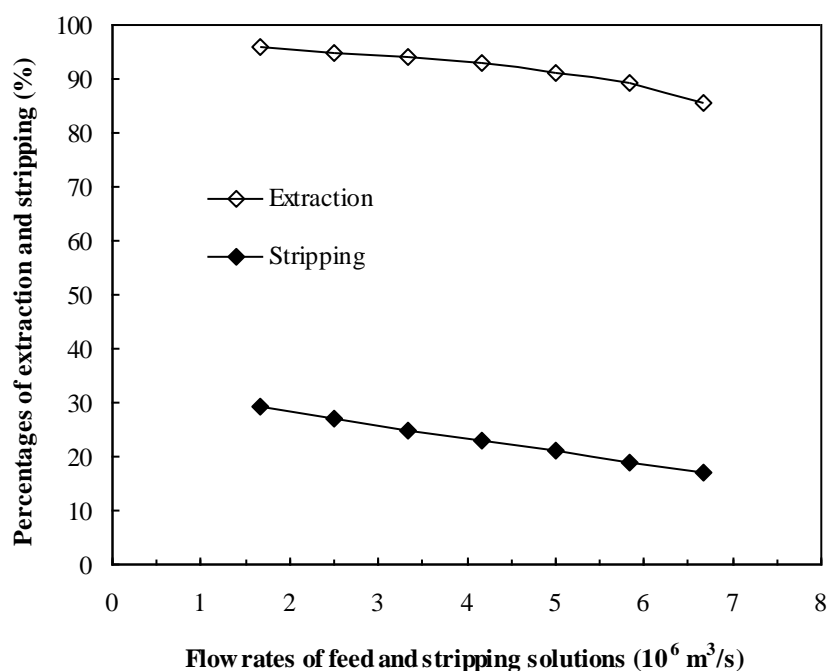


**Figure 4. 7** Influences of flow rates of feed and stripping solutions on the extraction and stripping of Pb(II) using 0.03 M D2EHPA as the extractant with 0.9 M HCl as the stripping solution and 1 mg/L  $\text{PbCl}_2$  as feed solution.

#### 4.5.5 Reaction order and reaction rate constant

The reaction order and reaction rate constant for extraction and stripping of Pb(II) in Eqs. (4.3) and (4.4) were determined through integration method. The integral concentrations of Pb(II) were plotted versus time. Results are shown in Table 4.3. It was clear that the highest *R*-square of extraction and stripping reactions, as shown in Figure 4.8, was obtained at second-order reaction. Thus, the reactions of Pb(II)

extraction and stripping were second-order with reaction rate constants of 0.03 and 0.19 L/mg s, respectively.

**Table 4. 3** Reaction orders ( $m/n$ ) and reaction rate constants of Pb(II) extraction and stripping ( $k_{EX}$  and  $k_{St}$ ).

$m/n$	Reaction	Plot	Reaction rate constant	$R^2$
1	Extraction	$\ln \frac{C_{A0}}{C_A}$ and $t$	$9.50 \times 10^{-3} \text{ s}^{-1}$	0.6920
	Stripping	$\ln \frac{C_{CO}}{C_{CO} - C_S}$ and $t$	$2.37 \times 10^{-2} \text{ s}^{-1}$	0.0878
2	Extraction	$\frac{1}{C_A} - \frac{1}{C_{A0}}$ and $t$	0.03 L/mg s	0.9812
	Stripping	$\frac{1}{C_{CO} - C_S} - \frac{1}{C_{CO}}$ and $t$	0.19 L/mg s	0.9796
3	Extraction	$\frac{1}{2C_A^2} - \frac{1}{2C_{A0}^2}$ and $t$	$0.08 \text{ L}^2/\text{mg}^2 \text{ s}$	0.8263
	Stripping	$\frac{1}{2(C_{CO} - C_S)^2} - \frac{1}{2C_{CO}^2}$ and $t$	$3.60 \text{ L}^2/\text{mg}^2 \text{ s}$	0.8252

*Note:*  $C_A$ , concentration of lead ions in the feed solution at time  $t$ ;  $C_{A0}$ , initial concentration of lead ions in the feed solution;  $C_{CO}$ , initial concentration of lead ions in the organic extractant;  $C_S$ , concentration of lead ions in the stripping solution at time  $t$ .

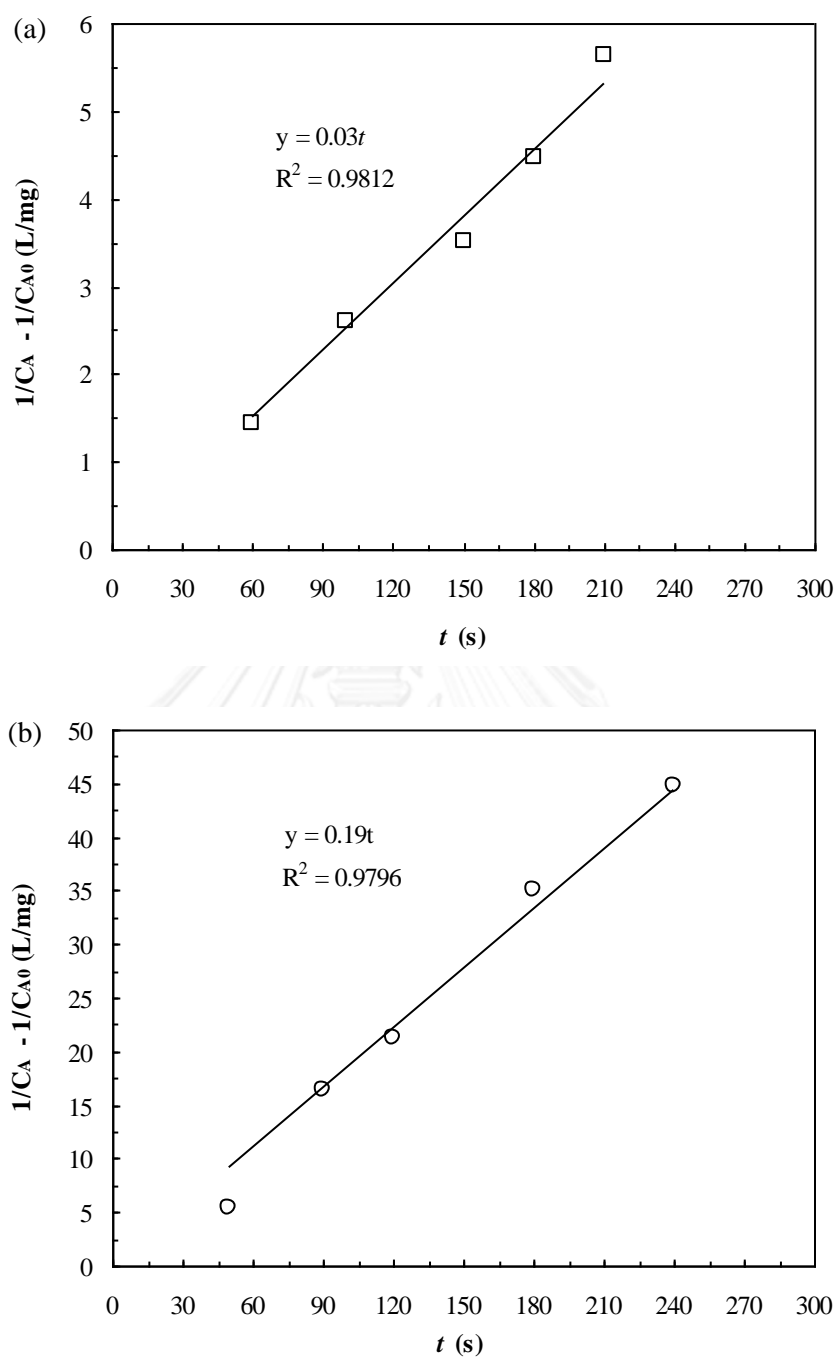


Figure 4. 8 Plots of integral concentrations of Pb(II) versus time: (a) extraction reaction, (b) stripping reaction.

#### 4.5.6 Validation of the model with experimental results

Results from the experiment, under various flow rates of feed and stripping solutions, were used to validate the model equations for predicting lead ion concentration in both feed and stripping solutions. These equations can be found in Eqs. (4.12) and (4.18), respectively. Flow rates of feed and stripping solutions were varied from  $1.7 \times 10^{-6}$  to  $6.7 \times 10^{-6}$  m<sup>3</sup>/s. Operating time was 600 s. As shown in Figure 4.9, concentrations of Pb(II) in feed and stripping solutions, calculated from the model of this work, were in line with the results observed from the experiment. Average percent deviation was 3% for both feed and stripping sides. Low average percent deviation indicated that lead-ion transport from the feed to stripping phases depended on axial convection, mass accumulation and reactions at liquid-membrane interfaces.

In Figure 4.9, the models of this work along with Chaturabul et al. [23] (based on convection transport, mass accumulation and reaction – neglecting diffusion) were compared with the model based on diffusion and convection transport (neglecting mass accumulation and reaction) of Kandwal et al. [24]. Our models, as stated, as well as Chaturabul et al. were improved in order to predict the concentration of metal ions in both feed and stripping solutions. Average percent deviation in the feed side was found to be 3% for our model and 8% for Chaturabul's model. This indicated again that lead-ion transport along the hollow fibers depended on axial convection, mass accumulation and reaction at liquid-membrane interfaces.



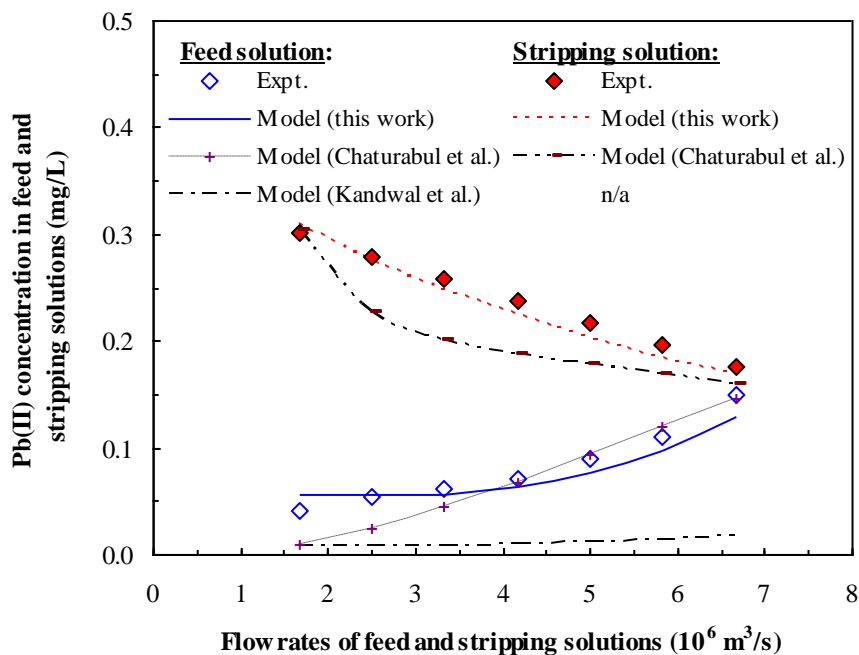


**Figure 4. 9** Comparison of Pb(II) concentration in the outlet feed and stripping solutions from the model and from the experiment at various flow rates of feed and stripping solutions using 0.03 M D2EHPA as the extractant with 0.9 M HCl as stripping solution and 1 mg/L PbCl<sub>2</sub> as feed solution.

Kandwal's model, in contrast, was developed in order to predict the concentration of metal ions only in the feed solution. On the feed side, it was noted that the models based on axial convection, mass accumulation and reaction were in good agreement with the experimental results. However, the model based on diffusion and convection transport did not fit with the experimental results.

For the stripping side, our model fitted in better with the experimental results than those of Chaturabul's model. Average percent deviation observed from our model was found to be 3% and from Chaturabul's model was 14%.

#### 4.6 Conclusion

It was noted that HFSLM using D2EHPA as the extractant can successfully separate a very low concentration of Pb(II) from both PbCl<sub>2</sub> and Pb(NO<sub>3</sub>)<sub>2</sub> solutions (1 mg/L). Thus, the discharge limit for the synthetic wastewater after treatment was found to be less than the regulatory limit of 0.2 mg/L. Using 0.03 M D2EHPA as the extractant, 0.9 M HCl as the stripping solution, and flow rates of feed and stripping solutions of  $1.7 \times 10^{-6}$  m<sup>3</sup>/s, the maximum percentage of Pb(II) extraction and stripping were 97% and 30%. Extraction and stripping of Pb(II) was second-order reaction. Reaction rate constants of extraction and stripping were 0.03 and 0.19 L/mg s, respectively. The concentration of Pb(II) predicted by the developed model in this work, based on axial convection, mass accumulation and reaction, was in good agreement with the experimental results. For predictions, in both feed and stripping phases, average percent deviation was 3%. This indicated that the transport of lead ions along the hollow fibers depended on axial convection, mass accumulation and reactions at liquid-membrane interfaces.

#### 4.7 Acknowledgements

Thanks to the Thailand Research Fund as well as Chulalongkorn University under the Royal Golden Jubilee Ph.D. Program (Grant No. PHD/0324/2551) for financial support. Sincere thanks are also extended to the Separation Laboratory, Department of Chemical Engineering, Chulalongkorn University, Bangkok, Thailand.

#### 4.8 Appendix A. Solving mathematics for the model of lead ions transport via HFSLM

The conservation of mass for lead ions, with regards to a small segment in the tube side ( $\Delta x$ ) of the hollow fiber, is shown as:

$$q_F C_{A,F}(x_{i-1}, t) - q_F C_{A,F}(x_i, t) + r_{A,Ex}(x_i, t) V_P = V_t \frac{dC_{A,F}(x_i, t)}{dt} \quad (A1)$$

Substituting Eq. (4.5) in Eq. (A1) and dividing by the volumetric flow rate of feed solution, the mass conservation in segments 1, 2, 3, ...,  $i$  can be written as:

$$C_{A,F}(x_0, t) - C_{A,F}(x_1, t) - \frac{V_P}{q_F} \beta C_{A,F}(x_1, t) - \frac{V_P}{q_F} \alpha = \frac{V_t}{q_F} \frac{dC_{A,F}(x_1, t)}{dt} \quad (A2)$$

$$C_{A,F}(x_1, t) - C_{A,F}(x_2, t) - \frac{V_P}{q_F} \beta C_{A,F}(x_2, t) - \frac{V_P}{q_F} \alpha = \frac{V_t}{q_F} \frac{dC_{A,F}(x_2, t)}{dt} \quad (A3)$$

$$C_{A,F}(x_2, t) - C_{A,F}(x_3, t) - \frac{V_P}{q_F} \beta C_{A,F}(x_3, t) - \frac{V_P}{q_F} \alpha = \frac{V_t}{q_F} \frac{dC_{A,F}(x_3, t)}{dt} \quad (A4)$$

·  
·  
·

$$C_{A,F}(x_{i-1}, t) - C_{A,F}(x_i, t) - \frac{V_P}{q_F} \beta C_{A,F}(x_i, t) - \frac{V_P}{q_F} \alpha = \frac{V_t}{q_F} \frac{dC_{A,F}(x_i, t)}{dt} \quad (A5)$$

Defining  $a = 1 + (V_P / q_F) \beta$  and  $b = (V_P / q_F) \alpha$ , Eqs. (A2)–(A5) can be rewritten as:

$$C_{A,F}(x_0,t) - aC_{A,F}(x_1,t) - b = \frac{V_t}{q_F} \frac{dC_{A,F}(x_1,t)}{dt} \quad (A6)$$

$$C_{A,F}(x_1,t) - aC_{A,F}(x_2,t) - b = \frac{V_t}{q_F} \frac{dC_{A,F}(x_2,t)}{dt} \quad (A7)$$

$$C_{A,F}(x_2,t) - aC_{A,F}(x_3,t) - b = \frac{V_t}{q_F} \frac{dC_{A,F}(x_3,t)}{dt} \quad (A8)$$

·  
·  
·

$$C_{A,F}(x_{i-1},t) - aC_{A,F}(x_i,t) - b = \frac{V_t}{q_F} \frac{dC_{A,F}(x_i,t)}{dt} \quad (A9)$$

Defining:

$$\tau_F = \frac{V_t}{aq_F} \quad (A10)$$

Using Eq. (A10) and taking Laplace transform of Eqs. (A6)–(A9), the following equations are obtained:

$$C_{A,F}(x_1, s) = \frac{1}{a} \left[ \frac{1}{(\tau_F s + 1)} \right] C_{A,F}(x_0, s) - \frac{b}{a} \left[ \frac{1}{s(\tau_F s + 1)} \right] \quad (\text{A11})$$

$$C_{A,F}(x_2, s) = \frac{1}{a} \left[ \frac{1}{(\tau_F s + 1)} \right] C_{A,F}(x_1, s) - \frac{b}{a} \left[ \frac{1}{s(\tau_F s + 1)} \right] \quad (\text{A12})$$

$$C_{A,F}(x_3, s) = \frac{1}{a} \left[ \frac{1}{(\tau_F s + 1)} \right] C_{A,F}(x_2, s) - \frac{b}{a} \left[ \frac{1}{s(\tau_F s + 1)} \right] \quad (\text{A13})$$

$$C_{A,F}(x_i, s) = \frac{1}{a} \left[ \frac{1}{(\tau_F s + 1)} \right] C_{A,F}(x_{i-1}, s) - \frac{b}{a} \left[ \frac{1}{s(\tau_F s + 1)} \right] \quad (\text{A14})$$

Substituting Eq. (A11) in Eq. (A12) gives:

$$C_{A,F}(x_2, s) = \left( \frac{1}{a} \right)^2 \left( \frac{1}{\tau_F s + 1} \right)^2 C_{A,F}(x_0, s) - \frac{b}{a^2} \left[ \frac{1}{s(\tau_F s + 1)^2} \right] - \frac{b}{a} \left[ \frac{1}{s(\tau_F s + 1)} \right] \quad (\text{A15})$$

Substituting Eq. (A15) in Eq. (A13) gives:

$$C_{A,F}(x_3, s) = \left( \frac{1}{a} \right)^3 \left( \frac{1}{\tau_F s + 1} \right)^3 C_{A,F}(x_0, s) - \frac{b}{a^3} \left[ \frac{1}{s(\tau_F s + 1)^3} \right] - \frac{b}{a^2} \left[ \frac{1}{s(\tau_F s + 1)^2} \right] - \frac{b}{a} \left[ \frac{1}{s(\tau_F s + 1)} \right] \quad (\text{A16})$$

$$\therefore C_{A,F}(x_i, s) = \left(\frac{1}{a}\right)^i \left(\frac{1}{\tau_F s + 1}\right)^i C_{A,F}(x_0, s) - \sum_{i=1}^n \left(\frac{b}{a^i}\right) \left[\frac{1}{s(\tau_F s + 1)^i}\right] \quad (\text{A17})$$

Solving  $C_{A,F}(x_1, s)$ ,  $C_{A,F}(x_2, s)$  and  $C_{A,F}(x_3, s)$

$$\text{Let } C_0(s) = \frac{C_0}{s}$$

$$C_{A,F}(x_1, s) = \frac{1}{a} \left[ \frac{1}{s(\tau_F s + 1)} \right] C_{A,F}(x_0, t) - \frac{b}{a} \left[ \frac{1}{s(\tau_F s + 1)} \right] \quad (\text{A18})$$

$$C_{A,F}(x_1, s) = \frac{1}{a} \left[ \frac{1}{s} - \frac{1}{s + 1/\tau_F} \right] C_{A,F}(x_0, t) - \frac{b}{a} \left[ \frac{1}{s} - \frac{1}{s + 1/\tau_F} \right] \quad (\text{A19})$$

$$C_{A,F}(x_1, t) = \frac{1}{a} \left[ 1 - e^{-t/\tau_F} \right] C_{A,F}(x_0, t) - \frac{b}{a} \left[ 1 - e^{-t/\tau_F} \right] \quad (\text{A20})$$

$$C_{A,F}(x_2, s) = \left(\frac{1}{a}\right)^2 \frac{1}{s(\tau_F s + 1)^2} C_{A,F}(x_0, t) - \frac{b}{a^2} \left[ \frac{1}{s(\tau_F s + 1)^2} \right] - \frac{b}{a} \left[ \frac{1}{s(\tau_F s + 1)} \right] \quad (\text{A21})$$

$$C_{A,F}(x_2, s) = \left(\frac{1}{a}\right)^2 \left[ \frac{1}{s} - \frac{1}{s + 1/\tau_F} - \frac{1/\tau_F}{(s + 1/\tau_F)^2} \right] C_{A,F}(x_0, t) - \frac{b}{a^2} \left[ \frac{1}{s} - \frac{1}{s + 1/\tau_F} - \frac{1/\tau_F}{(s + 1/\tau_F)^2} \right] - \frac{b}{a} \left[ \frac{1}{s} - \frac{1}{s + 1/\tau_F} \right] \quad (\text{A22})$$

$$\begin{aligned}
C_{A,F}(x_2, t) &= \left(\frac{1}{a}\right)^2 \left[ 1 - e^{-t/\tau_F} - \left(\frac{t}{\tau_F}\right) e^{-t/\tau_F} \right] C_{A,F}(x_0, t) - \\
&\quad \frac{b}{a^2} \left[ 1 - e^{-t/\tau_F} - \left(\frac{t}{\tau_F}\right) e^{-t/\tau_F} \right] - \frac{b}{a} \left[ 1 - e^{-t/\tau_F} \right]
\end{aligned} \tag{A23}$$

$$\begin{aligned}
C_{A,F}(x_3, s) &= \left(\frac{1}{a}\right)^3 \frac{1}{s(\tau_F s + 1)^3} C_{A,F}(x_0, t) - \frac{b}{a^3} \left[ \frac{1}{s(\tau_F s + 1)^3} \right] - \\
&\quad \frac{b}{a^2} \left[ \frac{1}{s(\tau_F s + 1)^2} \right] - \frac{b}{a} \left[ \frac{1}{s(\tau_F s + 1)} \right]
\end{aligned} \tag{A24}$$

$$\begin{aligned}
C_{A,F}(x_3, s) &= \left(\frac{1}{a}\right)^3 \left[ \frac{1}{s} - \frac{\tau_F}{\tau_F s + 1} - \frac{\tau_F}{(\tau_F s + 1)^2} - \frac{\tau_F}{(\tau_F s + 1)^3} \right] C_{A,F}(x_0, t) - \\
&\quad \frac{b}{a^3} \left[ \frac{1}{s} - \frac{\tau_F}{\tau_F s + 1} - \frac{\tau_F}{(\tau_F s + 1)^2} - \frac{\tau_F}{(\tau_F s + 1)^3} \right] - \\
&\quad \frac{b}{a^2} \left[ \frac{1}{s} - \frac{1}{s + 1/\tau_F} - \frac{1/\tau_F}{(s + 1/\tau_F)^2} \right] - \frac{b}{a} \left[ \frac{1}{s} - \frac{1}{s + 1/\tau_F} \right]
\end{aligned} \tag{A25}$$

$$\begin{aligned}
C_{A,F}(x_3, t) = & \left(\frac{1}{a}\right)^3 \left[ 1 - e^{-t/\tau_F} - \left(\frac{t}{\tau_F}\right) e^{-t/\tau_F} - \frac{1}{2!} \left(\frac{t}{\tau_F}\right)^2 e^{-t/\tau_F} \right] C_{A,F}(x_0, t) - \\
& \frac{b}{a^3} \left[ 1 - e^{-t/\tau_F} - \left(\frac{t}{\tau_F}\right) e^{-t/\tau_F} - \frac{1}{2!} \left(\frac{t}{\tau_F}\right)^2 e^{-t/\tau_F} \right] - \\
& \frac{b}{a^2} \left[ 1 - e^{-t/\tau_F} - \left(\frac{t}{\tau_F}\right) e^{-t/\tau_F} \right] - \frac{b}{u} \left[ 1 - e^{-t/\tau_F} \right] \quad (A26)
\end{aligned}$$

$$\begin{aligned}
\therefore C_{A,F}(x_i, t) = & \left(\frac{1}{a}\right)^i \left[ 1 - \sum_{j=1}^i \frac{1}{(j-1)!} \left(\frac{t}{\tau_F}\right)^{j-1} e^{-t/\tau_F} \right] C_{A,F}(x_0, t) - \\
& \sum_{j=1}^i \left(\frac{b}{a^j}\right) \left[ 1 - \sum_{j=1}^i \frac{1}{(j-1)!} \left(\frac{t}{\tau_F}\right)^{j-1} e^{-t/\tau_F} \right] \quad (A27)
\end{aligned}$$

Substituting Eq. (A10) in Eq. (A27), the equation for calculating concentration of lead ions in the outlet feed solution,  $C_{A,F}(x_i, t)$ , is achieved:

$$\begin{aligned}
C_{A,F}(x_i, t) = & \left(\frac{1}{a}\right)^i \left[ 1 - \sum_{j=1}^i \frac{1}{(j-1)!} \left(\frac{taq_F}{V_t}\right)^{j-1} e^{-taq_F/V_t} \right] C_{A,F}(x_0, t) - \\
& \sum_{j=1}^i \left(\frac{b}{a^j}\right) \left[ 1 - \sum_{j=1}^i \frac{1}{(j-1)!} \left(\frac{taq_F}{V_t}\right)^{j-1} e^{-taq_F/V_t} \right] \quad (A28)
\end{aligned}$$



For the stripping phase, the conservation of mass for lead ions, with regards to a small segment in shell side ( $\Delta\bar{x}$ ) of the hollow fiber, is shown below:

$$q_{St}C_{A,St}(\bar{x}_{i-1},t) - q_{St}C_{A,St}(\bar{x}_i,t) + r_{A,St}(\bar{x}_i,t)V_p = V_s \frac{dC_{A,St}(\bar{x}_i,t)}{dt} \quad (A29)$$

$$\text{where } V_s = \left( \frac{\sqrt{3}}{4} d_o^2 - \frac{\pi r_o^2}{2} \right) \Delta\bar{x}$$

$$\Delta\bar{x} = \frac{L}{i}$$

Substituting Eq. (4.6) in Eq. (A29) and dividing by the volumetric flow rate of stripping solution, the mass conservation in segments 1, 2, 3, ...,  $i$  can be written as follows:

$$C_{A,St}(\bar{x}_0,t) - C_{A,St}(\bar{x}_1,t) + \frac{V_p}{q_{St}} \varphi C_{A,St}(\bar{x}_1,t) + \frac{V_p}{q_{St}} \gamma = \frac{V_s}{q_{St}} \frac{dC_{A,St}(\bar{x}_1,t)}{dt} \quad (A30)$$

$$C_{A,St}(\bar{x}_1,t) - C_{A,St}(\bar{x}_2,t) + \frac{V_p}{q_{St}} \varphi C_{A,St}(\bar{x}_2,t) + \frac{V_p}{q_{St}} \gamma = \frac{V_s}{q_{St}} \frac{dC_{A,St}(\bar{x}_2,t)}{dt} \quad (A31)$$

$$C_{A,St}(\bar{x}_2,t) - C_{A,St}(\bar{x}_3,t) + \frac{V_p}{q_{St}} \varphi C_{A,St}(\bar{x}_3,t) + \frac{V_p}{q_{St}} \gamma = \frac{V_s}{q_{St}} \frac{dC_{A,St}(\bar{x}_3,t)}{dt} \quad (A32)$$

·  
·  
·

$$C_{A,St}(\bar{x}_{i-1},t) - C_{A,St}(\bar{x}_i,t) + \frac{V_p}{q_{St}} \varphi C_{A,St}(\bar{x}_i,t) + \frac{V_p}{q_{St}} \gamma = \frac{V_s}{q_{St}} \frac{dC_{A,St}(\bar{x}_i,t)}{dt} \quad (A33)$$

Defining:

$$g = 1 - \frac{V_p}{q_{St}} \varphi$$

$$h = \frac{V_p}{q_{St}} \gamma,$$

Eqs. (A30)–(A33) can be rewritten as:

$$C_{A,St}(\bar{x}_0, t) - gC_{A,St}(\bar{x}_1, t) + h = \frac{V_s}{q_{St}} \frac{dC_{A,St}(\bar{x}_1, t)}{dt} \quad (\text{A34})$$

$$C_{A,St}(\bar{x}_1, t) - gC_{A,St}(\bar{x}_2, t) + h = \frac{V_s}{q_{St}} \frac{dC_{A,St}(\bar{x}_2, t)}{dt} \quad (\text{A35})$$

$$C_{A,St}(\bar{x}_2, t) - gC_{A,St}(\bar{x}_3, t) + h = \frac{V_s}{q_{St}} \frac{dC_{A,St}(\bar{x}_3, t)}{dt} \quad (\text{A36})$$

·  
·  
·

$$C_{A,St}(\bar{x}_{i-1}, t) - gC_{A,St}(\bar{x}_i, t) + h = \frac{V_s}{q_{St}} \frac{dC_{A,St}(\bar{x}_i, t)}{dt} \quad (\text{A37})$$

Defining:

$$\tau_{St} = \frac{V_s}{gq_{St}} \quad (\text{A38})$$

Using Eq. (A38) and taking Laplace transform of Eqs. (A34)–(A37) gives:

$$C_{A,St}(\bar{x}_1, s) = \frac{1}{g} \left[ \frac{1}{(\tau_{St}s + 1)} \right] C_{A,St}(\bar{x}_0, s) + \frac{h}{g} \left[ \frac{1}{s(\tau_{St}s + 1)} \right] \quad (A39)$$

$$C_{A,St}(\bar{x}_2, s) = \frac{1}{g} \left[ \frac{1}{(\tau_{St}s + 1)} \right] C_{A,St}(\bar{x}_1, s) + \frac{h}{g} \left[ \frac{1}{s(\tau_{St}s + 1)} \right] \quad (A40)$$

$$C_{A,St}(\bar{x}_3, s) = \frac{1}{g} \left[ \frac{1}{(\tau_{St}s + 1)} \right] C_{A,St}(\bar{x}_2, s) + \frac{h}{g} \left[ \frac{1}{s(\tau_{St}s + 1)} \right] \quad (A41)$$

$$\dots$$

$$C_{A,St}(\bar{x}_i, s) = \frac{1}{g} \left[ \frac{1}{(\tau_{St}s + 1)} \right] C_{A,St}(\bar{x}_{i-1}, s) + \frac{h}{g} \left[ \frac{1}{s(\tau_{St}s + 1)} \right] \quad (A42)$$

Solving Eqs. (A39)–(A42) by the same concept described in Eqs. (A15)–(A27) results in the following equation:

$$C_{A,St}(\bar{x}_i, t) = \left( \frac{1}{g} \right)^i \left[ 1 - \sum_{j=1}^i \frac{1}{(j-1)!} \left( \frac{t}{\tau_{St}} \right)^{j-1} e^{-t/\tau_{St}} \right] C_{A,St}(\bar{x}_0, t) + \sum_{j=1}^i \left( \frac{h}{g^j} \right) \left[ 1 - \sum_{j=1}^i \frac{1}{(j-1)!} \left( \frac{t}{\tau_{St}} \right)^{j-1} e^{-t/\tau_{St}} \right] \quad (A43)$$

Substituting Eq. (A38) in Eq. (A43) gives an equation for the calculation of lead ions concentration in the outlet stripping solution,  $C_{A,St}(x'_i, t)$ , as shown below:

$$C_{A,St}(\bar{X}_i, t) = \left(\frac{1}{g}\right)^i \left[ 1 - \sum_{j=1}^i \frac{1}{(j-1)!} \left(\frac{tgq_{St}}{V_s}\right)^{j-1} e^{-tgq_{St}/V_s} \right] C_{A,St}(\bar{X}_0, t) + \sum_{j=1}^i \left(\frac{h}{g^j}\right) \left[ 1 - \sum_{j=1}^i \frac{1}{(j-1)!} \left(\frac{tgq_{St}}{V_s}\right)^{j-1} e^{-tgq_{St}/V_s} \right] \quad (\text{A44})$$

#### 4.9 References

- [1] L. Gurel, L. Altas, H. Buyukgungor, *Environmental Engineering Science* 22 (2005) 411.
- [2] M. Singanan, A. Abebaw, S. Vinodhini, *Bulletin of the Chemical Society of Ethiopia* 19 (2005) 289.
- [3] D. Marani, G. Macchi, M. Pagano, *Water Research* 29 (1995) 1085.
- [4] M.Z. Barciszewska, M. Szymanski, E. Wyszko, J. Pas, L. Rychlewski, J. Barciszewski, *Mutation Research/Reviews in Mutation Research* 589 (2005) 103.
- [5] E.K. Silbergeld, *Mutation Research/Reviews in Mutation Research* 533 (2003) 121.
- [6] Thailand Regulatory Discharge Standards, vol. 2, Ministry of Industry, Thailand, 1996.
- [7] Q. Chen, Z. Luo, C. Hills, G. Xue, M. Tyrer, *Water Research* 43 (2009) 2605.
- [8] M. Eloussaief, M. Benzina, *Journal of Hazardous materials* 178 (2010) 753.
- [9] O. Gerçel, H.F. Gerçel, *Chemical Engineering Journal* 132 (2007) 289.
- [10] Y. Xue, H. Hou, S. Zhu, *Journal of Hazardous materials* 162 (2009) 391.
- [11] B. Mandal, N. Ghosh, *Desalination* 250 (2010) 506.
- [12] B.S. Inbaraj, J.S. Wang, J.F. Lu, F.Y. Siao, B.H. Chen, *Bioresource Technology* 100 (2009) 200.

- [13] I.M. Coelho, M.M. Cardoso, R.M.C. Viegas, J.P.S.G. Crespo, *Separation and Purification Technology* 19 (2000) 183.
- [14] M.F. San Roman, E. Bringas, R. Ibanez, I. Ortiz, *Journal of Chemical Technology and Biotechnology* 85 (2010) 2.
- [15] N.M. Kocherginsky, Q. Yang, L. Seelam, *Separation and Purification Technology* 53 (2007) 171.
- [16] U. Pancharoen, A.W. Lothongkum, S. Chaturabul, Mass transfer in hollow fiber supported liquid membrane for As and Hg removal from produced water in upstream petroleum operation in the gulf of Thailand, in: M. El-Amin (Ed.), *Mass Transfer in Multiphase Systems and Its Applications*, InTech, India, 2011.
- [17] R. Guell, E. Antico, V. Salvado, C. Fontas, *Separation and Purification Technology* 62 (2008) 389.
- [18] D. Buachuang, P. Ramakul, N. Leepipatpiboon, U. Pancharoen, *Journal of Alloys and Compounds* 509 (2011) 9549.
- [19] L.D. Mafu, T.A.M. Msagati, B.B. Mamba, *Physics and Chemistry of the Earth* 50–52 (2012) 121.
- [20] S.A. Ansari, P.K. Mohapatra, D.R. Raut, M. Kumar, B. Rajeswari, V.K. Manchanda, *Journal of Membrane Science* 337 (2009) 304.
- [21] A. Mtibe, T.A.M. Msagati, A.K. Mishra, B.B. Mamba, *Physics and Chemistry of the Earth* 50–52 (2012) 239.
- [22] P.V. Vernekar, Y.D. Jagdale, A.W. Patwardhan, A.V. Patwardhan, S.A. Ansari, P.K. Mohapatra, V.K. Manchanda, *Chemical Engineering Research and Design* 91 (2013) 141.
- [23] S. Chaturabul, K. Wongkaew, U. Pancharoen, *Separation Science and Technology* 48 (2012) 93.

- [24] P. Kandwal, S. Dixit, S. Mukhopadhyay, P.K. Mohapatra, *Chemical Engineering Journal* 174 (2011) 110.
- [25] P. Ramakul, U. Mooncluen, Y. Yanachawakul, N. Leepipatpiboon, *Journal of Industrial and Engineering Chemistry* 18 (2012) 1606.
- [26] W. Zhang, C. Cui, Z. Hao, *Chinese Journal of Chemical Engineering* 18 (2010) 48.
- [27] J.W. Choi, K.S. Cho, B.K. Oh, I.J. Youn, J. Jeong, S. Park, W.H. Lee, *Chinese Journal of Chemical Engineering* 7 (2001) 230.
- [28] Q. Yang, N.M. Kocherginsky, *Journal of Membrane Science* 297 (2007) 121.
- [29] U. Pancharoen, T. Wongsawa, A.W. Lothongkum, *Separation Science and Technology* 46 (2011) 2183.
- [30] A. Escobar, K.A. Schimmel, J. de Gyves, E.R. de San Miguel, *Journal of Chemical Technology and Biotechnology* 79 (2004) 961.
- [31] T. Gumi, M. Oleinikova, C. Palet, M. Valiente, M. Munoz, *Analytica Chimica Acta* 408 (2000) 65.
- [32] C.-V.I. Gherasim, G. Bourceanu, R.-I. Olariu, C. Arsene, *Journal of Membrane Science* 377 (2011) 167.
- [33] R.S. Juang, J.Y. Su, *Industrial and Engineering Chemistry Research* 31 (1992) 2395.
- [34] E.G. Rochow, E.W. Abel, *The Chemistry of Germanium, Tin and Lead*, Pergamon, England, 1973.
- [35] C.W. Wood, A.K. Holliday, *Inorganic Chemistry*, third ed., Butterworth, England, 1967.
- [36] E. Uedee, P. Ramakul, U. Pancharoen, A.W. Lothongkum, *Korean Journal of Chemical Engineering* 25 (2008) 1486.

## CHAPTER V

### A GENERATING FUNCTION APPLIED ON A REACTION MODEL FOR THE SELECTIVE SEPARATION OF Pb(II) AND Hg(II) VIA HFSLM

Sira Suren<sup>a</sup>, Ura Pancharoen<sup>a,\*</sup>, Noppawat Thamphiphit<sup>a</sup>,  
Natchanun Leepipatpiboon<sup>b,\*\*</sup>

<sup>a</sup>*Department of Chemical Engineering, Faculty of Engineering, Chulalongkorn University, Bangkok 10330, Thailand*

<sup>b</sup>*Chromatography and Separation Research Unit, Department of Chemistry, Faculty of Science, Chulalongkorn University, Patumwan, Bangkok 10330, Thailand*

จุฬาลงกรณ์มหาวิทยาลัย  
CHULALONGKORN UNIVERSITY

---

This article has been published in Journal: Journal of Membrane Science.

Page: 23–33. Volume: 448. Year: 2013.

---

## 5.1 Abstract

The separation of Pb(II) and Hg(II) via a hollow fiber supported liquid membrane (HFSLM) is presented. The experiment studied the influence of types of extractants, the concentration of selected extractants, setting modules, operating time together with flow rates of feed and stripping solutions. The mathematical model used to predict the concentration of Pb(II) and Hg(II) in both feed and stripping solutions was developed based on chemical reactions. The results clearly showed that a double-module HFSLM can selectively separate Pb(II) and Hg(II) at a very low concentration. Optimum condition was achieved using 0.03 M D2EHPA and 0.06 M Aliquat 336 as the extractant for first and second modules. The flow rates of the feed and stripping solutions were 100 mL/min. The complicated series of differential equations arising from the model was solved using the concept of Generating Function. The concentration of Pb(II) and Hg(II) in feed and stripping solutions, obtained from the model, fitted well with that from the experimental results as shown in Figure 5.10. This indicated that the extraction and stripping reactions were important factors that governed the rate of Pb(II) and Hg(II) transport across the liquid membrane phase.

**Keywords:** Generating Function; Separation; Pb(II); Hg(II); HFSLM.



## 5.2 Introduction

Wastewater from offshore oil and gas production is usually contaminated with toxic metals such as lead and mercury. Quantities of lead and mercury exposed to the environment continuously intensify with the quantity of wastewater generated by the activities of offshore oil and gas production. Lead and mercury can cause acute and chronic poisoning in humans [1–4]. The Thailand Ministry of Industry and the Ministry of Natural Resources and Environment [5] established regulatory discharge limits for lead and mercury from industrial wastewaters. The Ministry stipulated that limits should be no higher than 0.2 and 0.05 mg/L. In practice, conventional methods, i.e. adsorption, ion exchange, coagulation and precipitation, are used to treat toxic metals in wastewater. Wastewater treatment is controlled by on-line monitors. However, sometimes the concentration of toxic metals in wastewater, after treatment, is over the water-quality standard [6,7]. Inbaraj et al. [8] reported that conventional methods are always ineffective in treating a very low concentration of metal ions contaminated in mg/L or  $\mu\text{g/L}$  level.

Several studies have shown that hollow fiber supported liquid membrane (HFSLM) is an effective method for separating a very low concentration of metal ions from various aqueous solutions. This method allows for both simultaneous extraction and stripping processes of target ions in one single-step operation, with high selectivity [9,10]. Many advantages of HFSLM over traditional methods include lower energy consumption, lower capital and operating costs and less solvent used [11]. HFSLM has a high surface area that contributes to the adequate rates of separation for industrial purposes [12,13]. It can be utilized in many applications in industries,

such as chemical, food and pharmaceutical processing [12,14,15]. Hollow fiber modules can be connected in parallel or in series for a larger capacity [16]. Therefore, HFSLM is suitable for use as a secondary method in order to effectively manage a very low concentration of metal ions.

Recent studies have investigated the use of HFSLM for separating various trace metal ions from aqueous solutions or wastewater. Güell et al. [17] for example, reported on the separation of Cr(VI) at a concentration level of  $\mu\text{g/L}$  from different aqueous matrices via HFSLM using trioctyl methyl ammonium chloride (Aliquat 336) as the extractant. Results demonstrated that this system was most efficient in removing Cr(VI) from different aqueous samples: liquid membrane was stable during an operating time of 8 days non-stop. Buachuang et al. [18] separated tantalum ions from dilute hydrofluoric media across HFSLM. Aliquat 336 diluted in kerosene was used as the liquid membrane. The percentage of tantalum extraction was 80% using 0.3 M HCl in the feed solution, 0.06 M Aliquat 336 in the liquid membrane and 0.2 M  $\text{NaClO}_4$  as the stripping solution. Mafu et al. [19] separated As(III) from wastewater by HFSLM. Results showed that 50% of As(III) was removed using *n*-undecane and di-*n*-hexyl ether mixtures (3:1%v/v) as the liquid membrane and  $\text{H}_2\text{SO}_4$  as the stripping solution. Mtibe et al. [20] applied HFSLM in conjunction with high-performance liquid chromatography (HPLC) to separate dibutyl phthalate (DBP), benzyl butyl phthalate (BBP) and diethylhexyl phthalate (DEHP) from wastewater.

HFSLM has many advantages and researchers are interested in using HFSLM in order to manage a large volume of wastewater contaminated with a very low concentration of toxic ions [21]. Since the reliable mathematical models provide an understanding of the transport mechanism of the target species across the liquid

membrane from the feed side to the stripping side, they therefore, are required. The models also help in the scale-up of the HFSLM system [22].

Most models have been developed based on the principle of a facilitated diffusional transport mechanism neglecting the chemical reactions in the system. Kandwal et al. [23] established a mathematical model describing the transport of Cs(I) through HFSLM based on the facilitated diffusional transport mechanism: the chemical reactions were neglected. Results showed that the said mathematical model was acceptable. Vernekar et al. [22] developed a model for the transport of Co(II) across HFSLM diffusional transport, neglecting the complexation and de-complexation reactions. Results indicated that the controlling step of Co(II) transport was the diffusion in the liquid membrane phase. However, Yang and Kocherginsky [24] found that the transport of Cu(II) across the liquid membrane also depended on the chemical reactions. Pancharoen et al. [21] developed a mathematical model describing the transport of Cu(II) via HFSLM. The model was developed based on chemical reaction at the feed-liquid-membrane interface, neglecting the diffusion. The modeled results fitted well with the experimental data. This confirmed that the transport of Cu(II) via HFSLM was controlled by the chemical reaction. However, this model describes the transport of target ions only in the feed side. A mathematical model, therefore, based on chemical reaction was developed in this work to describe the transport of target ions across HFSLM from feed side to stripping side.

Developing a mathematical model based on chemical reactions leads to a complicated series of differential equations. The concept of Generating Function has been used to solve the series of differential equations in catalytic polymerization

which are not easy to solve due to difficulty in integrating. By using this concept, chemical kinetic problems have been overcome in many cases [25].

This work studied the selective extraction and stripping of a very low concentration of lead and mercury ions from synthetic wastewater in order to comply with the regulatory discharge limit. Types of extractants, concentration of the selected extractants, setting modules, operating time together with the flow rates of feed and stripping solutions were investigated. A mathematical model based on chemical reactions was developed to describe the transport of lead and mercury ions in both feed and stripping sides. The complicated series of differential equations arising from the model was solved by the concept of the Generating Function. The results achieved by the experiment were compared to those obtained from the model.

### 5.3 Modeling of lead and mercury ions transport

#### 5.3.1 Transport mechanisms of lead and mercury ions across the liquid membrane phase

$\text{PbCl}_2$  and  $\text{HgCl}_2$  dissolved in  $\text{NaCl}$  solution were used as feed solution.  $\text{PbCl}_2$  dissociates to cations while  $\text{HgCl}_2$  in the presence of chloride ions associates to anions [26]. In HFSLM operation, both feed and stripping solutions are fed into the tube and shell sides of the hollow fibers, respectively. Both solutions are separated by an organic extractant embedded in the supported liquid membrane. Figs. 5.1 and 5.2 show the schematics of the mass transports of target metal ions ( $\text{Pb(II)}$  and  $\text{Hg(II)}$ )

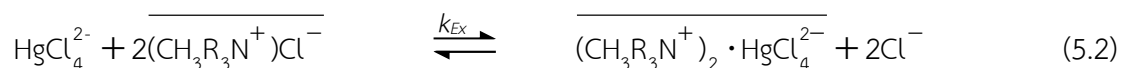
across the liquid membrane phase. The target metal ions in the feed solution react with the organic extractant at the feed–liquid-membrane interface resulting in the formation of a metal–extractant complex. Then, the complex species diffuses across the liquid membrane phase to the liquid-membrane–stripping interface due to its concentration gradient. Subsequently, it reacts with the stripping solution. After that, the target metal ions are released into the stripping phase while the extractant diffuses back towards the feed–liquid-membrane interface and reacts once again with the target metal ions from the feed phase.

The extraction of Pb(II) by di-(2-ethylhexyl)phosphoric acid (D2EHPA,  $\overline{\text{HR}}$ ) at the feed–liquid-membrane interface, as shown in Figure 5.1, is described by [27]



The overbar represents the species in the liquid membrane phase.

The extraction of Hg(II) by  $(\text{CH}_3\text{R}_3\text{N}^+)\text{Cl}^-$  (Aliquat 336) at the feed–liquid-membrane interface, as shown in Figure 5.2, is described by [28]



At the liquid–membrane–stripping interface, the complex species  $\overline{\text{PbR}_2}$  reacts continuously with  $\text{H}^+$  from the stripping solution and then releases Pb(II) into the stripping phase as follows:

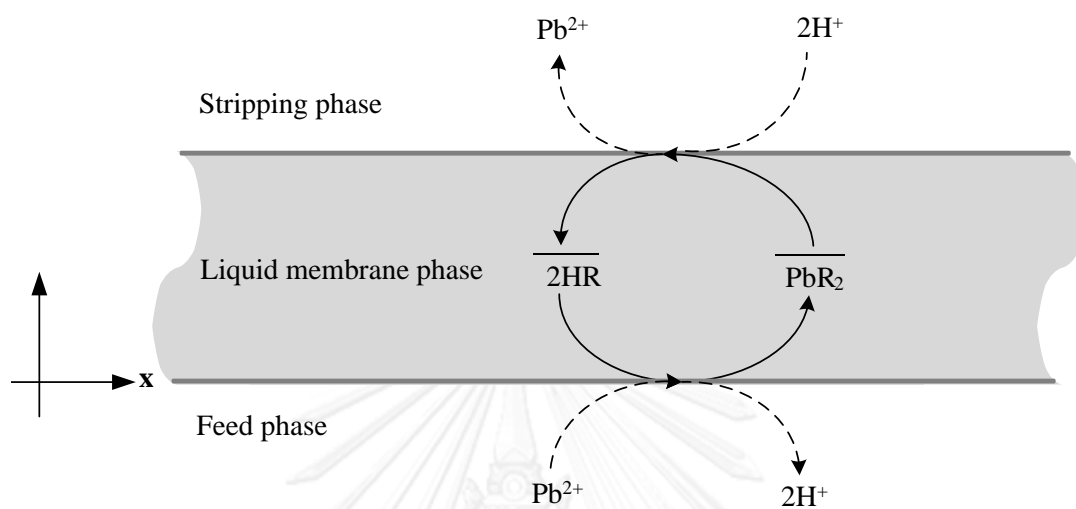


**Figure 5. 1** Schematic of mass transport of Pb(II) across the liquid membrane phase using  $\overline{\text{HR}}$  (D2EHPA) as the extractant and HCl as the stripping solution.

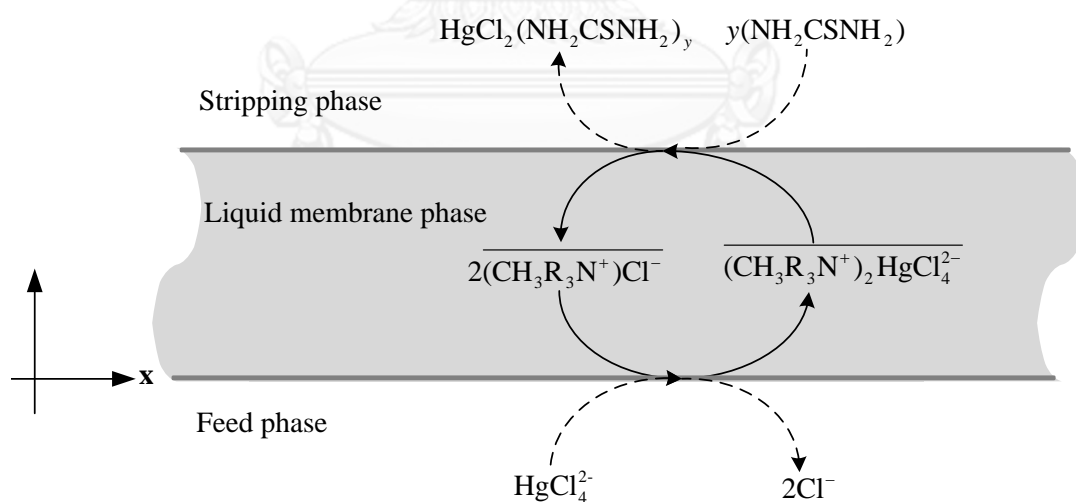
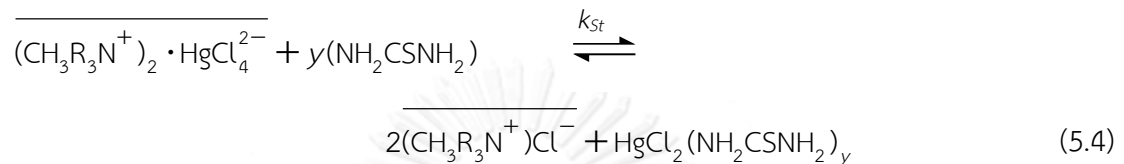


**Figure 5. 2** Schematic of mass transport of Hg(II) across the liquid membrane phase using  $(\text{CH}_3\text{R}_3\text{N}^+)\text{Cl}^-$  (Aliquat 336) as the extractant and  $\text{NH}_2\text{CSNH}_2$  (thiourea) as the stripping solution.

In the case of the species  $\overline{(\text{CH}_3\text{R}_3\text{N}^+)_2 \cdot \text{HgCl}_4^{2-}}$ , at the liquid-membrane-stripping interface, it reacts continuously with  $\text{NH}_2\text{CSNH}_2$  (thiourea) from stripping solution and then releases  $\text{Hg(II)}$  into the stripping phase as follows [28]:



In the hollow fiber operation, metal ion in the complex, occurring at the feed-liquid-membrane interface, is stripped out continuously by the stripping agent at the liquid-membrane-stripping interface. Therefore, the total reaction in Eqs. (5.1) and (5.2) can be considered as the forward reaction.

The reaction rate of extraction of  $\text{Pb(II)}$  and  $\text{Hg(II)}$  ( $r_{A,Ex}$ ) can be described as follows:

$$r_{A,Ex}(x,t) = -k_{Ex} C_{A,F}^m(x,t) \quad (5.5)$$

where  $x$  is the longitudinal axis of the hollow fiber in the feed phase,  $k_{Ex}$  is the reaction rate constant of extraction,  $t$  is the extraction time,  $C_{A,F}$  is the concentration of metal ions in the feed solution (mg/L) and  $m$  is the reaction order of extraction.

To strip metal ions, the stripping solution is kept at an excess concentration. Therefore, the total reaction of stripping of  $\text{Pb(II)}$  and  $\text{Hg(II)}$  in Eqs. (5.3) and (5.4) can

be considered as the forward reaction. Thus, the reaction rate of stripping of Pb(II) and Hg(II) ( $r_{A,St}$ ) can be written as

$$r_{A,St}(x',t) = k_{St} C_{A,St}^n(x',t) \quad (5.6)$$

where  $x'$  is the longitudinal axis of the hollow fiber in the stripping phase,  $k_{St}$  is the reaction rate constant of stripping,  $C_{A,St}$  is the concentration of metal ions in the stripping solution and  $n$  is the reaction order of stripping.

### 5.3.2 Developing the mathematical model

A mathematical model based on the chemical reaction was developed to predict the concentration of lead and mercury ions in both feed and stripping solutions for extraction and stripping via HFSLM.

The mathematical model for the feed phase was developed based on the following assumptions:

1. The feed-phase physical properties viz. temperature, pressure and volume are constant.
2. The hollow-fiber inside diameter is very small. Thus, the concentration profiles of lead and mercury ions in the radial direction are constant, meaning that the diffusion fluxes of these ions in the feed phase occur only in the axial direction.
3. Only the complex species which occurs from the extraction reaction, not metal ions, can transport into the liquid membrane phase.



4. The rate of transport of lead and mercury ions from the feed phase to the liquid-membrane phase is controlled by the extraction reaction at the feed-liquid-membrane interface.

For the stripping of lead and mercury ions into the stripping phase, a mathematical model was developed under the following assumptions:

1. The stripping-phase physical properties viz. temperature, pressure and volume are constant.
2. Only the lead and mercury ions which result from the stripping reaction at the liquid-membrane-stripping interface, not complex species, can be stripped into the stripping phase.
3. The rate of transport of lead and mercury ions from the liquid-membrane-stripping interface to the stripping phase is controlled by the stripping reaction at the liquid-membrane-stripping interface.

The conservation of mass for the transport of metal ions in the feed and stripping phases is considered at small segments of the hollow fibers, as shown in Figure 5.3.

In the feed phase, the conservation of mass for metal ions in each small segment ( $\Delta x$ ) is described by

$$q_F C_{A,F}(x_{i-1}, t) - q_F C_{A,F}(x_i, t) + r_{A,Ex}(x_i, t) V_p = V_t \frac{dC_{A,F}(x_i, t)}{dt} \quad (5.7)$$

where  $q_F$  is the volumetric flow rate of the feed solution,  $i$  is the number of small segments,  $V_p$  is the pore volume of a small segment of the hollow fiber and  $V_t$  is the volume of a small segment on the tube side of the hollow fiber.

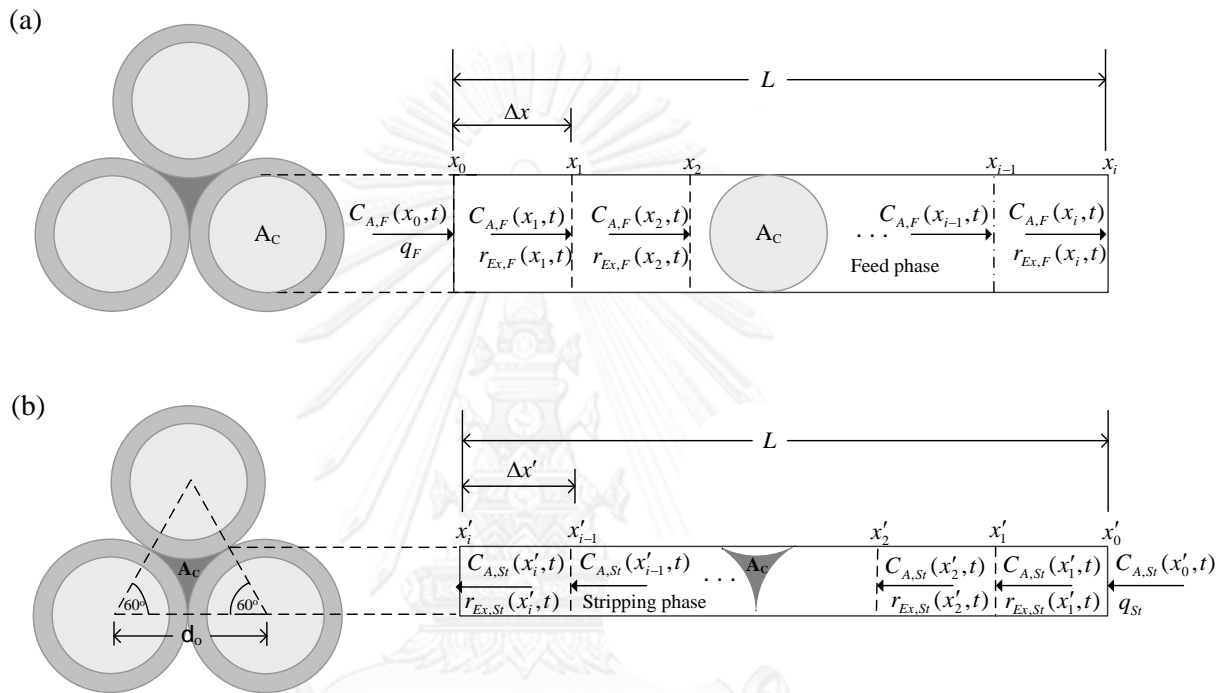


**Figure 5. 3** Schematic of the transport mechanism of metal ions through small segments: (a) feed phase (tube side), (b) stripping phase (shell side).

Solving Eq. (5.7) by the concept of the Generating Function, as described in detail in Appendix A, the equation for estimating the concentration of metal ions in the outlet feed ( $C_{A,F}(x_i, t)$ ) is obtained as shown below:

$$C_{A,F}(x_i, t) = -C_{A,F}(0,0)e^{(-\lambda tq_F)/V_t} \sum_{l=1}^i \frac{1}{(j-l)!} \left(\frac{1}{\lambda}\right)^l \cdot \left(\frac{tq_F}{V_t}\right)^{i-l} +$$

$$\frac{V_t \alpha}{q_F \lambda} e^{(-\lambda tq_F)/V_t} \sum_{l=1}^i \frac{1}{(j-l)!} \left(\frac{tq_F}{V_t}\right)^{i-l} \sum_{j=1}^l \left(\frac{1}{\lambda}\right)^{j-1} - \frac{V_p \alpha}{q_F} \sum_{l=1}^i \frac{1}{\lambda^{j-l+1}} + C_{A,F}(0,0) \frac{1}{\lambda^i} \quad (5.8)$$

The parameters in Eq. (5.8) are described in detail in Appendix A.

In the case of the stripping phase for counter-current flow, the conservation of mass of metal ions at segment  $i$  can be expressed as follows:

$$q_{St} C_{A,St}(x'_{i-1}, t) - q_{St} C_{A,St}(x'_i, t) + r_{A,St}(x'_i, t) V_p = V_s \frac{dC_{A,St}(x'_i, t)}{dt} \quad (5.9)$$

where  $q_{St}$  denotes the volumetric flow rate of the stripping solution and  $V_s$  is the volume of a small segment on the shell side of the hollow fiber.

Solving Eq. (5.9) by the concept of Generating Function, the equation for estimating the concentration of metal ions in the outlet stripping solution ( $C_{A,St}(x'_i, t)$ ) is obtained as shown below:

$$C_{A,St}(x'_i, t) = -C_{A,St}(x'_0, 0)e^{t\theta_{q_{St}}/V_s} \sum_{l=1}^i \frac{1}{(i-l)!} \left(\frac{1}{\theta}\right)^l \cdot \left(\frac{tq_{St}}{V_s}\right)^{i-l} -$$

$$\frac{V_s \gamma}{\theta_{q_{St}}} e^{t\theta_{q_{St}}/V_s} \sum_{l=1}^i \frac{1}{(i-l)!} \left(\frac{tq_{St}}{V_s}\right)^{i-l} \sum_{j=1}^l \left(\frac{1}{\theta}\right)^{j-1} + \frac{V_p \gamma}{q_{St}} \sum_{l=1}^i \frac{1}{\theta^{i-l+1}} + C_{A,St}(x'_0, 0) \frac{1}{\theta^i} \quad (5.10)$$

where  $C_{A,St}(x'_0, 0)$  is the initial concentration of metal ions in the stripping solution at position  $x'_0$ . The other parameters in Eq. (5.10) are described in detail in Appendix A.

## 5.4 Experimental

### 5.4.1 Reagents and solutions

The four types of extractants studied were D2EHPA (Merck Ltd.), Cyanex 471 (tri-isobutylphosphine sulfide, Cytec Canada Inc.), Aliquat 336 (Cognis Ltd.) and TOA (tri-n-octylamine, Sigma-Aldrich) all of which were uniformly mixed with the diluent i.e. toluene (Merck Ltd). Synthetic wastewater as feed solution was prepared by dissolving  $PbCl_2$  (Sigma-Aldrich Co.LLC),  $HgCl_2$  (Ajax Finechem Pty Ltd.) and NaCl (LobaChemie) in distilled water at a concentration of 1.0 mg/L of  $PbCl_2$  and  $HgCl_2$  together with a concentration of 1000 mg/L of NaCl. Hydrochloric acid (Merck Ltd.) and thiourea (RFLC) were found to be the best stripping for recovery of lead and mercury ions [29,30] and were further selected as the stripping solutions. The concentration of HCl was 0.9 M and that of thiourea was 0.1 M. These concentrations were selected because they were found to be the most suitable [29,30].

### 5.4.2 Apparatus

**Table 5. 1** Attributes of the hollow fiber module.

Attributes	Details
Material	Polypropylene
Module diameter	6.3 cm
Number of hollow fibers	10,000
Inside diameter of a hollow fiber	0.024 cm
Outside diameter of a hollow fiber	0.030 cm
Effective length of a hollow fiber	20.3 m
Contact area	$1.4 \times 10^4 \text{ cm}^2$
Area per unit volume	$29.3 \text{ cm}^2 \text{ cm}^{-3}$
Pore size	$3 \times 10^{-6} \text{ cm}$
Porosity	25%
Tortuosity	2.6

The hollow fiber module (Liqui-Cel Extra-flow 2.5 in. x 8 in.; Hoechst Celanese, Bridgewater, NJ) – consisting of 10,000 microporous polypropylene fibers which are woven into fabric and wrapped around a central feeder tube in order to supply the shell-side fluid – was used to study the separation of Pb(II) and Hg(II). Its attributes are listed in Table 5.1 [31]. Feed and stripping solutions were agitated by a magnetic stirrer (model CMT-V1) from Protronics Intertrade Co. Ltd. (Thailand). An inductively coupled plasma optical emission spectrometer (ICP-OES) (model JY-2000;

HORIBA Jobin Yvon, Edison NJ, USA) was used to determine the concentration of metal ions.

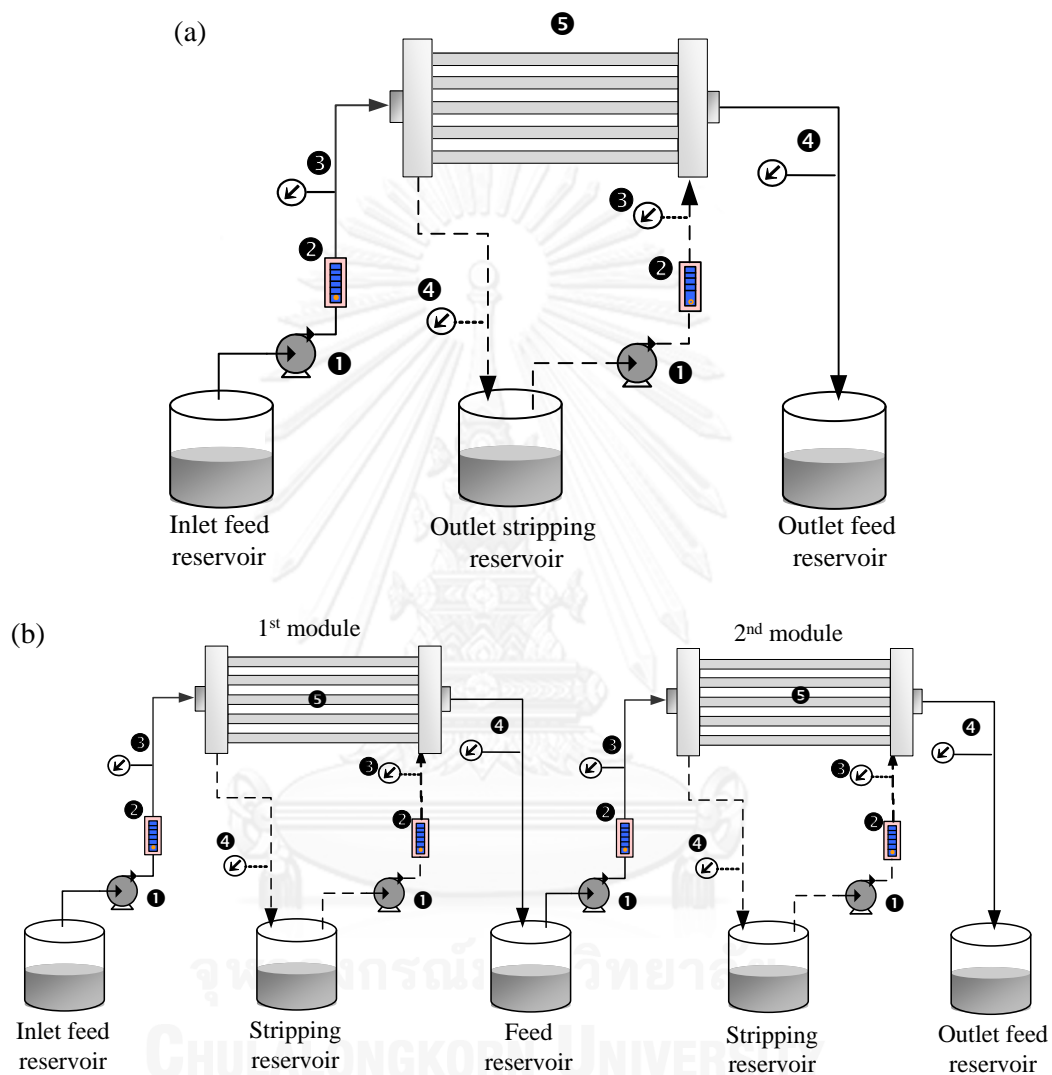


**Figure 5. 4** Schematic diagram of lead and mercury ion separation via HFSLM by counter-current flow patterns of feed and stripping solutions: (1) gear pumps, (2) flow meters, (3) inlet pressure gauges, (4) outlet pressure gauges, (5) hollow fiber modules.

### 5.4.3 Procedures

Liquid membrane – an extractant mixed with toluene – was circulated along the tube and shell sides of the hollow fibers simultaneously, until it filled in the hollow-fiber micropores with a total volume of about 52 mL. After that, distilled water was fed through the tube and shell sides of the hollow fibers to remove the excess liquid membrane. Subsequently, feed (synthetic wastewater) and stripping solutions were fed counter-currently into the tube and shell sides of the hollow fibers. The flow patterns of feed and stripping solutions were single-pass flow and circulating flow which were the best flow patterns observed from previous work [29]. The influence of types of extractants and the concentration of the selected extractant were investigated using single module HFSLM, as shown in Figure 5.4(a), with 0.9 M HCl as stripping solution. The volume of feed and stripping solutions was 1 L. Samples of feed and stripping solutions of 10 mL each were taken at 10 min.

A double-module HFSLM, as shown in Figure 5.4(b), was applied in order to selectively separate lead and mercury ions. One module was used to selectively separate lead ions. The other module was used to selectively separate mercury ions. In the double-module HFSLM, modes of setting modules, operating time and flow rates of both feed and stripping solutions were studied using 8 L of feed solution and 1 L of stripping solution. Feed and stripping solutions were collected every 10 min for 80 min. All samples collected from the experiment determined the concentration of metal ions by ICP-OES. The results of both flow rates of feed and stripping solutions were used in order to verify the validity of the model which is shown by the average percent deviation:

$$\% \text{ Deviation} = \frac{\sum_{j=1}^l ((C_{\text{Expt.}} - C_{\text{Model}}) / C_{\text{Expt.}})_j}{l} 100 \quad (5.11)$$

## 5.5 Results and discussion

### 5.5.1 Influences of extractants

From a review of the literature, D2EHPA showed high performance in the extraction of lead ions [27,32–34]. On the other hand, Cyanex 471, Aliquat 336 and TOA showed high efficiency in the extraction of mercury ions [30,35,36]. Thus, all of the above were chosen to study the selective extraction of lead and mercury ions. The experiment was conducted using a single-module hollow fiber with 0.9 M HCl as stripping solution. As shown in Figure 5.5, D2EHPA was the best extractant for the selective extraction of lead ions. This corresponded to the fact that D2EHPA is an acidic extractant which reacts well with Pb(II) cations. Mercury in anions form does not react with an acid extractant i.e., D2EHPA [37]. In the case of the extraction of mercury ions, Cyanex 471 was the best extractant. TOA and Aliquat 336, however, attained a higher selective extraction of mercury ions than Cyanex 471 did. It can be explained that TOA and Aliquat 336 are basic extractants which react well with anions but do not react with cations. The extraction percentage of mercury ions by Aliquat 336 was higher than that by TOA. This is because Aliquat 336 has a higher basicity than TOA [38]. D2EHPA and Aliquat 336 were chosen for further study with regards to their relevant variables of concentrations, setting modules and operating time in order to selectively extract lead and mercury ions, respectively.



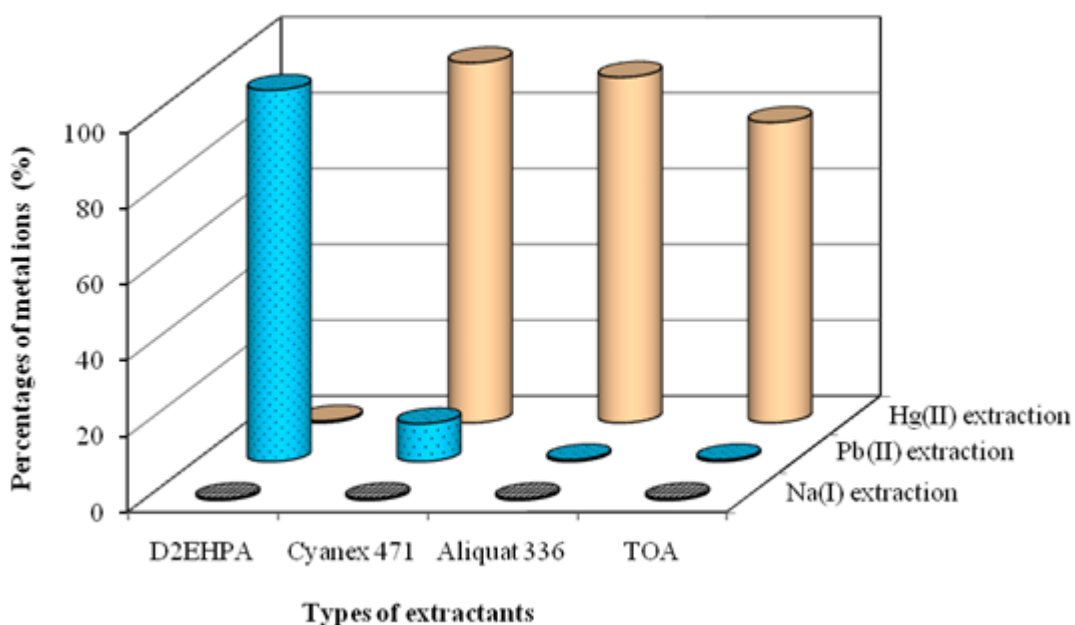


**Figure 5. 5** Percentages of metal ions versus types of extractants (0.03 M each) by single-module hollow fiber at flow rates of feed and stripping solutions of 100 mL/min with 0.9 M HCl.

### 5.5.2 Influence of D2EHPA concentration on the selective extraction of lead ions

To selectively extract Pb(II) from synthetic wastewater containing Pb(II) and Hg(II) and Na(I), D2EHPA was selected. Its concentration varied from  $5 \times 10^{-8}$  to 0.09 M. Results are shown in Figure 5.6. Extraction percentage of Pb(II) dramatically increased as D2EHPA concentration increased. This was in agreement with the chemical kinetics where reaction rate of extraction of Pb(II) increased when the concentration of D2EHPA was increased. Extraction percentage of Pb(II) increased to 98% at D2EHPA concentration up to 0.03 M. Percentage of Pb(II) stripping was lower

than that of Pb(II) extraction since there was an accumulation of metal–extractant complex in the liquid membrane. Only some metal–extractant complexes reached the liquid-membrane–stripping interface to react with the stripping solution. In order to study the other variables, 0.03 M D2EHPA was selected.

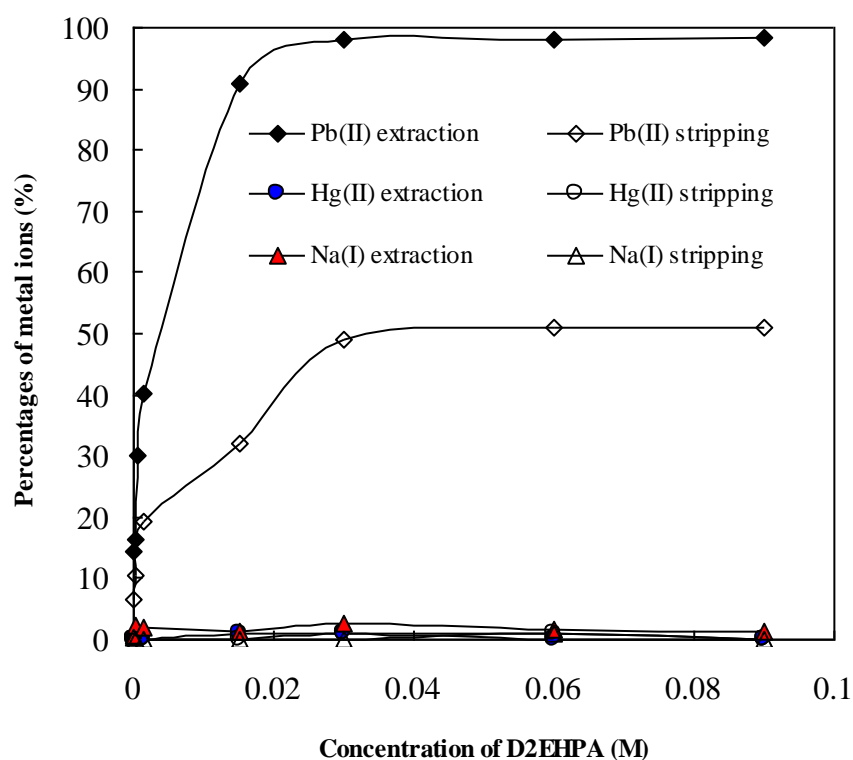
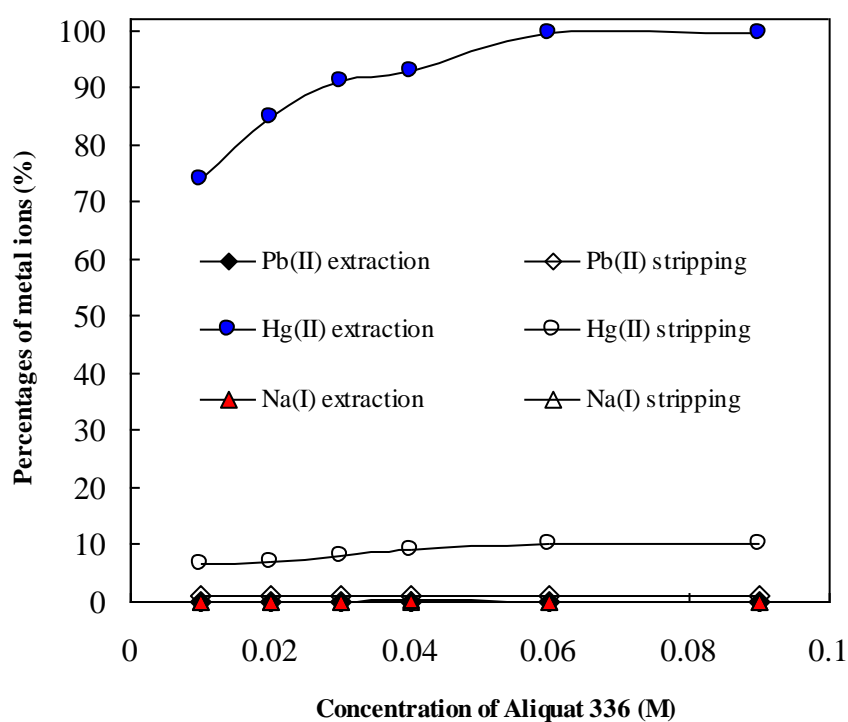


Figure 5. 6 Percentages of metal ions versus concentration of D2EHPA by single-module hollow fiber at flow rates of feed and stripping solutions of 100 mL/min with 0.9 M HCl.

### 5.5.3 Influence of Aliquat 336 concentration on the selective extraction of mercury ions

Aliquat 336 and thiourea were used as the extractant and the stripping solution, respectively, to study the selective separation of Hg(II). The concentration of

Aliquat 336 varied from 0.01 to 0.09 M but that of thiourea was fixed at 0.1 M. As shown in Figure 5.7, extraction percentage of Hg(II) increased when Aliquat 336 concentration increased in accordance with chemical kinetics. The extraction percentage of Hg(II) increased to about 100% at Aliquat 336 concentration up to 0.06 M. Thus, 0.06 M Aliquat 336 was chosen to study further variables.



**Figure 5. 7** Percentages of metal ions versus concentration of Aliquat 336 by single-module hollow fiber at flow rates of feed and stripping solutions of 100 mL/min with 0.1 M thiourea.

#### 5.5.4 Influences of setting modules

To selectively separate Pb(II) and Hg(II) from synthetic wastewater containing Pb(II), Hg(II), and Na(I), a double-module HFSLM was applied. One module was used to selectively separate Pb(II) and another module was used to selectively separate Hg(II). The percentages of lead and mercury extractions versus setting modules are shown in Figure 5.8.

Figure 5.8(a) shows the percentages of lead and mercury extractions using 0.03 M D2EHPA as the extractant for the first module and 0.06 M Aliquat 336 as the extractant for the second module. 0.9 M HCl and 0.1 M thiourea were used as the stripping solutions for the first and second modules, respectively. It was observed that lead ions were almost totally extracted in the first module while mercury ions were almost completely extracted in the second module. This was because the first module contained D2EHPA which has a small value of acid dissociation constant. It reacts with only cations like Pb(II). The second module contained Aliquat 336 having a small value of base dissociation constant which reacts well with anions like Hg(II).

In Figure 5.8(b), for the first module, 0.06 M Aliquat 336 was used as the extractant with 0.1 M thiourea as the stripping solution. In the second module, 0.03 M D2EHPA was used as the extractant with 0.9 M HCl as the stripping solution. Results clearly showed that mercury ions were almost completely extracted in the first module, without extraction of lead ions because this module contained Aliquat 336. As for lead ions, in the second module, they were highly extracted since this module contained D2EHPA.

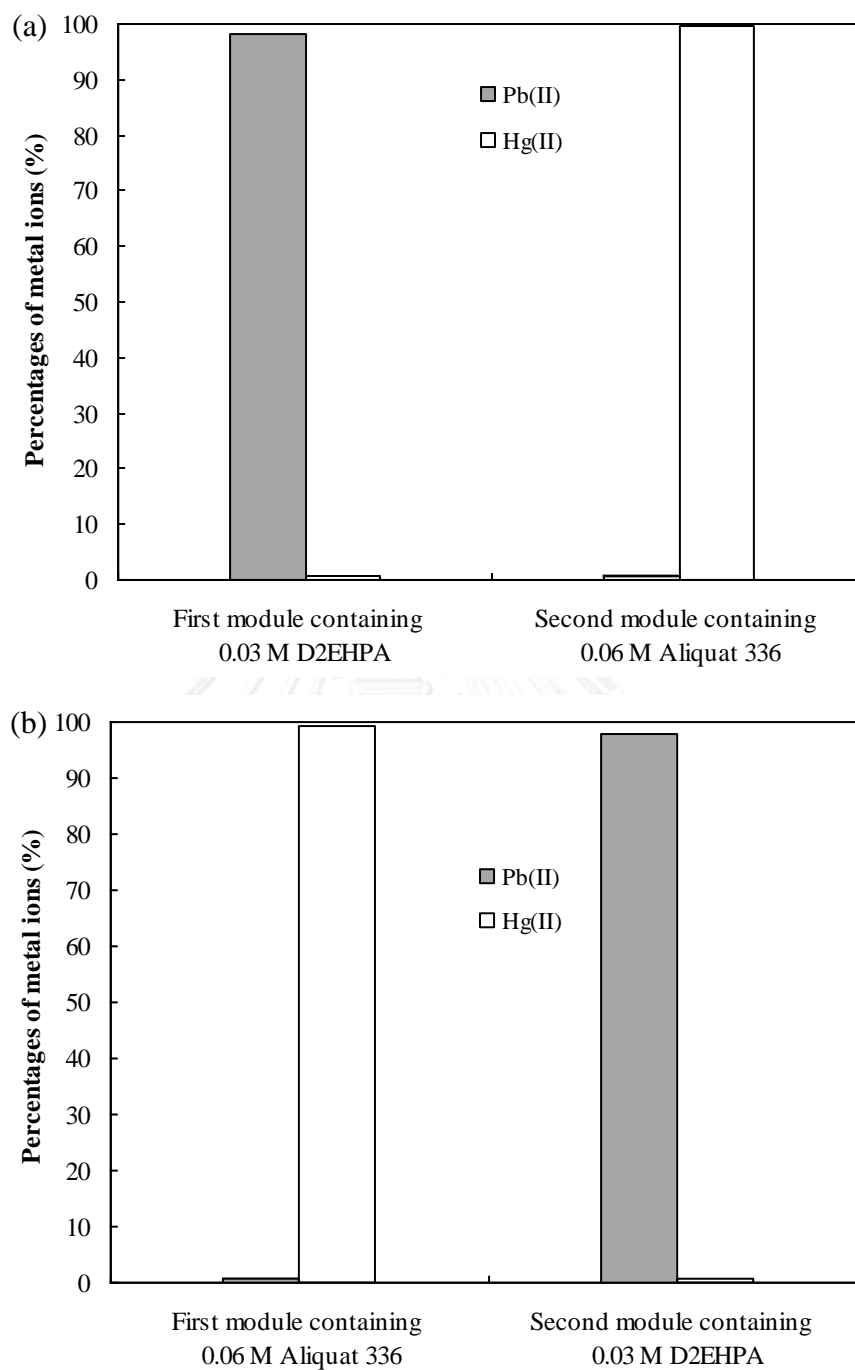


**Figure 5. 8** Percentages of extraction of metal ions versus setting modules with flow rates of feed and stripping solutions of 100 mL/min: (a) 0.9 M HCl and 0.1 M thiourea as the stripping solution for the first module and the second module, respectively, (b) 0.1 M thiourea and 0.9 M HCl as the stripping solution for the first module and the second module, respectively.

### 5.5.5 Influence of operating time

The influence of operating time was investigated using double-module hollow fiber. The first and second modules were set to selectively separate lead ions and mercury ions, respectively. In the first module, 0.03 M D2EHPA was used as the extractant and 0.9 M HCl was used as the stripping solution. For the second module, the extractant and stripping were 0.06 M Aliquat 336 and 0.1 M thiourea, respectively. Concentration of lead and mercury ions in inlet feed solution was 1 mg/L. The results are shown in Figure 5.9(a)–(d).

With regards to the separation of Pb(II), in the first module (Figure 5.9(a) and (b)), Pb(II) was extracted immediately from the feed solution. Moreover, its concentration in the stripping solution increased continuously with operating time. This resulted from the continual accumulation of Pb(II) due to the circulation of stripping solution. After 20 min, Pb(II) concentration in the stripping solution reached a higher level than that in the inlet feed solution. This was because Pb(II) in excess HCl is converted to anions [39] which cannot recombine with D2EHPA extractant.

In the case of Hg(II) separation, in the second module (Figure 5.9(c) and (d)), Hg(II) was also extracted immediately from the feed solution. Hg(II) was then stripped continuously into the stripping solution. Its concentration in the stripping solution reached a higher level than that in the inlet feed solution after 60 min.

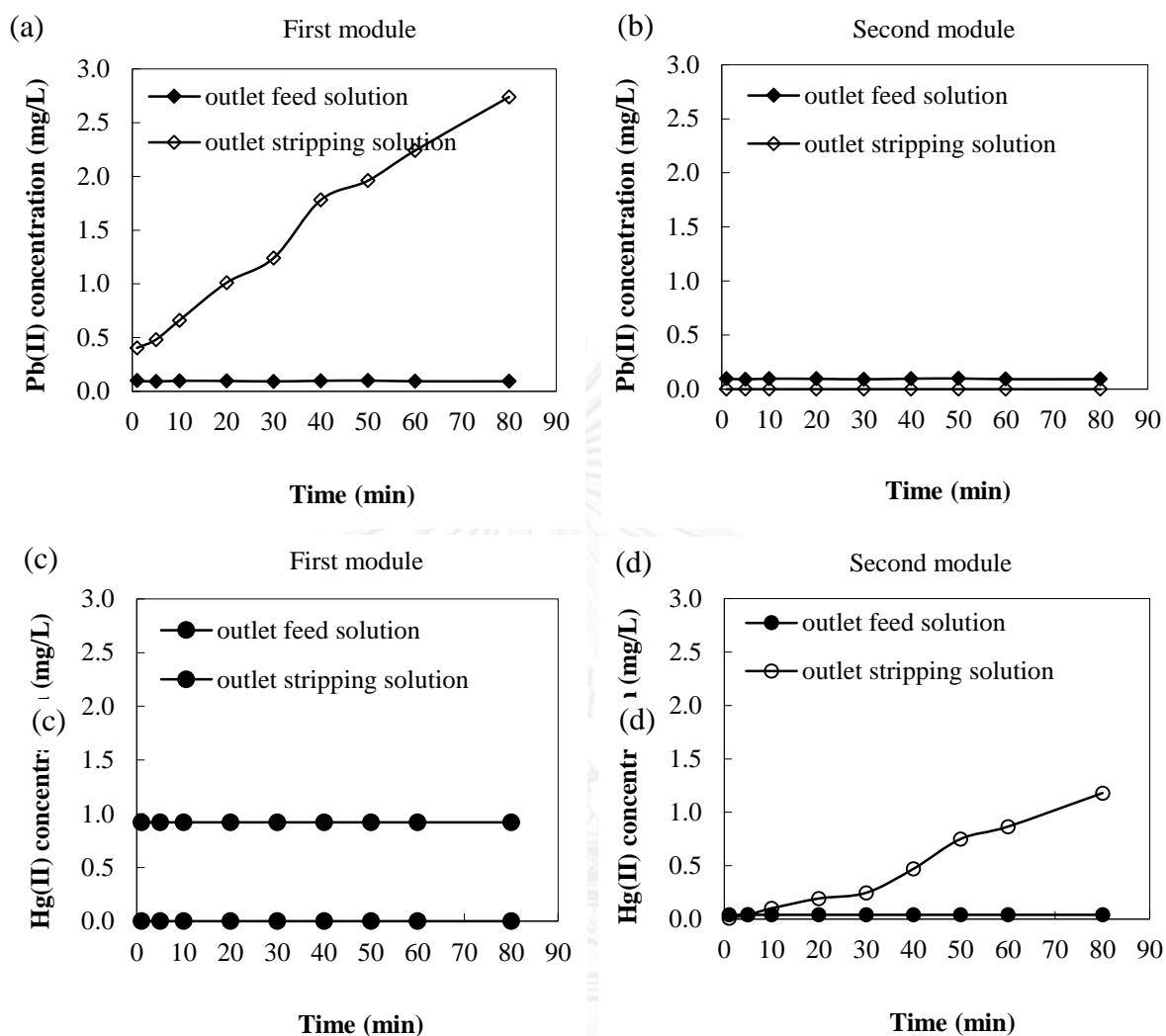


**Figure 5. 9** Concentration of metal ions versus operating time with flow rates of feed and stripping solutions of 100 mL/min, first module (a and c) using 0.03 M D2EHPA and 0.9 M HCl as the extractant and stripping solution, second module (b and d) using 0.06 M Aliquat 336 and 0.1 M thiourea as the extractant and stripping solution: (a) and (b) for Pb(II), (c) and (d) for Hg(II).

### 5.5.6 Parameters used in the model

**Table 5. 2** Reaction orders ( $m/n$ ) versus reaction rate constants of Pb(II) and Hg(II) extraction and stripping ( $k_{EX}$  and  $k_{St}$ ).

$m/n$	Reaction	Plot	Reaction rate constant*		$R^2$	
			Pb(II)	Hg(II)	Pb(II)	Hg(II)
1	Extraction	$\ln \frac{C_{A0}}{C_A}$ and $t$	0.57 min <sup>-1</sup>	0.72 min <sup>-1</sup>	0.5667	0.2396
	Stripping	$\ln \frac{C_{CO}}{C_{CO} - C_S}$ and $t$	1.42 min <sup>-1</sup>	1.98 min <sup>-1</sup>	0.0841	0.5972
2	Extraction	$\frac{1}{C_A} - \frac{1}{C_{A0}}$ and $t$	1.51 L/mg min	1.20 L/mg min	0.9788	0.9980
	Stripping	$\frac{1}{C_{CO} - C_S} - \frac{1}{C_{CO}}$ and $t$	11.20 L/mg min	9.25 L/mg min	0.9801	0.9997
3	Extraction	$\frac{1}{2C_A^2} - \frac{1}{2C_{A0}^2}$ and $t$	5.00 L <sup>2</sup> /mg <sup>2</sup> min	2.70 L <sup>2</sup> /mg <sup>2</sup> min	0.8263	0.9036
	Stripping	$\frac{1}{2(C_{CO} - C_S)^2} - \frac{1}{2C_{CO}^2}$ and $t$	219.16 L <sup>2</sup> /mg <sup>2</sup> min	104.12 L <sup>2</sup> /mg <sup>2</sup> min	0.8113	0.7745

\* Reaction rate constant of Pb(II) extraction obtained from previous work [29];  $C_A$ , concentration of metal ions in the feed solution at time  $t$ ;  $C_{A0}$ , initial concentration of metal ions in the feed solution;  $C_{CO}$ , initial concentration of metal ions in the organic extractant; and  $C_S$ , concentration of metal ions in the stripping solution at time  $t$ .

The reaction rate constant and reaction order for extraction and stripping of Pb(II) and Hg(II) in Eqs. (5.5) and (5.6) were determined using integration and graphical methods plotted between the integral concentrations of Pb(II) and Hg(II) versus time. Results are shown in Table 5.2. It was clear that the highest  $R^2$  of extraction and



stripping reactions was obtained at second-order reactions. Thus, both extraction and stripping reactions of Pb(II) and Hg(II) were second-order. The other relevant parameters to be used in the model, as described in detail in Appendix A, are listed in Table 5.3.

**Table 5. 3** Values of relevant parameters used in the model.

Parameters	Prediction	
	Pb(II)	Hg(II)
$C_{A,F(0,0)}$ (mg/L)	1.0	1.0
$V_t$ ( $10^4$ cm <sup>3</sup> )	4.59	4.59
$V_s$ ( $10^5$ cm <sup>3</sup> )	3.68	3.68
$i$ (dimensionless)	100	100
$\alpha$ (mg/L min)	-0.457	-0.190
$\beta$ (min <sup>-1</sup> )	1.661	0.960
$\gamma$ (mg/L min)	-0.038	-0.024
$\varphi$ (min <sup>-1</sup> )	1.301	0.941

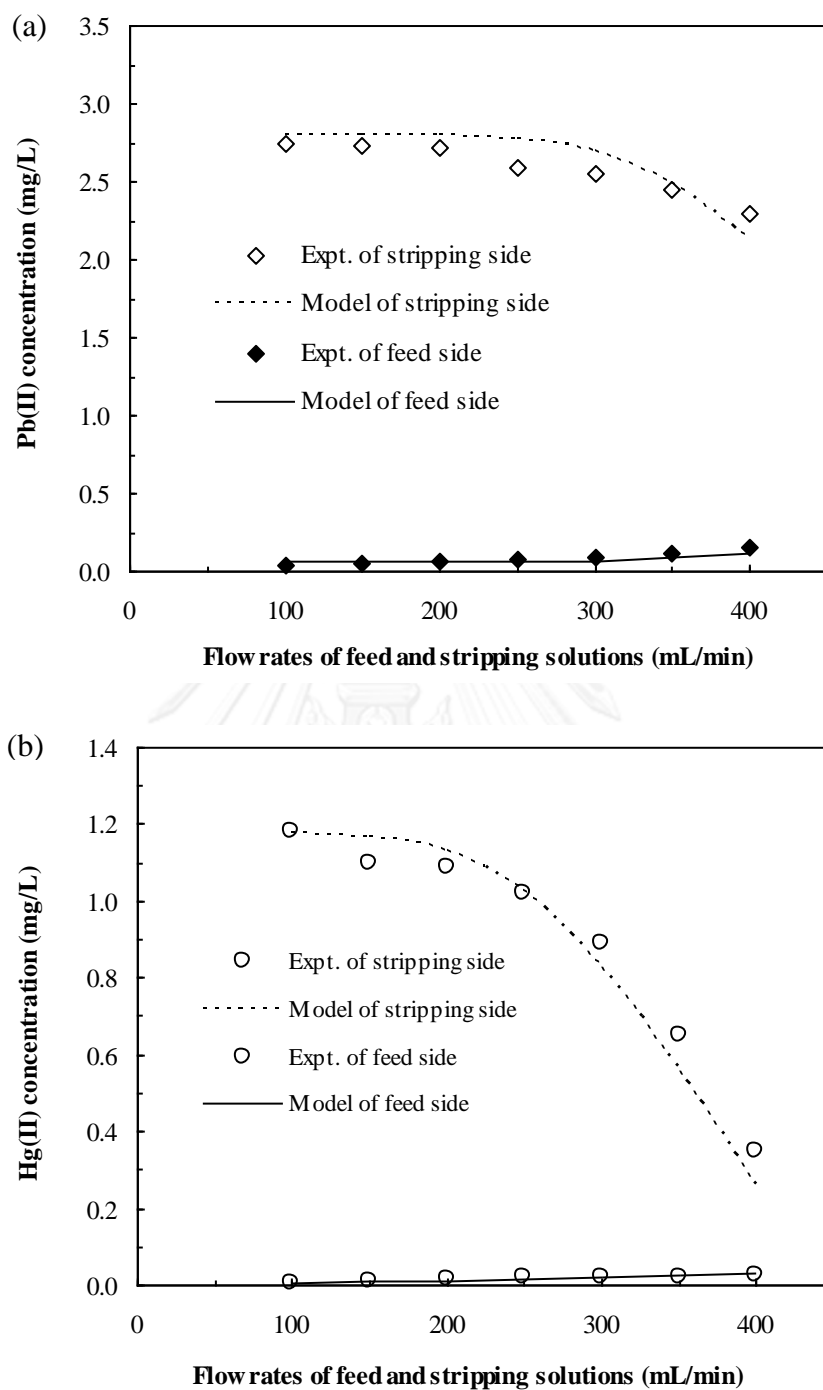
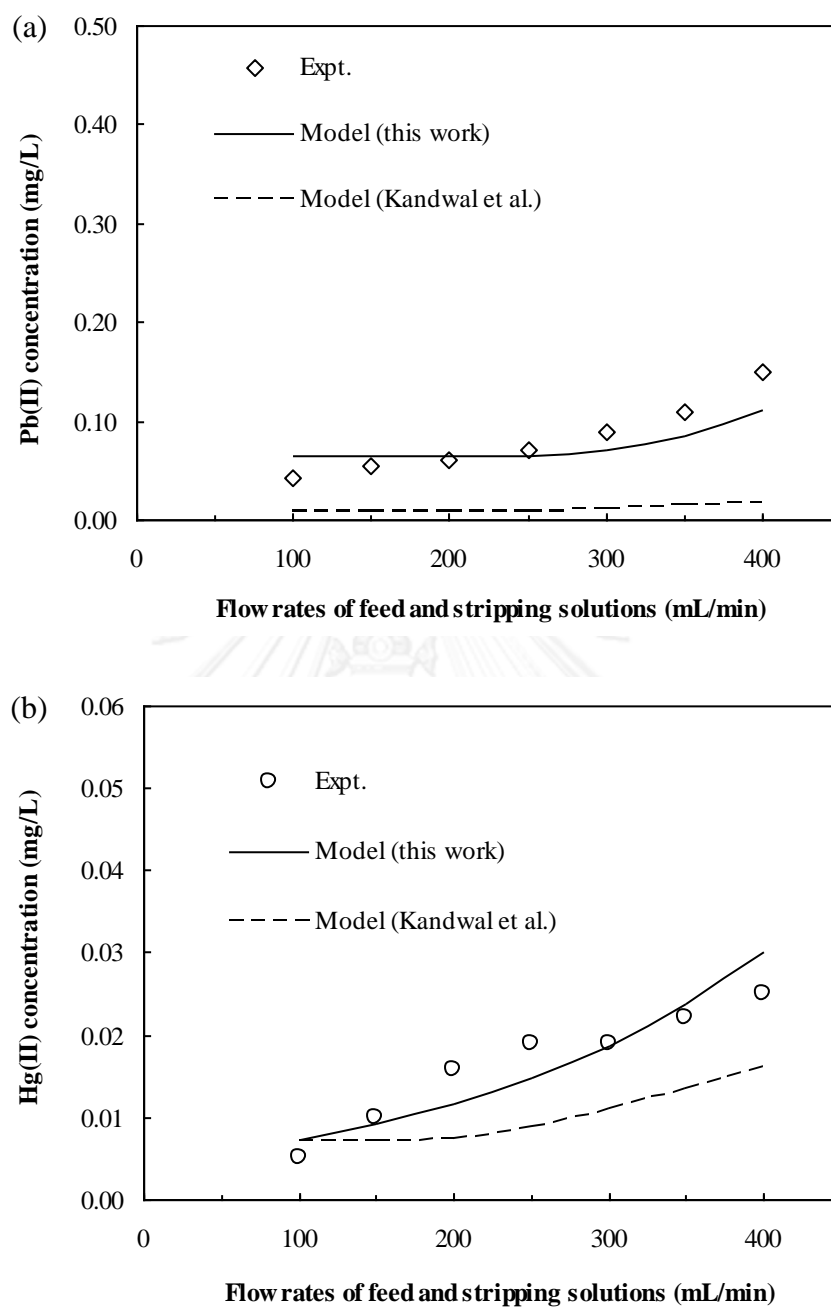


Figure 5. 10 Concentrations of Pb(II) and Hg(II) versus flow rates of feed and stripping solutions: (a) first module using 0.03 M D2EHPA and 0.9 M HCl as the extractant and stripping solution, respectively, (b) second module using 0.06 M Aliquat 336 and 0.1 M thiourea as the extractant and stripping solution, respectively.



**Figure 5. 11** Comparison of concentrations of Pb(II) and Hg(II) in the feed solution, obtained from experimental results and mathematical model results: (a) first module using 0.03 M D2EHPA and 0.9 M HCl as the extractant and stripping solution, respectively, (b) second module using 0.06 M Aliquat 336 and 0.1 M thiourea as the extractant and stripping solution, respectively.

### 5.5.7 Validation of the model with the experimental results

The experiment, under various flow rates of both feed and stripping solutions, was carried out in order to validate model prediction. It was investigated by using a continuous flow of both feed and circulating flow of stripping solutions at flow rates between 100 and 400 mL/min. Operating time was 80 min. The concentration of Pb(II) and Hg(II) in feed and stripping solutions, from both experimental results and model results calculated by Eqs. (5.8) and (5.10), are shown in Figure 5.10. Results showed that the concentration of Pb(II) and Hg(II) in feed solutions slowly increased with higher flow rates of feed and stripping solutions, while their concentration in the stripping solutions showed opposite results. This was because of less residence time, as reported by Uedee et al. [40]. Therefore, flow rates of both feed and stripping solutions at 100 mL/min are recommended.

Concentration of Pb(II) and Hg(II) in feed and stripping solutions predicted by the model fitted well with the experimental results. Average percent deviation was 2% and 5% for predictions in the feed and stripping phases, respectively. Results indicated that the extraction and stripping reactions at both feed-liquid-membrane and liquid-membrane-stripping interfaces are important factors that govern the rate of lead and mercury ions transport across the liquid membrane.

### 5.5.8 Comparison of the models

Figure 5.11 shows the comparison of concentration of lead and mercury ions in feed solutions obtained from the experimental results and from the models (this

work and Kandwal et al. [23]). The model of Kandwal et al. was developed based on the principle of a facilitated diffusional transport mechanism (neglecting mass accumulation and chemical reactions). It can be seen that the model results, from the present work, were in good agreement with the experimental results. Average percent deviations were about 2% for both  $\text{PbCl}_2$  and  $\text{HgCl}_2$  solutions; whereas the results of the model by Kandwal et al. did not match the experimental results. This confirmed that the chemical reaction is a very important factor in controlling the rate of transport of lead and mercury ions along the hollow fibers.

## 5.6 Conclusion

Double-module HFSLM showed a high selective separation of  $\text{Pb(II)}$  and  $\text{Hg(II)}$  from synthetic wastewater containing  $\text{Pb(II)}$ ,  $\text{Hg(II)}$ , and  $\text{Na(I)}$ . D2EHPA and Aliquat 336 were found to be the best extractants for the selective extraction of  $\text{Pb(II)}$  and  $\text{Hg(II)}$ , respectively. Optimum condition was achieved using 0.03 M D2EHPA and 0.9 M HCl as the extractant and stripping solution for the first module with 0.06 M Aliquat 336 and 0.1 M thiourea as the extractant and stripping solution, respectively, for the second module. The concentration of lead and mercury ions in the stripping solutions increased linearly with operating time. Their concentration in the stripping solutions reached a higher level than that in the inlet feed solution after 20 and 60 min, respectively.

Reaction rate constants of extraction and stripping of  $\text{Pb(II)}$  were 1.51 and 11.20 L/mg min and of  $\text{Hg(II)}$  were 1.20 and 9.25 L/mg min. Concentration of  $\text{Pb(II)}$  and  $\text{Hg(II)}$  predicted by the developed model, based on the chemical reactions and

solved by the concept of Generating Function, were in good agreement with the experimental results. Average percent deviations were 2% and 5% for predictions in the feed and stripping phases. This indicated that chemical reactions at the liquid membrane interfaces were important factors that govern the rate of Pb(II) and Hg(II) transport across the liquid membrane phase.

### 5.7 Acknowledgements

The authors are very grateful for the financial support of the Thailand Research Fund and Chulalongkorn University under the Royal Golden Jubilee Ph.D. Program (Grant no. PHD/0324/2551), and the Asahi Glass Foundation. Sincere thanks are also extended to our research group and the Separation Laboratory, Department of Chemical Engineering, Chulalongkorn University, Bangkok, Thailand.

### 5.8 Appendix A. The developed-model mathematics and assumptions for metal-ion transport through HFSLM

The conservation of mass of metal ions in each small segment for feed phase is as shown below:

$$q_F C_{A,F}(x_{i-1}, t) - q_F C_{A,F}(x_i, t) + r_{A,Ex}(x_i, t) V_P = V_t \frac{dC_{A,F}(x_i, t)}{dt} \quad (\text{A.1})$$

Linearization of the reaction rate of extraction ( $r_{A,Ex}(x_i, t)$ ) in Eq. (A.1) using the Taylor series gives the following equation:

$$r_{A,Ex}(x_i, t) = -[\alpha + \beta C_{A,F}(x_i, t)] \quad (A.2)$$

where

$$\alpha = (1 - m)k_{EX} C_{A,F}^m(0,0)$$

$$\beta = mk_{EX} C_{A,F}^{m-1}(0,0)$$

$C_{A,F}(0,0)$  is the initial concentration of metal ions in the feed solution.

By substituting Eq. (A.2) into Eq. (A.1) and dividing by the volumetric flow rate, the following equation is obtained:

$$\frac{V_t}{q_F} \frac{dC_{A,F}(x_i, t)}{dt} = C_{A,F}(x_{i-1}, t) - \left(1 + \frac{V_P}{q_F} \beta\right) C_{A,F}(x_i, t) - \frac{V_P}{q_F} \alpha \quad (A.3)$$

$$V_t = \pi r_i^2 \Delta x, \quad V_P = \pi (r_o^2 - r_i^2) \Delta x \varepsilon, \quad \Delta x = \frac{L}{i}$$

where  $r_i$  and  $r_o$  are the inner and outer radius of the hollow fibers,  $\varepsilon$  is the porosity of the hollow fiber and  $L$  is the effective length of the hollow fibers.

Considering the conservation of mass in segments 1, 2, 3, ...,  $i$  based on Eq. (A.3), the following series of differential equations is obtained:

$$\frac{V_t}{q_F} \frac{dC_{A,F}(x_1, t)}{dt} = C_{A,F}(x_0, t) - \left(1 + \frac{V_p}{q_F} \beta\right) C_{A,F}(x_1, t) - \frac{V_p}{q_F} \alpha \quad (\text{A.4})$$

$$\frac{V_t}{q_F} \frac{dC_{A,F}(x_2, t)}{dt} = C_{A,F}(x_1, t) - \left(1 + \frac{V_p}{q_F} \beta\right) C_{A,F}(x_2, t) - \frac{V_p}{q_F} \alpha \quad (\text{A.5})$$

$$\frac{V_t}{q_F} \frac{dC_{A,F}(x_3, t)}{dt} = C_{A,F}(x_2, t) - \left(1 + \frac{V_p}{q_F} \beta\right) C_{A,F}(x_3, t) - \frac{V_p}{q_F} \alpha \quad (\text{A.6})$$

·  
·  
·

$$\frac{V_t}{q_F} \frac{dC_{A,F}(x_i, t)}{dt} = C_{A,F}(x_{i-1}, t) - \left(1 + \frac{V_p}{q_F} \beta\right) C_{A,F}(x_i, t) - \frac{V_p}{q_F} \alpha \quad (\text{A.7})$$

The series of differential equations in Eqs. (A.4)–(A.7) can be solved by using the concept of Generating Function. The definition of Generating Function [25,41] is

$$\mathcal{C}_A(Z, t) = C_{A0}Z^0 + C_{A1}Z^1 + C_{A2}Z^2 + \dots \quad (\text{A.8})$$

where

$$\begin{aligned} \mathcal{C}_A(Z, 0) &= C_A(x_0, 0)Z^0 + C_A(x_1, 0)Z^1 + C_A(x_2, 0)Z^2 + \dots = C_A(x_0, 0)Z^0 \\ &= C_A(x_0, 0) = C_A(0, 0) \end{aligned}$$

and  $Z$  is a complex quantity.



Eq. (A.8) can be represented as

$$\frac{\partial \mathcal{C}_A(Z,t)}{\partial t} = Z^0 \frac{dC_A(x_0,t)}{dt} + Z^1 \frac{dC_A(x_1,t)}{dt} + Z^2 \frac{dC_A(x_2,t)}{dt} + Z^3 \frac{dC_A(x_3,t)}{dt} + \dots \quad (\text{A.9})$$

By multiplying the series of differential equations in Eqs. (A.4)–(A.7) by  $Z^1, Z^2, Z^3, \dots, Z^i$ , and then summing them up, the following equation is obtained:

$$\begin{aligned} \frac{V_t}{q_F} \left[ \frac{dC_{A,F}(x_0,t)}{dt} + Z \frac{dC_{A,F}(x_1,t)}{dt} + Z^2 \frac{dC_{A,F}(x_2,t)}{dt} + Z^3 \frac{dC_{A,F}(x_3,t)}{dt} + \dots \right] = \\ Z \left[ C_{A,F}(x_0,t) + Z C_{A,F}(x_1,t) + Z^2 C_{A,F}(x_2,t) + \dots \right] - \\ \lambda \left[ C_{A,F}(x_0,t) + Z C_{A,F}(x_1,t) + Z^2 C_{A,F}(x_2,t) + Z^3 C_{A,F}(x_3,t) + \dots \right] - \\ \frac{V_t}{q_F} \alpha \left[ Z + Z^2 + Z^3 + \dots \right] + \lambda C_{A,F}(x_0,t) \end{aligned} \quad (\text{A.10})$$

where  $\lambda = (1 + (V_t/q_F)\beta)$ .

From the definition of the Generating Function, Eq. (A.10) can be rewritten as follows:

$$\frac{V_t}{q_F} \frac{\partial \mathcal{C}_{A,F}(Z,t)}{\partial t} = Z \mathcal{C}_{A,F}(Z,t) - \lambda \mathcal{C}_{A,F}(Z,t) - \frac{V_t}{q_F} \alpha \sum_{j=1}^i Z^j + \lambda C_{A,F}(x_0,t) \quad (\text{A.11})$$

By integrating Eq. (A.11) and using the boundary condition from Eq. (A.8), the following equation is obtained:

$$C_{A,F}(Z,t) = \left[ \frac{ZC_{A,F}(0,0)e^{(tq_F/V_t)Z}}{(Z-\lambda)} - \frac{(V_t\alpha/q_F)\sum_{j=1}^i Z^j}{(Z-\lambda)} e^{(tq_F/V_t)Z} \right] e^{(-\lambda tq_F/V_t)} + \frac{(V_p\alpha/q_F)\sum_{j=1}^i Z^j}{(Z-\lambda)} - \frac{\lambda C_{A,F}(0,0)}{(Z-\lambda)} \quad (\text{A.12})$$

By the distribution of  $Z$  function in Eq. (A.12) into polynomial form and using the method of undetermined coefficients, an equation for estimating the concentration of metal ions in the outlet feed solution ( $C_{A,F}(x_i,t)$ ) is obtained, as shown in Eq. (A.13):

$$C_{A,F}(x_i,t) = -C_{A,F}(0,0)e^{(-\lambda tq_F/V_t)} \sum_{l=1}^i \frac{1}{(j-l)!} \left(\frac{1}{\lambda}\right)^l \cdot \left(\frac{tq_F}{V_t}\right)^{i-l} + \frac{V_t\alpha}{q_F\lambda} e^{(-\lambda tq_F/V_t)} \sum_{l=1}^i \frac{1}{(j-l)!} \left(\frac{tq_F}{V_t}\right)^{i-l} \sum_{j=1}^l \left(\frac{1}{\lambda}\right)^{j-1} - \frac{V_p\alpha}{q_F} \sum_{l=1}^i \frac{1}{\lambda^{i-l+1}} + C_{A,F}(0,0) \frac{1}{\lambda} \quad (\text{A.13})$$

At the stripping phase, the conservation of mass of metal ions in segment  $i$  is shown below:

$$q_{St}C_{A,St}(x'_{i-1},t) - q_{St}C_{A,St}(x'_i,t) + r_{A,St}(x'_i,t)V_p = V_s \frac{dC_{A,St}(x'_i,t)}{dt} \quad (\text{A.14})$$

To linearize the term of  $r_{A,St}(x'_i, t)$  in Eq. (A.14), the Taylor series is applied:

$$r_{A,St}(x'_i, t) = \gamma + \varphi C_{A,St}(x'_i, t) \quad (\text{A.15})$$

where  $\gamma = (1 - n)k_{St}C_{A,St}^n(x'_0, 0)$

$$\varphi = nk_{St}C_{A,St}^{n-1}(x'_0, 0)$$

Substituting Eq. (A.15) in Eq. (A.14) and dividing by the volumetric flow rate of stripping solution, the following equation is obtained:

$$\frac{V_s}{q_{St}} \frac{dC_{A,St}(x'_i, t)}{dt} = C_{A,St}(x'_{i-1}, t) - \left(1 - \frac{V_p}{q_{St}}\varphi\right)C_{A,St}(x'_i, t) + \frac{V_p}{q_{St}}\gamma \quad (\text{A.16})$$

$$\text{where } V_s = \left( \frac{\sqrt{3}}{4}d_o^2 - \frac{\pi\omega_o^2}{2} \right) \Delta x'$$

$$\Delta x' = \frac{L}{i}$$

where  $d_o$  is the outer diameter of the hollow fiber.

The conservation of mass in the stripping phase at segments 1, 2, 3, ...,  $i$  based on Eq. (A.16) can be expressed by the following series of differential equations:

$$\frac{V_s}{q_{St}} \frac{dC_{A,St}(x'_1, t)}{dt} = C_{A,St}(x'_0, t) - (1 - \frac{V_P}{q_{St}} \varphi) C_{A,St}(x'_1, t) + \frac{V_P}{q_{St}} \gamma \quad (\text{A.17})$$

$$\frac{V_s}{q_{St}} \frac{dC_{A,St}(x'_2, t)}{dt} = C_{A,St}(x'_1, t) - (1 - \frac{V_P}{q_{St}} \varphi) C_{A,St}(x'_2, t) + \frac{V_P}{q_{St}} \gamma \quad (\text{A.18})$$

$$\frac{V_s}{q_{St}} \frac{dC_{A,St}(x'_3, t)}{dt} = C_{A,St}(x'_2, t) - (1 - \frac{V_P}{q_{St}} \varphi) C_{A,St}(x'_3, t) + \frac{V_P}{q_{St}} \gamma \quad (\text{A.19})$$

·  
·  
·

$$\frac{V_s}{q_{St}} \frac{dC_{A,St}(x'_i, t)}{dt} = C_{A,St}(x'_{i-1}, t) - (1 - \frac{V_P}{q_{St}} \varphi) C_{A,St}(x'_i, t) + \frac{V_P}{q_{St}} \gamma \quad (\text{A.20})$$

Solving the series of differential equations in Eqs. (A.17)–(A.20) by the same concept described in Eqs. (A.4)–(A.13), the equation for estimating the concentration of metal ions in the outlet stripping solution ( $C_{A,St}(x'_i, t)$ ) is obtained as shown in Eq. (A.21):

$$C_{A,St}(x'_i, t) = -C_{A,St}(x'_0, 0) e^{t\theta_{q_{St}}/V_s} \sum_{l=1}^i \frac{1}{(i-l)!} \left(\frac{1}{\theta}\right)^l \cdot \left(\frac{tq_{St}}{V_s}\right)^{i-l} - \frac{V_s \gamma}{\theta q_{St}} e^{t\theta_{q_{St}}/V_s} \sum_{l=1}^i \frac{1}{(i-l)!} \left(\frac{tq_{St}}{V_s}\right)^{i-l} \sum_{j=1}^l \left(\frac{1}{\theta}\right)^{j-1} + \frac{V_P \gamma}{q_{St}} \sum_{l=1}^i \frac{1}{\theta^{i-l+1}} + C_{A,St}(x'_0, 0) \frac{1}{\theta^i} \quad (\text{A.21})$$

where  $\theta = (1 - (V_P/q_{St})\varphi)$ .

$C_{A,St}(x'_0,0)$  is estimated from the experimental mass-transfer flux of metal-ion transport across the liquid membrane phase from the feed phase to the stripping phase ( $J_{Expt.}$ ). The experimental mass-transfer flux can be estimated from [42]

$$J_{Expt.} = \frac{q_{St} \Delta C_{A,St}}{A} \quad (A.22)$$

where  $A$  is the effective mass-transfer area and  $\Delta C_{A,St}$  is the difference in the concentration of metal ions between the outlet and inlet stripping solutions obtained from the experiment.

The experimental mass-transfer flux can also be estimated from [42]

$$J_{Expt.} = \frac{V_{St}}{A} \frac{dC_{A,St}}{dt} \quad (A.23)$$

Applying Eq. (A.23), the following equation is obtained:

$$J_{Expt.} = \frac{V_{St,x'_i}}{A} k_{St} C_{A,St}^n(x'_i, t) \quad (A.24)$$

where  $V_{St,x'_i}$  is the volume of the stripping phase at position  $x'_i$ .

Considering the small segment at position  $x'_0$ ,  $C_{A,St}(x'_i, t)$  is equal to  $C_{A,St}(x'_0, 0)$ . Therefore, from Eqs. (A.22) and (A.24),  $C_{A,St}(x'_0, 0)$  in Eq. (A.21) can be calculated, as shown below:

$$C_{A,St}(x'_0, 0) = \left( J_{Expt.} \cdot \frac{A_0}{V_{St, x'_0} k_{St}} \right)^{1/n} \quad (A.25)$$

where  $V_{St, x'_0}$  is the volume of the stripping phase at position  $x'_0$  and  $A_0$  is the effective mass-transfer area at position  $x'_0$ .

## 5.9 References

- [1] M.Z. Barciszewska, M. Szymanski, E. Wyszko, J. Pas, L. Rychlewski, J. Barciszewski, Lead toxicity through the leadzyme, *Mutation Research: Reviews in Mutation Research* 589 (2005) 103–110.
- [2] E.K. Silbergeld, Facilitative mechanisms of lead as a carcinogen, *Mutation Research: Fundamental and Molecular Mechanisms of Mutagenesis* 533 (2003) 121–133.
- [3] S. Diez, Human health effects of methyl mercury exposure, *Reviews of Environmental Contamination and Toxicology* 198 (2009) 111–132.
- [4] W.L. Hughes, A physicochemical rationale for the biological activity of mercury and its compounds, *Annals of the New York Academy of Sciences* 65 (2006) 454–460.

- [5] Thailand Regulatory Discharge Standards 2, Ministry of Industry, Thailand, 1996.
- [6] D.L. Gallup, J.B. Strong, Removal of mercury and arsenic from produced water, Chevron Corporation (2007) 1–9.
- [7] S. Gupta, M. Chakraborty, Z.V.P. Murthy, Optimization of process parameters for mercury extraction through pseudo-emulsion hollow fiber strip dispersion system, *Separation and Purification Technology* 114 (2013) 43–52.
- [8] B.S. Inbaraj, J.S. Wang, J.F. Lu, F.Y. Siao, B.H. Chen, Adsorption of toxic mercury (II) by an extracellular biopolymer poly( $\gamma$ -glutamic acid), *Bioresource Technology* 100 (2009) 200–207.
- [9] I.M. Coelho, M.M. Cardoso, R.M.C. Viegas, J.P.S.G. Crespo, Transport mechanisms and modelling in liquid membrane contactors, *Separation and Purification Technology* 19 (2000) 183–197.
- [10] P.C. Rout, K. Sarangi, A comparative study on extraction of Mo(VI) using both solvent extraction and hollow fiber membrane technique, *Hydrometallurgy* 133 (2013) 149–155.
- [11] M.F. San Roman, E. Bringas, R. Ibanez, I. Ortiz, Liquid membrane technology: fundamentals and review of its applications, *Journal of Chemical Technology and Biotechnology* 85 (2010) 2–10.
- [12] N.M. Kocherginsky, Q. Yang, L. Seelam, Recent advances in supported liquid membrane technology, *Separation and Purification Technology* 53 (2007) 171–177.

- [13] P.K. Mohapatra, V.K. Manchanda, Liquid membrane-based separations of actinides, in: A.K. Pabby, S.S.H. Rizvi, A.M. Sastre (Eds.), *Handbook of Membrane Separations: Chemical, Pharmaceutical, Food and Biotechnological Applications*, CRC Press, United States, 2009, pp. 883–918.
- [14] B.F. Jirjis, S. Luque, Chapter 9—practical aspects of membrane system design in food and bioprocessing applications, in: Z.F. Cui, H.S. Muralidhara (Eds.), *Membrane Technology*, Butterworth-Heinemann, Oxford, 2010, pp. 179–212.
- [15] Z. Lazarova, B. Syska, K. Schügerl, Application of large-scale hollow fiber membrane contactors for simultaneous extractive removal and stripping of penicillin G, *Journal of Membrane Science* 202 (2002) 151–164.
- [16] U. Pancharoen, A.W. Lothongkum, S. Chaturabul, Mass transfer in hollow fiber supported liquid membrane for As and Hg removal from produced water in upstream petroleum operation in the gulf of Thailand, in: M. El-Amin (Ed.), *Mass Transfer in Multiphase Systems and its Applications*, InTech, India, 2011, pp. 499–524.
- [17] R. Guell, E. Antico, V. Salvado, C. Fontas, Efficient hollow fiber supported liquid membrane system for the removal and preconcentration of Cr(VI) at trace levels, *Separation and Purification Technology* 62 (2008) 389–393.
- [18] D. Buachuang, P. Ramakul, N. Leepipatpiboon, U. Pancharoen, Mass transfer modeling on the separation of tantalum and niobium from dilute hydrofluoric media through a hollow fiber supported liquid membrane, *Journal of Alloys and Compounds* 509 (2011) 9549–9557.



- [19] L.D. Mafu, T.A.M. Msagati, B.B. Mamba, The enrichment and removal of arsenic (III) from water samples using HFSLM, *Physics and Chemistry of the Earth* 50–52 (2012) 121–126.
- [20] A. Mtibe, T.A.M. Msagati, A.K. Mishra, B.B. Mamba, Determination of phthalate ester plasticizers in the aquatic environment using hollow fibre supported liquid membranes, *Physics and Chemistry of the Earth* 50–52 (2012) 239–242.
- [21] U. Pancharoen, T. Wongsawa, A.W. Lothongkum, A reaction flux model for extraction of Cu(II) with LIX84I in HFSLM, *Separation Science and Technology* 46 (2011) 2183–2190.
- [22] P.V. Vernekar, Y.D. Jagdale, A.W. Patwardhan, A.V. Patwardhan, S.A. Ansari, P. K. Mohapatra, V.K. Manchanda, Transport of cobalt(II) through a hollow fiber supported liquid membrane containing di-(2-ethylhexyl) phosphoric acid (D2EHPA) as the carrier, *Chemical Engineering Research and Design* 91 (2013) 141–157.
- [23] P. Kandwal, S. Dixit, S. Mukhopadhyay, P.K. Mohapatra, Mass transport modeling of Cs(I) through hollow fiber supported liquid membrane containing calix-[4]-bis(2,3-naphtho)-crown-6 as the mobile carrier, *Chemical Engineering Journal* 174 (2011) 110–116.
- [24] Q. Yang, N.M. Kocherginsky, Copper removal from ammoniacal wastewater through a hollow fiber supported liquid membrane system: modeling and experimental verification, *Journal of Membrane Science* 297 (2007) 121–129.
- [25] K.W. McLaughlin, C.M. Bertolucci, Applications of generating functions to polymerization kinetics. 3.: general procedure illustrated for propagation with monomer conversion, *Journal of Mathematical Chemistry* 14 (1993) 71–78.

- [26] Y. Kawamura, M. Mitsuhashi, H. Tanibe, H. Yoshida, Adsorption of metal ions on polyaminated highly porous chitosan chelating resin, *Industrial and Engineering Chemistry Research* 32 (1993) 386–391.
- [27] T. Gumi, M. Oleinikova, C. Palet, M. Valiente, M. Munoz, Facilitated transport of lead(II) and cadmium(II) through novel activated composite membranes containing di-(2-ethyl-hexyl)phosphoric acid as carrier, *Analytica Chimica Acta* 408 (2000) 65–74.
- [28] F.d.M. Fabrega, M.B. Mansur, Liquid-liquid extraction of mercury (II) from hydrochloric acid solutions by Aliquat 336, *Hydrometallurgy* 87 (2007) 83–90.
- [29] S. Suren, T.Wongsawa, U. Pancharoen, T. Prapasawat, A.W. Lothongkum, Uphill transport and mathematical model of Pb(II) from dilute synthetic leadcontaining solutions across hollow fiber supported liquid membrane, *Chemical Engineering Journal* 191 (2012) 503–511.
- [30] A.W. Lothongkum, S. Suren, S. Chaturabul, N. Thamphiphit, U. Pancharoen, Simultaneous removal of arsenic and mercury from natural-gas-co-produced water from the Gulf of Thailand using synergistic extractant via HFSLM, *Journal of Membrane Science* 369 (2011) 350–358.
- [31] Membrana–Charlotte, Celgard, LLC, 13800 South Lakes Drive, Charlotte, North Carolina 28273, USA.
- [32] A. Escobar, K.A. Schimmel, J. de Gyves, E.R. de San Miguel, Hollow-fiber dispersion-free extraction and stripping of Pb(II) in the presence of Cd(II) using D2EHPA under recirculating operation mode, *Journal of Chemical Technology and Biotechnology* 79 (2004) 961–973.

- [33] C.-V.I. Gherasim, G. Bourceanu, R.-I. Olariu, C. Arsene, Removal of lead(II) from aqueous solutions by a polyvinyl-chloride inclusion membrane without added plasticizer, *Journal of Membrane Science* 377 (2011) 167–174.
- [34] L. Gurel, L. Altas, H. Buyukgungor, Removal of lead from wastewater using emulsion liquid membrane technique, *Environmental Engineering Science* 22 (2005) 411–420.
- [35] U. Pancharoen, S. Somboonpanya, S. Chaturabul, A.W. Lothongkum, Selective removal of mercury as  $\text{HgCl}_4^{2-}$  from natural gas well produced water by TOA via HFSLM, *Journal of Alloys and Compounds* 489 (2010) 72–79.
- [36] K. Chakrabarty, P. Saha, A.K. Ghoshal, Simultaneous separation of mercury and lignosulfonate from aqueous solution using supported liquid membrane, *Journal of Membrane Science* 346 (2010) 37–44.
- [37] L. Iberhan, M. Wisniewski, Extraction of arsenic(III) and arsenic(V) with Cyanex 925, Cyanex 301 and their mixtures, *Hydrometallurgy* 63 (2002) 23–30.
- [38] B. Wassink, D. Dreisinger, J. Howard, Solvent extraction separation of zinc and cadmium from nickel and cobalt using Aliquat 336, a strong base anion exchanger, in the chloride and thiocyanate forms, *Hydrometallurgy* 57 (2000) 235–252.
- [39] C.W. Wood, A.K. Holliday, *Inorganic Chemistry*, third ed., Butterworth, England, 1967.
- [40] E. Uedee, P. Ramakul, U. Pancharoen, A.W. Lothongkum, Performance of hollow fiber supported liquid membrane on the extraction of mercury(II) ions, *Korean Journal of Chemical Engineering* 25 (2008) 1486–1494.
- [41] I. Pázsit, L. Pál, *Neutron Fluctuations*, 2008, Elsevier; Amsterdam, 315–329.

- [42] Z. Ren, W. Zhang, Y. Liu, Y. Dai, C. Cui, New liquid membrane technology for simultaneous extraction and stripping of copper(II) from wastewater, *Chemical Engineering Science* 62 (2007) 6090–6101.



CHAPTER VI  
MEASUREMENT ON THE SOLUBILITY OF ADIPIC ACID IN VARIOUS  
SOLVENTS AT HIGH TEMPERATURE AND ITS  
THERMODYNAMICS PARAMETERS

Sira Suren <sup>a,b</sup>, Niti Sunsandee <sup>a,b</sup>, Magdalena Stolcova <sup>b</sup>, Milan Hronec <sup>b</sup>,  
Natchanun Leepipatpiboon <sup>c</sup>, Ura Pancharoen <sup>a,\*</sup>, Soorathep Kheawhom <sup>a,\*\*</sup>

<sup>a</sup> *Department of Chemical Engineering, Faculty of Engineering, Chulalongkorn University, Bangkok 10330, Thailand*

<sup>b</sup> *Department of Organic Technology, Faculty of Chemical and Food Technology, Slovak University of Technology in Bratislava, Bratislava 81237, Slovak Republic*

<sup>c</sup> *Chromatography and Separation Research Unit, Department of Chemistry, Faculty of Science, Chulalongkorn University, Patumwan, Bangkok 10330, Thailand*

---

This article has been published in Journal: Fluid Phase Equilibria.

Page: 332–337. Volume: 360. Year: 2013.

---

## 6.1 Abstract

This work presents measurements of the solubility of adipic acid in water, acetic acid, acetic acid-water mixture (ratio of 1:1, v/v), cyclohexanol and cyclohexanone at the temperatures ranging from 303.0 to 403.0 K. The reliability experimental method used in this work for studying the solubility of adipic acid was verified using the published solubility data at low temperatures. The modified Apelblat equation was applied in order to correlate the solubility of adipic acid in the above mentioned solvents. The results showed that our method was found to be acceptable for measuring the solubility of adipic acid at high temperatures. The solubilities of adipic acid obtained from the modified Apelblat equation fitted well with the experimental data. The total average relative deviation was 2.55%. Moreover, the molar enthalpy and the molar entropy of dissolutions of adipic acid in water, acetic acid, acetic acid-water mixtures, cyclohexanol and cyclohexanone at temperatures ranging from 303.0 to 403.0 K were calculated.

**Keywords:** Adipic acid; Solubility; Apelbat equation; Enthalpy of solution; Entropy of solution.

## 6.2 Introduction

Adipic acid is an important substance in chemical industries. It is ranked in the top ten by the term of volume used [1]. It is used as a raw material in the productions of polyamide [2,3], polyurethane, polyester resins, plasticizers, lubricants

[4], carpet fibers, specialty foams, reinforcements, and several items of clothing [5]. Oxidation of cyclohexanone-cyclohexanol mixture with nitric acid is the conventional route for preparing adipic acid [1]. In the industry, it is mainly produced by oxidation of cyclohexane with air and nitric acid [6]. After oxidization process, crude adipic acid has to be purified to obtain pure adipic acid [7].

Crystallization is one of the most purification methods for recovering the target components from the solution. To recover the target component by crystallization, its solubility data is required [8,9]. For separation by crystallization, a suitable solvent system should yield an adequately high solubility at the starting conditions in order to entirely dissolve the product without a dramatic increase in the volume of solution but also allow a significant decrease in solubility at the end of the process to reduce the product losses and increase the process yield [10].

The solubility of substances is one of the most considerable parameters in the development of solution theory [11–18]. However, the solubility data of some substances that have been reported are limited [19–21]. This lack of data results from the problems in the sampling of solutions at high temperatures and pressures [22].

To obtain the solubility data of compounds at high temperatures, it requires a high experimental effort which is very sophisticated and time consuming [23,24]. Some thermodynamic models have been developed to predict the solubility of certain substances to reduce this effort to a minimum. The modification of the Apelblat equation model is widely used to correlate the solubility data of some substances. It provides the acceptable data of solubility at different temperatures

[25–28]. Moreover, it can also be applied to calculate the molar enthalpy and the molar entropy of dissolutions of compounds [28].

As far as we know, only a few data of the solubility of adipic acid in several organic solvents and aqueous solutions [7,29–31] was measured at low temperatures. However, this solubility data is far from the industrial conditions. Therefore, in this work, the solubility data of adipic acid was measured in various solvents (water, acetic acid, acetic acid–water mixture (ratio of 1:1, v/v), cyclohexanol and cyclohexanone) in the temperatures ranging from 303.0 to 403.0 K. The modified Apelblat equation model was applied to correlate the solubility data of adipic acid. The model was verified by comparing the solubility data obtained from the model with those gained from the experimental results.

## 6.3 Experimental

### 6.3.1 Materials

Adipic acid ( $C_6H_{10}O_4$ , MW 146.14 g/mol, melting point 424.0–425.0 K [32]) and acetic acid ( $CH_3CO_2H$ , MW 60.05 g/mol) were purchased from Sigma–Aldrich. Cyclohexanol ( $C_6H_{12}O$ , MW 100.16 g/mol) and cyclohexanone ( $C_6H_{10}O$ , MW 98.15 g/mol) were bought from Mikrochem<sup>®</sup>, Slovakia. Water used in the experiments was distilled water. All chemicals were used without further purification. The source and mass fraction purity of chemicals are concluded in Table 6.1.



**Table 6. 1** Source and mass fraction purity of chemicals.

Chemical name	Source	Purity /% mass	Analysis method
Adipic acid	Sigma–Aldrich	99	HPLC
Acetic acid	Sigma–Aldrich	99	HPLC
Cyclohexanol	Mikrochem	95	HPLC
Cyclohexanone	Mikrochem	99	HPLC

### 6.3.2 Apparatus and procedures

The solubility of adipic acid in various solvents was measured by our published method [33,34] which is the equilibrium method. The experiment was performed in a 50-mL reactor made from stainless steel as shown in Figure 6.1. Within the reactor, the Teflon<sup>®</sup> container, which has a hole of 0.5 cm<sup>3</sup>, was kept over the solution level. Before each experiment was carried out, both solvent (25 mL) and excess adipic acid had been measured and subsequently deposited into the reactor. A magnetic stirring rotor was put into the reactor so that adipic acid and solvent could be adequately mixed. After the reactor containing adipic acid and solvent has been firmly closed, it was heated in a thermostated silicone oil bath. This silicone oil bath was linked with the stirrer and thermocouple with an uncertainty  $\pm 0.1$  K so that the system could reach the required temperature. The preliminary experiments showed that equilibrium could be achieved when the concentration of adipic acid in the liquid-phase solution become unchanging after stirring for 90 min. Therefore, the system was retained in the static state for 180 min until the solution become homogeneous and all of the suspended particles deposited on the bottom.

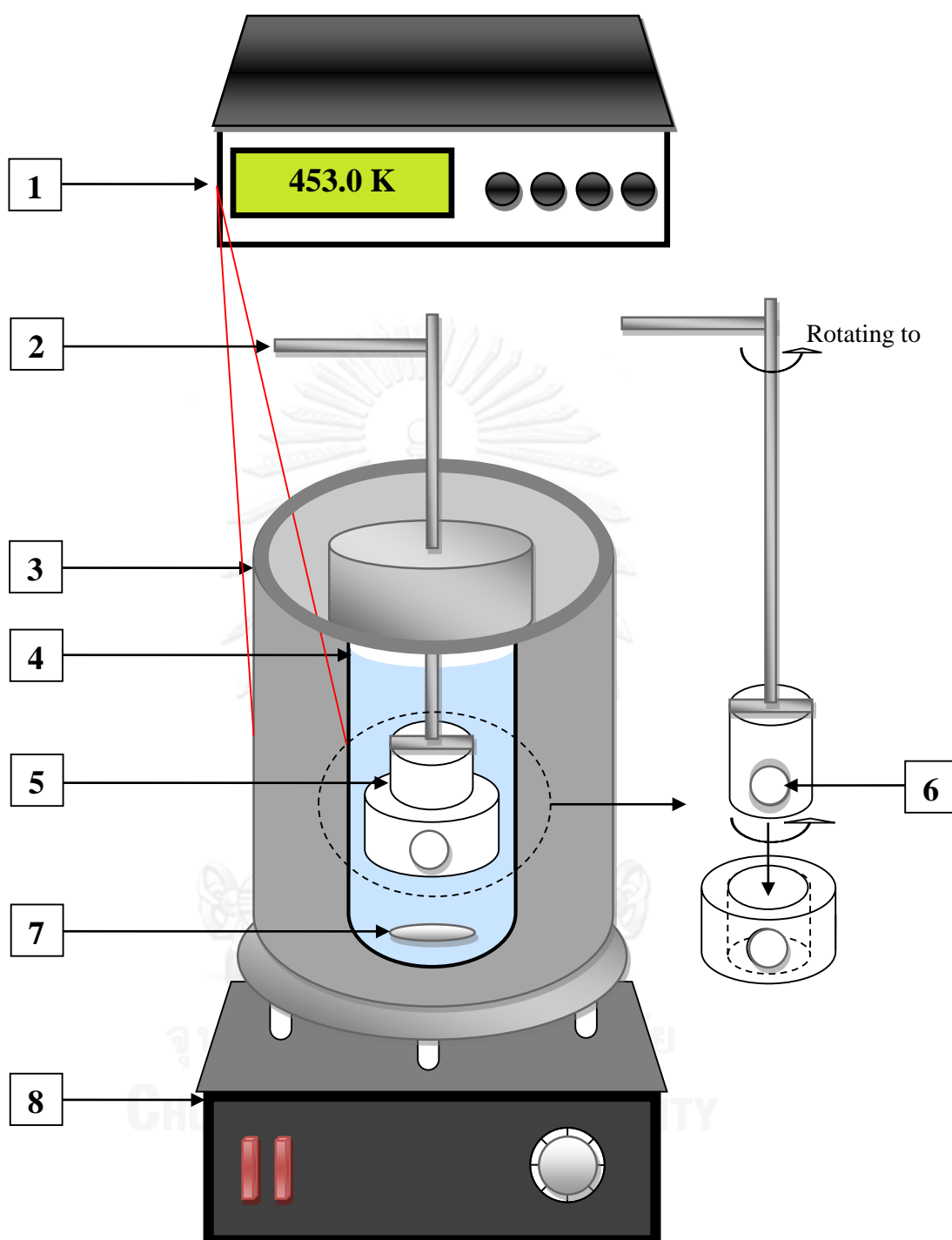


**Figure 6. 1** The experimental apparatus: (1) temperature control, (2) Teflon<sup>®</sup> container holder, (3) silicone oil bath, (4) stainless steel reactor, (5) Teflon<sup>®</sup> container, (6) Teflon<sup>®</sup> container hole, (7) magnetic bar, (8) stirrer controller.

At the experimental temperature, about 0.5 mL of a solution sample was withdrawn by pushing a Teflon<sup>®</sup> container into the solution. Then, the Teflon<sup>®</sup> container hole was opened by rotating the Teflon<sup>®</sup> container holder to the sampling position and waiting for 1 min so that the sample solution flowed in to the Teflon<sup>®</sup> hole. After that, the sampler hole was closed by turning the Teflon<sup>®</sup> container holder back and pulled from the middle of solution to over the solution level. Subsequently, the reactor was cooled to the ambient temperature by cooling water (most of the solute would crystallize) to avoid the vaporization of the solvent. After that, the reactor was opened. The closed Teflon<sup>®</sup> container was washed three times with 100-mL distilled water and then air-dried. The amount of the sample withdrawn into the Teflon<sup>®</sup> container was determined as the weight difference of the container – before and after sampling. Then, the Teflon<sup>®</sup> container was opened. The collected sample was transferred into the volumetric flask and analyzed by high-performance liquid chromatography (HPLC). Each experiment was repeated at least three times.

### 6.3.3 Analyses

HPLC was used to analyze the concentrations of adipic acid in various solvents. A Shimadzu (Japan) instrument consisting of a LC10AD high-pressure binary solvent delivery system, a Rheodyne injector equipped with 20- $\mu$ L sample loop and a Shimadzu SPD-M10Vp photodiode-array detector was used. The Class-10 software was used to control the system, data acquisition and integration. The compounds were separated on the LiChrospher 100 RP-18e column (250  $\times$  4.0 mm, 5  $\mu$ m) (Merck, Germany) at the ambient temperature. A mixture of acetonitrile and 10-

mmol/L aqueous solution of monosodium dihydrogen phosphate buffer adjusted to pH of 2.9 at a ratio of 10:90% (v/v) was used for elution. The flow rate of mobile phase was 1.0 mL/min. The compounds were detected at 210 nm. For sample quantification, external calibration was used. To obtain the calibration standards, serial dilution of adipic acid in the mobile phase was used. The linearity was assessed by standard solution preparation from 0.4 to 2 mg/mL. The determination precision was calculated from triplicated injections. The pH of the aqueous mobile phase was measured by a pH meter SevenMulti™ Modular Expansion model (Mettler-Toledo, Greifensee, Switzerland). An analytical balance (Mettler ae-260 type) with an uncertainty of 0.0001 g was used for all the mass measurements.

## 6.4 Results and discussion

### 6.4.1 Verification of the experimental method

The reliability of the experimental method used in this work for studying the solubility of adipic acid was verified using the published solubility data obtained in water [30], acetic acid, cyclohexanol and cyclohexanone [29] at low temperatures. The results are shown in Figure 6.2, the mole fractions of adipic acid solubilities ( $x_i$ ) in these solvents measured by our method are in accordance with those available in the literature.

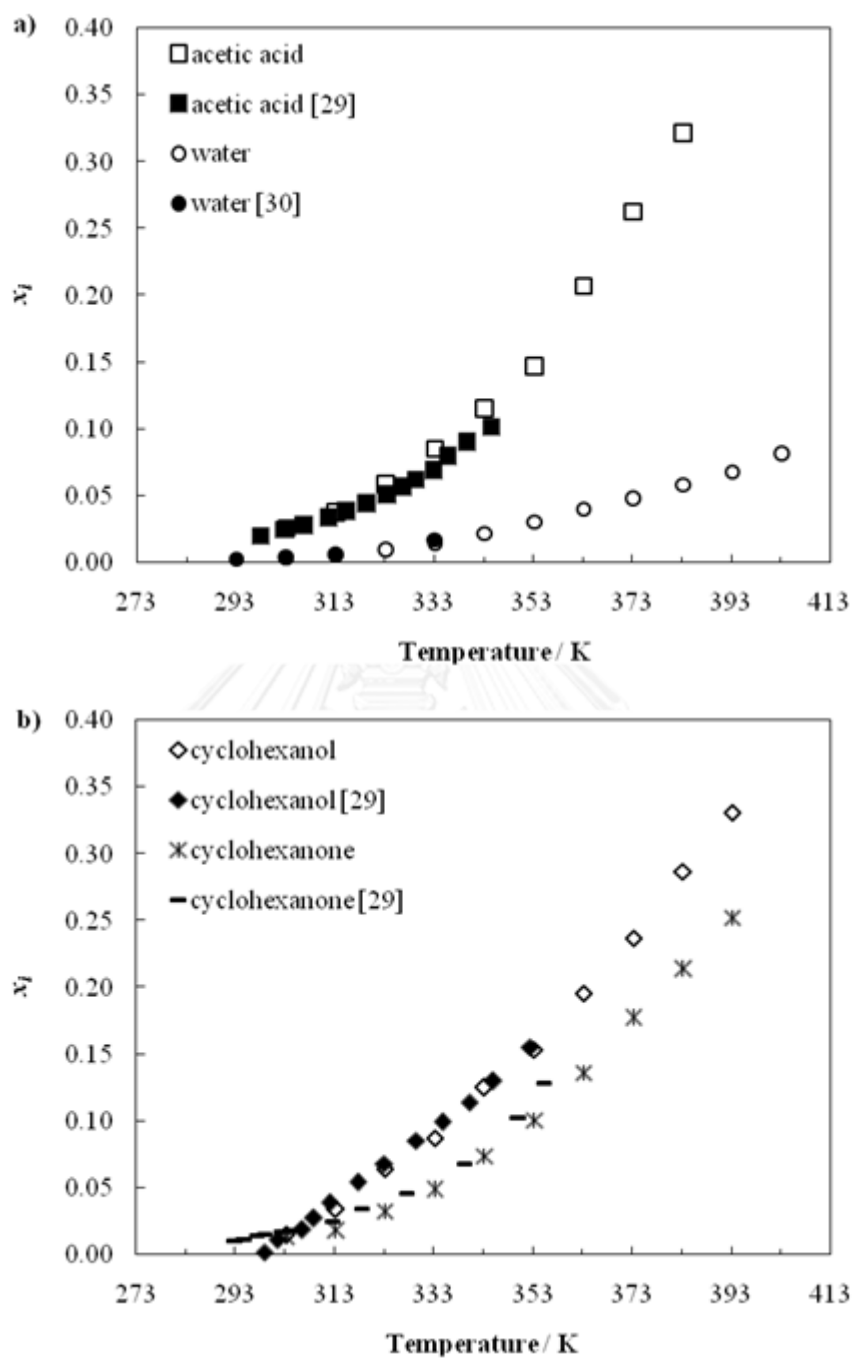


**Figure 6. 2** Comparison of the literature and experimental mole fraction of adipic acid solubility ( $x_i$ ) against temperature: (a) in acetic acid and water, (b) in cyclohexanol and cyclohexanone.

## 6.4.2 Solubility of adipic acid in various solvents

**Table 6. 2** Mole fraction of adipic acid solubility ( $x_i$ ) in solvents at different temperature (T).<sup>a</sup>

T (K)	$x_i$				
	Water	Acetic acid	Acetic acid+water (ratio 1:1, v/v)	Cyclohexanol	Cyclohexanone
303.0	0.004	0.026	0.006	0.015	0.013
313.0	0.006	0.037	0.016	0.034	0.019
323.0	0.009	0.059	0.016	0.064	0.032
333.0	0.015	0.085	0.026	0.087	0.049
343.0	0.022	0.116	0.040	0.125	0.074
353.0	0.031	0.147	0.051	0.154	0.100
363.0	0.040	0.207	0.070	0.195	0.136
373.0	0.048	0.263	0.085	0.237	0.178
383.0	0.058	0.322	0.096	0.287	0.214
393.0	0.068		0.108	0.331	0.252
403.0	0.082				

<sup>a</sup> Standard uncertainties  $u$  are  $u(T) = \pm 0.1\text{K}$ ,  $u(x_i) = \pm 0.001$ .

The mole fractions of adipic acid solubilities in water, acetic acid, acetic acid-water mixture (ratio of 1:1, v/v), cyclohexanol and cyclohexanone were measured in the temperatures ranging from 303.0 to 403.0 K. The results shown in Table 6.2 indicates that the mole fraction of adipic acid solubility in all studied

solvents increases with temperature. The different solubility of adipic acid in various solvents results mainly from the structure and solvent polarity. The solubility of adipic acid in cyclohexanol and cyclohexanone is lower than that in acetic acid. This probably attributes to the incompatible structures. Adipic acid has a chain structure while cyclohexanol and cyclohexanone have a ring structure [29]. Moreover, the polarities of cyclohexanol and cyclohexanone are lower than that of acetic acid [35].

#### 6.4.3 Modeling of solubility data

To predict the concentration of adipic acid in saturated aqueous and organic solutions, the modified Apelblat equation was used. This equation (assuming that the enthalpy of solution depends directly on the temperature [36,37]) is widely used to calculate the solubilities of some organic compounds in various solvents. The modified Apelblat equation is expressed as shown below:

$$\ln x_i = A + \frac{B}{T} + C \ln(T) \quad (6.1)$$

where  $x_i$  is the mole fraction of adipic acid solubility in a solution;  $A$ ,  $B$  and  $C$  are the parameters obtained from the curve fitting of experimental solubility data using a non-linear optimization method [33]; and  $T$  is the temperature in Kelvin (K).

For prediction of the solubility of adipic acid in the predetermined solutions, by fitting of experimental solubility data – shown in Table 6.2 – the parameters  $A$ ,  $B$  and  $C$  were obtained. The values of these are listed in Table 6.3.

**Table 6. 3** Parameters (*A*, *B* and *C*) in the modified Apelblat equation model obtained by curve fitting the experimental solubility data and validity of the model for prediction of the adipic acid solubility in various solvents.<sup>a</sup>

Solvents	<i>A</i>	<i>B</i>	<i>C</i>	Average relative deviation ( <i>E</i> , %)
Water	273.24	-17313.30	-38.82	1.87
Acetic acid	101.16	-8316.00	-13.55	2.22
Acetic acid+water (ratio 1:1 v/v)	309.24	-19015.00	-44.04	2.58
Cyclohexanol	398.50	-23581.00	-56.86	4.06
Cyclohexanone	171.06	-12117.00	-23.70	2.01
Total average relative deviation (%)				2.55

<sup>a</sup> Standard uncertainties *u* are  $u(A) = u(B) = u(C) = u(E) = \pm 0.01$ .

The validation of the modified Apelblat equation was verified by the average relative deviation (*ARD*) [28], as shown in Eq. (6.2):

$$ARD = \frac{1}{N} \sum_{i=1}^N \left| \frac{x_{Exp.} - x_{Cal.}}{x_{Exp.}} \right| \times 100\% \quad (6.2)$$

where *N* is the number of experimental data;  $x_{Exp.}$  and  $x_{Cal.}$  are the experimental and calculated mole fraction solubilities, respectively.

Using Eq. (6.1), the solubility of adipic acid in water, acetic acid, acetic acid-water mixture (ratio of 1:1, v/v), cyclohexanol and cyclohexanone can be



estimated. The results, as seen in Figure 6.3, show that the solubility data calculated using the modified Apelblat equation model fit well with the measured experimental results. The validity of the modified Apelblat equation is summarized in Table 6.3.

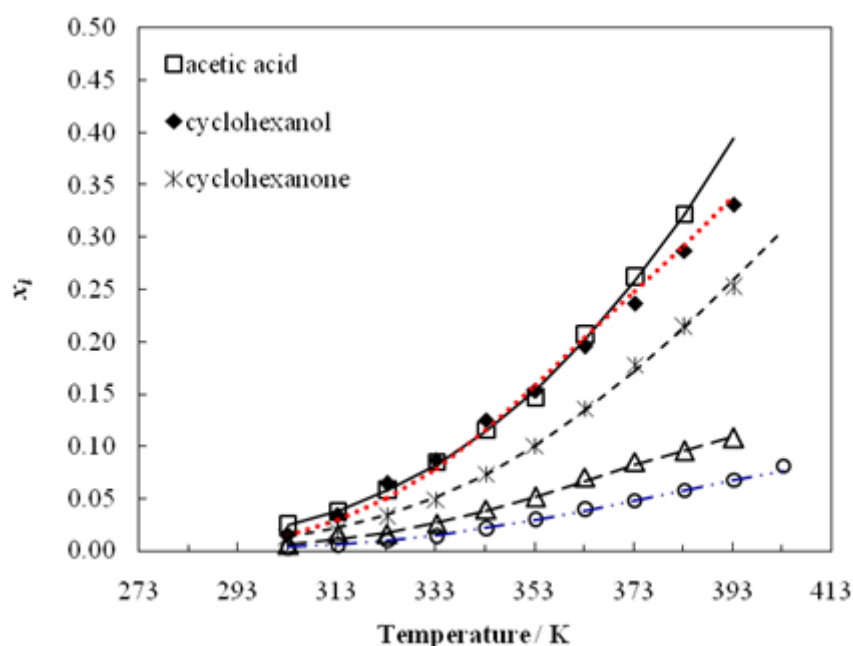


**Figure 6. 3** Mole fraction of adipic acid solubility ( $x_i$ ) in various solvents against temperature obtained from experimental results and from the modified Apelblat equation model.

As shown in Table 6.3, the modified Apelblat equation is well agreed with the experimental results. The average relative deviations between experimental results and results gained from the modified Apelblat equation are lower than 4.06%, and the total average relative deviation is 2.55%. Therefore, this model can be used to calculate the solubility of adipic acid in the studied solvents.

#### 6.4.4 Molar enthalpy and molar entropy of dissolutions

Modified Apelblat equation can be applied to calculate the molar enthalpy and molar entropy of dissolutions ( $\Delta_{sol}H$  and  $\Delta_{sol}S$ ) of solid compounds [28]. Due to a process of pseudochemical reaction, the relationship between equilibrium constant and activities of the dissolution process of solid in liquid can be expressed as [38]:

$$K_i = \frac{a_i}{a_s a_w} \quad (6.3)$$

where  $K_i$  is the solid dissolution equilibrium constant;  $a_i$  is the activity of adipic acid in the solution;  $a_s$  is the activity of pure solid; and  $a_w$  is the activity of pure liquid.

Due to standard-state solid and liquid, it is considered that each of  $a_s$  and  $a_w$  is a constant, and  $K_i$  can be written as [28]:

$$K_i = \frac{\gamma_i x_i}{a_s a_w} \quad (6.4)$$

where  $\gamma_i$  is the activity coefficient of adipic acid in the solution.

It is assumed that  $\gamma_i$  is independent of composition. When the temperature derivative is taken, the temperature dependence of  $\gamma_i$  is ignored also. Therefore,  $\gamma_i$  in

Eq. (6.4) can be merged into  $a_s a_w$  [27]. By taking a logarithm of Eq. (6.4), the following equation can be obtained:

$$\ln K_i = \ln x_i + J \quad (6.5)$$

where  $J = \ln \gamma_i - \ln a_s a_w$ .  $J$  is a temperature-independent constant.

According to the modified Van't Hoff method together with the basis of the Gibbs equation [39] and using Eq. (6.5), the molar enthalpy of dissolution  $\Delta_{sol}H$  can be obtained as:

$$\Delta_{sol}H = -R \frac{d \ln x_i}{dT^{-1}} \quad (6.6)$$

where  $R$  is the gas constant.

Substituting Eq. (6.1) into Eq. (6.6) and using values of parameters  $B$  and  $C$  in Table 6.3, the molar enthalpy of dissolution, as shown in Table 6.4, is obtained.

**Table 6. 4** Molar enthalpy of dissolution ( $\Delta_{sol}H$ ) of adipic acid in various solvents.<sup>a</sup>

$T$ (K)	$\Delta_{sol}H$ (kJ/mol)				
	Water	Acetic acid	Acetic acid+water (ratio 1:1, v/v)	Cyclohexanol	Cyclohexanone
303.0	46.1	35.0	47.1	52.8	41.0
313.0	42.9	33.9	43.4	48.0	39.0
323.0	39.7	32.7	39.8	43.3	37.1
333.0	36.4	31.6	36.2	38.6	35.2
343.0	33.2	30.5	32.5	33.9	33.1
353.0	30.0	29.4	28.8	29.1	31.2
363.0	26.8	28.2	25.1	24.4	29.2
373.0	23.5	27.1	21.5	19.7	27.2
383.0	20.3	26.0	17.8	14.9	25.3
393.0	17.1	24.9	14.2	10.2	23.3
403.0	13.9	23.7	10.5	5.5	21.3

<sup>a</sup> Standard uncertainties  $u$  are  $u(T) = \pm 0.1$  K,  $u(\Delta_{sol}H) = \pm 0.1$  kJ/mol.

As shown in Table 6.4,  $\Delta_{sol}H$  is higher than zero. It indicates that the course of adipic acid dissolving in water, acetic acid, acetic acid-water mixture (ratio of 1:1, v/v), cyclohexanol and cyclohexanone was endothermic [28]. This means that the energy of the mixture is higher than the energy of the components.

According to the fundamental thermodynamic relation [40], the molar entropy of dissolution of adipic acid can be calculated as shown in the following relation [28].

$$\Delta_{sol}S = R \left( C - \frac{B}{T} \right) \quad (6.7)$$

**Table 6. 5** Molar entropy of dissolution ( $\Delta_{sol}S$ ) of adipic acid in various solvents.<sup>a</sup>

T (K)	$\Delta_{sol}S$ (J/mol K)				
	Water	Acetic acid	Acetic acid+water (ratio 1:1, v/v)	Cyclohexanol	Cyclohexanone
303.0	152.1	115.4	155.4	174.0	135.3
313.0	136.9	108.2	138.7	153.4	124.7
323.0	122.7	101.3	123.1	135.0	114.7
333.0	109.5	94.9	108.4	115.8	105.4
343.0	96.8	88.9	94.6	98.6	96.5
353.0	84.9	83.1	81.5	82.5	88.2
363.0	73.7	77.8	69.2	67.2	80.4
373.0	63.0	72.7	57.6	52.7	72.9
383.0	53.0	67.8	46.5	39.0	65.9
393.0	43.4	63.2	36.0	26.0	59.2
403.0	34.3	58.7	26.0	13.6	52.9

<sup>a</sup> Standard uncertainties  $u$  are  $u(T) = \pm 0.1$  K,  $u(\Delta_{sol}S) = \pm 0.1$  J/mol K.

Adding values of parameters  $C$  and  $B$  in Table 6.3 into Eq. (6.7), the molar entropy of dissolution can be calculated. The results are shown in Table 6.5.

As shown in Table 6.5, molar entropy of dissolution for adipic acid in studied solvent is higher than zero. Tables 6.4 and 6.5 show that  $\Delta_{sol}H$  and  $\Delta_{sol}S$  are positive. It indicates that dissolving of adipic acid in studied solvents is an entropy-driving process [28].

## 6.5 Conclusion

This work presents the measurement of adipic acid solubility in water, acetic acid, acetic acid-water mixture (ratio of 1:1, v/v), cyclohexanol and cyclohexanone at temperatures ranging from 303.0 to 403.0 K. The reliability experimental method used in this work for studying the solubility of adipic acid was verified by the published solubility data at low temperatures. The solubility of adipic acid in the studied solvents was correlated with the modified Apelblat equation. The results clearly showed that the solubility data obtained from our method were acceptable for measuring the solubility of adipic acid. The solubilities of adipic acid obtained from the modified Apelblat equation fitted well with the experimental data. The total average relative deviation was 2.55%. The molar enthalpy and the molar entropy of dissolutions of adipic acid in water, acetic acid, acetic acid-water mixture (ratio of 1:1, v/v), cyclohexanol and cyclohexanone at the temperatures ranging from 303.0 to 403.0 K were calculated. The results showed that their values were positive, indicating that the system was endothermic and entropy-driving process.

## 6.6 List of symbols

$A$	parameter in the modified Apelblat equation
$a_i$	activity of adipic acid in the solution
$ARD$	average relative deviation (%)
$a_s$	activity of pure solid
$a_w$	activity of pure liquid
$B$	parameter in the modified Apelblat equation
$C$	parameter in the modified Apelblat equation
$J$	temperature-independent constant
$K_i$	solid dissolution equilibrium constant
$N$	number of experimental data
$R$	gas constant (J/mol K)
$T$	temperature (K)
$x_{Cal.}$	calculated mole fraction solubility
$x_{Exp.}$	experimental mole fraction solubility
$x_i$	mole fraction of adipic acid solubility

### Greek letter

$\gamma_i$	activity coefficient of adipic acid in the solution
------------	---

## Symbol

$\Delta_{sol}H$  molar enthalpy of dissolution (kJ/mol)

$\Delta_{sol}S$  molar entropy of dissolution (J/mol K)

## 6.7 Acknowledgements

The authors are very grateful to financial supports by the Thailand Research Fund and Chulalongkorn University under the Royal Golden Jubilee Ph.D. Program (Grant No. PHD/0324/2551) and Dutsadi Phiphat. Sincere thanks also go to the Laboratory of Catalyzed Processes, Department of Organic Technology, Faculty of Chemical and Food Technology, Slovak University of Technology in Bratislava, Bratislava, Slovak Republic for kindly supplying all chemical compounds and instruments for analyses and measurements.

## 6.8 References

- [1] M. Vafaezadeh, M.M. Hashemi, M. Shakourian-Fard, *Catal. Commun.* 26 (2012) 54–57.
- [2] X.J. Shen, *Guangxi Chem. Ind.* 27 (1998) 34–35.
- [3] S.J. Yu, *J. Liaoyang Petrochem. College* 16 (2000) 13–15.
- [4] G.N. Glew, H.J. Hildebrand, *J. Phys. Chem.* 60 (1956) 616–618.
- [5] M.G. Buonomenna, G. Golemme, M.P. De Santo, E. Drioli, *Org. Process Res. Dev.* 14 (2009) 252–258.
- [6] J. Shao, Z. Zeng, W. Xue, C. Wu, *Chin. J. Chem. Eng.* 14 (2006) 780–783.



- [7] B. Shen, Q. Wang, Y. Wang, X. Ye, F. Lei, X. Gong, *J. Chem. Eng. Data* 58 (2013) 938–942.
- [8] J. Hur, J.P. O’Connell, K.-K. Bae, K.-S. Kang, J.W. Kang, *Int. J. Hydrogen Energy* 36 (2011) 8187–8191.
- [9] H. Encheng, L. Honglai, S. Jiangang, S. Jianlan, H. Ying, *Chin. J. Chem. Eng.* 3 (1995) 155–162.
- [10] J. Thati, F.L. Nordström, Å.C. Rasmuson, *J. Chem. Eng. Data* 55 (2010) 5124–5127.
- [11] P. Jain, K. Sepassi, S.H. Yalkowsky, *Int. J. Pharm.* 360 (2008) 122–147.
- [12] J. Qing-Zhu, M. Pei-Sheng, Z. Huan, X. Shu-Qian, W. Qiang, Q. Yan, *Fluid Phase Equilib.* 250 (2006) 165–172.
- [13] A.G. Carr, J.W. Tester, *Fluid Phase Equilib.* 337 (2013) 288–297.
- [14] J. Nti-Gyabaah, R. Chmielowski, V. Chan, Y.C. Chiew, *Int. J. Pharm.* 359 (2008) 111–117.
- [15] A. Noubigh, M. Cherif, E. Provost, M. Abderrabba, *J. Chem. Thermodyn.* 40 (2008) 1612–1616.
- [16] A. Valtz, C. Coquelet, D. Richon, *J. Chem. Thermodyn.* 39 (2007) 426–432.
- [17] E.M. Gonc, alves, M.E. Minas da Piedade, *J. Chem. Thermodyn.* 47 (2012) 362–371.
- [18] A. Jouyban, S. Soltanpour, W.E. Acree Jr., *Chem. Eng. Data.* 55 (2010) 5252–5257.
- [19] Q. Jia, P. Ma, S. Ma, C. Wang, *Chin. J. Chem. Eng.* 15 (2007) 710–714.
- [20] Z. Ding, R. Zhang, B. Long, L. Liu, H. Tu, *Fluid Phase Equilib.* 292 (2010) 96–103.

- [21] Y. Miyano, K. Nakanishi, *J. Chem. Thermodyn.* 35 (2003) 519–528.
- [22] Q.-b. Wang, H.-b. Xu, X. Li, *Fluid Phase Equilib.* 233 (2005) 81–85.
- [23] J. Cassens, F. Ruether, K. Leonhard, G. Sadowski, *Fluid Phase Equilib.* 299 (2010) 161–170.
- [24] F.L. Mota, A.P. Carneiro, A.J. Queimada, S.P. Pinho, E.A. Macedo, *Eur. J. Pharm. Sci.* 37 (2009) 499–507.
- [25] W. Sun, W. Qu, L. Zhao, *Chem. Eng. Data.* 55 (2010) 4476–4478.
- [26] F.-x. Chen, M.-r. Zhao, C.-c. Liu, F.-f. Peng, B.-z. Ren, *J. Chem. Thermodyn.* 50 (2012) 1–6.
- [27] F.-a. Wang, L.-c. Wang, J.-c. Song, L. Wang, H.-s. Chen, *J. Chem. Eng. Data* 49 (2004) 1539–1541.
- [28] C.-L. Zhang, F. Zhao, Y. Wang, *J. Mol. Liq.* 159 (2011) 170–172.
- [29] F. Lihua, M. Peisheng, X. Zhengle, *Chin. J. Chem. Eng.* 15 (2007) 110–114.
- [30] A.N. Gaivoronskii, V.A. Granzhan, *J. Appl. Chem.* 78 (2005) 404–408.
- [31] C. Bretti, R.M. Cigala, F. Crea, C. Foti, S. Sammartano, *Fluid Phase Equilib.* 263 (2008) 43–54.
- [32] Material Safety Data Sheet of Adipic Acid, Sigma-Aldrich Co. LLC, 2012.
- [33] N. Sunsandee, S. Suren, N. Leepipatpiboon, M. Hronec, U. Pancharoen, *Fluid Phase Equilib.* 338 (2013) 217–223.
- [34] N. Sunsandee, M. Hronec, M. Štolcová, N. Leepipatpiboon, U. Pancharoen, *J. Mol. Liq.* 180 (2013) 252–259.
- [35] C. Reichardt, *Solvents and Solvent Effects in Organic Chemistry*, third ed., Wiley-VCH, Weinheim, 2003.
- [36] A. Apelblat, E. Manzurola, *J. Chem. Thermodyn.* 31 (1999) 85–91.

- [37] A. Apelblat, E. Manzurola, *J. Chem. Thermodyn.* 33 (2001) 147–153.
- [38] F.A. Wang, *Molecular Thermodynamics and Chromatographic Retention*, first ed., Meteorology Press, Beijing, 2001.
- [39] D. Bourgois, D. Thomas, J.-L. Fanlo, J. Vanderschuren, *J. Chem. Eng. Data* 51(2006) 1212–1215.
- [40] J.M. Prausnitz, R.N. Lichtenthaler, E.G. Azevedo, *Molecular Thermodynamics of Fluid-Phase Equilibria*, third ed., Prentice Hall PTR, New Jersey, 1999.



CHAPTER VII  
SOLUBILITY MEASUREMENT AND CORRELATION OF 4-ALKYL BENZOIC  
ACIDS IN AQUEOUS SOLUTIONS

Sira Suren <sup>a,b</sup>, Milan Hronec <sup>b</sup>, Ura Pancharoen <sup>a,\*</sup>, Soorathep Kheawhom <sup>a,\*\*</sup>

<sup>a</sup> *Department of Chemical Engineering, Faculty of Engineering, Chulalongkorn University, Bangkok 10330, Thailand*

<sup>b</sup> *Department of Organic Technology, Faculty of Chemical and Food Technology, Slovak University of Technology in Bratislava, Bratislava, Slovak Republic*



จุฬาลงกรณ์มหาวิทยาลัย  
CHULALONGKORN UNIVERSITY

---

This article has been published in Journal: Journal of Molecular Liquids.

(in press).

---

## 7.1 Abstract

This work concerns the solubility measurement of 4-alkyl benzoic acids (4-iso-propylbenzoic, 4-methylbenzoic and 4-*tert*-butylbenzoic acids) in aqueous solutions at temperatures ranging from 303.2 to 433.2 K. The reliability of the experimental method used for studying the solubility of the above mentioned acids was verified using the published solubility data of 4-methylbenzoic acid in water at low temperatures. The results showed that the data obtained by means of our apparatus are acceptable for measuring the solubility of acids at high temperatures. Both the  $\lambda H$  equation and the modified Apelblat equation model were utilized to correlate the solubility of 4-alkyl benzoic acids in aqueous solutions. The solubilities of the studied acids obtained from the modified Apelblat equation were in good agreement with the experimental results, at total average relative deviation of 6.19%. The  $\lambda H$  equation did not correspond with the experimental results (total average relative deviation of 22.43%). Therefore, in order to predict the solubility of 4-iso-propylbenzoic, 4-methylbenzoic and 4-*tert*-butylbenzoic acids in aqueous solutions, a modified Apelblat equation was recommended. The modified Apelblat equation was also applied to determine the molar enthalpy and molar entropy of dissolutions of such acids in various solvents. The molar enthalpy and molar entropy of dissolutions observed were positive indicating that the dissolving of studied acids was an entropy-driven process.

**Keywords:** Solubility; 4-alkyl benzoic acids; High temperature; Enthalpy of dissolution; Entropy of dissolution.

## 7.2 Introduction

The solubility of solids in liquids is one of the most important process parameters and of scientific interest for the development of solution theory [1–7]. However, only limited solubility data have been reported in the literature. As far as we know, solubility data is available only for water and a few organic solvents at low temperatures. Unfortunately, this solubility data was gained under conditions far from industrial conditions.

The solubility data of substances is very important for chemical manufacturing processes and product designs [8,9]. Some processes require data for designing purification processes [10–12] e.g. precipitation [13] crystallization [14,15] chemical reaction systems [16] pollution prevention [17] as well as production and purification of chemical compounds [18]. For many separation and purification processes, a mixture of two or more solvents has been occasionally found to offer the best operation properties. Water mixed with alcohols or acids has been frequently used as solvent [9,19].

The 4-alkyl benzoic acids including 4-iso-propylbenzoic acid ( $C_{10}H_{12}O_2$ ), 4-methylbenzoic acid ( $C_8H_8O_2$ ) and 4-*tert*-butylbenzoic acid ( $C_{11}H_{14}O_2$ ) have been widely used in industry. In the production of medicines, 4-iso-propylbenzoic and 4-methylbenzoic acids are used [20]. 4-*tert*-butylbenzoic acid is used as raw material in order to produce alkyd resin modifier, cutting emulsion, lubricating oil additive, polypropylene nucleation agent, stabilizer, anti-oxidant in metal cutting emulsion, rust inhibitors in resin coatings and lubricating oil [21]. Only a few solubility data of 4-methylbenzoic acid ( $C_8H_8O_2$ ) were measured [20,22,23]. However, this data was

obtained only at low temperatures which are far from conditions used in industrial processes. There is a lack of useful solubility data of some acids because of problems in the sampling of solutions at high temperatures and pressures [14].

In order to gain solubility data of substances at high temperatures, sophisticated and time consuming experimental efforts are required [24]. To keep these experiments at a minimum, some thermodynamic models have been developed to calculate or predict the solubility of certain substances [25]. The thermodynamic models that are widely considered to correlate the solubility data of some substances are  $\lambda H$  equation and the modified Apelblat equation. These models provide acceptable data of solubilities of some compounds at different temperatures [19,20,26–29].

In previous work, a method to measure the solubility of methylbenzoic and 4-*tert*-butylbenzoic acids in water at high temperatures was successfully developed [30]. For this present work, this method is utilized to measure the solubility of 4-methylbenzoic acid and 4-*tert*-butylbenzoic acid in acetic acid solutions. Moreover, the solubility of 4-isopropyl benzoic in water and acetic acid solutions was also measured. Both the  $\lambda H$  equation and the modified Apelblat equation model were used in order to correlate the solubility of these acids at temperatures ranging from 303.2 to 433.2 K. Thus, in order to verify the validity of the models, the solubility data obtained from the experiment were compared to those determined from the models. Finally, the molar enthalpy and molar entropy of dissolutions of such acids in the studied solvents was estimated.

## 7.3 Experimental

### 7.3.1 Chemicals

The chemicals used were 4-iso-propylbenzoic acid ( $C_{10}H_{12}O_2$ , molecular weight 164.20 g/mol; melting point 545 K), 4-methylbenzoic acid ( $C_8H_8O_2$ , molecular weight 136.15 g/mol; melting point 453 K), 4-*tert*-butylbenzoic acid ( $C_{11}H_{14}O_2$ , molecular weight 178.23 g/mol; melting point 437 K) and acetic acid ( $CH_3CO_2H$ , molecular weight 60.05 g/mol). The source and purity of such chemicals are summarized in Table 7.1. All chemicals were used without further purification.

**Table 7. 1** Source and purity of the chemicals used.

Chemical name	Source	Purity (% mass)	Analytical method
4-iso-propylbenzoic acid	Sigma–Aldrich Co. LLC	98	GC
4-methylbenzoic acid	Sigma–Aldrich Co. LLC	98	n/a
4- <i>tert</i> -butylbenzoic acid	Sigma–Aldrich Co. LLC	99	GC
acetic acid	Sigma–Aldrich Co. LLC	99.7	GC



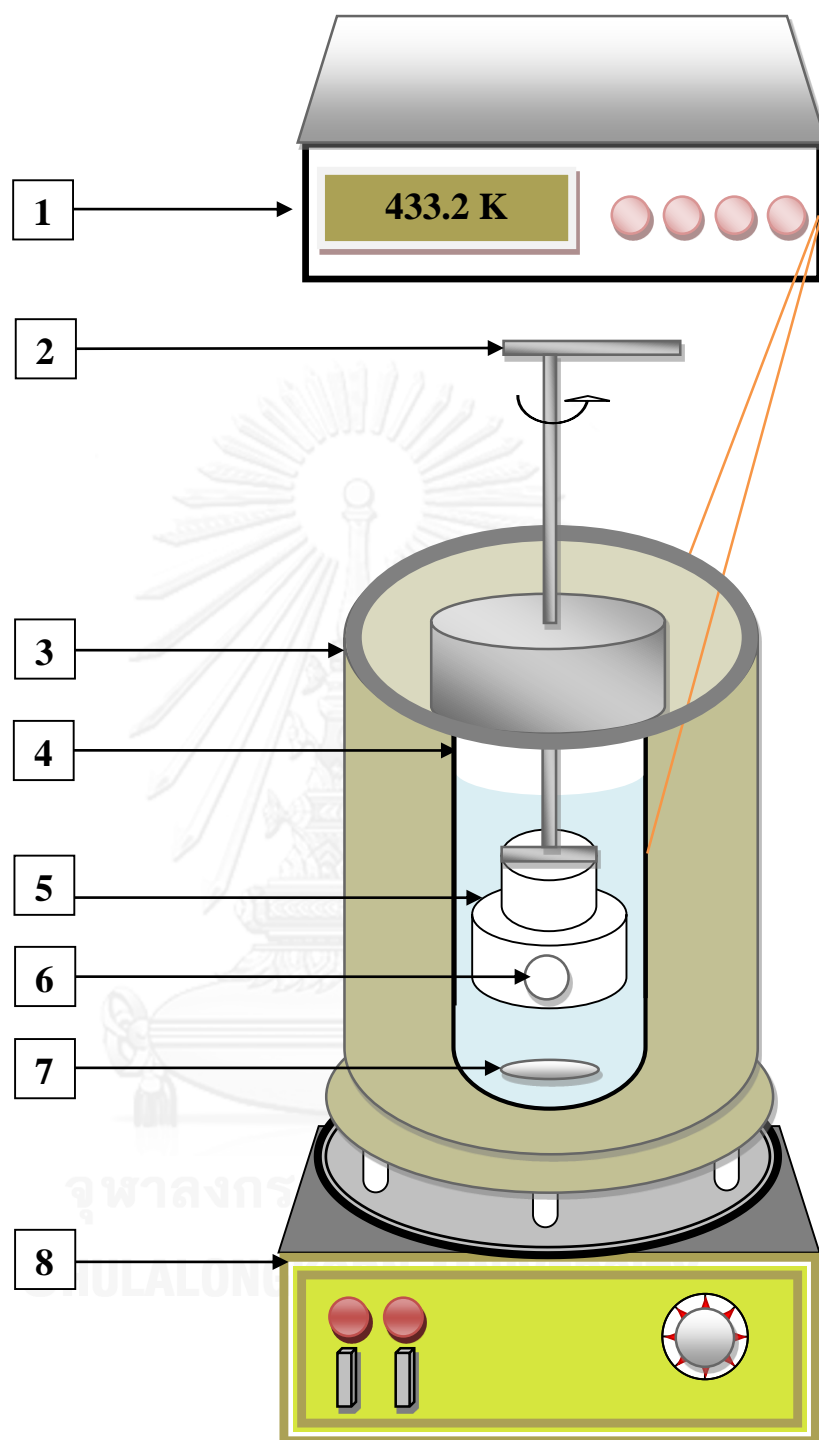


**Figure 7. 1** Experimental apparatus: (1) temperature control, (2) container handle (3) silicone oil bath, (4) stainless steel vessel, (5) Teflon® container, (6) Teflon® container hole, (7) magnetic bar, (8) stirrer controller.

### 7.3.2 Apparatus and procedures

The solubility of 4-iso-propylbenzoic, 4-methylbenzoic and 4-*tert*-butylbenzoic acids in aqueous solvents was measured by our published method [30,31] which is the equilibrium method. The experiment was performed in a 50-mL reactor made from stainless steel as shown in Figure 7.1. Before each experiment was carried out, both the solvent (approximate 25 mL) and excess studied acids were measured and subsequently deposited into the reactor. A magnetic stirring rotor was put into the reactor so that the studied acids and solvent could be adequately mixed. Then, the reactor was heated in a thermostated silicone oil bath. The silicone oil bath was linked with a thermocouple having an uncertainty  $\pm 0.1$  K, so that the system could reach the required temperature.

Preliminary experiments showed that equilibrium could be achieved when the concentration of the 4-alkyl benzoic acids in the liquid-phase solution becomes constant after stirring for 90 min. Thus, the system was kept in a static state for 120 min until the solution became homogeneous and all of the suspended particles were deposited on the bottom. Subsequently, at the experimental temperature, a sample of the solution (about 0.5 mL) was taken by pushing a Teflon<sup>®</sup> container into the solution. Through the rotation of the container handle, the container hole was uncovered and a sample of the solution flowed into the hole. After that, the Teflon<sup>®</sup> container was closed. Subsequently, the Teflon<sup>®</sup> container was pulled upwards through the solution right to the top. To avoid the vaporization of the solvent during sampling, the reactor was cooled to an ambient temperature by the cooling water. As a result, most of the solute crystallized. After the reactor was opened, the closed

Teflon<sup>®</sup> container was washed three times with 100-mL distilled water and then air-dried. The amount of the sample withdrawn into the Teflon<sup>®</sup> container was determined by the weight difference of the container – before and after sampling. Finally, the withdrawn sample was transferred into the volumetric flask and analyzed by high-performance liquid chromatography (HPLC). Each experiment was repeated at least three times.

### 7.2.3 Analyses

The solubility of the 4-alkyl benzoic acids was determined using HPLC. The chromatographic system was equipped with a Shimadzu LC10AD high-pressure binary solvent delivery system, using a Rheodyne injector provided with a 20- $\mu$ L sample loop and a Shimadzu SPD-M10Vp photodiode-array detector. Data analysis was carried out using Class 10 software for control of the system, data acquisition and integration. The analysis was conducted three times whereby the mean values were used for calculating the mole fraction solubility.

## 7.4 Results and discussion

### 7.4.1 Solubilities of 4-alkyl benzoic acids

To verify the reliability of the experimental method used in this work for measuring the solubility of the acids, the solubility data of the 4-methylbenzoic acid in water from the literature [20,32], at low temperatures, was compared to the

experimental results as obtained through our procedures. As shown in Figure 7.2, the mole fraction solubilities ( $x_i$ ) of 4-methylbenzoic acid in water, as measured by our method, are in accordance with those available in the literature.

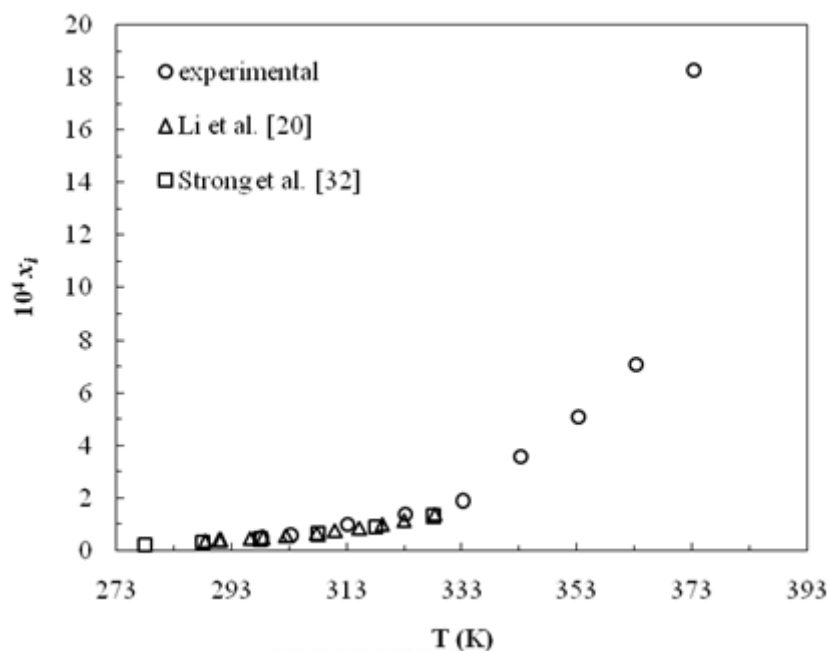


**Figure 7. 2** Comparison of mole fraction solubility ( $x_i$ ) of 4-methylbenzoic acid in water.

In this work, the solubilities of the 4-iso-propylbenzoic in water and acetic acid solutions, 4-methylbenzoic and 4-*tert*-butylbenzoic acids in acetic acid solutions were measured in the temperatures ranging from 303.2 to 433.2 K. As shown in Tables 7.2a – c, the mole fraction solubility of all the studied benzoic acids was found to increase with an increase in temperature and increase in the volume ratio of acetic acid-water mixture. Similar dependence but at lower temperatures was observed by Li et al. [20] and Strong et al. [30] for the solubility of 4-methylbenzoic acid in acetic acid and water.

**Table 7. 2** Mole fraction solubility ( $x_i$ ) of 4-alkyl benzoic acids.a) Mole fraction solubility ( $x_i$ ) of 4-iso-propylbenzoic acid in various solvents.

Temp. (K)	$10^3 x_i$		
	Water	Acetic acid+water (ratio 1:1, v/v)	Acetic acid+water (ratio 1.5:1, v/v)
303.2	1.33	3.97	13.10
313.2	1.55	4.25	15.38
318.2	1.98	4.95	15.59
323.2	1.76	5.45	17.71
328.2	2.68	6.36	18.68
333.2	2.45	7.41	21.57
338.2	3.61	8.17	23.46
343.2	3.98	8.56	25.75
353.2	4.89	12.26	
363.2	6.22	16.12	
368.2	8.89	18.25	
373.2	9.76	21.12	
383.2	12.83		

b) Mole fraction solubility ( $x_i$ ) of 4-methylbenzoic acid in various solvents.

Temp. (K)	$10^3 x_i$		
	Water [30]	Acetic acid+water (ratio 1:1, v/v)	Acetic acid+water (ratio 1.5:1, v/v)
298.2	0.05	-	-
303.2	0.06	0.44	1.25
313.2	0.10	0.62	1.47
323.2	0.14	1.12	2.06
333.2	0.19	1.50	3.00
343.2	0.36	1.84	4.12
353.2	0.51	3.63	6.26
363.2	0.71	6.17	9.77
373.2	1.83	8.93	14.23
383.2	2.77	12.06	19.35
393.2	4.53	15.96	27.38
403.2	7.14	20.01	37.74
413.2	11.23	31.60	51.14
423.2	13.48	50.73	68.99
433.2	39.82	72.76	98.88

c) Mole fraction solubility ( $x_i$ ) of 4-*tert*-butylbenzoic acid in various solvents.

Temp. (K)	$10^3 x_i$		
	Water [30]	Acetic acid+water (ratio 1:1, v/v)	Acetic acid+water (ratio 1.5:1, v/v)
303.2	0.50	1.22	3.12
313.2	0.80	3.22	5.69
323.2	1.53	3.36	7.68
333.2	1.63	5.02	9.68
343.2	2.50	7.30	12.39
353.2	3.89	10.29	17.77
363.2	5.56	13.57	23.43
373.2	9.12	19.48	27.43
383.2	10.45	27.53	41.55
393.2	15.50	31.25	57.56
403.2	21.20	44.15	72.06
413.2	29.68	57.37	

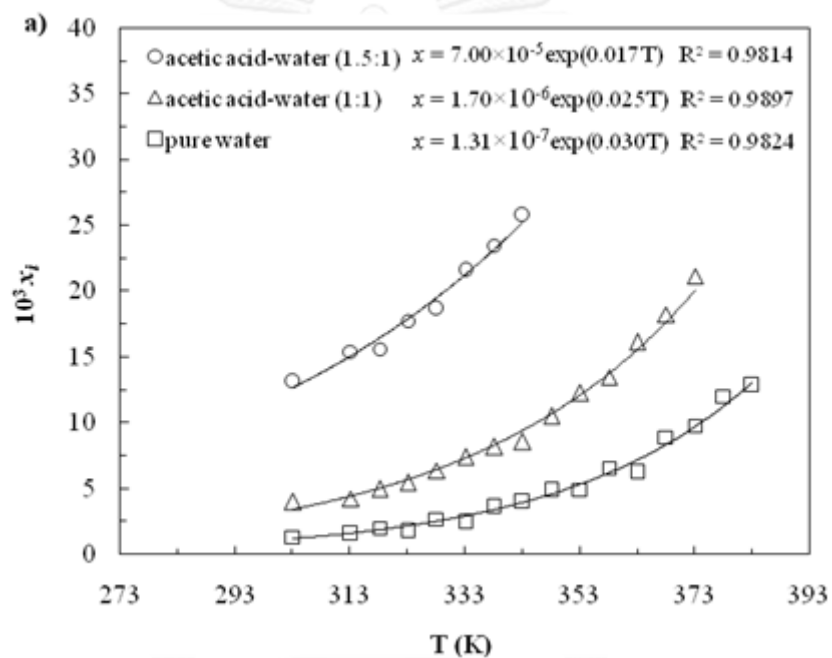
## 7.4.2 Modeling of solubility data

### 7.4.2.1 Empirical formula

In this work, an empirical formula, as shown in Eq. (7.1) [31,33] was used to correlate the mole fraction solubilities of 4-*iso*-propylbenzoic, 4-methylbenzoic and 4-*tert*-butylbenzoic acids in aqueous solutions.

$$x_i = k_1 \exp(k_2 T) \quad (7.1)$$

where  $x_i$  is the mole fraction solubility of a solute component  $i$  in the solvent;  $k_1$  and  $k_2$  are constant parameters in the empirical formula and  $T$  is the temperature in Kelvin (K).





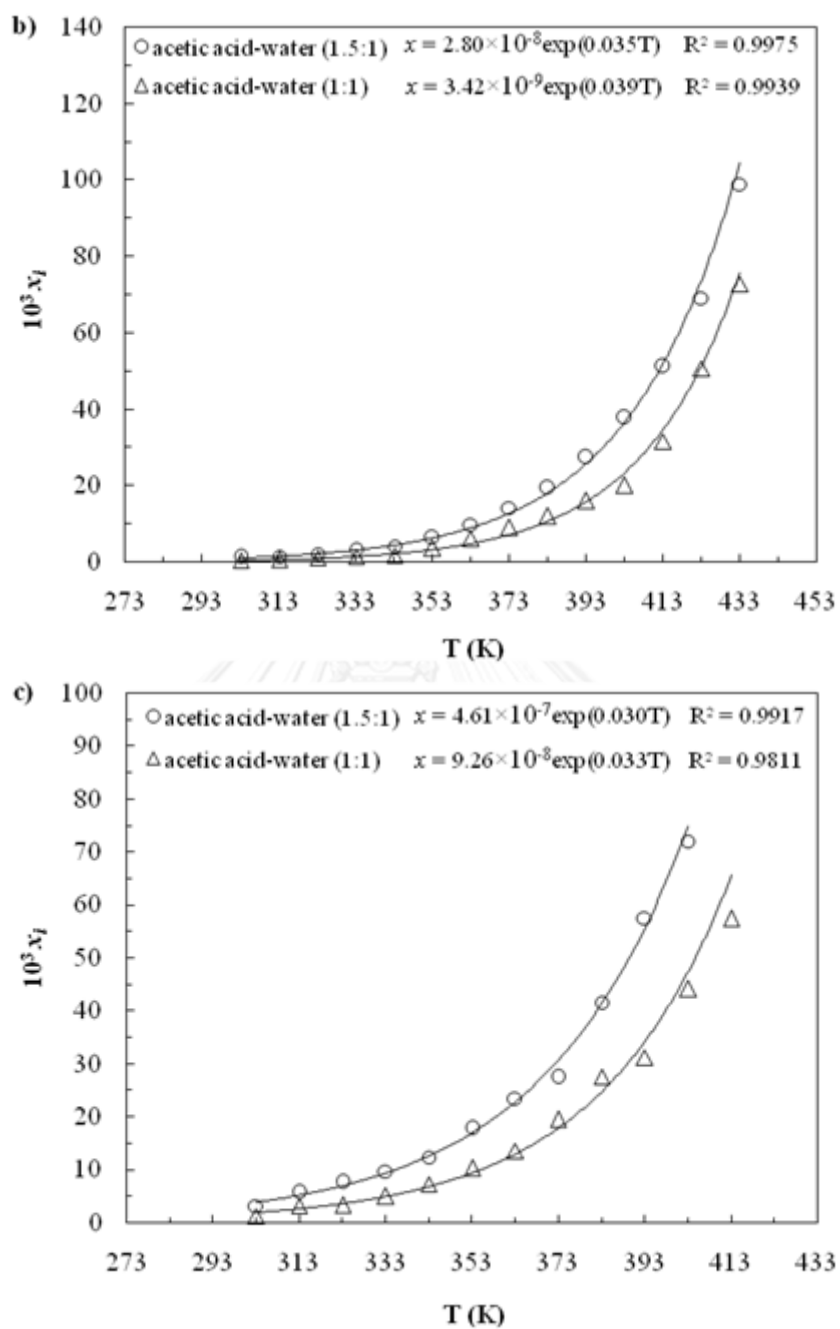


**Figure 7. 3** Mole fraction solubilities ( $x_i$ ) of acids in various solvents against temperature and their empirical formula correlation: (a) mole fraction solubility of 4-iso-propylbenzoic acid, (b) mole fraction solubility of 4-methylbenzoic acid, (c) mole fraction solubility of 4-tert-butylbenzoic acid.

The experimental solubility data of 4-alkyl benzoic acids and their empirical formulas are shown in Figure 7.3a – c. By comparing data from the empirical formula with the experimental solubility data, it was shown that all regressions attained high R-square ( $R^2 > 0.99$ ). This indicated that the experimental data is satisfactory described by using the above empirical formula.

#### 7.4.2.2 $\lambda H$ equation

The model of the  $\lambda H$  equation, as shown in Eq. (7.2), is widely used to correlate the solubility of organic acids in saturated aqueous solutions [26]. This model was first derived by Buchowski et al. [34]. The  $\lambda H$  equation, which only includes two parameters,  $\lambda$  and  $H$ , gives a good prediction of the solubility of many systems.

$$\ln \left[ 1 + \frac{\lambda(1-x_i)}{x_i} \right] = \lambda H \left[ \frac{1}{T} - \frac{1}{T_m} \right] \quad (7.2)$$

where  $\lambda$  and  $H$  are equation parameters;  $T$  and  $T_m$  is the equilibrium temperature and the melting point of the considered acid (K).

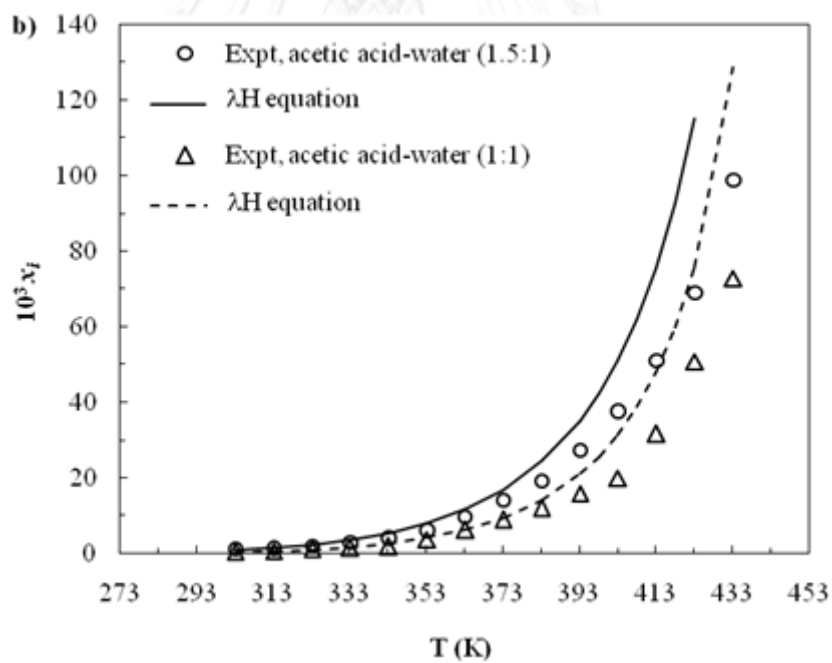
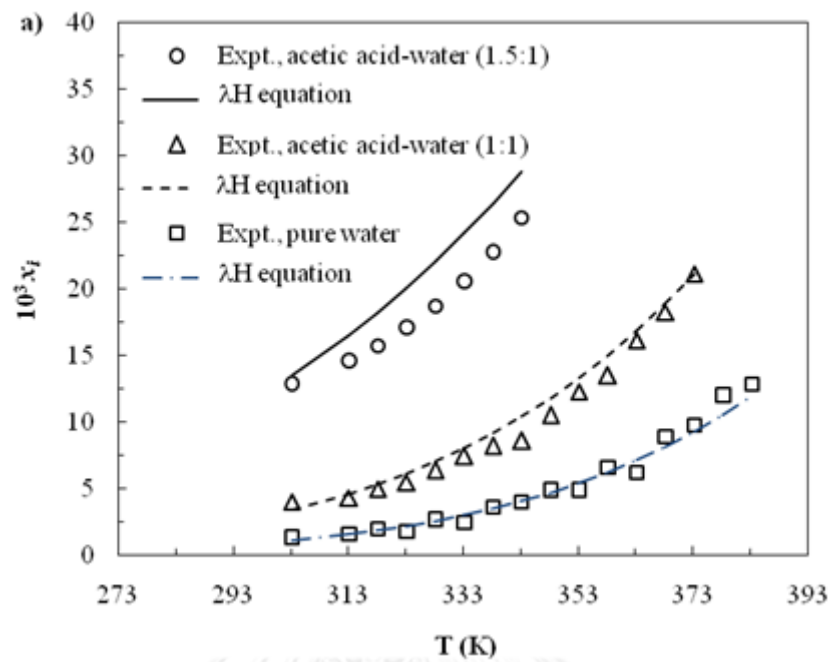
$\lambda$  and  $H$  are adjustable parameters which are estimated from the solubility data by the nonlinear regression [19]. By using Eq. (7.2) and the solubility data, as summarized in Table 7.2, the parameters  $\lambda$  and  $H$  for the prediction of the solubility

of 4-iso-propylbenzoic, 4-methylbenzoic and 4-tert-butylbenzoic acids in pure water and acetic acid-water mixture can be obtained. The optimized values for parameters  $\lambda$  and  $H$  are listed in Table 7.3.

The solubilities of 4-iso-propylbenzoic, 4-methylbenzoic and 4-tert-butylbenzoic acids in aqueous solvents estimated by the  $\lambda H$  equation are shown in Figure 7.4. As seen from the results in Figure 7.4, the solubility of considered benzoic acids in pure water and in mixture of acetic acid/water, as predicted by the  $\lambda H$  equation, did not correspond to the experimental results. It can be stated that the  $\lambda H$  equation cannot be applied for predicting the solubility of 4-iso-propylbenzoic, 4-methylbenzoic and 4-tert-butylbenzoic acids in the studied solvents.

**Table 7. 3** Parameters used in the  $\lambda H$  equation model for 4-iso-propylbenzoic, 4-methylbenzoic and 4-tert-butylbenzoic acids in various solvents.

Compound	$\lambda \times 10^3$	$H \times 10^{-3}$	$R^2$
4-iso-propylbenzoic acid:			
in acetic acid+water (ratio 1:5, v/v)	180.76	100.40	0.9910
in acetic acid+water (ratio 1:1, v/v)	221.44	129.50	0.9940
in water	161.41	218.90	0.9900
4-methylbenzoic acid:			
in acetic acid-water (1.5:1)	139.34	335.47	0.9920
in acetic acid+water (ratio 1:1, v/v)	102.21	509.01	0.9904
4-tert-butylbenzoic acid:			
in acetic acid+water (ratio 1:5, v/v)	142.99	260.45	0.9900
in acetic acid+water (ratio 1:1, v/v)	107.78	403.63	0.9981



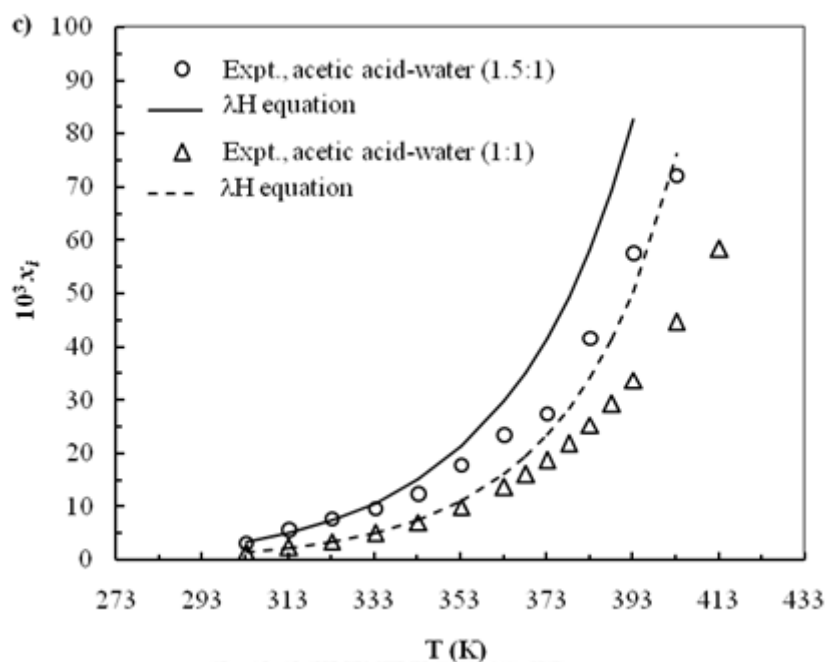


**Figure 7. 4** Mole fraction solubilities ( $x_i$ ) of acids in various solvents against temperature obtained from experimental results and from the  $\lambda H$  equation model: (a) mole fraction solubility of 4-iso-propylbenzoic acid, (b) mole fraction solubility of 4-methylbenzoic acid, (c) mole fraction solubility of 4-*tert*-butylbenzoic acid.

#### 7.4.2.3 Modified Apelblat equation

For calculation of the solubilities of some organic compounds in various solvents, the modified Apelblat equation was derived. This equation (assuming that the enthalpy of the solution is directly proportional to the temperature [30,35,36]) was used to predict the concentration of 4-iso-propylbenzoic, 4-methylbenzoic, and 4-*tert*-butylbenzoic acids in saturated aqueous solution. The modified Apelblat equation is expressed by the following equation:

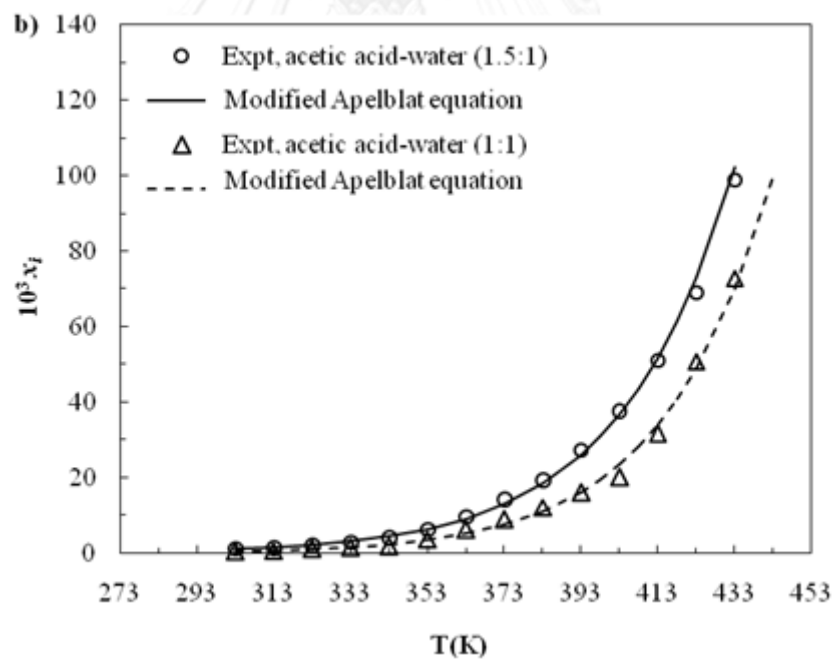
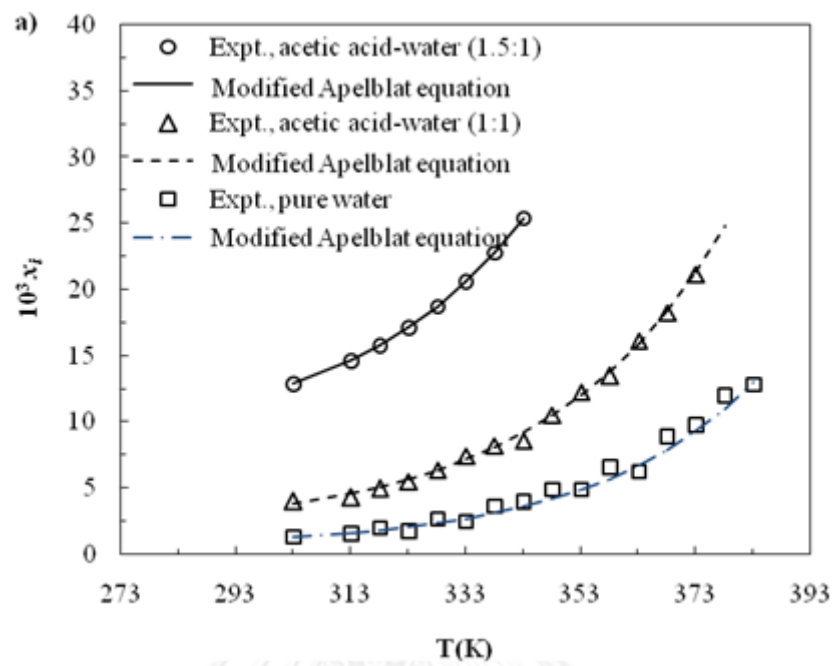
$$\ln x_i = A + \frac{B}{T} + C \ln(T) \quad (7.3)$$

where  $A$ ,  $B$  and  $C$  are the parameters in the modified Apelblat equation.

**Table 7. 4** Parameters ( $A$ ,  $B$  and  $C$ ) in the modified Apelblat equation model obtained by fitting the experimental solubility data.

Compound	$A$	$B$	$C$
4-iso-propylbenzoic acid:			
in acetic acid+water (ratio 1.5:1, v/v)	-267.12	11,008.00	39.63
in acetic acid+water (ratio 1:1, v/v)	-244.30	9,406.00	36.35
in water	-256.69	9,599.00	38.21
4-methylbenzoic acid:			
in acetic acid+water (ratio 1.5:1, v/v)	-157.27	4,065.70	23.98
in acetic acid+water (ratio 1:1, v/v)	-134.05	2,336.00	20.75
4- <i>tert</i> -butylbenzoic acid:			
in acetic acid+water (ratio 1.5:1, v/v)	-93.70	1,443.00	14.58
in acetic acid+water (ratio 1:1, v/v)	-36.36	-1,903.00	6.33

Parameters  $A$ ,  $B$  and  $C$  in Eq. (7.3) can be calculated by fitting the experimental solubility data via a non-linear optimization method [30]. In order to obtain these parameters, for predicting the concentration of 4-iso-propylbenzoic, 4-methylbenzoic and 4-*tert*-butylbenzoic acids in aqueous solutions, the solubility data, as summarized in Table 7.2a – c, were used. The calculated parameters  $A$ ,  $B$  and  $C$  are shown in Table 7.4.



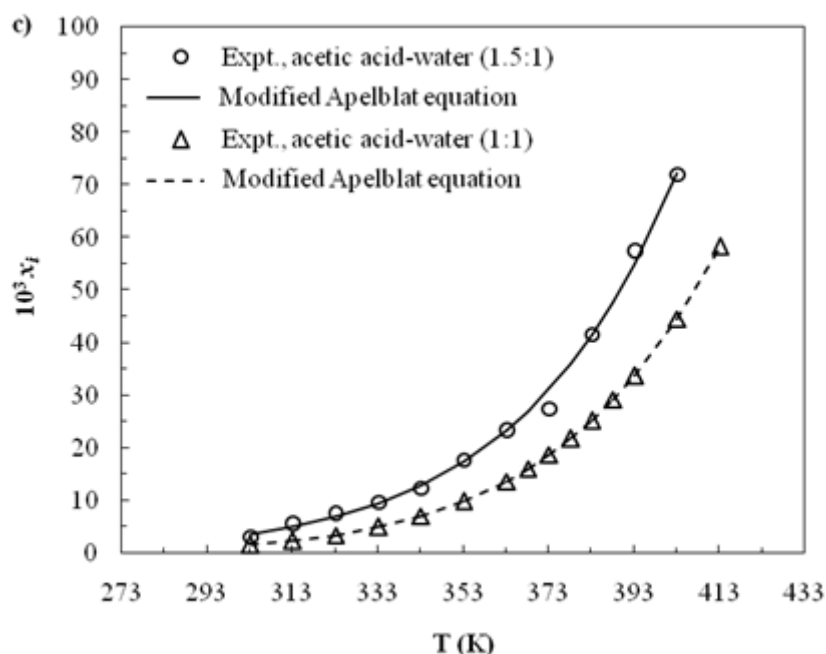


**Figure 7. 5** Mole fraction solubilities ( $x_i$ ) of acids in various solvents against temperature obtained from experimental results and from the modified Apelblat equation model: (a) mole fraction solubility of 4-iso-propylbenzoic acid, (b) mole fraction solubility of 4-methylbenzoic acid, (c) mole fraction solubility of 4-*tert*-butylbenzoic acid.

Using parameters summarized in Table. 7.4 and Eq. (7.3), the mole fraction solubility of 4-iso-propylbenzoic, 4-methylbenzoic, and 4-*tert*-butylbenzoic acids in the studied solvents can be estimated. The results in Figure 7.5 show that the mole fraction solubility data calculated using the modified Apelblat equation model are in good agreement with the measured experimental results.



#### 7.4.2.4 Comparison of the models

The validation of the  $\lambda H$  equation and the modified Apelblat equation models were verified by the average relative deviation ( $E$ ), as shown in Eq (7.4),

$$E = \frac{1}{N} \sum_{i=1}^N \left| \frac{x_{Exp.} - x_{Cal.}}{x_{Exp.}} \right| \times 100\% \quad (7.4)$$

where  $N$  is the number of experimental data;  $x_{Exp.}$  and  $x_{Cal.}$  are the experimental and calculated mole fraction solubility data.

The comparison of the validity of the  $\lambda H$  equation and the modified Apelblat equation models is summarized in Table 7.5.

As shown in Table 7.5, the data predicted from the modified Apelblat equation is in good agreement with the experimental results. The total average relative deviation between the experimental results and results predicted from the modified Apelblat equation is 6.19%. As regards the  $\lambda H$  equation, this did not correspond to the experimental results (total average relative deviation of 22.43%). Therefore, to predict the solubility of 4-iso-propylbenzoic, 4-methylbenzoic and 4-*tert*-butylbenzoic acids in pure water and acetic acid-water mixture, the modified Apelblat equation is recommended.

**Table 7. 5** Comparison of the validity of the  $\lambda H$  equation and the modified Apelblat equation models for the prediction of the solubility of 4-iso-propylbenzoic, 4-methylbenzoic and 4-*tert*-butylbenzoic acids in various solvents.

Compound	Average relative deviation ( $E, \%$ )	
	$\lambda H$ equation	Modified Apelblat equation
4-iso-propylbenzoic acid:		
in acetic acid+water (ratio 1.5:1, v/v)	11.80	2.55
in acetic acid+water (ratio 1:1, v/v)	9.67	3.90
in water	11.56	6.29
4-methylbenzoic acid:		
in acetic acid+water (ratio 1.5:1, v/v)	37.30	8.15
in acetic acid+water (ratio 1:1, v/v)	32.77	8.59
4- <i>tert</i> -butylbenzoic acid:		
in acetic acid+water (ratio 1.5:1, v/v)	23.78	6.48
in acetic acid+water (ratio 1:1, v/v)	30.10	7.39
Total average relative deviation (%)	22.43	6.19

#### 7.4.3 Molar enthalpy and molar entropy of dissolutions

The molar enthalpy and molar entropy of solid-compound dissolutions ( $\Delta_{sol}H$  and  $\Delta_{sol}S$ ) can be calculated by the Modified Apelblat equation [37]. Due to a process of pseudo-chemical reaction, the relationship between the equilibrium constant and the activities of the dissolution process of solid in liquid can be expressed as [38]:

$$K_i = \frac{a_i}{a_s a_w} \quad (7.5)$$

where  $K_i$  is the equilibrium constant of solid dissolution;  $a_i$  is the activity of acids in the solution;  $a_s$  is the activity of pure solid; and  $a_w$  is the activity of pure liquid.

According to standard-state liquid and solid, it is regarded as each of  $a_s$  and  $a_w$  is a constant, and  $K_i$  can be represented as [37]:

$$K_i = \frac{\gamma_i x_i}{a_s a_w} \quad (7.6)$$

where  $\gamma_i$  is the activity coefficient of acid in the solution.

It is assumed that  $\gamma_i$  is an independent composition. When the temperature derivative is taken, the temperature dependence of  $\gamma_i$  is ignored also. Therefore,  $\gamma_i$  in Eq. (7.6) can be merged into  $a_s a_w$  [28]. Taking a logarithm of Eq. (7.6) gives:

$$\ln K_i = \ln x_i + J \quad (7.7)$$

where  $J = \ln \gamma_i - \ln a_s a_w$

$J$  is a temperature-independent constant.

According to the modified Van't Hoff method together with the basis of the Gibbs equation [6] and using Eq. (7.7), the molar enthalpy of dissolution can be obtained as:

$$\Delta_{sol}H = -R \frac{d \ln K_i}{dT^{-1}} \quad (7.8)$$

where  $R$  is the gas constant.

Substituting Eq. (7.7) into Eq. (7.8) gives the following equation:

$$\Delta_{sol}H = -R \frac{d \ln x_i}{dT^{-1}} \quad (7.9)$$

Substituting Eq. (7.3) into Eq. (7.9) obtains:

$$\Delta_{sol}H = RT \left( C - \frac{B}{T} \right) \quad (7.10)$$

By using Eq. (7.10) and the values of parameters  $B$  and  $C$  from Table 7.4, the molar enthalpy of dissolution is achieved. These values are shown in Table 7.6.

**Table 7. 6** Molar enthalpy and molar entropy of dissolutions ( $\Delta_{sol}H$  and  $\Delta_{sol}S$ ) of 4-alkyl benzoic acids in various solvents.

a) Molar enthalpy and molar entropy ( $\Delta_{sol}H$  and  $\Delta_{sol}S$ ) of 4-iso-propylbenzoic acid in various solvents.

T (K)	$\Delta_{sol}H$ (J/mol)			$\Delta_{sol}S$ (J/mol K)		
	Water	Acetic acid+water (ratio 1:1, v/v)	Acetic acid+water (ratio 1.5:1, v/v)	Water	Acetic acid+water (ratio 1:1, v/v)	Acetic acid+water (ratio 1.5:1, v/v)
303.2	13,415.4	13,415.4	83,63.0	44.3	44.3	27.6
313.2	16,437.7	16,437.7	11,658.0	52.5	52.5	37.2
318.2	17,948.9	17,948.9	13,305.5	56.4	56.4	41.8
323.2	19,460.0	19,460.0	14,953.0	60.2	60.2	46.3
328.2	20,971.2	20,971.2	16,600.5	63.9	63.9	50.6
333.2	22,482.3	22,482.3	18,248.0	67.5	67.5	54.8
338.2	23,993.5	23,993.5	19,895.5	71.0	71.0	58.8
343.2	25,504.6	25,504.6	21,543.1	74.3	74.3	62.8
353.2	27,015.8	28,526.9	23,190.6	77.6	80.8	66.6
363.2	28,526.9	31,549.2	24,838.1	80.8	86.9	70.3
368.2	30,038.1	33,060.4	26,485.6	83.9	89.8	74.0
373.2	31,549.2	34,571.6	28,133.1	86.9	92.6	77.5
383.2	33,060.4	37,593.9	29,780.6	89.8	98.1	80.9

b) Molar enthalpy and molar entropy ( $\Delta_{sol}H$  and  $\Delta_{sol}S$ ) of 4-methylbenzoic acid dissolutions in various solvents.

T (K)	$\Delta_{sol}H$ (J/mol)		$\Delta_{sol}S$ (J/mol K)	
	Acetic acid+water (ratio 1:1, v/v)	Acetic acid+water (ratio 1.5:1, v/v)	Acetic acid+water (ratio 1:1, v/v)	Acetic acid+water (ratio 1.5:1, v/v)
303.2	32,878.4	26,638.2	107.4	87.9
313.2	34,603.6	28,632.0	108.5	91.4
323.2	36,328.9	30,625.8	110.5	94.8
333.2	38,054.1	32,619.6	112.4	97.9
343.2	39,779.4	34,613.4	114.2	100.9
353.2	41,504.7	36,607.2	115.9	103.7
363.2	43,229.9	38,601.0	117.5	106.3
373.2	44,955.2	40,594.8	119.0	108.8
383.2	46,680.4	42,588.6	120.5	111.2
393.2	48,405.7	44,582.5	121.8	113.4
403.2	50,130.9	45,579.4	123.7	114.5
413.2	51,856.2	46,576.3	124.9	115.5
423.2	53,581.4	47,573.2	126.1	116.6
433.2	55,306.7	48,570.1	126.6	117.6

c) Molar enthalpy and molar entropy ( $\Delta_{sol}H$  and  $\Delta_{sol}S$ ) of 4-*tert*-butylbenzoic acid in various solvents.

T (K)	$\Delta_{sol}H$ (J/mol)		$\Delta_{sol}S$ (J/mol K)	
	Acetic acid+water	Acetic acid+water	Acetic acid+water	Acetic acid+water
	(ratio 1:1 v/v)	(ratio 1.5:1 v/v)	(ratio 1:1 v/v)	(ratio 1.5:1 v/v)
303.2	31,777.4	24,751.5	104.8	81.6
313.2	32,303.7	25,963.8	103.2	82.9
323.2	32,830.0	27,176.0	101.6	84.1
333.2	33,356.3	28,388.3	100.1	85.2
343.2	33,882.6	29,600.5	98.7	86.3
353.2	34,408.9	30,812.8	97.4	87.3
363.2	34,935.2	32,025.0	96.2	88.2
373.2	35,461.5	33,237.3	95.0	89.1
383.2	35,987.8	34,449.5	93.9	89.9
393.2	36,514.1	35,661.8	92.9	90.7
403.2	37,040.4	36,874.0	91.9	91.5
413.2	37,566.7	38,086.3	90.9	92.2
423.2	38,093.0	39,298.5	90.0	92.9

As shown in Table 7.6,  $\Delta_{sol}H$  is a positive value indicating that the course of 4-iso-propylbenzoic acid, 4-methylbenzoic acid and 4-*tert*-butylbenzoic acid in studied solvents was endothermic [37]. This means that the energy of the components is lower than the energy of the mixture.

According to the fundamental thermodynamic relation [39], the molar entropy of dissolution of studied acids can be calculated as shown in the following relation [37].

$$\Delta_{sol}S = R \left( C - \frac{B}{T} \right) \quad (7.11)$$

From Eq. (7.11) and values of the parameters  $C$  and  $B$ , as shown in Table 7.4, the molar entropy of dissolution can be obtained. These values are shown above in Table 7.6.

As shown in Table 7.6, molar entropy of dissolution for 4-alkyl benzoic acids in studied solvents is positive. Again, as shown in Table 7.6, both  $\Delta_{sol}H$  and  $\Delta_{sol}S$  are higher than zero indicating that the dissolving of 4-iso-propylbenzoic acid, 4-methylbenzoic acid and 4-*tert*-butylbenzoic acid in studied solvents is an entropy-driven process [37].



## 7.5 Conclusion

This work experimentally studied the solubility of 4-iso-propylbenzoic, 4-methylbenzoic and 4-*tert*-butylbenzoic acids in water and acetic acid/water mixture at a temperature ranging from 303.2 to 433.2 K. The experimental procedures, applied for the study of these benzoic acids in this work, was verified by comparing the measured data of the solubility of 4-methylbenzoic acid in water with the literature data concerning this acid at lower temperatures. The  $\lambda H$  equation and the modified Apelblat equation models were used to predict the solubility of 4-iso-propylbenzoic, 4-methylbenzoic and 4-*tert*-butylbenzoic acids in aqueous solvents at high temperatures. The modified Apelblat equation was recommended in order to predict the solubility of considered acids and was applied to determine molar enthalpy and molar entropy of dissolutions of 4-alkyl benzoic acids in various solvents. The molar enthalpy and molar entropy of dissolutions observed were positive indicating that the dissolving of the acids studied was an entropy-driven process.

## 7.6 Nomenclature

$a_i$	activity of acids in the solution
$a_s$	activity of pure solid
$a_w$	activity of pure liquid
$A$	parameter in the modified Apelblat equation
$B$	parameter in the modified Apelblat equation

$C$	parameter in the modified Apelblat equation
$E$	average absolute deviation
$H$	parameter in the $\lambda H$ equation
$J$	temperature-independent constant
$k_1$	constant parameter in the empirical formula
$k_2$	constant parameter in the empirical formula
$K_i$	equilibrium constant of solid dissolution
$N$	number of experimental data
$R$	gas constant (J/mol K)
$T$	temperature in Kelvin (K)
$T_m$	melting point of the considered 4-alkyl benzoic acid (K)
$x_{Cal.}$	calculated mole fraction solubility data
$x_{Exp.}$	experimental mole fraction solubility data
$x_i$	mole fraction solubility of the solute component $i$ in the solvent

#### Greek letter

$\lambda$	parameter in the $\lambda H$ equation
$\gamma_i$	activity coefficient of acid in the solution

#### Symbol

$\Delta_{sol}H$	molar enthalpy of solid-compound dissolution (J/mol)
$\Delta_{sol}S$	molar entropy of solid-compound dissolution (J/mol K)

## 7.7 Acknowledgements

The authors are very grateful for the financial support given by the Thailand Research Fund and Chulalongkorn University under the Royal Golden Jubilee Ph.D. Program (Grant No. PHD/0324/2551) and Dutsadi Phiphat. Sincere thanks are also given to the Laboratory of Catalyzed Processes, Department of Organic Technology, Faculty of Chemical and Food Technology, Slovak University of Technology in Bratislava, Bratislava, Slovak Republic, for kindly supplying all chemical compounds and instruments for analyses and measurements.

## 7.8 References

- [1] Q. Jia, P. Ma, S. Ma, C. Wang, Solid-liquid equilibria of benzoic acid derivatives in 1-octanol, *Chin. J. Chem. Eng.* 15 (2007) 710-714.
- [2] S.N. Reddy, G. Madras, Modeling of ternary solubilities of solids in supercritical carbon dioxide in the presence of cosolvents or cosolutes, *J. Supercrit. Fluids.* 63 (2012) 105-114.
- [3] S.N. Reddy, G. Madras, Mixture solubilities of nitrobenzoic acid isomers in supercritical carbon dioxide, *J. Supercrit. Fluids* 70 (2012) 66-74.
- [4] C. Saal, A.C. Petereit, Optimizing solubility: kinetic versus thermodynamic solubility temptations and risks, *Eur. J. Pharm. Sci.* 47 (2012) 589-595.
- [5] A.G. Carr, J.W. Tester, Prediction of the solubility of quartz in salt solutions from 25°C to 900°C using the 3-parameter Non-Random Two-Liquid (NRTL) model, *Fluid Phase Equilib.* 337 (2013) 288-297.

- [6] D. Bourgois, D. Thomas, J.-L. Fanlo, J. Vanderschuren, Solubilities at high dilution of toluene, ethylbenzene, 1,2,4-trimethylbenzene, and hexane in di-2-ethylhexyl, diisooheptyl, and diisononyl phthalates, *J. Chem. Eng. Data.* 51 (2006) 1212-1215.
- [7] A. Jouyban, S. Soltanpour, W.E. Acree, Solubility of acetaminophen and ibuprofen in the mixtures of polyethylene glycol 200 or 400 with ethanol and water and the density of solute-free mixed solvents at 298.2 K, *J. Chem. Eng. Data.* 55 (2010) 5252-5257.
- [8] J. Cassens, F. Ruether, K. Leonhard, G. Sadowski, Solubility calculation of pharmaceutical compounds – a priori parameter estimation using quantum-chemistry, *Fluid Phase Equilib.* 299 (2010) 161-170.
- [9] W. Song, P. Ma, L. Fan, Z. Xiang, Solubility of glutaric acid in cyclohexanone, cyclohexanol, their five mixtures and acetic acid, *Chin. J. Chem. Eng.* 15 (2007) 228-232.
- [10] J. Nti-Gyabaah, R. Chmielowski, V. Chan, Y.C. Chiew, Solubility of lovastatin in a family of six alcohols: ethanol, 1-propanol, 1-butanol, 1-pentanol, 1-hexanol, and 1-octanol, *Int. J. Pharm.* 359 (2008) 111-117.
- [11] A.I. Kholkin, V.V. Belova, G.L. Pashkov, I.Y. Fleitlikh, V.V. Sergeev, Solvent binary extraction, *J. Mol. Liq.* 82 (1999) 131-146.
- [12] H. Weingärtner, W. Schröer, Liquid-liquid phase separations and critical behavior of electrolyte solutions driven by long-range and short-range interactions, *J. Mol. Liq.* 65-66 (1995) 107-114.

- [13] B. Coto, C. Martos, J.L. Peña, R. Rodríguez, G. Pastor, Effects in the solubility of  $\text{CaCO}_3$ : experimental study and model description, *Fluid Phase Equilib.* 324 (2012) 1-7.
- [14] Q.-b. Wang, H.-b. Xu, X. Li, Solubility of terephthalic acid in aqueous acetic acid from 423.15 to 513.15 K, *Fluid Phase Equilib.* 233 (2005) 81-85.
- [15] K. Maeda, Y. Asakuma, K. Fukui, Configurations of solute molecules from homogeneous binary solution during crystallization on molecular dynamics simulations, *J. Mol. Liq.* 122 (2005) 43-48.
- [16] D.A. Crerar, G.M. Anderson, Solubility and solvation reactions of quartz in dilute hydrothermal solutions, *Chem. Geol.* 8 (1971) 107-122.
- [17] E. Madejón, A.P. de Mora, E. Felipe, P. Burgos, F. Cabrera, Soil amendments reduce trace element solubility in a contaminated soil and allow regrowth of natural vegetation, *Environ. Pollut.* 139 (2006) 40-52.
- [18] J. Thati, F.L. Nordström, Å.C. Rasmuson, Solubility of benzoic acid in pure solvents and binary mixtures, *J. Chem. Eng. Data.* 55 (2010) 5124-5127.
- [19] Z. Ding, R. Zhang, B. Long, L. Liu, H. Tu, Solubilities of m-phthalic acid in petroleum ether and its binary solvent mixture of alcohol + petroleum ether, *Fluid Phase Equilib.* 292 (2010) 96-103.
- [20] D.-Q. Li, D.-Z. Liu, F.-A. Wang, Solubility of 4-methylbenzoic acid between 288 K and 370 K, *J. Chem. Eng. Data.* 46 (2001) 234-236.
- [21] China Haohua Chemical Co.,Ltd  
<<http://haohua.chemchina.com/haohuaen/cpyfw/gscp/jxhcp/webinfo/2012/01/1326633216220307.htm>> (accessed 07.08.13).

- [22] E. Manzurola, A. Apelblat, Solubilities of l-glutamic acid, 3-nitrobenzoic acid, p-toluic acid, calcium-l-lactate, calcium gluconate, magnesium-dl-aspartate, and magnesium-l-lactate in water, *J. Chem. Thermodyn.* 34 (2002) 1127-1136.
- [23] J. Marrero, J. Abildskov, Solubility and Related Properties of Large Complex Chemicals, DECHEMA: Chemistry Data Series, Frankfurt, 2003.
- [24] F.L. Mota, A.P. Carneiro, A.J. Queimada, S.P. Pinho, E.A. Macedo, Temperature and solvent effects in the solubility of some pharmaceutical compounds: measurements and modeling, *Eur. J. Pharm. Sci.* 37 (2009) 499-507.
- [25] W.L. Jorgensen, E.M. Duffy, Prediction of drug solubility from structure, *Adv. Drug Delivery Rev.* 54 (2002) 355-366.
- [26] F. Lihua, M. Peisheng, X. Zhengle, Measurement and correlation for solubility of adipic acid in several solvents, *Chin. J. Chem. Eng.* 15 (2007) 110-114.
- [27] H. Li, J. Liu, J. Zhu, L. Zhao, Y. Zhang, Solubility of pimelic acid in water, *Russ. J. Phys. Chem. A.* 85 (2011) 1472-1474.
- [28] F.-a. Wang, L.-c. Wang, J.-c. Song, L. Wang, H.-s. Chen, Solubilities of bis(2,2,6,6-tetramethyl-4-piperidinyloxy) maleate in hexane, heptane, octane, m-xylene, and tetrahydrofuran from (253.15 to 310.15) K, *J. Chem. Eng. Data.* 49 (2004) 1539-1541.
- [29] W. Sun, W. Qu, L. Zhao, Solubilities of 4-formylbenzoic acid in ethanoic acid, water, and ethanoic acid/water mixtures with different compositions from (303.2 to 473.2) K, *J. Chem. Eng. Data.* 55 (2010) 4476-4478.

- [30] N. Sunsandee, S. Suren, N. Leepipatpiboon, M. Hronec, U. Pancharoen, Determination and modeling of aqueous solubility of 4-position substituted benzoic acid compounds in a high-temperature solution, *Fluid Phase Equilib.* 338 (2013) 217-223.
- [31] N. Sunsandee, M. Hronec, M. Štolcová, N. Leepipatpiboon, U. Pancharoen, Thermodynamics of the solubility of 4-acetylbenzoic acid in different solvents from 303.15 to 473.15K, *J. Mol. Liq.* 180 (2013) 252-259.
- [32] L. Strong, R. Neff, I. Whitesel, Thermodynamics of dissolving and solvation processes for benzoic acid and the toluic acids in aqueous solution, *J. Solution Chem.* 18 (1989) 101-114.
- [33] J.W. Williams, F. Bender, R.A. Alberty, C.D. Cornwell, J.E. Harriman, *Experimental Physical Chemistry*, McGraw-Hill, New York, 1970.
- [34] H. Buchowski, A. Khiat, Solubility of solids in liquids: one-parameter solubility equation, *Fluid Phase Equilib.* 25 (1986) 273-278.
- [35] A. Apelblat, E. Manzurola, Solubilities of o-acetylsalicylic, 4-aminosalicylic, 3,5-dinitrosalicylic, and p-toluic acid, and magnesium-DL-aspartate in water from  $T=(278 \text{ to } 348) \text{ K}$ , *J. Chem. Thermodyn.* 31 (1999) 85-91.
- [36] A. Apelblat, E. Manzurola, Solubilities of manganese, cadmium, mercury and lead acetates in water from  $T= 278.15 \text{ K}$  to  $T= 340.15 \text{ K}$ , *J. Chem. Thermodyn.* 33 (2001) 147-153.
- [37] C.-L. Zhang, F. Zhao, Y. Wang, Thermodynamics of the solubility of sulfamethazine in methanol, ethanol, 1-propanol, acetone, and chloroform from 293.15 to 333.15 K, *J. Mol. Liq.* 159 (2011) 170-172.

- [38] F.A. Wang, Molecular Thermodynamics and Chromatographic Retention, Meteorology Press, Beijing, 2001.
- [39] J.M. Prausnitz, R.N. Lichtenthaler, E.G. Azevedo, Molecular Thermodynamics of Fluid-Phase Equilibria, third ed., Prentice Hall PTR, Upper Saddle River, New Jersey, 1999.





## CHAPTER VIII

### CONCLUSION

#### 8.1 Conclusion

According to the results in this work and previous findings, hollow fiber supported liquid membrane (HFSLM) is proved to be most effective for the separation of a relatively low concentration of various target species, e.g., metal ions<sup>(10-14)</sup>, organic compounds<sup>(75,76)</sup> and enantiomers<sup>(77-79)</sup>. In this work, HFSLM can successfully separate lead, mercury and arsenic ions in ppm level from synthetic water and produced water. The concentrations of discharged lead, mercury and arsenic ions comply with the regulatory discharge limits of which the concentrations are not higher than 0.2, 0.005 and 0.25 ppm, respectively. Simultaneous extraction and stripping of target ions in a single-step operation of the HFSLM system makes the separation unit very compact with less operating time. Other advantages of the HFSLM over traditional methods (e.g., chemical precipitation, coagulation, adsorption and ion exchange) include less extractant and solvent, low energy consumption, low capital and operating costs, and high selectivity. It is worth to be noted that selective separation can be attained by using a mixture of two types of extractants so-called synergistic extractant together with connecting hollow fiber modules in series or in parallel, while higher capacity can be attained by connecting hollow fiber modules in parallel. However, in this work selective separation of lead(II) and mercury(II) ions was obtained by applying D2EHPA (an acidic extractant) and Aliquat 336 (a basic

extractant) in two hollow fiber modules connected in series, i.e, D2EHPA and Aliquat 336 in the first and second modules, respectively.

The overall contents of this dissertation cover the following studies:

The superior extraction of mercury ions compared with arsenic ions was obtained. Mercury ions in produced water were almost totally extracted by Aliquat 336, Bromo-PADAP, Cyanex 923 and Cyanex 471. Of all the extractants, Aliquat 336 showed the best performance in the extraction of mercury ions. Synergistic separation of arsenic ions was remarkably obtained by using the mixture of 0.22 M Aliquat 336 and 0.06 M Cyanex 471 with 0.2 M H<sub>2</sub>SO<sub>4</sub> in feed solution, 0.1 M of thiourea as a stripping solution, continuous operation HFSLM using a single module of the HFSLM and equal flow rates of feed and stripping solutions of 100 mL/min. The concentrations of discharged mercury and arsenic ions complied with the regulatory discharge limits at 1-cycle separation (approximately 40 min) and 3-cycle separation, respectively. The synergistic coefficient (*R*) for the extraction of arsenic ions was 2.8 indicating that the synergistic extraction of arsenic ions by the mixture of Aliquat 336 and Cyanex 471 was moderate compared with the synergistic extraction of zirconium ions (*R* = 30.4) and hafnium ions (*R* = 18.3) by the mixture of Cyanex 921 and Cyanex 272<sup>(55)</sup>. To enhance the synergistic extraction of arsenic ions, further study on the mixture of other extractants was recommended.

According to the results of separation of lead(II) ions from synthetic water, high extraction and stripping of lead(II) ions from Pb(NO<sub>3</sub>)<sub>2</sub> and PbCl<sub>2</sub> solutions were observed. The concentrations of lead(II) ions in the stripping solution was higher than

that in the inlet feed solution of about 2.7 times. The concentration of discharged lead(II) ions complied with the regulatory discharge limit by using 0.03 M D2EHPA as the extractant, 0.9 M HCl as the stripping solution, semi-batch operation HFSLM using a single module of the HFSLM, operating time of 80 min, and equal flow rates of feed and stripping solutions of 100 mL/min. It should be noted that the concentration of lead(II) ions in the stripping solution increased with the concentration of HCl. However, in order to ensure a longer lifetime of the polypropylene hollow fibers, 0.9 M HCl is recommended. Further, to obtain a high concentration of lead(II) ions in the stripping solution and less-stripping solution consumption, semi-batch operation HFSLM is recommended. It was found that the kinetics of  $\text{Pb}(\text{NO}_3)_2$  and  $\text{PbCl}_2$  extraction corresponded to the second-order reaction with the rate constants of 1.49 and 1.51 L/mg min, respectively. The outlet concentrations of lead(II) ions in the  $\text{Pb}(\text{NO}_3)_2$  and  $\text{PbCl}_2$  feed solutions estimated by the reaction flux model from our research group<sup>(23)</sup> were in good agreement with the experimental data at the average percent deviations of 4% for  $\text{Pb}(\text{NO}_3)_2$  solution and 8% for  $\text{PbCl}_2$  solution. It indicated that the extraction of lead(II) ions by HFSLM depended on the convection and accumulation of lead(II) ions in the feed solution, and the reactions at feed-liquid membrane interface.

The semi-batch operation HFSLM using a double-module HFSLM in series was applied to attain the selective separation of lead(II) and mercury(II) ions. It was found that lead(II) and mercury(II) ions were selective separated from synthetic water by each module. The concentrations of discharged lead(II) and mercury(II) ions complied with the regulatory discharge limits. The optimum conditions were 0.03 M D2EHPA as the extractant and 0.9 M HCl as the stripping solution in the first module; 0.06 M

Aliquat 336 as the extractant and 0.1 M thiourea as the stripping solution in the second module at the operating time of 80 min, and equal flow rates of feed and stripping solutions of 100 mL/min. The concentrations of lead and mercury ions in the stripping solutions were higher than those in the inlet feed solution of about 2.7 and 1.2 times, respectively. The extraction and stripping of lead(II) and mercury(II) ions were found to be the second-order reaction. The reaction rate constants for the extraction of lead(II) and mercury(II) ions were 1.51 and 1.20 L/mg min, respectively. The reaction rate constants for the stripping of lead(II) and mercury(II) ions were 11.20 and 9.25 L/mg min, respectively.

To apply the HFSLM system to industrial applications, the reaction flux model considering the convection and accumulation of lead(II) and mercury(II) ions in the feed and stripping solutions and the reactions at liquid-membrane interfaces is recommended to predict suitable flow rates of feed and stripping solutions, and the extraction and stripping of the target species. The diffusion in liquid membrane was neglected. In this work, the models were solved by two methods, i.e., Laplace Transform and Generating Function. The results from the models agreed well with the experimental data. In case of using Laplace Transform, the average percent deviations for the prediction of extraction and stripping of lead(II) and mercury(II) ions were the same of about 3%. In case of using Generating Function, the average percent deviations for the prediction of extraction and stripping of lead(II) and mercury(II) ions were 2% and 5%, respectively. There was no significant difference in the solutions obtained by the models using the Laplace Transform and Generating Function. Low average percent deviations indicated that the extraction and stripping of lead(II) and mercury(II) ions via HFSLM corresponded to the reaction flux model. In

fact, the concentrations of lead, mercury and arsenic in the produced water from various wells are different. The reaction flux model is proved very helpful for the separation of the metal ions to attain high quality produced water or wastewater.

Solubilities of the extractant in feed and stripping solutions are important to the stability of the liquid membrane and of course to the efficiency separation by HFSLM. The suitable extractant should have low solubility in feed and stripping solutions but should have high solubility in the diluent<sup>(68)</sup>. The solubility data of the extractants in feed and stripping solutions must be known to select a suitable extractant for the HFSLM system.

The equilibrium method for the measurements of the solubilities of the organic acids was applied as learning cases for the measurement of the solubility of the extractant. The solubilities of adipic acid, 4-methylbenzoic acid, 4-iso-propylbenzoic acid and 4-*tert*-butylbenzoic acid attained from the equilibrium method in this work were in good agreement with those solubilities reported in the literature<sup>(69-72)</sup>. The modified Apelblat equation was found to be highly accurate compared with the  $\lambda H$  equation in the prediction of these organic acids. The total average relative deviation for the prediction of the solubilities by the modified Apelblat equation was about 6% while by the  $\lambda H$  equation was about 22%. The molar enthalpy and the molar entropy of dissolutions of adipic acid, 4-methylbenzoic acid, 4-iso-propylbenzoic acid and 4-*tert*-butylbenzoic acid estimated by the modified Apelblat equation were positive values indicating that the dissolving of these organic acids was endothermic and entropy-driven process.

## 8.2 Recommendations for future studies

1. The properties and contaminant ions of produced water from various reservoirs are different, and thus the results in this work corresponding to the produced water from Bualuang field might be different from the produced water other reservoirs. Accordingly, the separation of metal ions from produced water from different reservoirs is recommended because types of metal ions and the interference of different ions play a role in the extraction and stripping of metal ions.

2. Because the hollow fibers of the HFSLM module in this work are polypropylene, which cannot resist strong acids such as HCl, high concentration of acid and high temperature, therefore, other materials should be considered and too high concentration of acid and too high temperature should be avoided.

3. Measurement of the solubilities of various extractants in aqueous solutions should be studied.

## REFERENCES

- (1) Barciszewska, M.Z., M. Szymanski, E. Wyszko, J. Pas, L. Rychlewski, J. Barciszewski. Lead toxicity through the leadzyme. Mutat. Res., Rev. Mutat. Res. 589 (2005): 103-110.
- (2) Rochow, E.G., E.W. Abel, The Chemistry of Germanium, Tin and Lead, Pergamon Press, 1973.
- (3) Díez, S. Human health effects of methyl mercury exposure. Rev. Environ. Contam. Toxicol. 198 (2009): 111-132.
- (4) Pajuelo, E., I.D. Rodríguez-Llorente, M. Dary, A.J. Palomares. Toxic effects of arsenic on *Sinorhizobium-Medicago sativa* symbiotic interaction. Environ. Pollut. 154 (2008): 203-211.
- (5) Thailand Regulatory Discharge Standards 2, Ministry of Industry, Thailand, 1996.
- (6) Water Quality Standards, Ministry of Natural Resources and Environment, Thailand, 1996.
- (7) Gallup, D.L., J.B. Strong, Removal of mercury and arsenic from produced water, Chevron Corporation, 2007, pp. 1-9.
- (8) Guell, R., E. Antico, V. Salvado, C. Fontas. Efficient hollow fiber supported liquid membrane system for the removal and preconcentration of Cr(VI) at trace levels. Sep. Purif. Technol. 62 (2008): 389-393.
- (9) Ansari, S.A., P.K. Mohapatra, D.R. Raut, M. Kumar, B. Rajeswari, V.K. Manchanda. Performance of some extractants used for 'actinide partitioning' in a comparative hollow fibre supported liquid membrane transport study using simulated high level nuclear waste. J. Membr. Sci. 337 (2009): 304-309.
- (10) Zeng, C., F. Yang, N. Zhou. Hollow fiber supported liquid membrane extraction coupled with thermospray flame furnace atomic absorption spectrometry for the speciation of Sb(III) and Sb(V) in environmental and biological samples. Microchem. J. 98 (2011): 307-311.
- (11) Kandwal, P., S.A. Ansari, P.K. Mohapatra. Transport of cesium using hollow fiber supported liquid membrane containing calix[4]arene-bis(2,3-naphtho)crown-6 as the carrier extractant: Part II. Recovery from simulated high level waste and mass transfer modeling. J. Membr. Sci. 384 (2011): 37-43.
- (12) Weidong, Z., C. Chunhua, H. Zisu. Transport Study of Cu(II) Through Hollow Fiber Supported Liquid Membrane. Chin. J. Chem. Eng. 18 (2010): 48-54.
- (13) Es'haghi, Z., R. Azmoodeh. Hollow fiber supported liquid membrane microextraction of Cu<sup>2+</sup> followed by flame atomic absorption spectroscopy determination. Arabian J. Chem. 3 (2010): 21-26.

- (14) Bhattacharyya, A., P.K. Mohapatra, S.A. Ansari, D.R. Raut, V.K. Manchanda. Separation of trivalent actinides from lanthanides using hollow fiber supported liquid membrane containing Cyanex-301 as the carrier. J. Membr. Sci. 312 (2008): 1-5.
- (15) Coelho, I.M., M.M. Cardoso, R.M.C. Viegas, J.P.S.G. Crespo. Transport mechanisms and modelling in liquid membrane contactors. Sep. Purif. Technol. 19 (2000): 183-197.
- (16) Rout, P.C., K. Sarangi. A comparative study on extraction of Mo(VI) using both solvent extraction and hollow fiber membrane technique. Hydrometallurgy. 133 (2013): 149-155.
- (17) San Roman, M.F., E. Bringas, R. Ibanez, I. Ortiz. Liquid membrane technology: fundamentals and review of its applications. J. Chem. Technol. Biotechnol. 85 (2010): 2-10.
- (18) Kocherginsky, N.M., Q. Yang, L. Seelam. Recent advances in supported liquid membrane technology. Sep. Purif. Technol. 53 (2007): 171-177.
- (19) Mohapatra, P.K., V.K. Manchanda. Liquid membrane-based separations of actinides. in: Pabby, A.K., Rizvi, S.S.H., Sastre, A.M. (Eds.), Handbook of Membrane Separations: Chemical, Pharmaceutical, Food and Biotechnological Applications. CRC Press, pp. 883-918. (2009).
- (20) Parthasarathy, N., M. Pelletier, J. Buffle. Hollow fiber based supported liquid membrane: a novel analytical system for trace metal analysis. Analytica Chimica Acta 350 (1997): 183-195.
- (21) Jirjis, B.F., S. Luque, Chapter 9 - Practical aspects of membrane system design in food and bioprocessing applications, in: Z.F. Cui, H.S. Muralidhara (Eds.), Membrane Technology, Butterworth-Heinemann, Oxford, 2010, pp. 179-212.
- (22) Pancharoen, U., A.W. Lothongkum, S. Chaturabul, Mass transfer in hollow fiber supported liquid membrane for As and Hg removal from produced water in upstream petroleum operation in the gulf of Thailand, in: M. El-Amin (Ed.), Mass Transfer in Multiphase Systems and Its Applications, InTech, India, 2011, pp. 499-524.
- (23) Pancharoen, U., T. Wongsawa, A.W. Lothongkum. A reaction flux model for extraction of Cu(II) with LIX84I in HFSLM. Sep. Sci. Technol. 46 (2011): 2183-2190.
- (24) Vernekar, P.V., Y.D. Jagdale, A.W. Patwardhan, A.V. Patwardhan, S.A. Ansari, P.K. Mohapatra, V.K. Manchanda. Transport of cobalt(II) through a hollow fiber supported liquid membrane containing di-(2-ethylhexyl) phosphoric acid (D2EHPA) as the carrier. Chem. Eng. Res. Des. 91 (2013): 141-157.
- (25) Organization, W.H., Environmental Health Criteria 165: Inorganic Lead, Finland, World Health Organization, 1995.



- (26) Organization, W.H., Environmental Health Criteria 85:Lead – Environmental Aspects, Geneva, World Health Organization, 1989.
- (27) Wood, C.W., A.K. Holliday, Inorganic Chemistry, 3rd ed., England, Butterworth, 1967.
- (28) Gurel, L., L. Altas, H. Buyukgungor. Removal of lead from wastewater using emulsion liquid membrane technique. *Environ. Eng. Sci.* 22 (2005): 411-420.
- (29) US. EPA. Residential lead hazard standards - TSCA section 403. (2002).
- (30) Fabrega, F.d.M., M.B. Mansur. Liquid-liquid extraction of mercury (II) from hydrochloric acid solutions by Aliquat 336. *Hydrometallurgy*. 87 (2007): 83-90.
- (31) James, F.N., A textbook of inorganic chemistry for colleges, 1 ed., the United States of America, McGraw-Hill, 1921.
- (32) Friberg, L., Inorganic Mercury, Environmental Health Criteria 118, World Health Organization, Geneva, 1991.
- (33) Ayllett, B.J., The Chemistry of Zinc, Cadmium and Mercury, Oxford, Pergamon Press, 1973.
- (34) Ferens, C., U.S.E.P.A.O.o. Research, Development, A review of the physiological impact of mercurials, For sale by the Supt. of Docs., U.S. Govt. Print. Off., 1974.
- (35) A. Gomez-Caminero, P. Howe, M. Hughes, E. Kenyon, D.R. Lewis, M. Moore, J. Ng., A. Aitio, G. Becking, Arsenic and Arsenic Compounds, in: J. Ng (Ed.), Environmental Health Criteria 224, World Health Organization, Finland, 2001.
- (36) S.D. Wilson, W.R. Kelly, T.R. Holm, J.L. Talbott, Arsenic Removal in Water Treatment Facilities: Survey of Geochemical Factors and Pilot Plant Experiments, Midwest Technology Assistance Center, 2007.
- (37) Leermakers, M., W. Baeyens, M. De Gieter, B. Smedts, C. Meert, H.C. De Bisschop, R. Morabito, P. Quevauviller. Toxic arsenic compounds in environmental samples: Speciation and validation. *TrAC Trends in Analytical Chemistry* 25 (2006): 1-10.
- (38) Salgado, S.G., M.A.Q. Nieto, M.M.B. Simón. Assessment of total arsenic and arsenic species stability in alga samples and their aqueous extracts. *Talanta* 75 (2008): 897-903.
- (39) Functional groups.
- (40) Fromm, J.R. The Concept of Functional Groups. (2014).
- (41) MCT. MCT Redbook: solvent extraction reagents and applications.
- (42) Author, Solvent extraction and membranes, fundamentals and applications in new materials, in: Manuel, A., L.C. Jose, (Eds.), Book Solvent extraction and membranes, fundamentals and applications in new materials, CRC Press, the United States of America, 2008, pp. Pages

- (43) Gumi, T., M. Oleinikova, C. Palet, M. Valiente, M. Munoz. Facilitated transport of lead(II) and cadmium(II) through novel activated composite membranes containing di-(2-ethyl-hexyl)phosphoric acid as carrier. *Anal. Chim. Acta.* 408 (2000): 65-74.
- (44) Adebayo, A.O., K. Sarangi. Separation of copper from chalcopyrite leach liquor containing copper, iron, zinc and magnesium by supported liquid membrane. *Separation and Purification Technology* 63 (2008): 392-399.
- (45) Perez, M.E.M., J.A. Reyes-Aguilera, T.I. Saucedo, M.P. Gonzalez, R. Navarro, M. Avila-Rodriguez. Study of As(V) transfer through a supported liquid membrane impregnated with trioctylphosphine oxide (Cyanex 921). *J. Membr. Sci.* 302 (2007): 119-126.
- (46) Iberhan, L., M. Wisniewski. Removal of arsenic(III) and arsenic(V) from sulfuric acid solution by liquid-liquid extraction. *J. Chem. Technol. Biotechnol.* 78 (2003): 659-665.
- (47) Chapman, T.W., Chapter 8, Extraction – Metals Processing, in: R.W. Rousseau (Ed.), Handbook of Separation Process Technology, John Wiley & Sons, Inc., Canada, 1997, pp. 467–499.
- (48) Kawamura, Y., M. Mitsuhashi, H. Tanibe, H. Yoshida. Adsorption of metal ions on polyaminated highly porous chitosan chelating resin. *Ind. Eng. Chem. Res.* 32 (1993): 386-391.
- (49) Chakrabarty, K., P. Saha, A.K. Ghoshal. Simultaneous separation of mercury and lignosulfonate from aqueous solution using supported liquid membrane. *J. Membr. Sci.* 346 (2010): 37-44.
- (50) Atanassova, M. Synergistic solvent extraction and separation of lanthanide(III) ions with 4-benzoyl-3-phenyl-5-isoxazolone and the quaternary ammonium salt. *Solvent Extr. Ion Exch* 27 (2009): 159 - 171.
- (51) Choppin, G.R., A. Morgenstern. Thermodynamics of solvent extraction. *Solvent Extr. Ion Exch.* 18 (2000): 1029–1049.
- (52) Luo, F., D. Li, P. Wei. Synergistic extraction of zinc(II) and cadmium(II) with mixtures of primary amine N1923 and neutral organophosphorous derivatives. *Hydrometallurgy* 73 (2004): 31-40.
- (53) Guezzen, B., M.A. Didi. Removal of Zn(II) from aqueous acetate solution using Di(2-Ethylhexyl)phosphoric acid & tributylphosphate. *International Journal of Chemistry* 4 (2012): 32-41.
- (54) Wannachod, T., N. Leepipatpiboon, U. Pancharoen, K. Nootong. Synergistic effect of various neutral donors in D2EHPA for selective neodymium separation from lanthanide series via HFSLM. *J. Ind. Eng. Chem.* (2014)  
<http://dx.doi.org/10.1016/j.jiec.2014.01.014>.

- (55) Wang, L.Y., H.Y. Lee, M.S. Lee. Solvent extraction of zirconium and hafnium from hydrochloric acid solutions using acidic organophosphorus extractants and their mixtures with TOPO. *Mater. Trans., JIM* 54 (2013): 1460–1466.
- (56) Qiong, J., W. Jie, L. Ting-Ting, Z. Wei-Hong. Synergistic extraction of Zn(II) by mixtures of tri-butyl-phosphate and trialkyl amine extractant *Chin. J. Anal. Chem.* 36 (2008): 619–622.
- (57) Prapasawat, T., P. Ramakul, C. Satayaprasert, U. Pancharoen, A.W. Lothongkum. Separation of As(III) and As(V) by hollow fiber supported liquid membrane based on the mass transfer theory. *Korean Journal of Chemical Engineering* 25 (2008): 158-163.
- (58) Kandwal, P., S. Dixit, S. Mukhopadhyay, P.K. Mohapatra. Mass transport modeling of Cs(I) through hollow fiber supported liquid membrane containing calix-[4]-bis(2,3-naphtho)-crown-6 as the mobile carrier. *Chem. Eng. J.* 174 (2011): 110-116.
- (59) Chaturabul, S., K. Wongkaew, U. Pancharoen. Selective Transport of Palladium through a Hollow Fiber Supported Liquid Membrane and Prediction Model Based on Reaction Flux. *Sep. Sci. Technol.* 48 (2012): 93-104.
- (60) Yang, Q., N.M. Kocherginsky. Copper removal from ammoniacal wastewater through a hollow fiber supported liquid membrane system: modeling and experimental verification. *J. Membr. Sci.* 297 (2007): 121-129.
- (61) Lothongkum, A.W., S. Suren, S. Chaturabul, N. Thamphiphit, U. Pancharoen. Simultaneous removal of arsenic and mercury from natural-gas-co-produced water from the Gulf of Thailand using synergistic extractant via HFSLM. *J. Membr. Sci.* 369 (2011): 350-358.
- (62) Escobar, A., K.A. Schimmel, J. de Gyves, E.R. de San Miguel. Hollow-fiber dispersion-free extraction and stripping of Pb(II) in the presence of Cd(II) using D2EHPA under recirculating operation mode. *J. Chem. Technol. Biotechnol.* 79 (2004): 961-973.
- (63) Gherasim, C.-V.I., G. Bourceanu, R.-I. Olariu, C. Arsene. Removal of lead(II) from aqueous solutions by a polyvinyl-chloride inclusion membrane without added plasticizer. *J. Membr. Sci.* 377 (2011): 167-174.
- (64) Juang, R.S., J.Y. Su. Thermodynamic equilibria of the extraction of cobalt(II) from sulfate solutions with bis(2-ethylhexyl)phosphoric acid. *Ind. Eng. Chem. Res.* 31 (1992): 2395-2400.
- (65) Suren, S., T. Wongsawa, U. Pancharoen, T. Prapasawat, A.W. Lothongkum. Uphill transport and mathematical model of Pb(II) from dilute synthetic lead-containing solutions across hollow fiber supported liquid membrane. *Chem. Eng. J.* 191 (2012): 503-511.

- (66) Suren, S., U. Pancharoen, S. Kheawhom. Simultaneous extraction and stripping of lead ions via a hollow fiber supported liquid membrane: Experiment and modeling. Journal of Industrial and Engineering Chemistry (2013).
- (67) Suren, S., U. Pancharoen, N. Thamphiphit, N. Leepipatpiboon. A Generating Function applied on a reaction model for the selective separation of Pb(II) and Hg(II) via HFSLM. J. Membr. Sci. 448 (2013): 23-33.
- (68) Gallacher, L.V. Liquid Ion Exchange in Metal Recovery and Recycling
- (69) Gaivoronskii, A.N., V.A. Granzhan. Solubility of adipic acid in organic solvents and water. Russ. J. Appl. Chem. 78 (2005): 404-408.
- (70) F. Lihua, M. Peisheng, X. Zhengle. Measurement and correlation for solubility of adipic acid in several solvents. Chin. J. Chem. Eng. 15 (2007): 110-114.
- (71) Li, D.-Q., D.-Z. Liu, F.-A. Wang. Solubility of 4-methylbenzoic acid between 288 K and 370 K. J. Chem. Eng. Data. 46 (2001): 234-236.
- (72) Strong, L., R. Neff, I. Whitesel. Thermodynamics of dissolving and solvation processes for benzoic acid and the toluic acids in aqueous solution. J. Solution Chem. 18 (1989): 101-114.
- (73) Suren, S., N. Sunsandee, M. Stolcova, M. Hronec, N. Leepipatpiboon, U. Pancharoen, S. Kheawhom. Measurement on the solubility of adipic acid in various solvents at high temperature and its thermodynamics parameters. Fluid Phase Equilib. 360 (2013): 332-337.
- (74) Suren, S., M. Hronec, U. Pancharoen, S. Kheawhom. Solubility measurement and correlation of 4-alkyl benzoic acids in aqueous solutions. J. Mol. Liq. in press.
- (75) Mtibe, A., T.A.M. Msagati, A.K. Mishra, B.B. Mamba. Determination of phthalate ester plasticizers in the aquatic environment using hollow fibre supported liquid membranes. Phys. Chem. Earth. 50-52 (2012): 239-242.
- (76) Liu, Y., B. Shi. Hollow fiber supported liquid membrane for extraction of ethylbenzene and nitrobenzene from aqueous solution: A Hansen Solubility Parameter approach. Sep. Purif. Technol. 65 (2009): 233-242.
- (77) Sunsandee, N., P. Ramakul, U. Pancharoen, N. Leepipatpiboon. Enantioseparation of (S)-amlodipine from pharmaceutical industry wastewater by stripping phase recovery via HFSLM: Polarity of diluent and membrane stability investigation. Sep. Sci. Technol. 116 (2013): 405-414.
- (78) Sunsandee, N., P. Ramakul, N. Thamphiphit, U. Pancharoen, N. Leepipatpiboon. The synergistic effect of selective separation of (S)-amlodipine from pharmaceutical wastewaters via hollow fiber supported liquid membrane. Chem. Eng. J. 209 (2012): 201-214.

- (79) Sunsandee, N., N. Leepipatpiboon, P. Ramaku. Selective enantioseparation of levocetirizine via a hollow fiber supported liquid membrane and mass transfer prediction. Korean J. Chem. Eng. 30(6) (2013): 1312-1320.



## VITA

Mr. Sira Suren was born in Trang on November 3, 1983. He received his Bachelor's Degree in Chemical Engineering from Mahanakorn University of Technology in 2006. He worked at Bang PA-IN Paper Mill Industry Limited from January 2007 to June 2008. He continued his graduate study in Doctoral degree at Separation Technology Laboratory, Department of Chemical Engineering, Faculty of Engineering, Chulalongkorn University since 2008 and received scholarship from the Thailand Research Fund and Chulalongkorn University under the Royal Golden Jubilee Ph.D. Program. He spent one year to do the research at Department of Organic Technology, Faculty of Chemical and Food Technology, Slovak University of Technology in Bratislava, Slovak.

